ANALYSIS OF HIGHER ORDER SHEAR-DEFORMABLE PLATES ON TWO PARAMETER ELASTIC FOUNDATION USING MODIFIED VLASOV MODEL

THESIS SUBMITTED

BY

ASHIS KUMAR DUTTA

DOCTOR OF PHILOSOPHY (ENGINEERING)

DEPARTMENT OF CONSTRUCTION ENGINEERING
FACULTY COUNCIL OF ENGINEERING & TECHNOLOGY
JADAVPUR UNIVERSITY
KOLKATA, INDIA

2024

INDEX No.:119/19/E of 2019

1. Title of the Thesis:

Analysis of Higher Order Shear-Deformable Plates on Two Parameter Elastic Foundation Using Modified Vlasov Model

2. Name, Designation and Institution of the Supervisors

(1) Prof. (Dr.) Debasish Bandyopadhyay
Professor
Department of Construction Engineering,
Jadavpur University, Kolkata- 700098
and
(2) Dr . Jagat Jyoti Mandal
Ex-Professor
Department of Civil Engineering,
NITTTR, Kolkata- 700106

25/06/2024

Dr. Jagat Jyoti Mandal
Ex-Professor, NIT Durgapur & NITTTR, Kolkata
Chartered Engineer & Geotechnical Consultant

25/06/24

Dr. Debasish Bandyopadhyay
Professor
Dept. of Construction Engineering
Jadavpur University, Salt Lake
Kolkata - 700 106

3. List of Publications:

Journal Publications: (7 Nos.)

1. **Dutta AK, Bandyopadhyay D, Mandal JJ (2024)** Application of strain energy approach in the analysis of circular plate with concentrated load resting on Pasternak-type foundation. Int J Adv Eng Sci Appl Math. https://doi.org/10.1007/s12572-024-00373-8
2. **Dutta AK, Bandyopadhyay D, Mandal JJ (2023)** Higher-Order Finite Element Vibration Analysis of Circular Raft on Winkler Foundation. Int J Geotech Earthq Eng 14:1–15. https://doi.org/10.4018/ijgee.324112
3. **Dutta AK, Bandyopadhyay D, Mandal JJ (2023)** Using Higher-Order Finite Element Analysis, a Circular Raft on an Elastic Foundation.pdf. Natl Acad Sci Lett. https://doi.org/https://doi.org/10.1007/s40009-023-01335-7
4. **Dutta AK, Bandyopadhyay D, Mandal JJ (2023)** Higher-Order Finite Element Analysis of Skew Plate on Elastic Foundation. Natl Acad Sci Lett 1–6. https://doi.org/10.1007/s40009-023-01212-3

25.06.2024.

5. **Dutta AK, Bandyopadhyay D, Mandal JJ (2022)** Skew Plate Vibration Analysis Using Modified Vlasov Model and Higher-Order Finite Element. ISET J Earthq Technol 59:151–178
6. **Dutta AK, Bandyopadhyay D, Mandal JJ (2021)** Free Vibration Analysis of Second-Order Continuity Plate Element Resting on Pasternak Type Foundation Using Finite Element Method. Int J Pavement Res Technol. https://doi.org/10.1007/s42947-021-00099-x
7. **Dutta AK, Bandyopadhyay D, Mandal JJ (2021)** Response Analysis of Second-Order Continuity Rectangular Plate Bending Element Resting on Elastic Foundation Using Modiied Vlasov Model. Int J Pavement Res Technol. https://doi.org/10.1007/s42947-021-00096-0

Book Chapter: (1 No)

1. **Dutta A.K., Bandyopadhyay D., Mandal J.J. (2021)** "Static Analysis of Thin Rectangular Plate Resting on Pasternak Foundation". In: Satyanarayana Reddy C.N.V., Saride S., Haldar S. (eds) Transportation, Water and Environmental Geotechnics. Lecture Notes in Civil Engineering, vol 159. Springer, Singapore. https://doi.org/10.1007/978-981-16-2260-1_21 (pp. 223-233)

4. List of Patents: Nil

5. List of Presentations in National/International/Conferences/Workshops:

1. **Dutta, A.K., Bandyopadhyay, D. & Mandal, J.J.(2024)** "Utilising a Modified Vlasov Model, Analyse a Plate-Bending Element Resting on an Elastic Foundation", in: Proc. of of ICI-IWC- 2024, Kolkata January 18-20, 2024.
2. **Dutta, A.K., Bandyopadhyay, D., and Mandal, J.J. (2022).** “Static Analysis of Thin Rectangular Plate Resting on Elastic Foundation Using Modified Vlasov Model.” Proceedings of the 12th Structural Engineering Convention - 2020,, p. 1531–37.

25.06.2024.

25/06/2024

Dr. Jagat Jyoti Mandal
Ex-Professor, NIT Durgapur & NITTTR, Kolkata
Chartered Engineer & Geotechnical Consultant

25/06/24

Dr. Debasish Bandyopadhyay
Professor
Dept. of Construction Engineering
Jadavpur University, Salt Lake
Kolkata - 700 106

"STATEMENT OF ORIGINALITY"

I, Ashis Kumar Dutta, registered on 11/06/2019 do hereby declare that this thesis entitled "**Analysis of Higher Order Shear-Deformable Plates on Two Parameter Elastic Foundation Using Modified Vlasov Model**" contains literature survey and original research work done by the undersigned candidate as part of Doctoral studies.

All information in this thesis have been obtained and presented in accordance with existing academic rules and ethical conduct. I declare that, as required by these rules and conduct, I have fully cited and referred all materials and results that are not original to this work.

I also declare that I have checked this thesis as per the "Policy on Anti Plagiarism, Jadavpur University, 2019", and the level of similarity as checked by iThenticate software is 4 %.

25.06.2024.

Signature of candidate

Date: 25.06.2024

25/06/2024

Dr. Jagat Jyoti Mandal
Ex-Professor, NIT Durgapur & NITTTR, Kolkata
Chartered Engineer & Geotechnical Consultant

25/06/24

Dr. Debasish Bandyopadhyay
Professor
Dept. of Construction Engineering
Jadavpur University, Salt Lake
Kolkata - 700 106

CERTIFICATE FROM THE SUPERVISORS

This is to certify that the thesis entitled "**Analysis of Higher Order Shear-Deformable Plates on Two Parameter Elastic Foundation Using Modified Vlasov Model**" submitted by Shri Ashis Kumar Dutta, who got his name registered on 11/06/2019 for the award of Ph. D. (Engg.) degree of Jadavpur University is absolutely based upon his own work under the supervision of Prof. (Dr.) Debasish Bandyopadhyay and Ex.-Prof. (Dr.) JagatJyoti Mandal that neither his thesis nor any part of the thesis has been submitted for any degree/ diploma or any other academic award anywhere before.

25.06.2024

25/06/2024

Dr. Jagat Jyoti Mandal
Ex-Professor, NIT Durgapur & NITTTR, Kolkata
Chartered Engineer & Geotechnical Consultant

25/06/24

Dr. Debasish Bandyopadhyay
Professor
Dept. of Construction Engineering
Jadavpur University, Salt Lake
Kolkata - 700 106

Dedicated

To

My Mother

and

My teacher Nayan Mukherjee who showed me the path I have walked on...........

ACKNOWLEDGEMENTS

I want to express my sincere thanks and a deep sense of gratitude to my mother, Tulsi Rani Dutta, my wife, Rakhi Dutta, and my only son, Pushkar Dutta; without their sacrifice and active cooperation, I couldn't have reached this point. I want to express my sincere thanks and a deep sense of gratitude to my thesis supervisors, Dr. Debasish Bandyopadhyay, Professor, Department of Construction Engineering, Jadavpur University, and Dr. JagatJyoti Mandal, Ex-Professor, Department of Civil Engineering, NITTTR, Kolkata, for their invaluable guidance, encouragement, and support in all aspects of conducting this research work. Without their help and advice, this study would not have been possible. I am grateful to both supervisors for entrusting me with this innovative research project and for their unwavering support and timely guidance in bringing it to a successful conclusion.

My sincere thanks to all the faculty members and technical support staff of the Construction Engineering Department for their help and cooperation. My sincere thanks to the Head of Department, Water Resources Investigation and Developement Department (WRI&DD), the Government of West Bengal, and all officials, colleagues, and staff of my esteemed department, WRI&DD, for their help and cooperation, as well as for giving me the necessary permission to conduct my research work. I want to express my special gratitude to Debashis Ray, Snehamoy Datta, Suvendu Kumar Ghosh, Debdatta Datta, Pradip De, Kalyan Mitra, Swarup Prokas Mukhopadhyay, Goutam Bondopadhyay, Prabal Kumar Tripathi, Kazi Badruzzaman, Samir Kumar Karmakar, Bikash Chandra Nandy, Anup Kumar Biswas, Dayal Chandra Santra, Partha Pratim Mukhopadhyay, and many more to my esteemed department, WRI&DD officials, and Jagannath Murmu, Sumit Sarkar, Biswaranjan Sinhamahapatra and other officials of the department of soil conservation , the Government of West Bengal. I am grateful to the Head of Department, all faculty members, and staff of the Construction Engineering Department for their valuable advice and guidance at the time of the inception of this research topic.

Last but not least, I want to express my gratitude to all of my friends and colleagues who assisted me in completing this research directly and indirectly. Thank you so much to everyone who helped me in any way during the entire journey of this PhD course.

Finally, I am grateful to the Almighty for inspiring me to complete this research work.

25.06.2024.

ABSTRACT

Plates on elastic foundations present widespread applications in civil engineering, for example, roadways, railway tracks, bridges, and airfields. These structures are subjected to static as well as dynamic loads. The study of numerical approaches has advanced to new dimensions in recent years, leading to more precise and efficient solution procedures. There are numerous situations where the Engineer has to use simple empirical techniques to design foundations that transfer the loads from the superstructure to the soil underneath. The "plate on elastic foundation" concept is widely used to solve typical soil foundation interaction problems. Appropriate analysis of the influence of suddenly applied load-moving mass requires proper modelling. An efficient vibration control process can be appropriately designed if the dynamic behaviour of the structural system is well estimated at the designed stage to prevent structural damage. Developing more realistic foundation models and simplified methods to solve this complex soil-structure interaction problem is essential for safe and economical design.

The present study attempted a workable approach for response analysis of plates on modified Vlasov foundations incorporating higher-order shear deformation theory (HSDT). The Poisson ratio of the soil is assumed to be constant from the top to a rigid surface to evaluate the soil parameters, i.e. Winkler/vertical parameter and shear parameter. Furthermore, the modulus of elasticity can be considered constant, varying linearly from top to bottom and quadratically from top to bottom. Finally, to evaluate the activated soil mass, the mass density of the soil is assumed to be constant for dynamic response analysis.

For static response analysis, different types of loading and boundary conditions for various irregular structural geometries are considered. In addition, free vibration and dynamic response analyses are carried out for stepped and suddenly applied loads. The results are compared with similar studies by other researchers, which show excellent conformity.

The present formulation's benefit is that it can efficiently analyze thin to thick rectangular, skew and solid circular plates resting on elastic foundations. The formulation is simple and requires less computational effort, resources and time. Moreover, parametric studies are carried out to obtain a response for different foundation parameters, loading and boundary conditions and types of loading.

Keywords: Modified Vlasov Model; Shear modulus; HSDT; Skewed Plate; Activated mass; Finite Element; Lock-free; Normal strain; Shear correction factor.

25.06.2024

25/06/2024

Dr. Jagat Jyoti Mandal
Ex-Professor, NIT Durgapur & NITTTR, Kolkata
Chartered Engineer & Geotechnical Consultant

25/06/24

Dr. Debasish Bandyopadhyay
Professor
Dept. of Construction Engineering
Jadavpur University, Salt Lake
Kolkata - 700 106

CONTENTS

LIST OF TABLES

LIST OF FIGURES

LIST OF ACRONYMS

FDM	-	Finite Difference Method
FEM	-	Finite Element Method
BEM	-	Boundary Element Method
HSDT	-	Higher-order Shear Deformation Theory
PBQ9	-	Nine - Noded Quardrilateral Plate Bending Element
DOF	-	Degrees of Freedom
EFHT	-	Extended Finite Hankel Transform
DQM	-	Differential Quadrature Method
PDE	-	Partial Differential Equation
PBQ4	-	Four - Noded Quardrilateral Plate Bending Element
PBR9	-	Nine - Noded Rectangular Plate Bending Element
PBR4	-	Four - Noded Rectangular Plate Bending Element
NI	-	Number of Iteration
UDL	-	Uniformly Distributed Load
PL	-	Point/Concentrated Load
4APB	-	Four - Noded Annular Plate Bending Element
PBS4	-	Four - Noded Skew Plate Bending Element
C	-	Clamped
S	-	Simply Supported
F	-	Free
PS	-	Present Study

LIST OF SYMBOLS

L/l/2a	Length of plate
B/2b	Width of plate
K_1, K_0	Modified Bessel functions of the second kind of first and zero orders
E_s,ν_s	Young's modulus of elasticity and Poisson's ratio of soil
E_0,ν_0	Effective modulus of elasticity and Poisson's ratio of soil
ρ_s	Mass density of soil
p (x) or f (x)	Load per unit length in the y-direction
K	Modulus of subgrade reaction (Winkler/Vertical parameter)
2t	Foundation parameter (Shear parameter)
K_f	Foundation parameter (Winkler/Vertical parameter)
V(x)	Shear force
M(x)	Bending moment
EI(x)	Bending stiffness around the z -axis
w	Displacement
P	Point load
M_0,M_A	Point moment
t	Time
u,v	Velocity
a	Acceleration
N	Shape function
M	Modal mass
K	Modal stiffness
m_1	Mass per unit length of the plate
m_0	Equivalent mass of soil participating in vibration
γ	Function of the characteristic of the foundation
ρ	Unit weight of the plate material
g	Gravitational acceleration
ξ	Damping ratio
ω	Natural circular frequency

Chapter 1
Introduction

1.1 General

Shallow foundations, typically in the shape of beams or plates, carry loads directly from the superstructures to the soil near the ground surface. As a result, shallow foundations remain popular. Several efforts have been made to improve the design and analysis of shallow foundation systems, and advancements have been acknowledged in modelling the soil media and the simulation of contact action between soil and foundation. The solution of plates resting on an elastic foundation can be linked to several critical practical situations. Direct applications include highway and airport runways, reinforced concrete pavements, building foundation slabs, etc. The foundation and the soil medium work together to resist and support the loads, complicating the integrated nature of the foundation and the soil medium. These structures are analyzed using the "plates on elastic foundation" approach. Adopting more practical and straightforward foundation models for the safe and economical design of transversely loaded plates on elastic foundations is very important. Plates or rafts are also used for foundations on soils of varying compressibility. Rigidity given by stiff slabs and beams is partially used to bridge over areas of more compressible soil. As a result, the foundation slab's differential settlement is decreased. Raft foundations can be used as a constructional convenience in a structure supported by a grid of pretty close-spaced columns.

Plates or Rafts of various shapes are used in practice. The most commonly used ones are rectangular, circular and annular in shape. They are subjected to different types of static and dynamic loads. Studying their response under various static and dynamic loading conditions is essential.

Analyses of plates on elastic foundations have broad applications in aerospace, civil and mechanical engineering. Many researchers consider the Love-Kirchhoff’s plate theory and the Mindlin plate model. Thin plate theory neglects transverse shear and normal transverse strain through the thickness of the plate. Reissner-Mindlin's theory assumes constant transverse shear strain through the thickness and neglects normal transverse strain, and a fictitious correction factor is introduced to account for correct shear energy. The limitations of Kirchhoff's plate and Mindlin's theory led to the development of higher-order shear deformation theories. Developing more realistic foundation models and simplified methods to solve this complex soil-structure interaction problem is crucial for safe and economical design. However, a theoretical approach cannot solve most problems, leading to numerical techniques like finite and boundary element methods.

A thorough investigation of the analysis and design of plate or raft foundations reveals that several approaches are used for various plate or raft kinds. The deformation characteristics of the soil medium, as well as the foundation's flexibility, should be taken into consideration when designing foundations that rely on soil media. Such interaction problems must always be treated analytically, necessitating considerable mathematical and computational work. It could be claimed that the time and effort put into these analyses may not be justified by the accuracy with which the various material parameters can be measured in a lab or situ or by the integrity of the fundamental assumptions regarding the response of the soil.

However, the traditional approaches to analysing soil-foundation interaction problems have distinct limitations, which the designer must know. For instance, the conventional design of footings, which relies on infinitely rigid foundation behaviour and uniform, planar, or parabolic contact stress distributions, completely ignores the flexural and deformational properties of the foundation as well as the deformational characteristics of the soil. These simple analyses essentially go against the fundamental tenets of indeterminate structural analysis. It should be understood that the interaction between the foundation and the structure should also be considered in a thorough analytical study of the soil foundation interaction problem. The behaviour of the soil-foundation system is significantly influenced by the structure's stiffness or by how the structural stiffness is transferred to the foundation.

1.2 Brief review of design methods for raft foundations

The assumptions made can be utilized to categorize the raft foundation analysis approach. Different approaches are used to analyze various kinds of rafts. The following are the general descriptions of the techniques used to examine multiple raft foundation types:

1.2.1 Rectangular Raft Foundations

Construction of water tanks, multi-story buildings, and other heavily loaded structures require rectangular raft foundations. They are typically examined using the techniques listed below.

(a) Conventional Methods (b) Numerical Methods

1.2.1.1 Conventional Methods

There are two approaches for analyzing the behaviour of raft foundations:

(i) Rigid Foundation approach (ii) Flexible foundation approach

Rigid foundation approach

The following assumptions are made when using a rigid foundation approach:

(a) The raft is stiff compared to the subsoil; its flexural displacement does not affect the contact pressure.

(b) The contact pressure is dispersed over a plane surface so that its centroid lies along the line of the action of the combined force of all loads acting on the raft.

Flexible foundation approach

According to the soil conditions, the raft's flexibility is considered to disperse the stress in the vicinity of the column. In this approach, differential settlements are substantial, but the raft is subjected to relatively low bending moments and shear stresses. Two theories are typically used for analysis.

(a) Hetenyi's theory (Hetenyi, 1946) states that an elastic foundation supports a flexible plate.
(b) A foundation supported by an elastic spring bed that is uniformly spaced, with a spring constant calculated using the co-efficient of sub-grade reaction, based on the Winkler model (Winkler, 1867). Simple problems can be solved manually based on these methods, but this has obvious limitations and several drawbacks.

1.2.1.2 Numerical Methods

Different numerical techniques like finite difference and finite element are used to analyze rectangular raft foundations.

Finite Difference Method (FDM)

The solution of the governing differential equations in finite difference form with suitable boundary conditions is the fundamental tenet of the finite difference technique. The process is then reduced to solving several simultaneous equations. The raft (seen as a thin plate) is often divided into square grids, and the soil is treated as a Winkler foundation. The differential equations for the plate's deflection are then produced in finite difference forms and computer-solved. The method for plates on a two-parameter elastic media can be expanded from that used for finite plates on the Winkler foundation. Finite difference analysis was used by (Pickett and McCormick, 1951) and (Janes, 1962) to examine rectangular plates on isotropic elastic half-space. (Straughan, 1990) studied a thin plate resting on a flexible foundation using the modified Vlasov model using FDM.

Finite Element Method (FEM)

(Buczkowski and Torbacki, 2001) developed an 18-node isoparametric interface element of zero-thickness that accounts for the shear deformation of the plate; details analyzed thick plates resting on a two-parameter elastic foundation.(Celik and Saygun, 1999a) developed a finite element formulation for plates on a flexible foundation incorporating the shear deformations in the plate's behaviour. The subsoil's effect combines the soil's elastic bending and shear deformation. (Daloglu and Ozgan, 2004) developed an iterative method to determine the subsoil depth affected by the load on the plate resting on an elastic foundation using stress distribution within the subsoil depending on the loading and dimension of the plate. (Kant, 1982) investigates the bending behaviour of a rectangular plate based on a higher-order displacement model and the three-dimensional Hooke's laws. The effects of transverse shear stresses on thick Mindlin plates with four and eight nodes resting on an elastic foundation were investigated by (Özgan and Daloğlu, 2008) using the modified Vlasov model. The modified Vlasov model and the finite element method were used by (Hamarat et al., 2012) to study the seismic behavior of a 3-D frame superstructure and a mat foundation resting on an elastic foundation. (Turhan, 1992) studied a thin plate resting on an elastic foundation using the modified Vlasov model using FEM. (Ozgan and Daloglu, 2007) developed an alternative plate element to analyze thick plates on the Winkler foundation. (Buczkowski and Torbacki, 2010) developed the finite element technique that accounts for soil material properties and incorporates the surrounding effect outside the plate. (Buczkowski et al., 2015) Employed a mixed first-order 16-node locking-free Mindlin plate resting on a two-parameter elastic foundation to analyse plates on elastic foundations. Using the modified Vlasov model , (Dutta et al., 2021) developed a second -order continuous rectangular plate bending element resting on a flexible foundation. The finite element method may be regarded as a generalization of standard structural analysis procedures and, in particular, the displacement method of analysis, which permits the evaluation of stresses and strains in two- and three-dimensional structures such as elastic continua, plates, shells and other complex structures. The critical distinction between the conventional methods of structural analysis and finite element technique is that the latter utilizes two- or three-dimensional structural elements to represent the elastic continuum. Using such elements the structural idealization is obtained merely by division of the original continuum region into segments of appropriate size and shape with all properties of the original system being retained in the individual elemental region. The earliest application of finite element method to the analysis of plates on elastic foundation is due to (Cheung and Zienkiewicz, 1965), assuming the soil to be a Winkler media. (Cheung and Nag, 1968) treated the soil to be isotropic elastic half-space. Later different researchers used different elemental idealization to solve the plate on elastic medium problem. (Fraser and Wardle, 1976) used the technique to a multi-layered soil system. (Rajapakse and Selvadurai, 1986) provided a brief literature review on the application of finite element technique in the interaction analysis of rectangular plates on elastic continuum. Generally the analysis is restricted to surface plate analysis, though practically, they are placed at some depth.

1.2.2 Circular Raft Foundations

Circular rafts are frequently employed for the foundations of industrial process towers and chimneys. Silos and other similar superstructures may also utilize them. According to the methodologies for finding solutions, the study of circular plates on elastic foundations can be roughly divided into the following categories.

(a) Closed-form solutions, (b) Numerical Methods

1.2.2.1 Closed-form solutions

There aren't many closed-form solutions for a circular plate on an elastic continuum (Borowicka, 1936), (Ishkova, 1947). The authors believed the traditional thin plate theory could accurately depict the plate's flexure. (Brown, 1969b; Brown, 1969a; Brown, 1974) studied the circular raft issues in homogeneous and non-homogeneous half-spaces with uniformly distributed stresses. (Hemsley, 1987) examined how an elastic circular raft would flex under various ground support configurations; the loading was either a uniform pressure load or a peripheral line load.

1.2.2.2 Numerical Methods

The analysis of a circular plate resting on an elastic foundation also uses many numerical approaches, including boundary element, finite element, and finite difference methods.

Boundary Element Method (BEM)

Considering the boundary element modelling for plates on elastic half-space, (Syngellakis and Bai, 1993) discussed applying the boundary element method to thin plates on the Boussinesq half-space. (Xiao, 2001) analyzed thick plates on elastic half-space using a unique, indirect boundary integral formulation form. In his analysis, results regarding two Hu functions (Hu, 1982) are obtained without reference to physical variables. (Weeën, 1982) derived a BEM for plate bending problems based on the shear deformable plate theory according to (Reissner, 1947). The formulation of (Xiao, 2001) produces hyper-singular kernels in the integral equations. (Mostafa Shaaban and Rashed, 2013) presents a new practical technique of using the Boundary Element Method (BEM) to solve plates on elastic half-space. The considered BEM is based on the formulation of (Weeën, 1982) for the shear deformable plate bending theory. A detailed study has been done by (Mandal and Ghosh, 1999) to predict the elastic settlement of rectangular raft foundations using a hybrid approach (FEM-BEM). A detailed study has been done by (Mandal and Roy, 2015) to predict the elastic settlement of rectangular piled raft foundation foundations using a hybrid FE-BE approach.

Finite Difference Method(FDM)

The circular plate problem has been studied by (Pickett and McCormick, 1951) and (Pickett et al., 1951) for the case of elastic half-space and elastic layer under a general non-symmetrical external stress. The method was also applied (Melerski, 1997) to simulate the elastic interaction of circular rafts with cross-anisotropic fluids.

Finite Element Method (FEM)

For the analysis of circular plates that are axisymmetrically loaded and supported by elastic foundations, (Utku et al., 2000) provide a 'mixed formulation' of both flexibility and stiffness terms generated from the standard plate theory equations for annular plates. (El-Zafrany and

Fadhil, 1996) They have analyzed thin plates resting on a two-parameter elastic foundation using the boundary element method. Finite grid solutions for circular plates on elastic foundations were created by (Karaşin et al., 2015). Using modified Vlasov models, designers have explored the flexural behaviour of uniformly loaded circular plates on elastic soil. Using modified Vlasov models, (Yue et al., 2020; Yue et al., 2019)investigated the bending analysis of thin circular plates supported by elastic foundations. (Vallabhan and Das, 1991b)An analytical method is suggested that produces a much stiffer response than FEA when the soil's Poisson ratio approaches 0.5. (Gunerathne et al., 2018)analyzed edge-to-centre tank settlement on elastic soil. (Gunerathne et al., 2019)consider numerous soil layers with varied characteristics and thicknesses and analyze the effect of soil layering circumstances on the flexural behaviour of big circular plates. (Elhuni et al., 2019) developed a continuum-based model to predict the flexural behaviour of a circular tank on an elastic foundation in polar coordinates.The analysis of circular raft by finite element technique is presented by (Hooper, 1974; Hooper, 1975) for distributed loading case (uniform or parabolic) by modeling the raft-soil system in axisymmetric finite elements. (Hooper and West, 1983) solved the circular raft problems on yielding soil by assuming Boussinesq type stress distribution for the soil. (Melerski, 1997) represented the plate by an assemblage of concentric ring elements and (Koning, 1997) 's solution to obtain the soil stiffness.

1.2.3 Dynamic response of raft foundations

Using the modified Vlasov model by finite element approach, (Hamarat et al., 2012) analyze the seismic behaviour of a 3-D frame superstructure and a mat foundation resting on an elastic basis. The mixed first-order transverse 16-node locking-free Mindlin plate resting on a two-parameter elastic foundation was used to obtain the natural frequencies of the plate by solving the eigenvalue problem (Buczkowski et al., 2015). Exact solutions were developed for the frequency analysis of rectangular Mindlin plates under in-plane loads resting on the elastic foundation of Pasternak by (Akhavan et al., 2009). Free vibration analysis of a dowelled rectangular isotropic thin plate on a Modified Vlasov foundation using the discrete singular convolution method was described in detail (Gibigaye et al., 2018). Using a modified Vlasov model using FEM (Turhan, 1992) analyzed in depth a thin plate lying on an elastic foundation. An updated Vlasov model using FDM (Straughan, 1990) analyzed a thin plate on an elastic foundation in depth. The dynamic response of Foundations on single and two-parameter media was investigated by (Mar et al., 1991). Using the modified Vlasov model, (Özgan and Daloğlu, 2008) examine the effect of transverse shear strains on thin and thick four-nodded and eight-nodded Mindlin plates lying on an elastic foundation.

A continuum-based model was created by (Elhuni et al., 2019) to forecast the flexural behaviour of an elastic soil layer supporting a circular tank foundation. The authors present the coupling problem for the traditional theory of plates on an elastic axis-symmetric circular foundation by considering the soil-structure system's horizontal and vertical displacement in the polar coordinate system. The issue of vibrations of circular plates resting on a Winkler foundation and elastically constrained against rotation and translation is addressed by (Rao and Rao, 2013). (Narita, 1985) investigated free elliptical plates comprehensively using the Ritz approach. The trial functions were performed using a power series. There were multiple elliptical plates with different ellipticities, and the first five frequency parameters were presented for each. (Kim and Dickinson, 1989)presented approximate natural frequencies and frequency characteristics for fully clamped and simply supported circular plates for completely free circular plates. (Gupta and Bhardwaj, 2004) investigated how an elastic foundation and a parabolic thickness variation affected the vibration of elliptical plates. Their study looked at the frequency and mode shapes of the first four vibration modes for different aspect ratios, taper, orthotropic, and foundation parameter values for free plates, simply supported and clamped edges.

The governing equations of an elastic circular plate on a tensionless foundation are obtained and numerically solved by (Guler and Celep, 1995a) to investigate the impact of the foundation's tensionless nature on the foundation and the plate's static and dynamic behaviours. On the opening page of (Leissa, 1993)., the vibration of a plate supported laterally by an elastic foundation was explored. Leissa reasoned that a full (Winkler) foundation simply results in a continual increase in the plate's squared natural frequency. (Salari et al., 1987)Also predicted this. (Laura et al., 1995) studied the vibration of a plate resting on an elastic foundation, in which a natural frequency connection is no longer valid. (Wang, 2005) studies have various goals. First, they'll calculate exact frequency determinants to validate and extend Laura's approximations for clamped and simply supported plates. Second, they analyze plates with free and moving edges. Past authors' assumptions of a fundamental axisymmetric mode may be erroneous. It shall be demonstrated. Using a variational formulation, (Ascione and

Grimaldi, 1984)investigated unilateral frictionless contact between a circular plate and a Winkler foundation. (Leissa, 1993) provided one of the early treatments of this issue by tabulating data for the frequency parameter for four vibration modes of a circular plate that was simply supported and had changing rotational stiffness. A circular plate on the Winkler foundation underwent a significant deflection (Zheng and Zhou, 1988). The axisymmetric dynamic response of a circular plate on an elastic foundation was investigated by (Ghosh, 1997a). Circular plates on an elastic foundation subjected to dynamic stresses are the subject of a dynamic analysis by (Wu and Lee, 2003) utilizing the Extended Finite Hankel Transform (EFHT) method. The terms of the spatial and time functions are first treated independently and then combined in the problem. The process of the spatial functions is carried out using BEM. (Sharma and Shivani, 2011), Their paper employed the differential quadrature method (DQM) for free vibration analysis of a circular plate of parabolically varying thickness resting on the Pasternak foundation. Using the three-dimensional elasticity theory and the improved Fourier series method, (Liu et al., 2016) investigated the free vibration of the thick annular sector plate on the Pasternak foundation with general boundary conditions. Four nodded sixteen degrees of freedom factor was considered by (Bogner et al., 1966) by adding one additional degree of freedom to every node.

The dynamic response of raft foundations is mainly restricted to the response analysis of different types of plates on elastic foundations with various boundary conditions. In most analyses, the foundation medium is in the form of a Winkler or a two-parameter soil. However, the parametric study on the dynamic response is limited.

Regarding the dynamic interaction analysis of the flexible rectangular foundation, pioneering work has been done by (Savidis and Richter, 1979), (Iguchi and Luco, 1981) and (Whittaker and Christiano, 1982). (Krenk and Schimdt, 1981) Using a direct method, they solved the axisymmetric problem of a vibrating circular plate on an elastic half-space. Different numerical techniques (FDM, FEM, and BEM) are used for the dynamic response analysis of plates on elastic foundations having different boundary conditions.

1.3 The objective of the present investigation

The present investigation aims to

- Develop a workable approach for analyzing thin to thick plates/rafts or slabs on elastic foundations based on a two-parameter model (modified Vlasov model).
- Suggest a unified solution technique for the response analysis of various plates or raft foundations under different static and dynamic loading types.
- Solve representative problems using realistic parameters to demonstrate the effectiveness and utility of the solution technique for the plate foundations' response analysis.
- Provide the designer realistic design parameters for the plate's design or, more specifically, reinforced concrete slabs, which may be easily handled using the adopted computational techniques.

1.4 Scope of the present study

Given the review of the literature outlined above, the scope of the present investigation is divided into the following steps:

Static response:

- Suggesting a unified approach for analyzing different types of raft/plate foundations, incorporating the effect of continuity and the semi-infinite character of the soil medium in the formulation. For this, FEM is best suited in which the semi-infinite soil domain is represented by Vlasov and Leont'ev model;
- The combined stiffness matrix of the soil plate system is obtained from the subsoil's stiffness matrix and the plate stiffness matrix, with compatible interface conditions.
- Incorporating the effect of higher-order shear deformation and the normal strain on response analysis.
- Study the effect of different parameters, such as thickness, shape, modulus of elasticity, Poisson's ratio of the raft and modulus of elasticity, Poisson's ratio and depth of the rigid base of the soil media, on the response of different raft foundations.

Dynamic response:

- Evaluation of natural frequencies of raft foundations of different shapes (rectangular, skew, circular and annular).
- Study the influence of different raft and half-space parameters on the natural frequencies.
- Incorporating the effect of higher-order shear deformation and the normal strain on vibration analysis.
- Study the effect of different parameters, such as thickness, shape, modulus of elasticity and Poisson's ratio of the raft and the soil media, on the response of different raft foundations.

1.5 Selection of the model and the computational technique

1.5.1 Winkler model

The Winkler model has been used for everyday design by practising engineers because of its simplicity. This model is developed on the assumption that the reaction forces per unit area at each point of the foundation are proportional to the deflection of the foundation itself. The vertical deformation characteristics of the foundation are defined by identical, independent, closely spaced, discrete and linearly elastic springs known as the modulus of sub-grade reaction, K (Hetenyi, 1946).

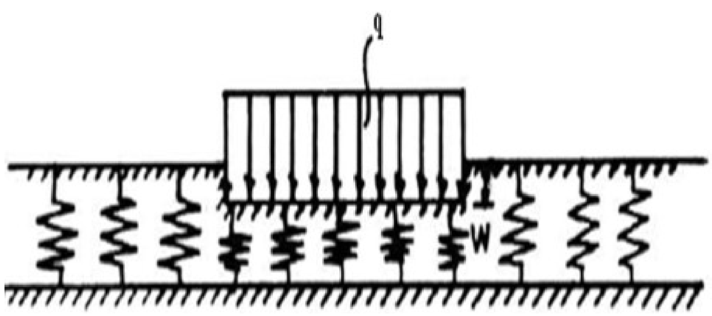

Fig. 1.1 Winkler foundations

In the Winkler model, the relationship between the external pressure and the deflection of the foundation surface under pressure is expressed as $q = Kw$ (Fig. 1.1) where w, the vertical displacement of the soil, is proportional to the contact pressure, q, at that point. The proportionality constant, K, is called “the modulus of sub-grade reaction" of the soil.

Where w is the plate's vertical displacement, i.e., displacement in the vertical z-direction, and q is the applied distributed load. The foundation parameter modulus of subgrade reaction can be evaluated from typical plate load tests. The modulus of sub-grade reaction (Ks) thus obtained is valid for 0.3 m wide footing. Corrections need to be applied to larger footings used for structures. A simple correction for a (B m × B m) square footing in a homogeneous cohesive soil with uniform elastic modulus, the modulus of sub-grade reaction can be estimated (Terzaghi, 1955) as K = Ks (0.3/ B) and in cohesionless soils, K = Ks [(B + 0.3)/ 2B]^2 and for the rectangular foundation of B × L, K = $K_{B \times B}$(1+B/L)/1.5 where $K_{B \times B}$ is the modulus of sub-grade reaction for square footing with dimensions B × B. According to (Bowles, 1996), if q is the bearing capacity causing a settlement of 25 mm, then K = 40qF where q is the allowable bearing pressure and F is the safety factor. The modulus of sub-grade reaction expressed by(Biot, 1937) according to the following relationship $K = \frac{0.95E_s}{b(1-v_s^2)}\left(\frac{E_s b^4}{EI(1-v_s^2)}\right)^{0.108}$.According to (Vesić, 1961), the modulus of sub-grade $K = \frac{0.65E_s}{b(1-v_s^2)}\sqrt[12]{\frac{E_s b^4}{EI}}$ where EI is the foundation flexural rigidity and b is the width of the foundation. According to (Galin, 1943) $K = \frac{\pi E_s}{2b(1-v_s^2)\log\left(\frac{L}{b}\right)}$ where L is the length of beam/footing/plate/foundation and (Lenczner, 1962) proposed $K = \frac{2E_s}{b\log\left[1+2\frac{H}{b}\right]}$ where H is the thickness of the soil layer.

1.5.2 Pasternak model

Attaching the spring ends to a plate that solely experiences transverse shear deformation, the spring components' existence in shear contact is assumed in this model. The vertical equilibrium of a shear plate is considered to get the load-deflection relation. $p = Kw - 2t\nabla^2 w$ (Fig. 1.2) gives the pressure-deflection relationship, where 2t denotes the shear modulus of the shear layer, and K denotes the vertical spring constant.

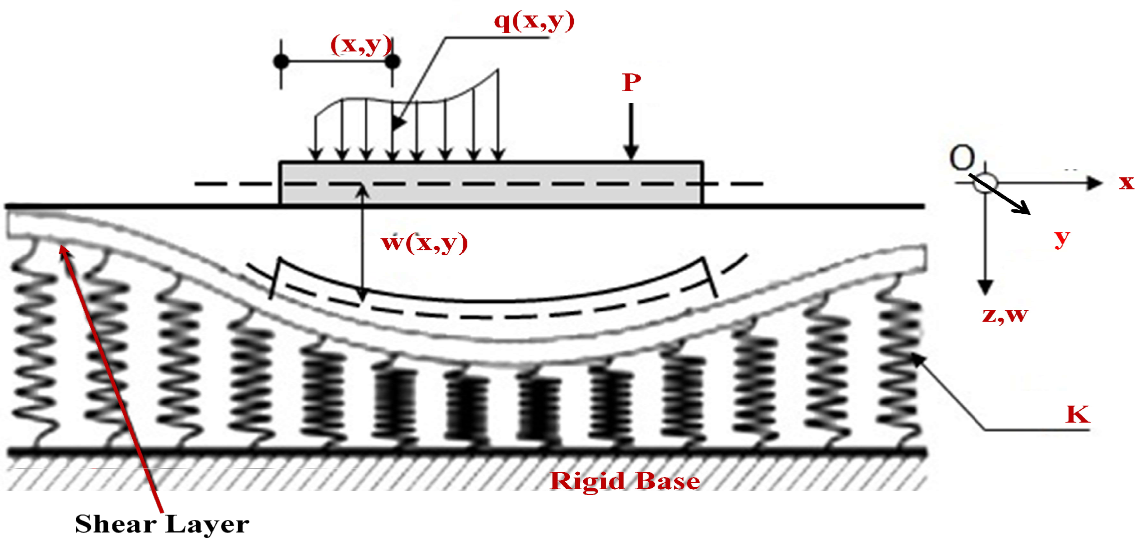

Fig. 1.2 (a) Pasternak foundations

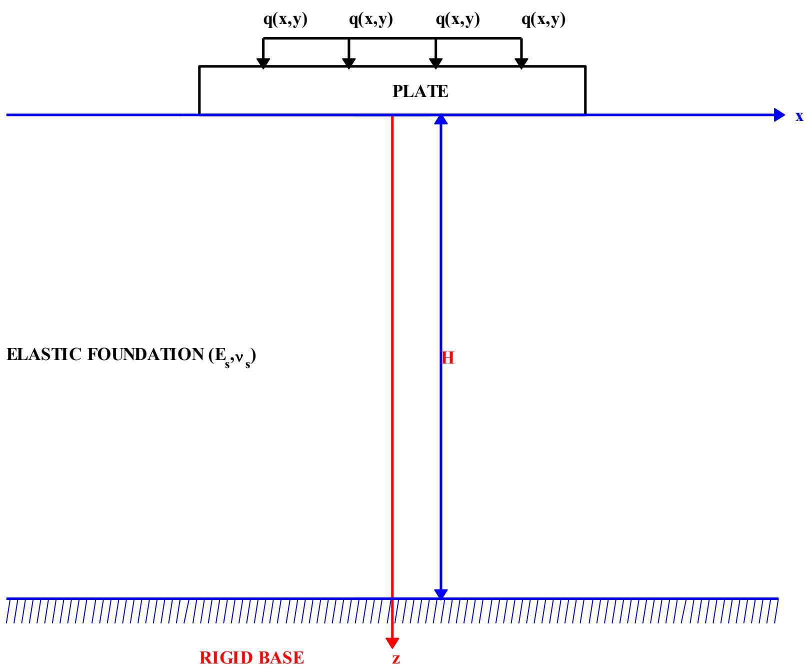

Fig. 1.2 (b) Pasternak foundations

The shear layer, thus, determines the consistency of this model. The vertical spring constant, K, and the shear parameter, 2t, which interacts with the vertical springs, are the two parameters that make up this two-parameter model. The (Selvaduari, 1979)method can calculate the parameters K and 2t values.

$K = \frac{E_s(1-v_s)}{H(1+v_s)(1-2v_s)}$ and $2t = \frac{E_s H}{6(1+v_s)}$. E_s, v_s - Young's modulus of elasticity and Poisson's ratio of the soil and according to Boussinesq's technique, H is the soil thickness corresponding to the end of the effect zone for the foundation. H = 2B, where B is a rectangular plate's width, and B is a circular plate's diameter.

1.5.3 Vlasov model

Adding a third parameter, γ, to describe the vertical deformation profile within the soil continuum (Selvaduari, 1979; Vlasov and Leont'ev, 1966) created a novel concept of the two-parameter model that has the advantage of determining soil parameters and dynamically activated mass depending on soil material properties, modulus of elasticity and Poisson's ratio (E_s, v_s), and the thickness of the subsoil (H). By utilizing an iterative process, (Vallabhan and Das, 1988) identified the parameter γ (Fig. 1.3) as a function of the foundational and structural characteristics and gave this model the name "modified Vlasov model." The parameters rely on the structure, the rigid base's depth, the soil's characteristics, and the kind and amount of loads.

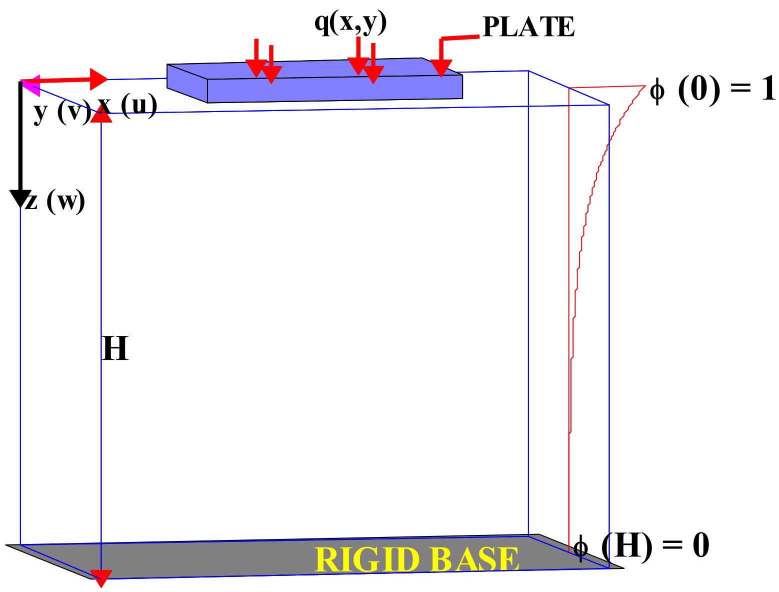

Fig. 1.3 Finite plates resting on two-parameter Elastic foundations

The solution of a plate on an elastic foundation is a statically indeterminate mechanics problem. A theoretical approach cannot solve most issues because the solution is very complicated. In solving this type of problem, one can use numerical methods. One of the most important goals of this work is to develop a realistic procedure for the response analysis of plates that will help practising engineers in the future. Most structural plates have holes and irregular geometries rather than ordinary rectangular shapes.

Moreover, the loading on the plate is entirely arbitrary. Therefore, selecting a finite-element model for the plate is considered efficient in accounting for different plate geometries, loading cases, and boundary conditions. However, based on practical considerations, the computer code developed here is limited to finite rectangular elements.

The values of the modulus of the sub-grade reaction, K, and the shear parameter, 2t, are computed within the computer program using the soil properties, etc.

A computer program is developed to solve some realistic cases of the loaded plate on elastic foundations to determine the dynamic response like displacements, velocity and acceleration. Where possible, a comparison is made between the results obtained by other researchers and the analytical method.

A few particular impediments to the traditional solution are introduced below (Hetenyi, 1950):

It is hard to expel soil impact when balance tends to isolate from the soil.

It is hard to apply different sorts of loads to a footing.

It is hard to change the cross area of the base.

It is hard to consider changes in sub-grade response along the foundation.

Consequently, numerical examinations of a plate laying on a flexible foundation appear in full detail, and viewpoints displaying (e.g., discretization reliance) will be discussed. Then, the after-effects of the numerical investigations are contrasted as the consequence of the general solution.

1.6 Application of Finite Element Method (FEM)

The finite element method was chosen as the numerical method to represent the behaviour of the plates in this work. Due to alternative numerical approaches, the finite difference method is reasonably practical for simple rectangular geometry. Still, its development becomes rather onerous when the rectangle has a hole or has been cut out. The benefit of using the finite element approach to analyze plates is that irregular geometry, generic loading, and arbitrary boundary conditions can all be applied relatively quickly. However, this study only uses specific rectangular, skew and solid circular finite elements.

This study suggests that the soil's material qualities, such as linear elasticity, homogeneity, and isotropy, be simplified. In addition, the model can be changed to consider the soil's time-dependent behaviour.

The present study uses a workable approach for analyzing a transversely loaded thin plate on a two-parameter elastic foundation using a modified Vlasov model, and second-order (C^2) compatible plate bending elements based on Kirchhoff's theory are attempted. The two soil parameters for the Vlasov foundation evaluation, the soil's modulus of elasticity and Poisson ratio are assumed to be constant from the top surface to the top of the rigid bottom base. The finite element method is used, and all the deformation stiffness matrices of plate and subsoil have been developed.

A Matlab code is written for the present formulation. Thus, the results are compared with similar studies by other researchers, showing excellent conformity.

It is concluded that the present approach is simple, effective and more reliable for static analysis of plates on two-parameter Vlasov foundations. Moreover, the convergence rate is a very high, straightforward method for getting stress results and takes less computational effort, resources and time.

A nine-nodded (PBQ9) Lagrange family plate bending element based on higher-order shear deformation theory incorporates the effects of normal strain adopted for static analysis of a thick plate resting on an elastic foundation using the modified Vlasov model. The formulations of the problem take into account the transverse shear strains and parabolic variation of normal strain through the thickness of the plate; hence, three-dimensional stress-strain relationships are utilized. The finite element method evaluates all the deformation stiffness matrices of plate and subsoil. Higher-order shear deformation theories (HSDTs) account for the shear deformation effects and overcome the use of fictitious shear correction factors. A Matlab code is written, and a convergence study is carried out. The results thus obtained are compared with the available results obtained by other researchers, showing excellent agreement. The central deflection and bending moment have been obtained parametrically for the different aspect ratios and foundation coefficients. The present formulation is completely lock-free and fits effectively into the analysis of thin to thick rectangular plates on elastic foundations using the modified Vlasov model with a reasonable convergence rate and accuracy.

1.7 Final Selection of the model and the computational technique

As can be determined from the previous emphasis, model selection is the most crucial step. The Vlasov and Leont'ev model, strengthened by Jones and Xenophontos and subsequently improved by Vallabhan and Das (three-parameter model), is used in this research. As mentioned earlier, this model considers shear strain in the soil stratum and results in a "dish-shaped" plate deformation profile. Refer to Figure 1.3. It also eliminates the necessity of attempting to determine values for the modulus of the subgrade reaction, K, or the shear parameter, t.

While the minimization of the required amount of data concerning the soil material properties and constitutive relationships is a definite goal of this research, a more overriding goal was the importance of constructing a realistic model. Chapter 3 presents the development of the theories and principles involved in utilizing this modelling approach.

One of the primary goals of the research is to develop a realistic procedure for the analysis of plates on an elastic foundation and a practical and easily applied procedure. The solution to this type of soil engineering problem, which involves equilibrium equations, constitutive relations, compatibility considerations, and complex boundary conditions, would require such an effort that a purely mathematical approach is impractical. An alternative approach is to use a numerical analysis technique that will provide approximate solutions close to the exact solutions required for practical engineering design problems.

To help ensure the acceptance of the method by practising engineers in small, medium, and large engineering offices, selecting a method that is at least within the storage capacity of microcomputers is essential. The computational method used in this research applies to the analysis of "thin to thick" plates, which experience minor to large deflections. Chapter 4 presents a detailed explanation of the application of the Finite-Element Method (FEM) to the analysis of plates on an elastic foundation as used in this research.

1.8 The organization of the Thesis

Five chapters make up the thesis. Chapter 1 introduces the problem being addressed and the overall approach to resolving it. In Chapter 2, the scope of the current inquiry is described together with an overview of the pertinent literature. In Chapter 3, the theoretical concepts are presented. The Finite Element Formulation (FEM) of plate/raft foundations of various shapes under static and dynamic loading are presented in Chapter 4. The results of the response analysis of plate/raft foundations of various shapes under static loading are presented in Chapter 5. This chapter also discusses the parametric effects on the natural frequency of the rafts and the results of the free vibration analysis of various raft foundations. Finally, concluding observations on the current investigation and the potential for additional research are included in Chapter 6.

Chapter 2
Literature Review

2.1 General

Raft foundations are generally used as foundation systems for constructing water tanks, multi-story buildings, and other heavily loaded structures. According to the requirement, rafts of different shapes are used. Rectangular, circular, and annular rafts are the most popular shapes. Various static and dynamic loads are applied on raft foundations.

Finite plates on an elastic medium with all their edges free are equivalent to plate/raft or mat foundations. Both continuity conditions at the plate-soil interface and the boundary conditions at the plate's borders shall be considered when analyzing finite plates. The following considerations shall be considered when solving the plate-soil interaction problem.

(i) Plate Shape: Typically, square or rectangular, circular, and annular finite plates are considered. In some situations, the plate can also be regarded as a semi-infinite strip with a finite width.

(ii) The type of soil media: Winkler, two-parameter, or elastic solid medium are considered as the supporting soil medium.

(iii) Boundary conditions: The boundary conditions at a plate's edge can be either fixed, simply supported, free, or elastically constrained against displacement and rotation.

(iv) External loading: Loading may be concentrated, uniformly distributed, or varying loads.

Several solution techniques are used depending on the problem at hand. The gradual evolution in the research of plates on elastic foundation problems highlighting pertinent literature is examined chronologically. A critical review outlines the focus of the current study at the end of this chapter.

2.2 Response under static loading

The pertinent literature is reviewed to explore the various solutions for the response analysis of plates on elastic foundations under static loads. In addition, studies on rectangular, skew, circular, and annular plates are reviewed to emphasize the variations in the approaches used.

2.2.1 Rectangular plates on elastic foundation

The problem of a rectangular plate on an elastic foundation has received the attention of researchers for several decades.

The single-parameter Winkler model is used to assess plates on elastic foundations, which neglects the shear deformations between the elastic springs that are closely spaced. The sub-grade response is a complex mathematical phenomenon that arises from the mechanical modelling of plate-subsoil interaction difficulties. The model by (Winkler, 1867) is predicated on the notion that each foundation point's reaction forces per unit area correspond to the foundation's deflection. The Winkler model has a problem in that it cannot account for the effect of loading outside the structure where soil displacement also occurs - by including a second medium that interacts with the Winkler's spring (Hetenyi, 1950; Filonenko-Borodich, 1940; Pasternak, 1954) developed two-parameter foundation models to address the shortcomings of the Winkler model.

The two-parameter model, developed by (Selvaduari, 1979; Vlasov and Leont'ev, 1966), have the advantage of allowing soil parameters to be determined based on the properties of the soil material, the Poisson's ratio and the modulus of elasticity, as well as the thickness of the subsoil (H).

By incorporating an arbitrary parameter, γ, to characterise the vertical deformation profile within the soil continuum, Vlasov and Leont'ev constructed a two-parameter model that has the benefit of calculating soil characteristics depending on soil material attributes and the thickness of the subsoil (Selvaduari, 1979). However, the γ parameter needs to be estimated for the Vlasov model. (Vallabhan and Das, 1991c) used an iterative process to determine the γ parameter as a function of the foundation's and structure's properties. They referred to this model as the "modified Vlasov model" and stressed that the parameters depend on the structure's and soil's characteristics, the kind and level of loading, and soil depth. (Mishra and Chakrabarti, 1997) Investigated the behaviour of rectangular plates supported by tensionless elastic foundations under shear and contact by finite element method. They developed a nine-noded Mindlin plate element to consider transverse shear effects. (Kant, 1982) examined the bending behaviour of a rectangular plate based on the three-dimensional Hooke's equations and a higher-order displacement model. (Dutta et al., 2021) studied a rectangular plate bending element with second-order continuity resting on an elastic foundation using a modified Vlasov model. Functionally graded thick plates resting on elastic foundations of the Pasternak type were examined by (Benyoucef et al., 2010). The Winkler-Pasternak foundation (CİVALEK, 2008) analyzes the bending behaviour of shear deformable rectangular plates. Radial basis functions were used by (Ferreira et al., 2010) to examine plates on Pasternak foundations. Mindlin plates on the Winkler foundation were studied by (Kobayashi and Sonoda, 1989). The elastic bending, buckling, and vibration problem of Levyplates on a two-parameter foundation were investigated by (Lam et al., 2000) by using Green's functions. Hybrid Trefftz finite elements were used by (Qin, 1994; Oin, 1995) to analyze the plate bending issue on an elastic foundation.The plate bending problem on a flexible foundation was examined by (Rouzegar and Sharifpoor, 2015) using a two-variable improved plate theory. (Vallabhan and Das, 1988) developed the modified Vlasov model; they estimated the parameter as a function of the foundation's properties and the structure's characteristics using an iterative process. The parameters are determined by the depth of the rigid base, the type of structure, the type and amount of loads, and the soil's characteristics. (Buczkowski and Torbacki, 2001) constructed an 18-node, zero-thickness isoparametric interface element to account for the plate's shear deformation. Their specific investigation concentrated on thick plates resting on a two-parameter foundation. A finite element formulation for plates on a flexible foundation was developed by (Celik and Saygun, 1999a) including shear deformations of the plates. (Daloglu and Ozgan, 2004) developed an iterative method to determine the subsurface's depth influenced by the plate's load resting on an elastic foundation by viewing the action of the subsoil as a synthesis of soil shear deformation and elastic bending. The effects of transverse shear strains on thin and thick four-noded and eight-noded Mindlin plates resting on an elastic foundation were examined by (Özgan and Daloğlu, 2008) using the modified Vlasov model. (Hamarat et al., 2012) analyze the seismic behaviour of a 3-D frame superstructure and a mat foundation resting on an elastic foundation using the modified Vlasov model and the finite element method.A detail study has been done by (Mandal and Ghosh, 1999) to predict the elastic settlement of rectangular raft foundation using a hybrid approach (FEM-BEM). Using a modified Vlasov model using FEM, (Turhan, 1992) analyzed in depth a thin plate lying on an elastic foundation. Using an updated Vlasov model using FDM, (Straughan, 1990) analyzed in depth a thin plate resting on an elastic foundation. A detail study has been done by (Mandal and Roy, 1996) to predict the elastic settlement of rectangular piled raft foundation foundation using a hybrid FE-BE approach. The finite element technique was used by (Buczkowski and Torbacki, 2010) by integrating the surrounding effect outside the plate and the material properties of soil. Using the modified Vlasov model by finite element approach, the mixed first-order transverse 16-node locking-free Mindlin plate resting on a two-parameter elastic foundation was used to study the bending of a thick plate by (Buczkowski et al., 2015). Plates on a two-parameter elastic foundation with various edge boundary conditions have been studied by (Katsikadelis and Kallivokas, 1986; Katsikadelis and Kallivokas, 1988) using the boundary integral equation (BIE) method and numerical assessment of the boundary integral equations. The numerical outcomes thus acquired are contrasted with those that can be gleaned from analytical outcomes.

The two-parameter model developed by (Vlasov and Leont'ev, 1966) was improved by (Vallabhan and Das, 1991c), utilising three parameters relating to the geometry and material properties of the soil continuum for a particular plate and loading. The authors used this model and a numerical model that applied the finite element method to resolve the rectangular, skew, and circular plate problems on a soil medium. The approach makes use of the properties of the soil rather than the soils co-efficient of subgrade reactivity.

For the thin plates supported independently on elastic homogeneous or non-homogeneous foundations, (Sapountazakis and Katsikadelis, 1992) employed the boundary element approach. The independent springs of the subgrade model are placed near each other. Consideration is given to both linear and non-linear variations of the subgrade reaction with deflection. Additionally, the plate and subgrade separate from one another. The linear portion of the controlling differential operator is integrally represented in the solution process, and the loading term includes the unidentified subgrade reaction. The outcomes for square and circular plates that are simply supported and clamped are presented.

For a thick plate of the Reissner type on a two-parameter foundation, (Jianguo et al., 1992) employed the direct boundary integral equation formulation. The auxiliary functions and their derivatives are combined linearly to represent the fundamental solutions of thick plates on a two-parameter foundation. A weighted residual technique is used to formulate the boundary integral equations. The resulting essential solutions are used as the kernel functions.

Numerical results for clamped circular plates and simply supported square plates show the method's precision.

(Caifeng and Hartley, 1994) developed a direct boundary element method to study the interaction between a thin rectangular plate and an elastic half-space foundation. The plate was subjected to the contact pressure at the bottom, and the external loads applied to the top surface. A thin plate boundary integral formulation serves as the foundation for plate bending. The Boussinesq solution is used to represent the dispersed contact pressure. The contact area and the exterior plate border are subject to boundary element discretization. The plate-half-space interface satisfies the compatibility requirements. There is good agreement when square plate numerical findings are compared to published results.

The boundary element equation of the foundation is not explicitly assembled with the finite element equation of the plate in (Feng and Owen, 1996) iterative scheme for the coupled FE/BE analysis of a plate-foundation interaction problem. Instead, an iterative procedure is proposed to obtain the final coupled equation. The plan lessens the need for computer storage and prevents the inaccuracy that the symmetry of the BE equations creates. A numerical example is given to highlight the advantages of the plan. The selection of a free parameter and a matrix in the solution determines how well the suggested method performs overall compared to the traditional direct solution of the unsymmetric equations resulting from the explicit coupling of the FE and BE equations.

To analyse plate-soil interaction problems, (Paiva de and Butterfield, 1997) developed a boundary element technique formulation where the subgrade reaction is considered to fluctuate linearly into triangle surface components. An integral over its borders is created from the integral in the domain of these elements. The outcomes produced by this formulation are contrasted with thin rectangular plate outcomes previously published.

(Rashed et al., 1998) presented an application of the boundary element method to thick plates on the Winkler foundation. The plate behaviour is modelled using the Reissner plate bending theory. Continuous springs describe the Winkler foundation model and are directly included in the governing differential equation. The boundary geometry and unknowns are modelled using quadratic isoparametric boundary elements. Compared to other published results, analytical data, and a 3-D solution, the results for simply supported and free-edge square plates produced using the formulation show good agreement.

2.2.2 Skew plates on elastic foundation

The mechanical modelling of skewed plate-subsoil interaction problems is a complex mathematical phenomenon, and sub-grade response depends upon many factors. (Morley, 1963) has presented a thorough overview of the analytical solution methods on skew plates. (Butalia et al., 1990) Have studied skew plates for various skew angles, stress conditions, and support conditions using the nine-noded Heterosis element. (Sengupta, 1995) used the specific three-noded element to investigate the performance of skew plates. Two more elements, element A and element B, developed by (Sengupta, 1991; Sengupta, 1993), are used to compare the outcomes. (Srinivasa et al., 2018) Investigated the bending behaviour of simply supported skew plates. Liew (Liew and Han, 1997) present the differential quadrature-based bending analysis of a thick, simply supported skew plate. A few researchers have addressed skewed plates on an elastic foundation because of their mathematical complexity. (Chun and Lim, 2011) investigated the behaviour of isotropic and orthotropic thick skewed plates on elastic foundations. (Chun and Ohga, 2012) Examined the analytical method to predict the bending behaviour of skewed thick plates on the Winkler foundation in detail. (Xenalevina Sidara and Maknun, 2020) studied the convergence behaviour of DKMQ elements in functionally graded skew plates (Joodaky and Joodaky, 2015) and developed semi-analytical solutions to study the behaviour of skew plates on Pasternak and Winkler foundations. Four noded sixteen degrees of freedom were considered by (Bogner et al., 1966) by adding one additional degree of freedom to every node. To the authors' knowledge, skew plates on elastic foundations with concentrated loads are still unavailable in the literature.

2.2.3 Circular plates on elastic foundation

(Buczkowski and Torbacki, 2001) presented an analytical approach to the analysis of the problem of a circular plate resting on a two-parameter elastic foundation subjected to various loadings and boundary conditions. (Celep, 1988; Celep and Turhan, 1990) Have published their assessments of circular plates using the Winkler foundation model. (Guler and Celep, 1995b; Güler and Guler, 2004) Used the Galerkin technique to estimate plate deflection on a two-parameter Pasternak foundation. The study examines the tensionless Pasternak foundation, which lifts plates.

The behaviour of circular plates had been investigated by (Galletly, 1959) to create a more accurate foundation model to fix Winkler's shortcomings. (Jones and Mazumdar, 1980) discussed the behaviour of plates on elastic foundations and the consequences of horizontal friction at the interface, which was examined using a variational technique. (Shukla et al., 2011) Analyze a thin circular elastic plate on a Pasternak foundation using the strain energy method to determine plate deflection and lift-off. (Olson and Lindberg, 1970) Produced two polar plate bending elements. The first element has 9 degrees of freedom (D.O.F.) in a circular plate, and the second has 12 in an annular plate. A continuum-based model was developed by (Elhuni et al., 2019) to forecast the flexural behaviour of a circular tank foundation resting on an elastic soil layer. The authors present the coupling problem for the traditional theory of plates on an elastic axis-symmetric circular foundation by considering the soil-structure system's horizontal and vertical displacement in the polar coordinate system. For studying the elastic behaviour of thin circular plates under various axis-symmetric loading and support conditions, (Melerski, 1989) suggested a variational formulation of the finite-difference approach. (Chandrashekhara and Antony, 1997) proposed a hybrid system that combines finite element and analytical methods to resolve annular slab-soil interaction issues. For the analysis of circular plates that are axisymmetrically loaded and supported by elastic foundations, (Utku et al., 2000) provide a 'mixed formulation' of both flexibility and stiffness terms generated from the standard plate theory equations for annular plates. (El-Zafrany and Fadhil, 1996) Thin plates resting on a two-parameter elastic foundation were analyzed using the boundary element method. Finite grid solutions for circular plates on elastic foundations were developed by (Karaşin et al., 2015). Using modified Vlasov models, designers have explored the flexural behaviour of uniformly loaded circular plates on elastic soil. Using modified Vlasov models, (Yue et al., 2020; Yue et al., 2019) investigated the bending analysis of thin circular plates supported by elastic foundations.

(Vallabhan and Das, 1991b) An analytical method is suggested that produces a much stiffer response than F.E.A. when the soil's Poisson ratio approaches 0.5. (Shi et al., 2014) analyzed edge-to-center tank settlement on elastic soil. (Gunerathne et al., 2019) consider numerous soil layers with varied characteristics and thicknesses and investigate the effect of soil layering circumstances on the flexural behaviour of big circular plates. (Davies et al., 1986) developed a continuum-based model to predict the flexural behaviour of a circular tank on an elastic foundation in polar coordinates.

With a higher-order displacement function considered, the analysis aims to establish an efficient method for determining the static response of a thin circular plate supported by elastic foundations. According to Kirchhoff's theory, a rectangular element needs four degrees of freedom at the right angle corner and at least six degrees at each non-right angle corner for a second-order (C^2) compatible type plate element (Krishnamoorthy, 1987).

2.3 Response under dynamic loading

The plate/raft or mat foundations, subjected to vertical vibrations, have infinite degrees of freedom. Contact pressure distribution under a raft depends on the soil type below and the vibration mode. Suppose the continuous system of the raft foundation is converted to a discrete system. In that case, it results in an eigenvalue problem of algebraic equations, giving the finite number of natural frequencies depending on the order of discretization of the system. The orthogonality of modes applies to both discrete and continuous systems adopted. The solution to this problem involves the study of the plate vibration theory, soil structure interaction and computational methods of vibrations.

Much research has been published on the vibration of plates with various edge conditions. These combinations are free, simply supported, clamped, etc. Compared to these, a few investigations have been undertaken for the dynamic response of completely free plates on elastic foundations, generally used for idealizing raft foundations. The works done on plates on elastic foundations are briefly described below.

2.3.1 Rectangular plates on elastic foundation

(Rajesh and Saheb, 2018) A coupled displacement approach will be used to investigate the free vibration analysis of Mindlin plates resting on the Pasternak basis. (Bahmyari and Rahbar-Ranji, 2012) The element-free Galerkin approach was used to study the vibration analysis of thin plates on Pasternak foundations. (Özgan and Daloğlu, 2015) Analyze the free vibration analysis of thick plates resting on an elastic Winkler foundation in detail. (Özgan and Daloğlu, 2012) Use the Modified Vlasov model with higher-order finite elements to investigate the free vibration study of thick plates resting on elastic foundations. (Özdemir, 2018) The eigenvector and Eigenvalue analysis of thick plates of first-order finite elements standing on elastic foundations are examined. The dynamic response of Foundations on single and two-parameter media was investigated by (Mar et al., 1991). Exact solutions were developed for the frequency analysis of rectangular Mindlin plates under in-plane loads resting on the elastic foundation of Pasternak by (Akhavan et al., 2009). Free vibration analysis of a dowelled rectangular isotropic thin plate on a Modified Vlasov foundation using the discrete singular convolution method was described in detail (Gibigaye et al., 2018). The nonlinear static and dynamic response for a clamped, rectangular composite plate resting on a two-parameter elastic basis was presented by (Chandrasekharappa, 1992). For dynamic analysis, transverse pressure pulse loading is applied to the plate, and the damping parameter is added to account for the damping typically applied to the structure.

The vertical response of flexible rectangular raft foundations under vibratory pressure was measured by (Molla and Ray, 1994). It is believed that the raft is resting on the Winkler medium. An analysis uses the finite element method and eight-noded, isoparametric plate-bending elements.

(Tameroglu, 1996) introduced a method for finding a solution for the free vibration of rectangular plates supported by elastic foundations (Winkler) with clamped boundaries and subject to uniform and continuous unidirectional forces in the mid-plane. The applied technique employs a non-orthogonal series expansion comprising a few carefully selected trigonometric functions for the plate's deflection surface. The fundamental frequency without a foundation is compared, and the results demonstrate good agreement with the widely used solutions.

For the dynamic plate-soil interaction of finite plates on uniform, layered, or Winkler soil, (Auersch, 1996) integrated the finite element and boundary element analysis methods. The compliance functions for a vertical point load and several vibration modes are calculated for a wide range of frequencies and actual plate and soil conditions. According to the data, the soil primarily influences low-frequency responses, whereas structural characteristics are more crucial for higher frequencies.

On an elastic foundation of the Winkler type, (Providakis, 1997) introduced a direct boundary element solution method for the dynamic analysis of thin elastoplastic flexural plates of arbitrary geometry. The technique uses the infinite plate's elastostatic fundamental solution. This generates surface and boundary integrals involving the effects of foundation pressure, plasticity, and inertia. For various edge boundary circumstances, the reaction of a square plate on a Winkler medium under various impact loads is described.

(Omurtag et al., 1997) A mixed finite element formulation based on the Gâteaux differential was used for various edge boundary conditions to perform free vibration analysis on a thin (Kirchoff) rectangular plate on Winkler and Pasternak foundations (for isotropic and orthotropic soil conditions). Concerning plates without foundation, the results agree with the available data. The numerical data presented in the research demonstrates that the orthotropic behaviour of the foundation appears to be less significant than the support conditions, variation in plate thickness, and interaction of the foundation concerning the angular natural frequencies.

2.3.2 Skew plates on elastic foundation

(Hassan and Kurgan, 2020) the extended Kantorovich approach was used to investigate the buckling analysis of thin skew isotropic plates resting on a Pasternak foundation. (Wang and Yuan, 2018) Studied the buckling analysis of thin skew isotropic plates under general in-plane loads by the modified differential quadrature method. A thorough examination of homogeneous and FGM skew plates resting on varied Winkler-Pasternak elastic foundations has been conducted using free vibration analysis by (Ketabdari et al., 2016).

2.3.3 Circular plates on elastic foundation

The issue of vibrations of circular plates resting on a Winkler foundation and elastically constrained against rotation and translation is addressed by (Rao and Rao, 2013). (Narita, 1985) investigated free elliptical plates comprehensively using the Ritz approach. The trial functions were performed using a power series. There were multiple elliptical plates with different ellipticities, and the first five frequency parameters were presented for each. (Kim and Dickinson, 1989) presented approximate natural frequencies and frequency characteristics for fully clamped and simply supported circular plates for completely free circular plates. (Gupta and Bhardwaj, 2004) investigated how an elastic foundation and a parabolic thickness variation affected the vibration of elliptical plates. Their study looked at the frequency and mode shapes of the first four vibration modes for different aspect ratios, taper, orthotropic, and foundation parameter values for free plates, simply supported edges and clamped edges.The governing equations of an elastic circular plate on a tensionless foundation are obtained and numerically solved in (Guler and Celep, 1995a) to investigate the impact of the foundation's tensionless nature on the foundation and the plate's static and dynamic behaviours. On the opening page of Leissa's renowned book (Leissa, 1993)., the vibration of a plate supported laterally by an elastic foundation was explored. Leissa reasoned that a full (Winkler) foundation simply results in a continual increase in the plate's squared natural frequency provided one of the early treatments of this issue by tabulating data for the frequency parameter for four vibration modes of a circular plate that was simply supported and had changing rotational stiffness. (Salari et al., 1987) also predicted this. (Laura et al., 1995) studied the vibration of a plate resting on an elastic foundation, in which a natural frequency connection is no longer valid. (Wang, 2005) studies have various goals. First, they'll calculate exact frequency determinants to validate and extend Laura's approximations for clamped and simply supported plates. Second, they analyze plates with free and moving edges. Past authors' assumptions of a fundamental axisymmetric mode may be erroneous. It shall be demonstrated. Using a variational formulation, (Ascione and Grimaldi, 1984) investigated unilateral frictionless contact between a circular plate and a Winkler foundation. A circular plate lying on the Winkler foundation underwent a significant deflection, which (Zheng and Zhou, 1988) examined. Ghosh investigated the axisymmetric dynamic response of a circular plate on an elastic foundation (Ghosh, 1997a). Circular plates on an elastic foundation subjected to dynamic stresses are the subject of a dynamic analysis by (Wu and Lee, 2003) utilizing the Extended Finite Hankel Transform (EFHT) method. The terms of the spatial and time functions are first treated independently and then combined in the problem. The process of the spatial functions is carried out using BEM. (Sharma and Shivani, 2011), in their paper differential quadrature method (DQM), have been employed for free vibration analysis of circular plates of parabolically varying thickness resting on the Pasternak foundation. Using the three-dimensional elasticity theory and the improved Fourier series method, (Liu et al., 2016) investigated. Circular plates on Winkler, Pasternak, and non-linear Winkler foundations subjected to uniformly distributed step loads are subject to non-linear dynamic responses that are governed by Von Karman partial differential equations, which (Smaill, 1990) reported numerical solutions to. Linear deflection is taken into account to verify the precision of the spatial finite difference representation and the Newmark recurrence technique used to model the time domain. For the purpose of comparing the findings, an accurate linear solution is constructed via model superposition. Both clamped and simply supported immovable edge boundary circumstances are discussed along with the effect of foundation parameters on the centre deflection. It is demonstrated that the foundation's effect causes the centre deflection to decrease as the magnitudes of the parameter values for both boundary conditions increase. It is taken into consideration how plate non-linearity affects the deflection of non-linear Winkler and Pasternak foundations.

Based on the classical theory of plates, (Gupta et al., 1990) addressed the axisymmetric vibrations of a polar orthotropic circular plate with variable thickness (linear and parabolic) sitting on an elastic foundation of Winkler type. The Ritz approach is used to get a rough answer to the issue. For the first three vibrational modes, the frequency characteristics of the plates with varying edge conditions are shown, together with a range of values for the taper parameters, foundation modulus, and rigidity ratio.

Using thick plates of various shapes supported by an elastic foundation of the Winkler type, (Bhattacharya and Banerjee, 1991) detailed an analysis of the non-linear dynamic response. In the inquiry, the conformal mapping approach is used. In-depth research is done on both the case of square plates that are simply supported and square plates with rounded corners.

A parametric analysis of the vertical oscillation of a flexible circular plate on the surface of an elastic half-space and an elastic layered system was provided by (Gucunski and Peek, 1993). Vertical oscillations have been analyzed to estimate the displacement and soil reaction distribution at the soil-plate contact and the impedance functions. The load distributions on the plate and the geometric and material characteristics of a soil system are among the study's parameters. The analysis results demonstrate that its surface layer's characteristics dominate a flexible plate's response. The results also show that a flexible plate behaves very differently from a stiff one.

For the axisymmetric forced and free vibration of simply supported and clamped circular plates on an elastic base, (Ghosh, 1997b) presented an analysis and numerical results. A

Winkler medium represents the elastic basis, while the Poisson-Kirchoff plate theory defines the plate.

2.4 Critical Review

Static reaction

The following important points are observed after reviewing the literature that is currently available on the response analysis of plates on elastic foundations:

The earlier study used the Rayleigh-Ritz method, series solution, and other traditional analytical techniques.

Later, to investigate the reaction of plate foundations, several numerical techniques like FDM, FEM, and BEM were employed.

Different problem-solving methods are often used for various plate foundation types.

Concerning several crucial factors like the impact of stiffness, breadth, etc., the literature on the interaction analysis of ring footings is relatively scant. Investigations are mainly focused on solid foundations.

Most studies only look at surface foundations; they don't detail how embedding affects response.

Although computationally sophisticated, most researchers saw the foundation soil as a Winkler or two-parameter Pasternak soil media, which does not accurately depict the continuum.

Dynamic reaction

Indirect techniques based on the superposition of foundation effects on the natural frequencies of thin plates with different boundary conditions are utilized in the free vibration analysis of raft foundations. Winkler or two-parameter Pasternak type soil media are the principal exceptions to the techniques.

The response of a raft foundation has received little parametric investigation. Non-dimensional frequency domain investigations make up the majority of the studies.

The reaction of various raft foundation types to transient loading is constrained. Investigations are primarily restricted to response analysis of plates on Winkler or two-parameter soils with various edge boundary conditions.

To the author's knowledge, there hasn't been any research on how to model the raft foundations as HSDT elements on the half-space.

Chapter 3
Mathematical Formulation

3.1 Introduction

Response analysis of different raft foundations under static and dynamic loads is carried out, and the theoretical formulation is presented in this Chapter and Finite Element Formulation (FEM) is presented in Chapter 4. It is essential to validate the proposed numerical algorithm and the computer code for accuracy, convergence and efficiency. For this purpose, a wide range of solutions reported in the literature has been considered. The results obtained from the proposed method are compared with the available solutions. Plates on elastic foundations represent a complex soil-structure interaction problem. Developing the equations for such issues and the associated solutions becomes challenging for the engineer. This chapter is devoted to the theoretical development of the equations, and Chapter 4 deals with the numerical techniques employed to arrive at the solutions. Most of the steps during the theoretical development are omitted; however, all the most critical steps are shown so that readers familiar with the Kirchhoff's theory, Mindlin theory and HSDT (Higher-order shear deformation) of plates and variational calculus may easily follow the derivations.

Two fundamentally different methods are employed in solid mechanics to derive the field equations and the boundary conditions for analysing complex structures using the displacement formulation. One technique commonly used involves the assumption of displacement functions and the subsequent development of the equilibrium equations. The other method assumes the displacement functions and applies the minimum potential energy principle. This research is chosen energy principle because it is easier to apply to this complex soil-structure interaction problem.

3.2 Response analysis of rectangular plate/raft on elastic foundations

3.2.1 Development of the theory of the Vlasov model

Most subsoil conditions can be approximated by having a relatively hard soil layer or rock at a finite depth, assuming that the subsoil has a finite uniform depth, where the displacements at the bottom are assumed to be zero and introduced a third parameter, γ which defines the distribution of the vertical displacement in the subsoil. For modelling the subsoil, to develop the differential equations of the soil continuum, Vlasov assumed three parameters, u,v and w, to describe the displacements of the soil in x, y and z directions. The displacements u and v in the x and y directions are very small in the case of the plate bending element compared to the displacement, w, in the vertical direction, z. Therefore, u,v can be assumed to be equal to zero. This simplification comes from the Vlasov and Leont'ev model. (Vlasov and Leont'ev, 1966) have developed a new concept on a two-parameter model that has the advantage of determining soil parameters and dynamically activated mass depending on soil material properties, modulus of elasticity, Poisson's ratio and mass density (E_s, v_s, ρ_s) and the thickness of the subsoil (H) by introducing a third parameter, γ, to characterize the vertical deformation profile within the soil continuum (Selvaduari, 1979). (Vallabhan and Das, 1988) determined the γ parameter as a function of the characteristic of the structure and the foundation using an iterative procedure and named this model a modified Vlasov model. The γ parameters depend on the properties of the soil, the depth of the soil or rigid base and the structure, as well as the type and magnitude of the loading (Fig. 3.1).

The two-parameter model developed by (Vlasov and Leont'ev, 1966) was improved by (Vallabhan and Das, 1991a) utilizing three parameters relating to the geometry and material properties of the soil continuum for a particular plate and loading. The authors resolved the rectangular, skew, and circular plate problems on a soil medium by combining this model with a numerical model that applied the finite element approach. The material qualities of the soil are employed in the analysis rather than the soils co-efficient of subgrade response.

The modified Vlasov model represents the subsurface because it considers soil shear strain and provides a dish-shaped deflection for a uniformly distributed load on the plate.

However, the γ parameter estimation is necessary for the Vlasov model. Using an iterative technique, (Vallabhan and Das, 1988) determined the γ parameter as a function of the characteristic of the foundation and the structure. They referred to this model as the "modified Vlasov model". They emphasized that the parameters are determined by the soil's structure, characteristics, type and magnitude of the loading and the depth of the soil, among other factors.

Vlasov made the following assumptions to simplify the derivation of the governing equations.

- The first assumption that he employed was to keep u(x, y, z) = 0; v(x, y, z) = 0 in the soil.

- The second assumption that he made in his formulation is to select only a single term describing the w displacement function, that is,
  w(x,y,z) = w(x,y)φ(z).

  Where φ (z) is the function describing the variation of the function w from the top of the soil to its bottom such that φ (0) = 1 and φ (H) = 0, it is further assumed that the displacements of the surface of the soil are equal to the displacements of the middle surface of the plate, w(x, y, 0) = w(x, y). It is a common practice in plates on elastic foundation studies to ignore the compatibility of horizontal (u, v) displacements at the interface. If we ignore this condition, we assume the soil interface is perfectly smooth. Thus, the analysis is performed in two categories. In the first category, the compatibility of u and v is neglected, making the soil a smooth boundary. In the second case, compatibility of u and v on the interface is enforced. With the assumed displacement fields, strains are calculated and subsequently related to stresses using elasticity theory. The soil medium is assumed to be an elastic, isotropic continuum, homogeneous within each layer, with Lame's constants λ_{si} and G_{si}. There is no slippage or separation between the plate and the surrounding soil or between the soil layers. For a material whose elastic properties are not a function of direction, only two independent elastic material constants are sufficient to describe its behaviour completely. This material is called "Isotropic linear elastic". The stress-strain relationship for this material is thus written as an extension of a transversely isotropic material.

(a)

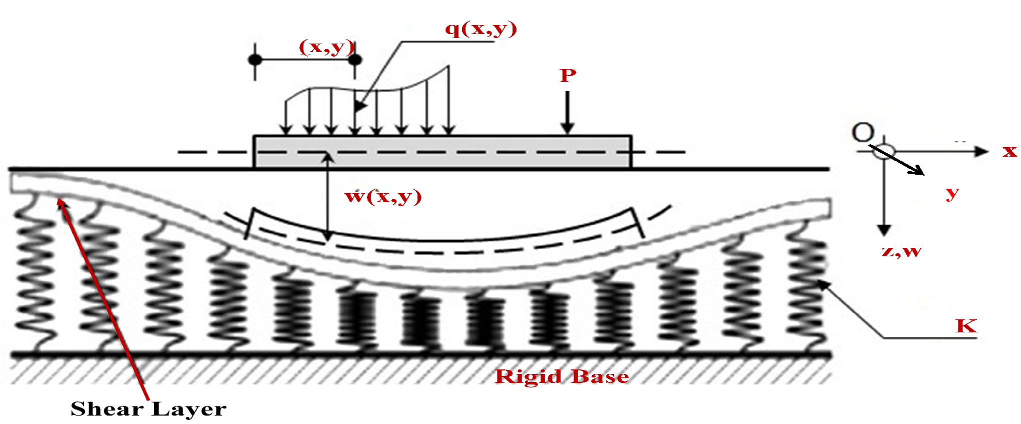

(b)

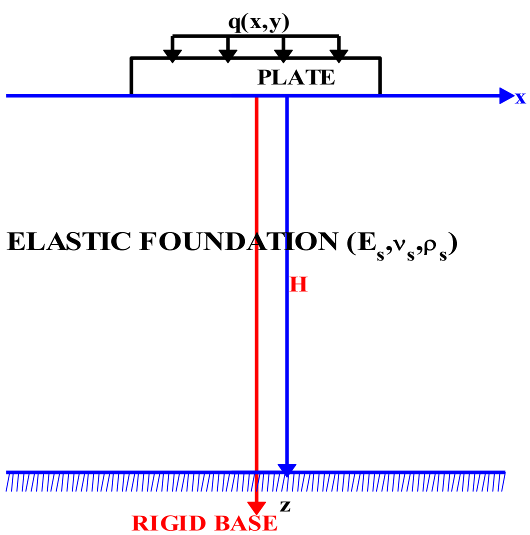

(c)

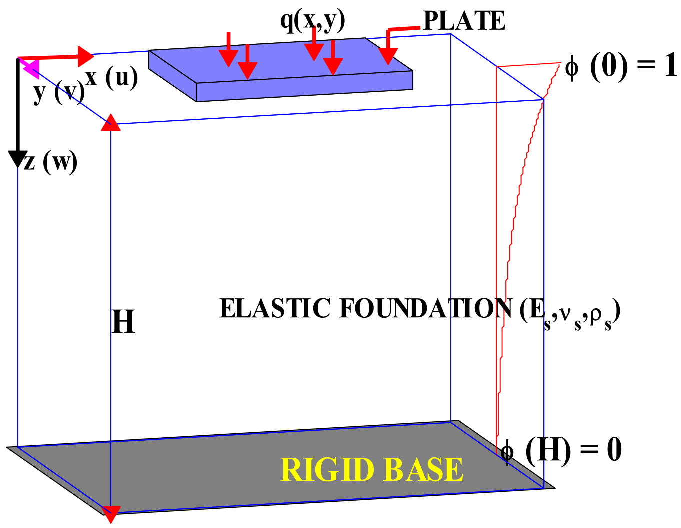

Rectangular plate

(d)

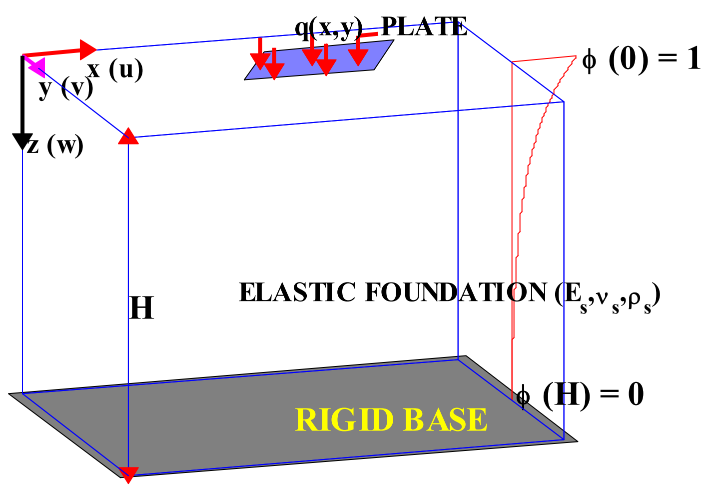

Skew plate

Fig. 3.1(a, b, c and d) Finite plates resting on two-parameters Elastic foundation (Rectangular and Skew)

The total potential energy in the soil-structure system may be

$$\Pi = \Pi_p + \Pi_s + V \qquad (3.2.1.1)$$

Π_p = The strain energy stored in the plate

Π_s = The strain energy stored in the soil

V = the potential energy of the external loads.

Plane Strain Condition

Plane strain conditions are assumed applicable to elastic half-space. Since lateral strains are minimal compared with vertical strains, they can be neglected. The strain components $\boldsymbol{\varepsilon}_{xx}$, $\boldsymbol{\varepsilon}_{yy}$ and γ_{xy} will therefore vanish. Strain field as follows

$$\varepsilon_{xx} = \frac{\partial u}{\partial x} = 0; \varepsilon_{yy} = \frac{\partial v}{\partial y} = 0; \varepsilon_{zz} = w\frac{\partial \varphi}{\partial z}; \gamma_{xy} = \frac{\partial u}{\partial y} + \frac{\partial v}{\partial x} = 0;$$

$$\gamma_{yz} = \frac{\partial w}{\partial y} + \frac{\partial v}{\partial z} = \frac{\partial w}{\partial y}\varphi; \gamma_{xz} = \frac{\partial u}{\partial z} + \frac{\partial w}{\partial x} = \frac{\partial w}{\partial x}\varphi$$

$$\begin{Bmatrix} \varepsilon_{xx} \\ \varepsilon_{y}y \\ \varepsilon_{zz} \\ \gamma_{xy} \\ \gamma_{yz} \\ \gamma_{xz} \end{Bmatrix} = \begin{bmatrix} 0 \\ 0 \\ w\frac{\partial \varphi}{\partial z} \\ 0 \\ \varphi\frac{\partial w}{\partial y} \\ \varphi\frac{\partial w}{\partial x} \end{bmatrix} \text{ and}$$

$$\begin{bmatrix} \sigma_{xx} \\ \sigma_{yy} \\ \sigma_{zz} \\ \tau_{xy} \\ \tau_{yz} \\ \tau_{xz} \end{bmatrix} = \frac{E_s}{(1+v_s)(1-2v_s)} \begin{bmatrix} 1-v_s & v_s & v_s & 0 & 0 & 0 \\ v_s & 1-v_s & v_s & 0 & 0 & 0 \\ v_s & v_s & 1-v_s & 0 & 0 & 0 \\ 0 & 0 & 0 & \frac{1-2v_s}{2} & 0 & 0 \\ 0 & 0 & 0 & 0 & \frac{1-2v_s}{2} & 0 \\ 0 & 0 & 0 & 0 & 0 & \frac{1-2v_s}{2} \end{bmatrix} \begin{bmatrix} 0 \\ 0 \\ w\frac{\partial \varphi}{\partial z} \\ 0 \\ \varphi\frac{\partial w}{\partial y} \\ \varphi\frac{\partial w}{\partial x} \end{bmatrix}$$

$$\therefore \begin{bmatrix} \sigma_{zz} \\ \tau_{yz} \\ \tau_{xz} \end{bmatrix} = \frac{E_s}{(1+v_s)(1-2v_s)} \begin{bmatrix} 1-v_s & 0 & 0 \\ 0 & \frac{1-2v_s}{2} & 0 \\ 0 & 0 & \frac{1-2v_s}{2} \end{bmatrix} \begin{bmatrix} w\frac{\partial \varphi}{\partial z} \\ \varphi\frac{\partial w}{\partial y} \\ \varphi\frac{\partial w}{\partial x} \end{bmatrix};$$

$$\overline{E} = \frac{E_s(1-v_s)}{(1+v_s)(1-2v_s)} \text{ and } G_s = \frac{E_s}{2(1+v_s)}$$

$$\therefore \sigma_{zz} = \overline{E}\varepsilon_{zz} = \overline{E}w\frac{\partial \varphi}{\partial z}; \tau_{yz} = G_s\frac{\partial w}{\partial y}\varphi \text{ and } \tau_{xz} = G_s\frac{\partial w}{\partial x}\varphi$$

$$\text{Strain energy}, \Pi_s = \tfrac{1}{2}\sigma_{ij}\varepsilon_{ij}dV = \tfrac{1}{2}\sigma_{ij}\varepsilon_{ij}dxdydz$$

$$\Pi_s = \tfrac{1}{2}\int\int\int\left(\sigma_{zz}\varepsilon_{zz} + \tau_{yz}\gamma_{yz} + \tau_{xz}\gamma_{xz}\right)dxdydz$$

Strain energy, $\Pi_s = \frac{1}{2}\int_0^H \int_{-\infty}^{\infty}\int_{-\infty}^{\infty}\left[\overline{E}\left(w\frac{\partial\varphi}{\partial z}\right)^2 + G_s\left(\frac{\partial w}{\partial y}\varphi\right)^2 + G_s\left(\frac{\partial w}{\partial x}\varphi\right)^2\right] dxdydz$

$$\Pi_s = \frac{1}{2}\int_0^H \int_{-\infty}^{\infty}\int_{-\infty}^{\infty}\left[\overline{E}w^2\left(\frac{\partial\varphi}{\partial z}\right)^2 + G_s\varphi^2\left[\left(\frac{\partial w}{\partial y}\right)^2 + \left(\frac{\partial w}{\partial x}\right)^2\right]\right] dxdydz$$

$$\Pi_s = \frac{1}{2}\int_0^H \int_{-\infty}^{\infty}\int_{-\infty}^{\infty}\left[\overline{E}w^2\left(\frac{\partial\varphi}{\partial z}\right)^2 + G_s\varphi^2\left[\left(\frac{\partial w}{\partial y}\right)^2 + \left(\frac{\partial w}{\partial x}\right)^2\right]\right] dxdydz$$

$$\Pi_s = \frac{1}{2}\int_{-\infty}^{\infty}\int_{-\infty}^{\infty}\left[Kw^2 + 2t\left\{\left(\frac{\partial w}{\partial y}\right)^2 + \left(\frac{\partial w}{\partial x}\right)^2\right\}\right] dxdy$$

$$K = \int_0^H \overline{E}\left(\frac{\partial\varphi}{\partial z}\right)^2 dz \text{ and } 2t = \int_0^H G_s\varphi^2 dz$$

Now, we obtain the governing differential equation for the foundation by taking the variation of φ and then equating it to zero:

$$\Pi_s = \frac{1}{2}\int_0^H \int_{-\infty}^{\infty}\int_{-\infty}^{\infty}\left[\overline{E}w^2\left(\frac{\partial\varphi}{\partial z}\right)^2 + G_s\varphi^2\left\{\left(\frac{\partial w}{\partial y}\right)^2 + \left(\frac{\partial w}{\partial x}\right)^2\right\}\right] dxdydz$$

$$\Pi_s = \frac{1}{2}\int_0^H\left[\int_{-\infty}^{\infty}\int_{-\infty}^{\infty}\overline{E}w^2 dxdy\right]\left(\frac{\partial\varphi}{\partial z}\right)^2 dz + \frac{1}{2}\int_0^H\left[\int_{-\infty}^{\infty}\int_{-\infty}^{\infty}G_s\left\{\left(\frac{\partial w}{\partial y}\right)^2 + \left(\frac{\partial w}{\partial x}\right)^2\right\}dxdy\right]\varphi^2 dz$$

$$\text{Now } m = \int_{-\infty}^{\infty}\int_{-\infty}^{\infty}\overline{E}w^2 dxdy \text{ and } n = \int_{-\infty}^{\infty}\int_{-\infty}^{\infty}G_s\left[\left(\frac{\partial w}{\partial y}\right)^2 + \left(\frac{\partial w}{\partial x}\right)^2\right]dxdy$$

$$\Pi_s = \frac{1}{2}\int_0^H\left[n\varphi^2 + m\left(\frac{\partial\varphi}{\partial z}\right)^2\right]dz;\ \text{Now } F_3 = \frac{1}{2}\left[n\varphi^2 + m\left(\frac{\partial\varphi}{\partial z}\right)^2\right];$$

$$\frac{\partial F_3}{\partial\varphi} = n\varphi \text{ and } \frac{\partial F_3}{\partial\left(\frac{d\varphi}{dz}\right)} = m\frac{\partial\varphi}{\partial z}$$

Now Euler-Lagrange equation,

$$\frac{\partial F_3}{\partial\varphi} - \frac{d}{dz}\left(\frac{\partial F_3}{\partial\left(\frac{d\varphi}{dz}\right)}\right) = 0 \ \therefore n\varphi - m\frac{\partial^2\varphi}{\partial z^2} = 0 \text{ or } -m\frac{\partial^2\varphi}{\partial z^2} + n\varphi = 0$$

Solution for the displacement dissipation function φ

$$\frac{\partial^2\varphi}{\partial z^2} - \frac{n}{m}\varphi = 0 \ \therefore \frac{\partial^2\varphi}{\partial z^2} - \left(\frac{\gamma}{H}\right)^2\varphi = 0$$

$$\text{Where } \left(\frac{\gamma}{H}\right)^2 = \frac{n}{m} = \frac{\int_{-\infty}^{\infty}\int_{-\infty}^{\infty}G_s\left[\left(\frac{\partial w}{\partial y}\right)^2 + \left(\frac{\partial w}{\partial x}\right)^2\right]dxdy}{\int_{-\infty}^{\infty}\int_{-\infty}^{\infty}\overline{E}w^2 dxdy} = \frac{(1-2v_s)}{2(1-v_s)}\frac{\int_{-\infty}^{\infty}\int_{-\infty}^{\infty}(\nabla w)^2 dxdy}{\int_{-\infty}^{\infty}\int_{-\infty}^{\infty}(w)^2 dxdy} \tag{3.2.1.2}$$

The general solution

$$\varphi(z) = Ae^{\frac{\gamma}{H}z} + Be^{-\frac{\gamma}{H}z} = A\left[\sinh\left(\frac{\gamma}{H}z\right) + \cosh\left(\frac{\gamma}{H}z\right)\right] + B\left[\cosh\left(\frac{\gamma}{H}z\right) - \sinh\left(\frac{\gamma}{H}z\right)\right]$$

$$\varphi(z) = (A+B)\cosh\left(\frac{\gamma}{H}z\right) + (A-B)\sinh\left(\frac{\gamma}{H}z\right) = C\cosh\left(\frac{\gamma}{H}z\right) + D\sinh\left(\frac{\gamma}{H}z\right)$$

The particular solution is given by and as per assumption,

$\varphi(0) = 1$ at $z = 0$, and $\varphi(H) = 0$ at $z = H$.

$$\therefore C\cosh(0) + D\sinh(0) = 1 \text{ and } C\cosh(\gamma) + D\sinh(\gamma) = 0$$

$$\text{or } C \times 1 + D \times 0 = 1 \text{ i.e. } C = 1;\ \therefore D = -\frac{\cosh(\gamma)}{\sinh(\gamma)}$$

$$\varphi(z) = \cosh\left(\frac{\gamma}{H}z\right) - \frac{\cosh(\gamma)}{\sinh(\gamma)}\sinh\left(\frac{\gamma}{H}z\right) = \frac{\cosh\left(\frac{\gamma}{H}z\right)\sinh(\gamma) - \sinh\left(\frac{\gamma}{H}z\right)\cos\ (\gamma)}{\sinh(\gamma)} = \frac{\sinh\left[\gamma\left(1-\frac{z}{H}\right)\right]}{\sinh(\gamma)}$$

$$\sinh(\alpha x) = \frac{e^{\alpha x} - e^{-\alpha x}}{2} \text{ and } \cosh(\alpha x) = \frac{e^{\alpha x} + e^{-\alpha x}}{2} \text{ and}$$

$$\sin(\alpha x) = \frac{e^{i\alpha x} - e^{-i\alpha x}}{2i} \text{ and } \cos(\alpha x) = \frac{e^{i\alpha x} + e^{-i\alpha x}}{2}$$

$$e^{\alpha x} = \sinh(\alpha x) + \cosh(\alpha x) \text{ and } e^{-\alpha x} = \cosh(\alpha x) - \sinh(\alpha x)$$

In this model, the loads only act on the plate domain in the lateral direction. They can consist of uniformly distributed loads on full plate or patch loads, line loads, concentrated loads, moments and any combination.

The strain energies of the plate may be written as

$$\Pi_p = \frac{1}{2}\int_\Omega \left(\frac{\partial^2 w}{\partial x^2}, \frac{\partial^2 w}{\partial y^2}, 2\frac{\partial^2 w}{\partial x\, \partial y}\right)[D]\left(\frac{\partial^2 w}{\partial x^2}, \frac{\partial^2 w}{\partial y^2}, 2\frac{\partial^2 w}{\partial x\, \partial y}\right)^T dxdy \tag{3.2.1.3}$$

$$V = -\frac{1}{2}\int_\Omega qwdxdy \tag{3.2.1.4}$$

Where w = the vertical displacement of the plate, i.e. displacement in z - direction,

q = the applied distributed load, σ, τ = normal and shear stress in the elastic foundation, ε, γ = normal and shear strain in the elastic foundation, H = depth of the subsoil, **Ω** = domain of the plate, and [D] = Plate rigidity matrix.

$$[D] = \frac{Eh^3}{12(1-v^2)}\begin{bmatrix} 1 & v & 0 \\ v & 1 & 0 \\ 0 & 0 & \frac{1-v}{2} \end{bmatrix} \tag{3.2.1.5}$$

E = the modulus of elasticity of the plate, h = thickness of the plate, and v = Poisson's ratio of the plate.

Using the strain-displacement equations of elasticity (Timoshenko) and the mentioned assumptions, the total potential energy of the plate-soil system in the domain of the plate can be written as

$$\Pi = \frac{1}{2}\int_{\Omega}\left(\frac{\partial^2 w}{\partial x^2}, \frac{\partial^2 w}{\partial y^2}, 2\frac{\partial^2 w}{\partial x\, \partial y}\right)[D]\left(\frac{\partial^2 w}{\partial x^2}, \frac{\partial^2 w}{\partial y^2}, 2\frac{\partial^2 w}{\partial x\, \partial y}\right)^{T} dxdy + \frac{1}{2}\int_{\Omega}[Kw^2 + 2t(\nabla w)^2]\, dxdy - \frac{1}{2}\int_{\Omega} q\, wdxdy \qquad (3.2.1.6)$$

Where K and 2t are the soil parameters defined as

$$K = \int_0^H \bar{E}\left(\frac{\partial \varphi}{\partial z}\right)^2 dz \text{ or } \int_0^H \frac{E_0}{(1-v_0{}^2)}\left(\frac{d\varphi}{dz}\right)^2 dz \text{ and } 2t = \int_0^H G_s\varphi^2 dz \text{ or } \int_0^H \frac{E_0}{2(1+v_0)}\varphi^2(z)\, dz$$

$$E_0 = \frac{E_s}{(1-v_s{}^2)} \text{ and } v_0 = \frac{v_s}{(1-v_s)}$$

$$\therefore \frac{E_0}{(1-v_0{}^2)} = \frac{E_s(1-v_s)}{(1+v_s)(1-2v_s)} \text{ and } \frac{E_0}{2(1+v_0)} = \frac{E_s}{2(1+v_s)}$$

E_s, v_s = Young's modulus of elasticity and Poisson's ratio of soil.

E_0, v_0 = Effective modulus of elasticity and Poisson's ratio of soil.

$$\varphi(z) = \frac{\sinh\left[\gamma\left(1-\frac{z}{H}\right)\right]}{\sinh(\gamma)} \text{ and } \frac{d\varphi}{dz} = -\frac{\gamma\cosh\left[\gamma\left(\frac{z}{H}-1\right)\right]}{H\sinh(\gamma)}$$

$$\varphi^2 = \frac{\sinh^2\left[\gamma\left(\frac{z}{H}-1\right)\right]}{\sinh^2\gamma} \text{ and } \left(\frac{d\varphi}{dz}\right)^2 = \frac{\gamma^2\cosh^2\left[\gamma\left(\frac{z}{H}-1\right)\right]}{H^2\sinh^2\gamma}$$

For constant E

$$K = \int_0^H \frac{E_0}{(1-v_0{}^2)}\left(\frac{d\varphi}{dz}\right)^2 dz = \frac{E_s(1-v_s)}{(1+v_s)(1-2v_s)}\int_0^H \frac{\gamma^2\cosh^2\left[\gamma\left(\frac{z}{H}-1\right)\right]}{H^2\sin\ ^2\gamma} dz$$

$$K = \frac{E_s(1-v_s)\gamma}{(1+v_s)(1-2v_s)H\sinh^2\gamma}\left[\frac{\gamma}{2} - \frac{\sinh(-2\gamma)}{4}\right] = \frac{E_s(1-v_s)\gamma}{(1+v_s)(1-2v_s)H\sinh^2\gamma}\left[\frac{\gamma}{2} + \frac{\sinh\gamma\cosh\gamma}{2}\right]$$

$$K = \frac{E_s(1-v_s)\gamma}{(1+v_s)(1-2v_s)H}\left(\frac{\sinh\gamma\cosh\gamma+\gamma}{2\sinh^2\gamma}\right) \qquad (3.2.1.7)$$

$$2t = \int_0^H \frac{E_0}{2(1+v_0)}\varphi^2(z)\, dz = \frac{E_s}{2(1+v_s)}\int_0^H \frac{\sinh^2\left[\gamma\left(\frac{z}{H}-1\right)\right]}{\sinh^2\gamma} dz = \frac{E_s}{2(1+v_s)}\left[\frac{H\sinh\left[2\gamma\left(\frac{z}{H}-1\right)\right]-2\gamma z}{2\gamma[\cosh(2\gamma)-1]}\right]_0^H$$

$$\cosh(2\gamma) = \cosh^2\gamma + \sinh^2\gamma \text{ and } 1 = \cosh^2\gamma - \sinh^2\gamma \therefore \cosh(2\gamma) - 1 = 2\sinh^2\gamma$$

$$2t = \frac{E_s}{2(1+v_s)}\left[-\frac{H}{2\sinh^2\gamma} + \frac{2H\sinh\gamma\cosh\gamma}{4\gamma\sinh^2\gamma}\right] = \frac{E_sH}{2\gamma(1+v_s)}\left(\frac{\sinh\gamma\mathrm{co}\quad\gamma-\gamma}{2\sinh^2\gamma}\right) \qquad (3.2.1.8)$$

γ parameter denotes the vertical deformation within the subsoil.

In the (Buczkowski and Torbacki, 2010), a linear variation of elasticity modulus E_s throughout the thickness of the foundation z was discussed, given as

$E_s(z) = E_1 + (E_2 - E_1)\frac{z}{H}$

$K = \frac{(1-v_s)}{8(1+v_s)(1-2v_s)H}\frac{\left(E_1-E_2+2E_1\gamma^2+2E_2\gamma^2-E_1\cosh(2\gamma)+E_2\cosh(2\gamma)+2E_1\gamma\sinh(2\gamma)\right)}{\sinh^2\gamma}$

$2t = \frac{H}{16\gamma^2(1+v_s)}\frac{\left(E_1-E_2-2E_1\gamma^2-2E_2\gamma^2-E_1\cosh(2\gamma)+E_2\cos\ \ (2\gamma)+2E_1\gamma \mathrm{si}\ \ \ (2\gamma)\right)}{\sinh^2\gamma}$

In the paper of (Celik and Omurtag, 2005), a quadratic variation of elasticity modulus Es throughout the thickness of the foundation z was discussed, given as

$E_s(z) = E_1 + (E_2 - E_1)\frac{z^2}{H^2}.$

Here , E_1 and E_2 are the elastic modulus of the subsoil at the top (at z = 0) and bottom (at z = H), respectively.

$K = \frac{(1-v_s)}{24\gamma H(1+v_s)(1-2v_s)}\frac{\left[8E_1\gamma^3+4E_2\gamma^3-3E_1\sinh(2\gamma)+3E_2\sinh(2\gamma)+6E_1\gamma-6E_2\gamma+6E_1\gamma^2\sinh(2\gamma)\right]}{\sinh^2\gamma}$

$2t = \frac{H}{48\gamma^3(1+v_s)}\frac{\left[3E_2\sinh(2\gamma)+6E_1\gamma-6E_2\gamma+6E_1\gamma^2\sinh(2\gamma)-8E_1\gamma^3-4E_2\gamma^3-3E_1\sinh(2\gamma)\right]}{\sinh^2\gamma}$

Using variational principles and minimizing the total potential energy of Equation (3.2.1.6) by taking variations in w and φ yields (Turhan, 1992).

$$\delta\Pi = \int_\Omega (D\nabla^4 w - 2t\nabla^2 w + Kw - q)\delta w dxdy + \int_0^H \left(-m\frac{\partial^2\varphi}{\partial z^2} + n\varphi\right)\delta\varphi dz + \text{boundary condition} = 0 \qquad (3.2.1.9)$$

Since the variations δw and δφ are not equal to zero, the terms in the parentheses and boundary conditions must equal zero.

Therefore, the field equation in the domain, **Ω**, can be written as

$D\nabla^4 w - 2t\nabla^2 w + Kw = q; \nabla^2 = \text{Laplacian operator} = \frac{\partial^2}{\partial x^2} + \frac{\partial^2}{\partial y^2}$ and

$\nabla^4 = \text{Bi} - \text{harmonic operator} = \nabla^2\nabla^2 = \frac{\partial^4}{\partial x^4} + \frac{2\,\partial^4}{\partial x^2\,\partial y^2} + \frac{\partial^4}{\partial y^4}$

Outside the plate domain, the field equation is

$-2t\nabla^2 w + Kw = 0$

The second expression within the parentheses in Equation (3.2.1.9) is the field equation for the deformation pattern of the soil in the vertical direction. The equation is

$$-m\frac{\partial^2\varphi}{\partial z^2} + n\varphi = 0 \qquad (3.2.1.10)$$

The Solution of Eq. (3.2.1.10) with the boundary conditions φ (0) = 1 and φ (H) = 0 yields

$\varphi(z) = \frac{\sinh\left[\gamma\left(1-\frac{z}{H}\right)\right]}{\sinh(\gamma)}$ At the surface , i.e ., at z = 0, φ = 1 , and at a depth H , at z = H, φ = 0.

The important point here is that the modulus of the sub-grade reaction, K, and the second parameter, 2t, which represents the shear deformation of the soil, are both dependent on the vertical deformation function γ and the depth of the soil, H, as can be seen in Eq. (3.2.1.7) and (3.2.1.8). Furthermore, the value of γ varies with the displacement of the plate and the depth of the subsoil. Therefore, the variables w, q, K, 2t, H and γ are all connected for a plate on an elastic foundation.

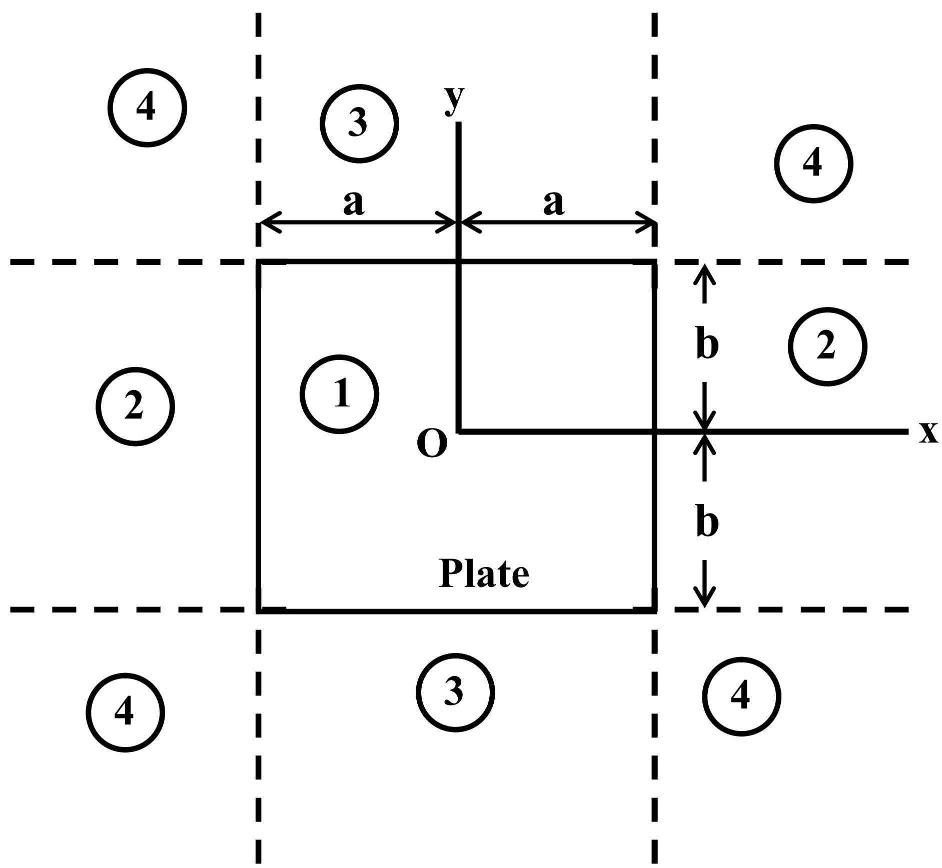

Fig. 3.2 is an illustration of a rectangular plate-soil surface divided into regions.

Outside plate domain for a rectangular plate with dimensions of 2a in the x direction and 2b in the y direction (Fig. 3.2), the assumed functions are,

for $a < x < \infty$ and $-b < y < b$; $w(x, y) = w_a e^{-\alpha(x-a)}$

for $b < y < \infty$ and $-a < x < a$; $w(x, y) = w_b e^{-\alpha(y-b)}$

and for a corner for $x < \infty$ and $y < b$; $w(x, y) = w_c e^{-\alpha(x-a)} e^{-\alpha(y-b)}$

Outside plate domain for a rectangular plate in the positive x direction

$\therefore\ 2t\frac{d^2w}{dx^2} - Kw = 0; \frac{d^2w}{dx^2} - \frac{K}{2t}w = 0; \frac{d^2w}{dx^2} - \alpha^2 w = 0$ where $\alpha^2 = \frac{K}{2t}$

General solution, $w(x) = Ae^{\alpha x} + Be^{-\alpha x}$

At $w(a) = w_a$ and $w(\infty) = 0$; $Ae^{\alpha a} + Be^{-\alpha a} = w_a$ and $A \times \infty + B \times 0 = 0$

i.e $A = 0$ and $B = w_a e^{\alpha a}$ $\therefore w(x) = w_a e^{-\alpha(x-a)}$ and $\frac{\partial w}{\partial x} = -\alpha w_a e^{-\alpha(x-a)}$

where, $w_a =$ vertical displacement of the plate at $x = a$,

$w_b =$ vertical displacement of the plate at $y = b$ and

$w_c =$ vertical displacement at the plate corner

In the positive direction of the x-axis (in regions 2)

$w(x,y) = w_a e^{-\alpha(x-a)}; \int_{-b}^{b}\int_{a}^{\infty}(w)^2 dxdy = \frac{1}{2\alpha}\int_{-b}^{b}(w_a)^2 dy;$

$\int_{-b}^{b}\int_{a}^{\infty}(\nabla w)^2 dxdy = \frac{\alpha}{2}\int_{-b}^{b}(w_a)^2 dy$

In the positive direction of the y-axis (in regions 3)

$w(x,y) = w_b e^{-\alpha(y-b)}; \int_{-a}^{a}\int_{b}^{\infty}(w)^2 dxdy = \frac{1}{2\alpha}\int_{-a}^{a}(w_b)^2 dx$

$\int_{-a}^{a}\int_{b}^{\infty}(\nabla w)^2 dxdy = \frac{\alpha}{2}\int_{-a}^{a}(w_b)^2 dx$

In the region $x > a, y > b$ (in regions 4)

$w(x,y) = w_c e^{-\alpha(x-a)} e^{-\alpha(y-b)}; \int_{a}^{\infty}\int_{b}^{\infty}(w)^2 dxdy = \frac{(w_C)^2}{4\alpha^2}; \int_{a}^{\infty}\int_{b}^{\infty}(\nabla w)^2 dxdy = \frac{(w_C)^2}{2}$

Outside the plate domain for a rectangular plate with dimensions of 2a in the x direction and 2b in the y direction, the equivalent boundary forces are due to the infinite soil domain on the plate boundary (Turhan, 1992). There are two types of stiffness to be considered. One is axial stiffness related to the displacement of the plate boundary in the transverse direction, and the other type is rotational stiffness associated with the rotation of the plate at its edge. Thus, the effect at a boundary other than the corner of the soil region is modelled by adding an equivalent to the stiffness term for a corner region, as shown in Figure 3.3. Minimizing the energy concerning displacement at that point, the equivalent corner reaction is $R = 1.5tw_c$. So the stiffness for the corner node is 1.5t.

Thus, the effect at the corner node of the soil region is modelled by adding 1.5t to the stiffness term representing the corner displacement. Vertical and rotational reaction forces for a continuous boundary can be obtained by

Stiffness is $\sqrt{2Kt}$ and rotational stiffness is $\frac{1}{2}(2t)\sqrt{\frac{2t}{K}}$

Where ‘a’ is the tributary length of the respective node.

Taking into consideration the above expressions, we obtain the expressions of the so-called fictive forces Q^{φ} and R^{φ} (Figure 3.3), with which the ground beyond the plate acts upon it.

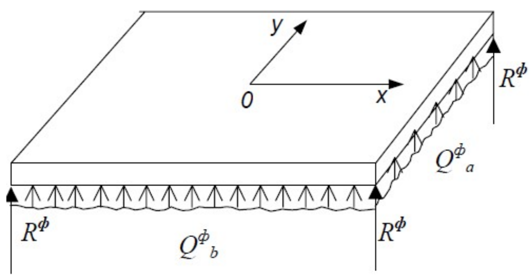

Fig. 3.3 Illustration of the boundary forces concentration of line stiffness on boundary nodal points.

Forces on the boundary nodes (Figure 3.3). $Q^{\varphi} = a\sqrt{2tK}w$ and $R^{\varphi} = 1.5tw_{c.}$The deflection of each node is represented by the letters w and w_c, respectively.

The iterative procedure

In this model, the solution technique is an iterative process dependent upon the value of the γ parameter. Therefore, γ is initially set equal to one and φ is calculated. These values are used to compute the sub-grade reaction, K, and soil shear parameter values, 2t, from Eqs. (3.2.1.7) and (3.2.1.8). With these values of K and 2t, the total coefficient matrix of the plate-soil system is constructed, and the set of simultaneous equations is solved to find the displacements at discrete points on the plate. The computed new value of γ is then compared with the presumptive original value using Equation (3.2.1.2), obtained using the measured plate displacements. A comparison between this calculated value of γ and the initial by assumed γ or previously calculated γ is then made. The analysis is stopped if the difference between the two successive γ values is within a prescribed tolerance. Otherwise, iteration is performed, and the process is repeated until convergence is obtained. Therefore, the mode shape parameter γ may be calculated at the end of any analysis step regarding vertical displacements of the foundation-subsoil system. More details of the Modified Vlasov model are available (Turhan, 1992; Celik and Saygun, 1999b; Straughan, 1990; Özgan and Daloğlu, 2008; Ozgan and Daloglu, 2009).

(a) (b) (c)

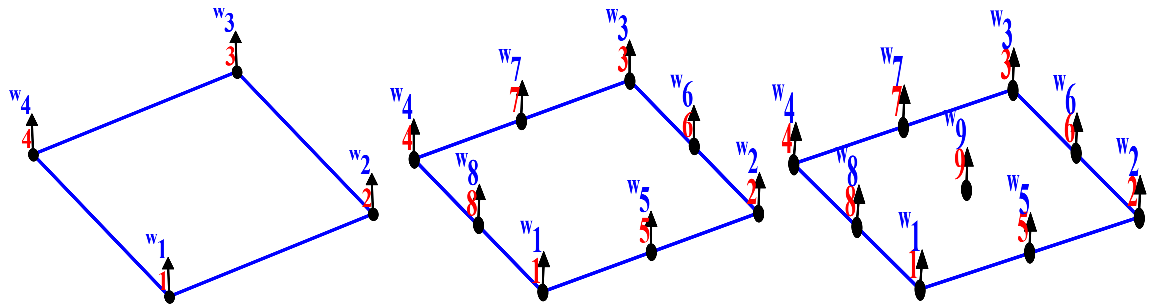

Fig. 3.4 (a,b and c) Four, Eight and Nine noded subsoil shear element

The integrals in equation (3.2.1.11) may be calculated in terms of the nodal displacements of the subsoil shear element within the plate domain is (Figure 3.4)

$$\int_{-b}^{b}\int_{-a}^{a}(\nabla w)^2 dxdy = \sum_{i=1}^{n}\frac{1}{2t}[w_i]^T[K_e]\,[w_i] \text{ and } \int_{-b}^{b}\int_{-a}^{a}(w)^2 dxdy = \sum_{i=1}^{m}A[w_i]^2$$

Where n, m, A, and w_i represent the element number, the node number, the tributary area of node i and the vertical deflection of the i^{th} node respectively.

Thin Rectangular Plate

The strain energy deformation in thin plates corresponding to bending and transverse shear and thickness stretch or contraction are taken as negligible; hence, it is a plane stress condition.

The displacement field for a thin plate is $u = -z\frac{\partial w}{\partial x}; v = -z\frac{\partial w}{\partial y}$ and w

strain field $\varepsilon_x = \frac{\partial u}{\partial x} = -z\frac{\partial^2 w}{\partial x^2}$;

$$\varepsilon_y = -z\frac{\partial^2 w}{\partial y^2} \text{ and } \gamma_{xy} = \frac{\partial u}{\partial y} + \frac{\partial v}{\partial x} = -2z\frac{\partial^2 w}{\partial x\,\partial y}$$

The constitutive law for plane stress conditions is

$$\begin{Bmatrix}\sigma_x\\ \sigma_y\\ \tau_{xy}\end{Bmatrix} = \frac{E}{(1-v^2)}\begin{bmatrix}1 & v & 0\\ v & 1 & 0\\ 0 & 0 & \frac{1-v}{2}\end{bmatrix}\begin{Bmatrix}\epsilon_x\\ \epsilon_y\\ \gamma_{xy}\end{Bmatrix} = -\frac{Ez}{(1-v^2)}\begin{bmatrix}1 & v & 0\\ v & 1 & 0\\ 0 & 0 & \frac{1-v}{2}\end{bmatrix}\begin{Bmatrix}\frac{\partial^2 w}{\partial x^2}\\ \frac{\partial^2 w}{\partial y^2}\\ 2\frac{\partial^2 w}{\partial x\,\partial y}\end{Bmatrix}$$

$$\therefore \sigma_x = -\frac{Ez}{(1-v^2)}\left(\frac{\partial^2 w}{\partial x^2} + v\frac{\partial^2 w}{\partial y^2}\right); \sigma_y = -\frac{Ez}{(1-v^2)}\left(v\frac{\partial^2 w}{\partial x^2} + \frac{\partial^2 w}{\partial y^2}\right); \tau_{xy} = -\frac{Ez}{(1+v)}\frac{\partial^2 w}{\partial x\,\partial y}$$

Strain energy, $\pi_p = \frac{1}{2}\sigma_{ij}\varepsilon_{ij}dV = \frac{1}{2}\sigma_{ij}\varepsilon_{ij}dxdydz = \frac{1}{2}\int\int\int\left(\sigma_x\varepsilon_x + \sigma_y\varepsilon_y + \tau_{xy}\gamma_{xy}\right)dxdydz$

$$\pi_p = \frac{1}{2}\frac{E}{(1-v^2)}\int\int\int_{-\frac{h}{2}}^{\frac{h}{2}}\left[\left(\frac{\partial^2 w}{\partial x^2} + v\frac{\partial^2 w}{\partial y^2}\right)\frac{\partial^2 w}{\partial x^2} + \left(v\frac{\partial^2 w}{\partial x^2} + \frac{\partial^2 w}{\partial y^2}\right)\frac{\partial^2 w}{\partial y^2} + 2(1-v)\left(\frac{\partial^2 w}{\partial x\,\partial y}\right)^2\right]z^2 dxdydz$$

$$\pi_p = \frac{D}{2}\int\int\left[\left(\frac{\partial^2 w}{\partial x^2} + \frac{\partial^2 w}{\partial y^2}\right)^2 - 2(1-v)\left\{\left(\frac{\partial^2 w}{\partial x^2}\right)\left(\frac{\partial^2 w}{\partial y^2}\right) - \left(\frac{\partial^2 w}{\partial x\,\partial y}\right)^2\right\}\right]dxdy = \frac{D}{2}\int\int\left[(\nabla^2 w)^2 - 2(1-v)\left\{\left(\frac{\partial^2 w}{\partial x^2}\right)\left(\frac{\partial^2 w}{\partial y^2}\right) - \left(\frac{\partial^2 w}{\partial x\,\partial y}\right)^2\right\}\right]dxdy$$

Where $\nabla^2 = \left(\frac{\partial^2}{\partial x^2} + \frac{\partial^2}{\partial y^2}\right)$ is the Laplacian operator and $D = \frac{Eh^3}{12(1-v^2)}$ is the flexural rigidity of plate.

The total potential energy of the soil-plate system subjected to a UDL of q is given by

$\Pi = \Pi_p + \Pi_s + V$

Now, the potential energy of the soil-plate system is

$$\Pi = \frac{D}{2}\int_{-a}^{a}\int_{-b}^{b}\left[(\nabla^2 w)^2 - 2(1-v)\left\{\left(\frac{\partial^2 w}{\partial x^2}\right)\left(\frac{\partial^2 w}{\partial y^2}\right) - \left(\frac{\partial^2 w}{\partial x\,\partial y}\right)^2\right\}\right]dxdy + \frac{1}{2}\int_0^H\int_{-\infty}^{\infty}\int_{-\infty}^{\infty}\left[\bar{E}w^2\left(\frac{\partial\varphi}{\partial z}\right)^2 + G_s\varphi^2\left[\left(\frac{\partial w}{\partial y}\right)^2 + \left(\frac{\partial w}{\partial x}\right)^2\right]\right]dxdydz - \int_{-a}^{a}\int_{-b}^{b}qwdxdy$$

We can now use the calculus of variations to obtain the equilibrium equations. For a stable equilibrium state to be reached, the first variation of the potential energy must be zero ($\delta\Pi = 0$). We consider the first plate soil system within the plate domain and take variations on w. Taking variations on w, we get the following

$$\Pi = \frac{D}{2}\int_{-a}^{a}\int_{-b}^{b}\left[(\nabla^2 w)^2 - 2(1-v)\left\{\left(\frac{\partial^2 w}{\partial x^2}\right)\left(\frac{\partial^2 w}{\partial y^2}\right) - \left(\frac{\partial^2 w}{\partial x\,\partial y}\right)^2\right\}\right]dxdy + \frac{1}{2}\int_0^H\int_{-a}^{a}\int_{-b}^{b}\left[\bar{E}w^2\left(\frac{\partial\varphi}{\partial z}\right)^2 + G_s\varphi^2\left[\left(\frac{\partial w}{\partial y}\right)^2 + \left(\frac{\partial w}{\partial x}\right)^2\right]\right]dxdydz - \int_{-a}^{a}\int_{-b}^{b}qwdxdy$$

$$\Pi = \frac{D}{2}\int_{-a}^{a}\int_{-b}^{b}\left[(\nabla^2 w)^2 - 2(1-v)\left\{\left(\frac{\partial^2 w}{\partial x^2}\right)\left(\frac{\partial^2 w}{\partial y^2}\right) - \left(\frac{\partial^2 w}{\partial x\,\partial y}\right)^2\right\}\right]dxdy + \frac{1}{2}\int_0^H\int_{-a}^{a}\int_{-b}^{b}\left[\bar{E}w^2\left(\frac{\partial\varphi}{\partial z}\right)^2 + G_s\varphi^2\left[\left(\frac{\partial w}{\partial y}\right)^2 + \left(\frac{\partial w}{\partial x}\right)^2\right]\right]dxdydz - \int_{-a}^{a}\int_{-b}^{b}qwdxdy$$

$$\Pi = \frac{D}{2}\int_{-a}^{a}\int_{-b}^{b}\left[(\nabla^2 w)^2 - 2(1-v)\left\{\left(\frac{\partial^2 w}{\partial x^2}\right)\left(\frac{\partial^2 w}{\partial y^2}\right) - \left(\frac{\partial^2 w}{\partial x\,\partial y}\right)^2\right\}\right] dxdy + \frac{1}{2}\int_{-a}^{a}\int_{-b}^{b}\left[Kw^2 + 2t\left[\left(\frac{\partial w}{\partial y}\right)^2 + \left(\frac{\partial w}{\partial x}\right)^2\right]\right] dxdy - \int_{-a}^{a}\int_{-b}^{b} qwdxdy$$

$$K = \int_0^H \overline{E}\left(\frac{\partial \varphi}{\partial z}\right)^2 dz \text{ and } 2t = \int_0^H G_s \varphi^2 dz$$

$$F = \frac{D}{2}\left(\left(\frac{\partial^2 w}{\partial x^2} + \frac{\partial^2 w}{\partial y^2}\right)^2 - 2(1-v)\left[\left(\frac{\partial^2 w}{\partial x^2}\right)\left(\frac{\partial^2 w}{\partial y^2}\right) - \left(\frac{\partial^2 w}{\partial x\,\partial y}\right)^2\right]\right) + \frac{1}{2}\left[Kw^2 + 2t\left[\left(\frac{\partial w}{\partial x}\right)^2 + \left(\frac{\partial w}{\partial y}\right)^2\right]\right] - qw$$

$$\frac{\partial F}{\partial w} = Kw - q; \frac{\partial F_1}{\partial\left(\frac{\partial w}{\partial x}\right)} = 2t\frac{\partial w}{\partial x}; \frac{\partial F}{\partial\left(\frac{\partial w}{\partial y}\right)} = 2t\frac{\partial w}{\partial y}; \frac{\partial F}{\partial\left(\frac{\partial^2 w}{\partial x^2}\right)} = D\left(\frac{\partial^2 w}{\partial x^2} + \frac{\partial^2 w}{\partial y^2}\right) - D(1-v)\frac{\partial^2 w}{\partial y^2};$$

$$\frac{\partial F}{\partial\left(\frac{\partial^2 w}{\partial y^2}\right)} = D\left(\frac{\partial^2 w}{\partial x^2} + \frac{\partial^2 w}{\partial y^2}\right) - D(1-v)\frac{\partial^2 w}{\partial x^2};$$

$$\frac{\partial F}{\partial w} - \frac{d}{dx}\left(\frac{\partial F}{\partial\left(\frac{\partial w}{\partial x}\right)}\right) - \frac{d}{dy}\left(\frac{\partial F}{\partial\left(\frac{\partial w}{\partial y}\right)}\right) + \frac{d^2}{dx^2}\left(\frac{\partial F}{\partial\left(\frac{\partial^2 w}{\partial x^2}\right)}\right) + \frac{d^2}{dy^2}\left(\frac{\partial F}{\partial\left(\frac{\partial^2 w}{\partial y^2}\right)}\right) = 0$$

$$Kw - q - 2t\frac{\partial^2 w}{\partial x^2} - 2t\frac{\partial^2 w}{\partial y^2} + D\left(\frac{\partial^4 w}{\partial x^4} + \frac{\partial^4 w}{\partial x^2\,\partial y^2}\right) + D\left(\frac{\partial^4 w}{\partial y^4} + \frac{\partial^4 w}{\partial x^2\,\partial y^2}\right) = 0$$

$$D\left(\frac{\partial^4 w}{\partial x^4} + 2\frac{\partial^4 w}{\partial x^2\,\partial y^2} + \frac{\partial^4 w}{\partial y^4}\right) - 2t\left(\frac{\partial^2 w}{\partial x^2} + \frac{\partial^2 w}{\partial y^2}\right) + Kw = q \qquad (3.2.1.11)$$

Therefore, the field equation in the domain, **Ω**, can be written as

$$D\nabla^4 w - 2t\nabla^2 w + Kw = q$$

$\nabla^2 =$ Laplacian operator $= \frac{\partial^2}{\partial x^2} + \frac{\partial^2}{\partial y^2}$ and

$\nabla^4 =$ Bi − harmonic operator $= \nabla^2\nabla^2 = \frac{\partial^4}{\partial x^4} + \frac{2\,\partial^4}{\partial x^2\,\partial y^2} + \frac{\partial^4}{\partial y^4}$

Mindlin Plate

The displacement field for the Mindlin plate is

$u = -z\theta_x, v = -z\theta_y$ and $w = w(x, y)$ strain field $\varepsilon_x = \frac{\partial u}{\partial x} = -z\frac{\partial \theta_x}{\partial x};$

$$\varepsilon_y = \frac{\partial v}{\partial y} = -z\frac{\partial \theta_y}{\partial y} \text{ and } \gamma_{xy} = \frac{\partial u}{\partial y} + \frac{\partial v}{\partial x} = -z\left(\frac{\partial \theta_x}{\partial y} + \frac{\partial \theta_y}{\partial x}\right); \varepsilon_z = \frac{\partial w}{\partial z} = 0;$$

$$\gamma_{xz} = \frac{\partial u}{\partial z} + \frac{\partial w}{\partial x} = -\theta_x + \frac{\partial w}{\partial x} \text{ and } \gamma_{yz} = \frac{\partial v}{\partial z} + \frac{\partial w}{\partial y} = -\theta_y + \frac{\partial w}{\partial y}; \therefore \sigma_x = \frac{E}{(1-v^2)}(\varepsilon_x + v\varepsilon_y);$$

$$\sigma_y = \frac{E}{(1-v^2)}(\varepsilon_y + v\varepsilon_x); \tau_{xy} = \frac{E\gamma_{xy}}{2(1+v)}; \tau_{xz} = \frac{E\gamma_{xz}}{2(1+v)} \text{ and } \tau_{yz} = \frac{E\gamma_{yz}}{2(1+v)}$$

$$\begin{Bmatrix} \sigma_x \\ \sigma_y \\ \tau_{xy} \end{Bmatrix} = \frac{E}{(1-v^2)} \begin{bmatrix} 1 & v & 0 \\ v & 1 & 0 \\ 0 & 0 & \frac{(1-v)}{2} \end{bmatrix} \begin{Bmatrix} \varepsilon_x \\ \varepsilon_y \\ \gamma_{xy} \end{Bmatrix} = \frac{E}{(1-v^2)} \begin{bmatrix} 1 & v & 0 \\ v & 1 & 0 \\ 0 & 0 & \frac{(1-v)}{2} \end{bmatrix} \begin{Bmatrix} -z\frac{\partial\theta_x}{\partial x} \\ -z\frac{\partial\theta_y}{\partial y} \\ -z\left(\frac{\partial\theta_x}{\partial y} + \frac{\partial\theta_y}{\partial x}\right) \end{Bmatrix}$$

$$\therefore \sigma_x = \frac{-Ez}{(1-v^2)}\left(\frac{\partial\theta_x}{\partial x} + v\frac{\partial\theta_y}{\partial y}\right); \sigma_y = \frac{-Ez}{(1-v^2)}\left(\frac{\partial\theta_y}{\partial y} + v\frac{\partial\theta_x}{\partial x}\right); \tau_{xy} = \frac{-Ez}{2(1+v)}\left(\frac{\partial\theta_x}{\partial y} + \frac{\partial\theta_y}{\partial x}\right);$$

$$\tau_{xz} = \frac{E}{2(1+v)}\left(\frac{\partial w}{\partial x} - \theta_x\right) \text{ and } \tau_{yz} = \frac{E}{2(1+v)}\left(\frac{\partial w}{\partial y} - \theta_y\right)$$

Mindlin introduced further a shear correction factor denoted by α to the expressions for τ_{xz} and τ_{yz} to ensure the agreement of the resultant shear stresses with the results of the rigorous theory of elasticity. Thus, the modified/corrected expressions for τ_{xz} and τ_{yz} become:

$$\tau_{xz} = \frac{E\alpha}{2(1+v)}\left(\frac{\partial w}{\partial x} - \theta_x\right) \text{ and } \tau_{yz} = \frac{E\alpha}{2(1+v)}\left(\frac{\partial w}{\partial y} - \theta_y\right)$$

The strain energy deformation in the Mindlin plate corresponding to bending and shear deformation is

$$\Pi_p = \frac{1}{2}\sigma_{ij}\varepsilon_{ij}dV = \frac{1}{2}\sigma_{ij}\varepsilon_{ij}dxdydz$$

$$\Pi_p = \frac{1}{2}\int\int\int(\sigma_x\varepsilon_x + \sigma_y\varepsilon_y + \sigma_z\varepsilon_z + \tau_{xy}\gamma_{xy} + \tau_{yz}\gamma_{yz} + \tau_{zx}\gamma_{xz})dxdydz$$

$$\therefore \Pi_p = \frac{1}{2}\int\int\int\left\{\frac{Ez}{(1-v^2)}\left(\frac{\partial\theta_x}{\partial x} + v\frac{\partial\theta_y}{\partial y}\right)z\frac{\partial\theta_x}{\partial x} + \frac{Ez}{(1-v^2)}\left(\frac{\partial\theta_y}{\partial y} + v\frac{\partial\theta_x}{\partial x}\right)z\frac{\partial\theta_y}{\partial y} + 0 + \frac{Ez}{2(1+v)}\left(\frac{\partial\theta_x}{\partial y} + \frac{\partial\theta_y}{\partial x}\right)z\left(\frac{\partial\theta_x}{\partial y} + \frac{\partial\theta_y}{\partial x}\right) + \frac{E\alpha}{2(1+v)}\left(\frac{\partial w}{\partial x} - \theta_x\right)\left(\frac{\partial w}{\partial x} - \theta_x\right) + \frac{E\alpha}{2(1+v)}\left(\frac{\partial w}{\partial y} - \theta_y\right)\left(\frac{\partial w}{\partial y} - \theta_y\right)\right\}dxdydz$$

$$\therefore \Pi_p = \frac{E}{2(1-v^2)}\int_{-a}^{a}\int_{-b}^{b}\int_{-h/2}^{h/2} z^2\left\{\left(\frac{\partial\theta_x}{\partial x}\right)^2 + \left(\frac{\partial\theta_y}{\partial y}\right)^2 + 2v\frac{\partial\theta_x}{\partial x}\frac{\partial\theta_y}{\partial y} + \frac{(1-v)}{2}\left(\frac{\partial\theta_x}{\partial y} + \frac{\partial\theta_y}{\partial x}\right)^2\right\}dxdydz + \frac{E\alpha}{4(1+v)}\int_{-a}^{a}\int_{-a}^{b}\int_{-h/2}^{h/2}\left\{\left(\frac{\partial w}{\partial x} - \theta_x\right)^2 + \left(\frac{\partial w}{\partial y} - \theta_y\right)^2\right\}dxdydz$$

$$\therefore \Pi_p = \frac{D}{2}\int_{-a}^{a}\int_{-b}^{b}\left\{\left(\frac{\partial\theta_x}{\partial x}\right)^2 + \left(\frac{\partial\theta_y}{\partial y}\right)^2 + 2v\frac{\partial\theta_x}{\partial x}\frac{\partial\theta_y}{\partial y} + \frac{(1-v)}{2}\left(\frac{\partial\theta_x}{\partial y} + \frac{\partial\theta_y}{\partial x}\right)^2\right\}dxdy + \frac{E\alpha h}{4(1+v)}\int_{-a}^{a}\int_{-b}^{b}\left\{\left(\frac{\partial w}{\partial x} - \theta_x\right)^2 + \left(\frac{\partial w}{\partial y} - \theta_y\right)^2\right\}dxdy$$

$$\Pi = \frac{D}{2}\int_{-a}^{a}\int_{-b}^{b}\left\{\left(\frac{\partial\theta_x}{\partial x}\right)^2 + \left(\frac{\partial\theta_y}{\partial y}\right)^2 + 2v\frac{\partial\theta_x}{\partial x}\frac{\partial\theta_y}{\partial y} + \frac{(1-v)}{2}\left(\frac{\partial\theta_x}{\partial y} + \frac{\partial\theta_y}{\partial x}\right)^2\right\}dxdy + \frac{E\alpha h}{4(1+v)}\int_{-a}^{a}\int_{-b}^{b}\left\{\left(\theta_x + \right.\right.$$

$$\left.\frac{\partial w}{\partial x}\right)^2 + \left(\theta_y + \frac{\partial w}{\partial y}\right)^2\Bigg\} dxdy + \frac{1}{2}\int_0^H \int_{-\infty}^{\infty}\int_{-\infty}^{\infty} \left[\overline{E}w^2\left(\frac{\partial \varphi}{\partial z}\right)^2 + G_s\varphi^2\left[\left(\frac{\partial w}{\partial y}\right)^2 + \left(\frac{\partial w}{\partial x}\right)^2\right]\right] dxdydz -$$

$$\int_{-a}^{a}\int_{-b}^{b} qw\, dxdy$$

$$\Pi =$$

$$\frac{D}{2}\int_{-a}^{a}\int_{-b}^{b}\left\{\left(\frac{\partial \theta_x}{\partial x}\right)^2 + \left(\frac{\partial \theta_y}{\partial y}\right)^2 + 2v\frac{\partial \theta_x}{\partial x}\frac{\partial \theta_y}{\partial y} + \frac{(1-v)}{2}\left(\frac{\partial \theta_x}{\partial y} + \frac{\partial \theta_y}{\partial x}\right)^2\right\} dxdy + \frac{E\alpha h}{4(1+v)}\int_{-a}^{a}\int_{-b}^{b}\Bigg\{\Big(\theta_x +$$

$$\left.\frac{\partial w}{\partial x}\right)^2 + \left(\theta_y + \frac{\partial w}{\partial y}\right)^2\Bigg\} dxdy + \frac{1}{2}\int_{-\infty}^{\infty}\int_{-\infty}^{\infty}\left(\int_0^H \overline{E}\left(\frac{\partial \varphi}{\partial z}\right)^2 dz\right) w^2\, dxdy +$$

$$\frac{1}{2}\int_{-\infty}^{\infty}\int_{-\infty}^{\infty}\left(\int_0^H G_s\varphi^2 dz\right)(\nabla w)^2\, dxdy - \int_{-a}^{a}\int_{-b}^{b} qw\, dxdy$$

$$\Pi =$$

$$\frac{D}{2}\int_{-a}^{a}\int_{-b}^{b}\left\{\left(\frac{\partial \theta_x}{\partial x}\right)^2 + \left(\frac{\partial \theta_y}{\partial y}\right)^2 + 2v\frac{\partial \theta_x}{\partial x}\frac{\partial \theta_y}{\partial y} + \frac{(1-v)}{2}\left(\frac{\partial \theta_x}{\partial y} + \frac{\partial \theta_y}{\partial x}\right)^2\right\} dxdy + \frac{E\alpha h}{4(1+v)}\int_{-a}^{a}\int_{-b}^{b}\Bigg\{\Big(\theta_x +$$

$$\left.\frac{\partial w}{\partial x}\right)^2 + \left(\theta_y + \frac{\partial w}{\partial y}\right)^2\Bigg\} dxdy + \frac{1}{2}\int_{-\infty}^{\infty}\int_{-\infty}^{\infty} Kw^2\, dxdy + \frac{1}{2}\int_{-\infty}^{\infty}\int_{-\infty}^{\infty} 2t\left[\left(\frac{\partial w}{\partial y}\right)^2 + \left(\frac{\partial w}{\partial x}\right)^2\right] dxdy -$$

$$\int_{-a}^{a}\int_{-b}^{b} qw\, dxdy$$

We can now use the calculus of variations to obtain the equilibrium equations. For a stable equilibrium state to be reached, the first variation of the potential energy must be zero ($\delta\Pi = 0$). First, we consider the plate soil system within the plate domain and take variations on w. Taking variations on w, we get the following

Strain energy of the plate soil system within the plate domain is

$$\Pi =$$

$$\frac{D}{2}\int_{-a}^{a}\int_{-b}^{b}\left\{\left(\frac{\partial \theta_x}{\partial x}\right)^2 + \left(\frac{\partial \theta_y}{\partial y}\right)^2 + 2v\frac{\partial \theta_x}{\partial x}\frac{\partial \theta_y}{\partial y} + \frac{(1-v)}{2}\left(\frac{\partial \theta_x}{\partial y} + \frac{\partial \theta_y}{\partial x}\right)^2\right\} dxdy + \frac{E\alpha h}{4(1+v)}\int_{-a}^{a}\int_{-b}^{b}\Bigg\{\Big(\theta_x +$$

$$\left.\frac{\partial w}{\partial x}\right)^2 + \left(\theta_y + \frac{\partial w}{\partial y}\right)^2\Bigg\} dxdy + \frac{1}{2}\int_{-a}^{a}\int_{-b}^{b} Kw^2\, dxdy + \frac{1}{2}\int_{-a}^{a}\int_{-b}^{b} 2t\left[\left(\frac{\partial w}{\partial y}\right)^2 + \left(\frac{\partial w}{\partial x}\right)^2\right] dxdy -$$

$$\int_{-a}^{a}\int_{-b}^{b} qw\, dxdy$$

$$F_1 = \frac{D}{2}\left\{\left(\frac{\partial \theta_x}{\partial x}\right)^2 + \left(\frac{\partial \theta_y}{\partial y}\right)^2 + 2v\frac{\partial \theta_x}{\partial x}\frac{\partial \theta_y}{\partial y} + \frac{(1-v)}{2}\left(\frac{\partial \theta_x}{\partial y} + \frac{\partial \theta_y}{\partial x}\right)^2\right\} + \frac{E\alpha h}{4(1+v)}\left\{\left(\theta_x + \frac{\partial w}{\partial x}\right)^2 +\right.$$

$$\left.\left(\theta_y + \frac{\partial w}{\partial y}\right)^2\right\} + \frac{1}{2}2t\left[\left(\frac{\partial w}{\partial x}\right)^2 + \left(\frac{\partial w}{\partial y}\right)^2\right] + \frac{1}{2}Kw^2 - qw.$$

$$\frac{\partial F_1}{\partial w}-\frac{d}{dx}\left(\frac{\partial F_1}{\partial\left(\frac{\partial w}{\partial x}\right)}\right)-\frac{d}{dy}\left(\frac{\partial F_1}{\partial\left(\frac{\partial w}{\partial y}\right)}\right)=0;\frac{\partial F_1}{\partial \theta_x}-\frac{d}{dx}\left(\frac{\partial F_1}{\partial\left(\frac{\partial \theta_x}{\partial x}\right)}\right)-\frac{d}{dy}\left(\frac{\partial F_1}{\partial\left(\frac{\partial \theta_x}{\partial y}\right)}\right)=0;\frac{\partial F_1}{\partial \theta_y}-\frac{d}{dx}\left(\frac{\partial F_1}{\partial\left(\frac{\partial \theta_y}{\partial x}\right)}\right)-$$

$$\frac{d}{dy}\left(\frac{\partial F_1}{\partial\left(\frac{\partial \theta_y}{\partial y}\right)}\right)=0$$

It is known as the Euler-Lagrange equation, which governs static equations of the equilibrium state of an elastic body.

$$\frac{\partial F_1}{\partial w}=Kw-q;\frac{\partial F_1}{\partial\left(\frac{\partial w}{\partial x}\right)}=2t\frac{\partial w}{\partial x}+\frac{E\alpha h}{2(1+v)}\left(\theta_x+\frac{\partial w}{\partial x}\right);\frac{\partial F_1}{\partial\left(\frac{\partial w}{\partial y}\right)}=2t\frac{\partial w}{\partial y}+\frac{E\alpha h}{2(1+v)}\left(\theta_y+\frac{\partial w}{\partial y}\right);$$

$$\frac{\partial F_1}{\partial \theta_x}=\frac{E\alpha h}{2(1+v)}\left(\theta_x+\frac{\partial w}{\partial x}\right);\frac{\partial F_1}{\partial\left(\frac{\partial \theta_x}{\partial x}\right)}=D\frac{\partial \theta_x}{\partial x}+Dv\frac{\partial \theta_y}{\partial y}$$

and $\frac{\partial F_1}{\partial\left(\frac{\partial \theta_x}{\partial y}\right)}=\frac{D(1-v)}{2}\left(\frac{\partial \theta_x}{\partial y}+\frac{\partial \theta_y}{\partial x}\right);\frac{\partial F_1}{\partial \theta_y}=\frac{E\alpha h}{2(1+v)}\left(\theta_y+\frac{\partial w}{\partial y}\right);$

$\frac{\partial F_1}{\partial\left(\frac{\partial \theta_y}{\partial y}\right)}=D\frac{\partial \theta_y}{\partial y}+Dv\frac{\partial \theta_x}{\partial x}$ and $\frac{\partial F_1}{\partial\left(\frac{\partial \theta_y}{\partial x}\right)}=\frac{D(1-v)}{2}\left(\frac{\partial \theta_x}{\partial y}+\frac{\partial \theta_y}{\partial x}\right)$

$$Kw-q-\frac{d}{dx}\left\{2t\frac{\partial w}{\partial x}+\frac{E\alpha h}{2(1+v)}\left(\theta_x+\frac{\partial w}{\partial x}\right)\right\}-\frac{d}{dy}\left\{2t\frac{\partial w}{\partial y}+\frac{E\alpha h}{2(1+v)}\left(\theta_y+\frac{\partial w}{\partial y}\right)\right\}=0$$

$$Kw-q-\left\{2t\frac{\partial^2 w}{\partial x^2}+\frac{E\alpha h}{2(1+v)}\left(\frac{\partial \theta_x}{\partial x}+\frac{\partial^2 w}{\partial x^2}\right)\right\}-\left\{2t\frac{\partial^2 w}{\partial y^2}+\frac{E\alpha h}{2(1+v)}\left(\frac{\partial \theta_y}{\partial y}+\frac{\partial^2 w}{\partial y^2}\right)\right\}=0$$

$$Kw-q-2t\left(\frac{\partial^2 w}{\partial x^2}+\frac{\partial^2 w}{\partial y^2}\right)-\frac{E\alpha h}{2(1+v)}\left(\frac{\partial \theta_x}{\partial x}+\frac{\partial \theta_y}{\partial y}+\frac{\partial^2 w}{\partial x^2}+\frac{\partial^2 w}{\partial y^2}\right)=0$$

$$\frac{E\alpha h}{2(1+v)}\left(\theta_x+\frac{\partial w}{\partial x}\right)-\frac{d}{dx}\left(D\frac{\partial \theta_x}{\partial x}+Dv\frac{\partial \theta_y}{\partial y}\right)-\frac{d}{dy}\left\{\frac{D(1-v)}{2}\left(\frac{\partial \theta_x}{\partial y}+\frac{\partial \theta_y}{\partial x}\right)\right\}=0$$

$$\frac{E\alpha h}{2(1+v)}\left(\theta_y+\frac{\partial w}{\partial y}\right)-\frac{d}{dy}\left(D\frac{\partial \theta_y}{\partial y}+Dv\frac{\partial \theta_x}{\partial x}\right)-\frac{d}{dx}\left\{\frac{D(1-v)}{2}\left(\frac{\partial \theta_x}{\partial y}+\frac{\partial \theta_y}{\partial x}\right)\right\}=0$$

The three governing PDE of the Mindlin plate on a two-parameter Vlasov foundation are

$$Kw-q-2t\left(\frac{\partial^2 w}{\partial x^2}+\frac{\partial^2 w}{\partial y^2}\right)-\frac{E\alpha h}{2(1+v)}\left(\frac{\partial \theta_x}{\partial x}+\frac{\partial \theta_y}{\partial y}+\frac{\partial^2 w}{\partial x^2}+\frac{\partial^2 w}{\partial y^2}\right)=0 \quad (3.2.1.12)$$

$$\frac{E\alpha h}{2(1+v)}\left(\theta_x+\frac{\partial w}{\partial x}\right)-\frac{d}{dx}\left(D\frac{\partial \theta_x}{\partial x}+Dv\frac{\partial \theta_y}{\partial y}\right)-\frac{d}{dy}\left[\frac{D(1-v)}{2}\left(\frac{\partial \theta_x}{\partial y}+\frac{\partial \theta_y}{\partial x}\right)\right]=0 \quad (3.2.1.13)$$

$$\frac{E\alpha h}{2(1+v)}\left(\theta_y+\frac{\partial w}{\partial y}\right)-\frac{d}{dy}\left(D\frac{\partial \theta_y}{\partial y}+Dv\frac{\partial \theta_x}{\partial x}\right)-\frac{d}{dx}\left[\frac{D(1-v)}{2}\left(\frac{\partial \theta_x}{\partial y}+\frac{\partial \theta_y}{\partial x}\right)\right]=0 \quad (3.2.1.14)$$

Shear correction factor

As previously mentioned, Mindlin's theory considers a constant transverse shear stress state. Such a solution does not correctly estimate the shear deformation work; a more realistic solution could be obtained by parabolic shear stress distribution. Therefore, a correction factor is introduced to better approximate the contribution of the shear deformation work. The factor is based on comparing the strain energy per unit width corresponding to the constant and the parabolic shear stress distribution.

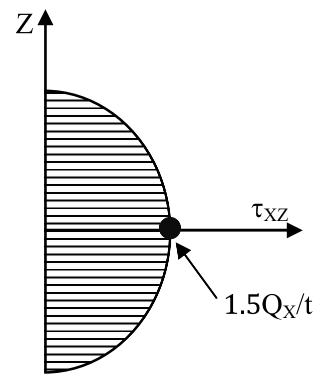

Fig. 3.5 Parabolic shear stress distributions

$$\Pi_{parabolic} = \int_{\frac{-t}{2}}^{\frac{t}{2}} \frac{1}{2}\frac{{\tau_{xz}}^2}{G}dz = \int_{\frac{-t}{2}}^{\frac{t}{2}} \frac{1}{2}\frac{\left(\frac{3Q_x}{2t}\right)^2\left[1-\left(\frac{2z}{t}\right)^2\right]^2}{G}dz = \frac{3{Q_x}^2}{5Gt} \quad \text{(Fig. 3.5)}$$

and $\Pi_{constant} = \int_{\frac{-t}{2}}^{\frac{t}{2}} \frac{1}{2}\frac{{\tau_{xz}}^2}{G}dz = \int_{\frac{-t}{2}}^{\frac{t}{2}} \frac{1}{2}\frac{\left(\frac{Q_x}{2t}\right)^2}{G}dz = \frac{{Q_x}^2}{2Gt}$

The ratio of the strain energies, in this case, is $\frac{\Pi_{constant}}{\Pi_{parabolic}} = \frac{\frac{{Q_x}^2}{2Gt}}{\frac{3{Q_x}^2}{5Gt}} = \frac{5}{6} = \alpha$

The shear correction factor for a rectangular section is 5/6; for a segment with complete warping restraint, it is 1; and for a section without any warping restraint, it is 2/3.

In this study, Higher-order displacement variations of each node written by (Kant, 1982),

$u(x,y,z) = z\theta_x(x,y) + z^3{\theta_x}^*(x,y); v(x,y,z) = z\theta_y(x,y) + z^3{\theta_y}^*(x,y)$

and $w(x,y,z) = w(x,y) + z^2w^*(x,y)$

The parameters θ^*_x, β^*_y, and w^* are the higher order terms in the Taylor series expansion and are all defined at $z = 0$.

$$\varepsilon_{xx} = \frac{\partial u}{\partial x} = z\frac{\partial\theta_x}{\partial x} + z^3\frac{\partial{\theta_x}^*}{\partial x}; \varepsilon_{yy} = \frac{\partial v}{\partial y} = z\frac{\partial\theta_y}{\partial y} + z^3\frac{\partial{\theta_y}^*}{\partial y} \text{ and } \varepsilon_{zz} = \frac{\partial w}{\partial z} = 2zw^*(x,y)$$

$$\gamma_{xy} = \frac{\partial v}{\partial x} + \frac{\partial u}{\partial y} = z\left(\frac{\partial\theta_x}{\partial y} + \frac{\partial\theta_y}{\partial x}\right) + z^3\left(\frac{\partial{\theta_x}^*}{\partial y} + \frac{\partial{\theta_y}^*}{\partial x}\right)$$

$$\gamma_{xz} = \frac{\partial u}{\partial z} + \frac{\partial w}{\partial x} = \theta_x + 3z^2\theta_x{}^* + \frac{\partial w}{\partial x} + z^2\frac{\partial w^*}{\partial x} = \left(\theta_x + \frac{\partial w}{\partial x}\right) + z^2\left(3\theta_x{}^* + \frac{\partial w^*}{\partial x}\right)$$

$$\gamma_{yz} = \frac{\partial v}{\partial z} + \frac{\partial w}{\partial y} = \theta_y + 3z^2\theta_y{}^* + \frac{\partial w}{\partial y} + z^2\frac{\partial w^*}{\partial y} = \left(\theta_y + \frac{\partial w}{\partial y}\right) + z^2\left(3\theta_y{}^* + \frac{\partial w^*}{\partial y}\right)$$

$$\begin{bmatrix}\sigma_{xx}\\ \sigma_{yy}\\ \sigma_{zz}\\ \tau_{xy}\\ \tau_{yz}\\ \tau_{xz}\end{bmatrix} = \frac{E}{(1+v)(1-2v)}\begin{bmatrix}1-v & v & v & 0 & 0 & 0\\ v & 1-v & v & 0 & 0 & 0\\ v & v & 1-v & 0 & 0 & 0\\ 0 & 0 & 0 & \frac{1-2v}{2} & 0 & 0\\ 0 & 0 & 0 & 0 & \frac{1-2v}{2} & 0\\ 0 & 0 & 0 & 0 & 0 & \frac{1-2v}{2}\end{bmatrix}\begin{Bmatrix}\varepsilon_{xx}\\ \varepsilon_{yy}\\ \varepsilon_{zz}\\ \gamma_{xy}\\ \gamma_{yz}\\ \gamma_{xz}\end{Bmatrix}$$

Lames constant, $\lambda = \frac{Ev}{(1+v)(1-2v)}$ and $G = \frac{E}{2(1+v)}$ $\therefore \lambda + 2G = \frac{E(1-v)}{(1+v)(1-2v)}$

$$\begin{bmatrix}\sigma_{xx}\\ \sigma_{yy}\\ \sigma_{zz}\\ \tau_{xy}\\ \tau_{yz}\\ \tau_{xz}\end{bmatrix} = \begin{bmatrix}\lambda+2G & \lambda & \lambda & 0 & 0 & 0\\ \lambda & \lambda+2G & \lambda & 0 & 0 & 0\\ \lambda & \lambda & \lambda+2G & 0 & 0 & 0\\ 0 & 0 & 0 & G & 0 & 0\\ 0 & 0 & 0 & 0 & G & 0\\ 0 & 0 & 0 & 0 & 0 & G\end{bmatrix}\begin{Bmatrix}\varepsilon_{xx}\\ \varepsilon_{yy}\\ \varepsilon_{zz}\\ \gamma_{xy}\\ \gamma_{yz}\\ \gamma_{xz}\end{Bmatrix}$$

The total potential energy of the soil-plate system subjected to a UDL of q is given by

$\Pi = \Pi_p + \Pi_s + V$

The strain energy deformation in the HSDT plate corresponding to bending, shear deformation and normal deformation is

Strain energy, $\Pi p = \frac{1}{2}\sigma_{ij}\varepsilon_{ij}dV = \frac{1}{2}\sigma_{ij}\varepsilon_{ij}dxdydz$

$$\Pi p = \frac{1}{2}\int\int\int\left(\sigma_{xx}\varepsilon_{xx} + \sigma_{yy}\varepsilon_{yy} + \sigma_{zz}\varepsilon_{zz} + \tau_{xy}\gamma_{xy} + \tau_{yz}\gamma_{yz} + \tau_{xz}\gamma_{xz}\right)dxdydz$$

$$\therefore \Pi_p = \frac{1}{2}\int\int\int\left(\left\{(\lambda+2G)\varepsilon_{xx} + \lambda\varepsilon_{yy} + \lambda\varepsilon_{zz}\right\}\varepsilon_{xx} + \left\{\lambda\varepsilon_{xx} + (\lambda+2G)\varepsilon_{yy} + \lambda\varepsilon_{zz}\right\}\varepsilon_{yy} + \left\{\lambda\varepsilon_{xx} + \lambda\varepsilon_{yy} + (\lambda+2G)\varepsilon_{zz}\right\}\varepsilon_{zz} + G\gamma_{xy}{}^2 + G\gamma_{yz}{}^2 + G\gamma_{xz}{}^2\right)dxdydz$$

$$\therefore \Pi_p = \frac{1}{2}(\lambda+2G)\int_{-a}^{a}\int_{-b}^{b}\int_{-h/2}^{h/2}\left(\varepsilon_{xx}{}^2 + \varepsilon_{yy}{}^2 + \varepsilon_{zz}{}^2\right)dxdydz + \lambda\int_{-a}^{a}\int_{-b}^{b}\int_{-h/2}^{h/2}\left(\varepsilon_{xx}\varepsilon_{yy} + \varepsilon_{xx}\varepsilon_{zz} + \varepsilon_{zz}\varepsilon_{yy}\right)dxdydz + \frac{G}{2}\int_{-a}^{a}\int_{-b}^{b}\int_{-h/2}^{h/2}\left(\gamma_{xy}{}^2 + \gamma_{yz}{}^2 + \gamma_{xz}{}^2\right)dxdydz$$

$$\varepsilon_{xx} = z\frac{\partial\theta_x}{\partial x} + z^3\frac{\partial\theta_x{}^*}{\partial x};\ \varepsilon_{yy} = z\frac{\partial\theta_y}{\partial y} + z^3\frac{\partial\theta_y{}^*}{\partial y};\ \varepsilon_{zz} = \frac{\partial w}{\partial z}$$

$$\gamma_{xy} = z\left(\frac{\partial\theta_x}{\partial y} + \frac{\partial\theta_y}{\partial x}\right) + z^3\left(\frac{\partial\theta_x{}^*}{\partial y} + \frac{\partial\theta_y{}^*}{\partial x}\right);\ \gamma_{xz} = \left(\theta_x + \frac{\partial w}{\partial x}\right) + z^2\left(3\theta_x{}^* + \frac{\partial w^*}{\partial x}\right);\ \gamma_{yz} = \left(\theta_y + \frac{\partial w}{\partial y}\right) + z^2\left(3\theta_y{}^* + \frac{\partial w^*}{\partial y}\right)$$

$$\therefore \Pi_p = \frac{(\lambda+2G)}{2}\int_{-a}^{a}\int_{-b}^{b}\int_{-h/2}^{h/2}\left[\left(z\frac{\partial\theta_x}{\partial x} + z^3\frac{\partial{\theta_x}^*}{\partial x}\right)^2 + \left(z\frac{\partial\theta_y}{\partial y} + z^3\frac{\partial{\theta_y}^*}{\partial y}\right)^2 + 4z^2w^*\right]dxdydz + \lambda\int_{-a}^{a}\int_{-b}^{b}\int_{-h/2}^{h/2}\left[\left(z\frac{\partial\theta_x}{\partial x} + z^3\frac{\partial{\theta_x}^*}{\partial x}\right)\left(z\frac{\partial\theta_y}{\partial y} + z^3\frac{\partial{\theta_y}^*}{\partial y}\right) + \left(2z^2\frac{\partial\theta_x}{\partial x} + 2z^4\frac{\partial{\theta_x}^*}{\partial x}\right)w^* + \left(2z^2\frac{\partial\theta_y}{\partial y} + 2z^4\frac{\partial{\theta_y}^*}{\partial y}\right)w^*\right]dxdydz + \frac{G}{2}\int_{-a}^{a}\int_{-b}^{b}\int_{-h/2}^{h/2}\left[\left\{z\left(\frac{\partial\theta_x}{\partial y} + \frac{\partial\theta_y}{\partial x}\right) + z^3\left(\frac{\partial{\theta_x}^*}{\partial y} + \frac{\partial{\theta_y}^*}{\partial x}\right)\right\}^2 + \left\{\left(\theta_y + \frac{\partial w}{\partial y}\right) + z^2\left(3{\theta_y}^* + \frac{\partial w^*}{\partial y}\right)\right\}^2 + \left(\theta_x + \frac{\partial w}{\partial x}\right) + z^2\left\{3{\theta_x}^* + \frac{\partial w^*}{\partial x}\right\}^2\right]dxdydz$$

Potential energy functional due to the applied transverse load $q_z(x, y)$

The potential energy functional due to the work done by the applied transverse distributed load $q_z(x, y)$ is denoted by V and given by the double integral over the plate domain:

$$V = -\int_{-a}^{a}\int_{-b}^{b} qw\, dxdy$$

Total potential energy functional, Π

The total potential energy functional for the HSDT plate on a two-parameter elastic foundation problem is the sum of the strain energy functional, the potential energy functional due to the distributed transverse loads and the potential energy functional due to the two-parameter elastic foundation Π.

$$\Pi = \frac{(\lambda+2G)}{2}\int_{-a}^{a}\int_{-b}^{b}\int_{-h/2}^{h/2}\left[\left(z\frac{\partial\theta_x}{\partial x} + z^3\frac{\partial{\theta_x}^*}{\partial x}\right)^2 + \left(z\frac{\partial\theta_y}{\partial y} + z^3\frac{\partial{\theta_y}^*}{\partial y}\right)^2 + 4z^2w^*\right]dxdydz + \lambda\int_{-a}^{a}\int_{-b}^{b}\int_{-h/2}^{h/2}\left[\left(z\frac{\partial\theta_x}{\partial x} + z^3\frac{\partial{\theta_x}^*}{\partial x}\right)\left(z\frac{\partial\theta_y}{\partial y} + z^3\frac{\partial{\theta_y}^*}{\partial y}\right) + \left(2z^2\frac{\partial\theta_x}{\partial x} + 2z^4\frac{\partial{\theta_x}^*}{\partial x}\right)w^* + \left(2z^2\frac{\partial\theta_y}{\partial y} + 2z^4\frac{\partial{\theta_y}^*}{\partial y}\right)w^*\right]dxdydz + \frac{G}{2}\int_{-a}^{a}\int_{-b}^{b}\int_{-h/2}^{h/2}\left[\left\{z\left(\frac{\partial\theta_x}{\partial y} + \frac{\partial\theta_y}{\partial x}\right) + z^3\left(\frac{\partial{\theta_x}^*}{\partial y} + \frac{\partial{\theta_y}^*}{\partial x}\right)\right\}^2 + \left\{\left(\theta_y + \frac{\partial w}{\partial y}\right) + z^2\left(3{\theta_y}^* + \frac{\partial w^*}{\partial y}\right)\right\}^2 + \left(\theta_x + \frac{\partial w}{\partial x}\right) + z^2\left\{3{\theta_x}^* + \frac{\partial w^*}{\partial x}\right\}^2\right]dxdydz + \frac{1}{2}\int_{0}^{H}\int_{-\infty}^{\infty}\int_{-\infty}^{\infty}\left[\bar{E}w^2\left(\frac{\partial\varphi}{\partial z}\right)^2 + G_s\varphi^2\left[\left(\frac{\partial w}{\partial y}\right)^2 + \left(\frac{\partial w}{\partial x}\right)^2\right]\right]dxdydz - \int_{-a}^{a}\int_{-b}^{b} qw\, dxdy$$

$$\Pi = \frac{(\lambda+2G)}{2}\int_{-a}^{a}\int_{-b}^{b}\int_{-h/2}^{h/2}\left[\left(z\frac{\partial\theta_x}{\partial x} + z^3\frac{\partial{\theta_x}^*}{\partial x}\right)^2 + \left(z\frac{\partial\theta_y}{\partial y} + z^3\frac{\partial{\theta_y}^*}{\partial y}\right)^2 + 4z^2w^*\right]dxdydz + \lambda\int_{-a}^{a}\int_{-b}^{b}\int_{-h/2}^{h/2}\left[\left(z\frac{\partial\theta_x}{\partial x} + z^3\frac{\partial{\theta_x}^*}{\partial x}\right)\left(z\frac{\partial\theta_y}{\partial y} + z^3\frac{\partial{\theta_y}^*}{\partial y}\right) + \left(2z^2\frac{\partial\theta_x}{\partial x} + 2z^4\frac{\partial{\theta_x}^*}{\partial x}\right)w^* + \left(2z^2\frac{\partial\theta_y}{\partial y} + 2z^4\frac{\partial{\theta_y}^*}{\partial y}\right)w^*\right]dxdydz + \frac{G}{2}\int_{-a}^{a}\int_{-b}^{b}\int_{-h/2}^{h/2}\left[\left\{z\left(\frac{\partial\theta_x}{\partial y} + \frac{\partial\theta_y}{\partial x}\right) + z^3\left(\frac{\partial{\theta_x}^*}{\partial y} + \frac{\partial{\theta_y}^*}{\partial x}\right)\right\}^2 + \left\{\left(\theta_y + \frac{\partial w}{\partial y}\right) +\right.\right.$$

$$z^2\left(3\theta_y{}^* + \frac{\partial w^*}{\partial y}\right)\Big\}^2 + \left(\theta_x + \frac{\partial w}{\partial x}\right) + z^2\left\{3\theta_x{}^* + \frac{\partial w^*}{\partial x}\right\}^2\Bigg]\,dxdydz +$$

$$\frac{1}{2}\int_{-\infty}^{\infty}\int_{-\infty}^{\infty}\left(\int_0^H \overline{E}\left(\frac{\partial\varphi}{\partial z}\right)^2 dz\right) w^2\,dxdy + \frac{1}{2}\int_{-\infty}^{\infty}\int_{-\infty}^{\infty}\left(\int_0^H G_s\varphi^2 dz\right)(\nabla w)^2\,dxdy - \int_{-a}^{a}\int_{-b}^{b} qw\,dxdy$$

$$\Pi = \frac{(\lambda+2G)}{2}\int_{-a}^{a}\int_{-b}^{b}\int_{-h/2}^{h/2}\left[\left(z\frac{\partial\theta_x}{\partial x} + z^3\frac{\partial\theta_x{}^*}{\partial x}\right)^2 + \left(z\frac{\partial\theta_y}{\partial y} + z^3\frac{\partial\theta_y{}^*}{\partial y}\right)^2 + 4z^2w^*\right]dxdydz +$$

$$\lambda\int_{-a}^{a}\int_{-b}^{b}\int_{-h/2}^{h/2}\left[\left(z\frac{\partial\theta_x}{\partial x} + z^3\frac{\partial\theta_x{}^*}{\partial x}\right)\left(z\frac{\partial\theta_y}{\partial y} + z^3\frac{\partial\theta_y{}^*}{\partial y}\right) + \left(2z^2\frac{\partial\theta_x}{\partial x} + 2z^4\frac{\partial\theta_x{}^*}{\partial x}\right)w^* + \left(2z^2\frac{\partial\theta_y}{\partial y} +\right.\right.$$

$$\left.\left.2z^4\frac{\partial\theta_y{}^*}{\partial y}\right)w^*\right]dxdydz + \frac{G}{2}\int_{-a}^{a}\int_{-b}^{b}\int_{-h/2}^{h/2}\left[\left\{z\left(\frac{\partial\theta_x}{\partial y} + \frac{\partial\theta_y}{\partial x}\right) + z^3\left(\frac{\partial\theta_x{}^*}{\partial y} + \frac{\partial\theta_y{}^*}{\partial x}\right)\right\}^2 + \left\{\left(\theta_y + \frac{\partial w}{\partial y}\right) +\right.\right.$$

$$z^2\left(3\theta_y{}^* + \frac{\partial w^*}{\partial y}\right)\Big\}^2 + \left(\theta_x + \frac{\partial w}{\partial x}\right) + z^2\left\{3\theta_x{}^* + \frac{\partial w^*}{\partial x}\right\}^2\Bigg]\,dxdydz + \frac{1}{2}\int_{-\infty}^{\infty}\int_{-\infty}^{\infty} Kw^2\,dxdy +$$

$$\frac{1}{2}\int_{-\infty}^{\infty}\int_{-\infty}^{\infty} 2t\left[\left(\frac{\partial w}{\partial y}\right)^2 + \left(\frac{\partial w}{\partial x}\right)^2\right]dxdy - \int_{-a}^{a}\int_{-b}^{b} qw\,dxdy$$

Where $K = \int_0^H \overline{E}\left(\frac{\partial\varphi}{\partial z}\right)^2 dz$ and $2t = \int_0^H G_s\varphi^2 dz$

$$\Pi = \frac{(\lambda+2G)}{2}\int_{-a}^{a}\int_{-b}^{b}\left[\frac{h^3}{12}\left(\frac{\partial\theta_x}{\partial x}\right)^2 + \frac{h^5}{40}\left(\frac{\partial\theta_x}{\partial x}\frac{\partial\theta_x{}^*}{\partial x}\right) + \frac{h^7}{448}\left(\frac{\partial\theta_x{}^*}{\partial x}\right)^2 + \frac{h^3}{12}\left(\frac{\partial\theta_y}{\partial y}\right)^2 + \frac{h^5}{40}\left(\frac{\partial\theta_y}{\partial y}\frac{\partial\theta_y{}^*}{\partial y}\right) +\right.$$

$$\left.\frac{h^7}{448}\left(\frac{\partial\theta_y{}^*}{\partial y}\right)^2 + \frac{h^3}{3}w^*\right]dxdy +$$

$$\lambda\int_{-a}^{a}\int_{-b}^{b}\left[\frac{h^5}{80}\left(\frac{\partial\theta_x}{\partial x}\frac{\partial\theta_y{}^*}{\partial y} + \frac{\partial\theta_x{}^*}{\partial x}\frac{\partial\theta_y}{\partial y}\right) + \frac{h^3}{12}\left(\frac{\partial\theta_x}{\partial x}\frac{\partial\theta_y}{\partial y}\right) + \frac{h^7}{448}\left(\frac{\partial\theta_x{}^*}{\partial x}\frac{\partial\theta_y{}^*}{\partial y}\right) + \frac{h^3}{6}w^*\frac{\partial\theta_x}{\partial x} + \frac{h^5}{40}w^*\frac{\partial\theta_x{}^*}{\partial x} +\right.$$

$$\left.\frac{h^3}{6}w^*\frac{\partial\theta_y}{\partial y} + \frac{h^5}{40}w^*\frac{\partial\theta_y{}^*}{\partial y}\right]dxdy + \frac{G}{2}\int_{-a}^{a}\int_{-b}^{b}\left[\frac{h^3}{12}\left(\frac{\partial\theta_x}{\partial y} + \frac{\partial\theta_y}{\partial x}\right)^2 + \frac{h^5}{40}\left(\frac{\partial\theta_x}{\partial y}\frac{\partial\theta_x{}^*}{\partial y} + \frac{\partial\theta_x}{\partial y}\frac{\partial\theta_y{}^*}{\partial x} + \frac{\partial\theta_x}{\partial y}\frac{\partial\theta_x{}^*}{\partial y} +\right.\right.$$

$$\left.\frac{\partial\theta_x}{\partial y}\frac{\partial\theta_y{}^*}{\partial x}\right) + \frac{h^7}{448}\left\{\left(\frac{\partial\theta_x{}^*}{\partial y}\right)^2 + 2\frac{\partial\theta_x{}^*}{\partial y}\frac{\partial\theta_y{}^*}{\partial x} + \left(\frac{\partial\theta_y{}^*}{\partial x}\right)^2\right\} + h\left\{\theta_y{}^2 + 2\theta_y\frac{\partial w}{\partial y} + \left(\frac{\partial w}{\partial y}\right)^2\right\} +$$

$$\frac{h^5}{80}\left\{9\theta_y{}^{*2} + 6\theta_y{}^*\frac{\partial w^*}{\partial y} + \left(\frac{\partial w^*}{\partial y}\right)^2\right\} + \frac{h^3}{6}\left(3\theta_y\theta_y{}^* + \theta_y\frac{\partial w^*}{\partial y} + 3\theta_y{}^*\frac{\partial w}{\partial y} + \frac{\partial w}{\partial y}\frac{\partial w^*}{\partial y}\right) + h\left\{\theta_x{}^2 +\right.$$

$$\left.2\theta_x\frac{\partial w}{\partial x} + \left(\frac{\partial w}{\partial x}\right)^2\right\} + \frac{h^5}{80}\left\{9\theta_x{}^{*2} + 6\theta_x{}^*\frac{\partial w^*}{\partial x} + \left(\frac{\partial w^*}{\partial x}\right)^2\right\} + \frac{h^3}{6}\left(3\theta_x\theta_x{}^* + \theta_x\frac{\partial w^*}{\partial x} + 3\theta_x{}^*\frac{\partial w}{\partial x} +\right.$$

$$\left.\left.\frac{\partial w}{\partial x}\frac{\partial w^*}{\partial x}\right)\right]dxdy + \frac{1}{2}\int_{-\infty}^{\infty}\int_{-\infty}^{\infty} Kw^2\,dxdy + \frac{1}{2}\int_{-\infty}^{\infty}\int_{-\infty}^{\infty} 2t\left[\left(\frac{\partial w}{\partial y}\right)^2 + \left(\frac{\partial w}{\partial x}\right)^2\right]dxdy -$$

$$\int_{-a}^{a}\int_{-b}^{b} qw\,dxdy$$

Now strain energy of the plate soil system within the plate domain is

$$\Pi = \frac{(\lambda+2G)}{2}\int_{-a}^{a}\int_{-b}^{b}\Bigg[\frac{h^3}{12}\left(\frac{\partial\theta_x}{\partial x}\right)^2 + \frac{h^5}{40}\left(\frac{\partial\theta_x}{\partial x}\frac{\partial\theta_x{}^*}{\partial x}\right) + \frac{h^7}{448}\left(\frac{\partial\theta_x{}^*}{\partial x}\right)^2 + \frac{h^3}{12}\left(\frac{\partial\theta_y}{\partial y}\right)^2 + \frac{h^5}{40}\left(\frac{\partial\theta_y}{\partial y}\frac{\partial\theta_y{}^*}{\partial y}\right) + \frac{h^7}{448}\left(\frac{\partial\theta_y{}^*}{\partial y}\right)^2 + \frac{h^3}{3}w^*\Bigg]dxdy + \lambda\int_{-a}^{a}\int_{-b}^{b}\Bigg[\frac{h^5}{80}\left(\frac{\partial\theta_x}{\partial x}\frac{\partial\theta_y{}^*}{\partial y} + \frac{\partial\theta_x{}^*}{\partial x}\frac{\partial\theta_y}{\partial y}\right) + \frac{h^3}{12}\left(\frac{\partial\theta_x}{\partial x}\frac{\partial\theta_y}{\partial y}\right) + \frac{h^7}{448}\left(\frac{\partial\theta_x{}^*}{\partial x}\frac{\partial\theta_y{}^*}{\partial y}\right) + \frac{h^3}{6}w^*\frac{\partial\theta_x}{\partial x} + \frac{h^5}{40}w^*\frac{\partial\theta_x{}^*}{\partial x} + \frac{h^3}{6}w^*\frac{\partial\theta_y}{\partial y} + \frac{h^5}{40}w^*\frac{\partial\theta_y{}^*}{\partial y}\Bigg]dxdy + \frac{G}{2}\int_{-a}^{a}\int_{-b}^{b}\Bigg[\frac{h^3}{12}\left(\frac{\partial\theta_x}{\partial y} + \frac{\partial\theta_y}{\partial x}\right)^2 + \frac{h^5}{40}\left(\frac{\partial\theta_x}{\partial y}\frac{\partial\theta_x{}^*}{\partial y} + \frac{\partial\theta_x}{\partial y}\frac{\partial\theta_y{}^*}{\partial x} + \frac{\partial\theta_x}{\partial y}\frac{\partial\theta_x{}^*}{\partial y} + \frac{\partial\theta_x}{\partial y}\frac{\partial\theta_y{}^*}{\partial x}\right) + \frac{h^7}{448}\left\{\left(\frac{\partial\theta_x{}^*}{\partial y}\right)^2 + 2\frac{\partial\theta_x{}^*}{\partial y}\frac{\partial\theta_y{}^*}{\partial x} + \left(\frac{\partial\theta_y{}^*}{\partial x}\right)^2\right\} + h\left\{\theta_y{}^2 + 2\theta_y\frac{\partial w}{\partial y} + \left(\frac{\partial w}{\partial y}\right)^2\right\} + \frac{h^5}{80}\left\{9\theta_y{}^{*2} + 6\theta_y{}^*\frac{\partial w^*}{\partial y} + \left(\frac{\partial w^*}{\partial y}\right)^2\right\} + \frac{h^3}{6}\left(3\theta_y\theta_y{}^* + \theta_y\frac{\partial w^*}{\partial y} + 3\theta_y{}^*\frac{\partial w}{\partial y} + \frac{\partial w}{\partial y}\frac{\partial w^*}{\partial y}\right) + h\left\{\theta_x{}^2 + 2\theta_x\frac{\partial w}{\partial x} + \left(\frac{\partial w}{\partial x}\right)^2\right\} + \frac{h^5}{80}\left\{9\theta_x{}^{*2} + 6\theta_x{}^*\frac{\partial w^*}{\partial x} + \left(\frac{\partial w^*}{\partial x}\right)^2\right\} + \frac{h^3}{6}\left(3\theta_x\theta_x{}^* + \theta_x\frac{\partial w^*}{\partial x} + 3\theta_x{}^*\frac{\partial w}{\partial x} + \frac{\partial w}{\partial x}\frac{\partial w^*}{\partial x}\right)\Bigg]dxdy + \frac{1}{2}\int_{-a}^{a}\int_{-b}^{b}Kw^2\,dxdy + \frac{1}{2}\int_{-a}^{a}\int_{-b}^{b}2t\left[\left(\frac{\partial w}{\partial y}\right)^2 + \left(\frac{\partial w}{\partial x}\right)^2\right]dxdy - \int_{-a}^{a}\int_{-b}^{b}qw\,dxdy$$

We can now use the calculus of variations to obtain the equilibrium equations. For a stable equilibrium state to be reached, first, the variation of the potential energy must be zero ($\delta\Pi = 0$). First, we consider the plate soil system within the plate domain and take variations on w. Taking variations on w, we get the following

$$F_1 = \frac{(\lambda+2G)}{2}\Bigg[\frac{h^3}{12}\left(\frac{\partial\theta_x}{\partial x}\right)^2 + \frac{h^5}{40}\left(\frac{\partial\theta_x}{\partial x}\frac{\partial\theta_x{}^*}{\partial x}\right) + \frac{h^7}{448}\left(\frac{\partial\theta_x{}^*}{\partial x}\right)^2 + \frac{h^3}{12}\left(\frac{\partial\theta_y}{\partial y}\right)^2 + \frac{h^5}{40}\left(\frac{\partial\theta_y}{\partial y}\frac{\partial\theta_y{}^*}{\partial y}\right) + \frac{h^7}{448}\left(\frac{\partial\theta_y{}^*}{\partial y}\right)^2 + \frac{h^3}{3}w^*\Bigg] + \lambda\Bigg[\frac{h^5}{80}\left(\frac{\partial\theta_x}{\partial x}\frac{\partial\theta_y{}^*}{\partial y} + \frac{\partial\theta_x{}^*}{\partial x}\frac{\partial\theta_y}{\partial y}\right) + \frac{h^3}{12}\left(\frac{\partial\theta_x}{\partial x}\frac{\partial\theta_y}{\partial y}\right) + \frac{h^7}{448}\left(\frac{\partial\theta_x{}^*}{\partial x}\frac{\partial\theta_y{}^*}{\partial y}\right) + \frac{h^3}{6}w^*\frac{\partial\theta_x}{\partial x} + \frac{h^5}{40}w^*\frac{\partial\theta_x{}^*}{\partial x} + \frac{h^3}{6}w^*\frac{\partial\theta_y}{\partial y} + \frac{h^5}{40}w^*\frac{\partial\theta_y{}^*}{\partial y}\Bigg] + \frac{G}{2}\Bigg[\frac{h^3}{12}\left(\frac{\partial\theta_x}{\partial y} + \frac{\partial\theta_y}{\partial x}\right)^2 + \frac{h^5}{40}\left(\frac{\partial\theta_x}{\partial y}\frac{\partial\theta_x{}^*}{\partial y} + \frac{\partial\theta_x}{\partial y}\frac{\partial\theta_y{}^*}{\partial x} + \frac{\partial\theta_x}{\partial y}\frac{\partial\theta_x{}^*}{\partial y} + \frac{\partial\theta_x}{\partial y}\frac{\partial\theta_y{}^*}{\partial x}\right) + \frac{h^7}{448}\left\{\left(\frac{\partial\theta_x{}^*}{\partial y}\right)^2 + 2\frac{\partial\theta_x{}^*}{\partial y}\frac{\partial\theta_y{}^*}{\partial x} + \left(\frac{\partial\theta_y{}^*}{\partial x}\right)^2\right\} + h\left\{\theta_y{}^2 + 2\theta_y\frac{\partial w}{\partial y} + \left(\frac{\partial w}{\partial y}\right)^2\right\} + \frac{h^5}{80}\left\{9\theta_y{}^{*2} + 6\theta_y{}^*\frac{\partial w^*}{\partial y} + \left(\frac{\partial w^*}{\partial y}\right)^2\right\} + \frac{h^3}{6}\left(3\theta_y\theta_y{}^* + \theta_y\frac{\partial w^*}{\partial y} + 3\theta_y{}^*\frac{\partial w}{\partial y} + \frac{\partial w}{\partial y}\frac{\partial w^*}{\partial y}\right) + h\left\{\theta_x{}^2 + 2\theta_x\frac{\partial w}{\partial x} + \left(\frac{\partial w}{\partial x}\right)^2\right\} + \frac{h^5}{80}\left\{9\theta_x{}^{*2} + 6\theta_x{}^*\frac{\partial w^*}{\partial x} + \left(\frac{\partial w^*}{\partial x}\right)^2\right\} + \frac{h^3}{6}\left(3\theta_x\theta_x{}^* + \theta_x\frac{\partial w^*}{\partial x} + 3\theta_x{}^*\frac{\partial w}{\partial x} + \frac{\partial w}{\partial x}\frac{\partial w^*}{\partial x}\right)\Bigg] + \frac{1}{2}2t\left[\left(\frac{\partial w}{\partial y}\right)^2 + \left(\frac{\partial w}{\partial x}\right)^2\right] + \frac{1}{2}Kw^2 - qw.$$

$$\frac{\partial F_1}{\partial w}-\frac{d}{dx}\left(\frac{\partial F_1}{\partial\left(\frac{dw}{dx}\right)}\right)-\frac{d}{dy}\left(\frac{\partial F_1}{\partial\left(\frac{dw}{dy}\right)}\right)=0 \tag{3.2.1.15}$$

$$\frac{\partial F_1}{\partial \theta_x}-\frac{d}{dx}\left(\frac{\partial F_1}{\partial\left(\frac{\partial \theta_x}{\partial x}\right)}\right)-\frac{d}{dy}\left(\frac{\partial F_1}{\partial\left(\frac{\partial \theta_x}{\partial y}\right)}\right)=0 \tag{3.2.1.16}$$

$$\frac{\partial F_1}{\partial \theta_y}-\frac{d}{dx}\left(\frac{\partial F_1}{\partial\left(\frac{\partial \theta_y}{\partial x}\right)}\right)-\frac{d}{dy}\left(\frac{\partial F_1}{\partial\left(\frac{\partial \theta_y}{\partial y}\right)}\right)=0 \tag{3.2.1.17}$$

$$\frac{\partial F_1}{\partial w^*}-\frac{d}{dx}\left(\frac{\partial F_1}{\partial\left(\frac{dw^*}{dx}\right)}\right)-\frac{d}{dy}\left(\frac{\partial F_1}{\partial\left(\frac{dw^*}{dy}\right)}\right)=0 \tag{3.2.1.18}$$

$$\frac{\partial F_1}{\partial {\theta_x}^*}-\frac{d}{dx}\left(\frac{\partial F_1}{\partial\left(\frac{\partial {\theta_x}^*}{\partial x}\right)}\right)-\frac{d}{dy}\left(\frac{\partial F_1}{\partial\left(\frac{\partial {\theta_x}^*}{\partial y}\right)}\right)=0 \tag{3.2.1.19}$$

$$\frac{\partial F_1}{\partial {\theta_y}^*}-\frac{d}{dx}\left(\frac{\partial F_1}{\partial\left(\frac{\partial {\theta_y}^*}{\partial x}\right)}\right)-\frac{d}{dy}\left(\frac{\partial F_1}{\partial\left(\frac{\partial {\theta_y}^*}{\partial y}\right)}\right)=0 \tag{3.2.1.20}$$

Are the six governing PDE of the HSDT plate on a two-parameter Vlasov foundation.

3.3 Response analysis of circular plate/raft on elastic foundations

3.3.1 Development of the theory of the Vlasov model

Plane strain conditions are assumed applicable to elastic half-space. Since lateral strains are minimal compared with vertical strains, they can be neglected.

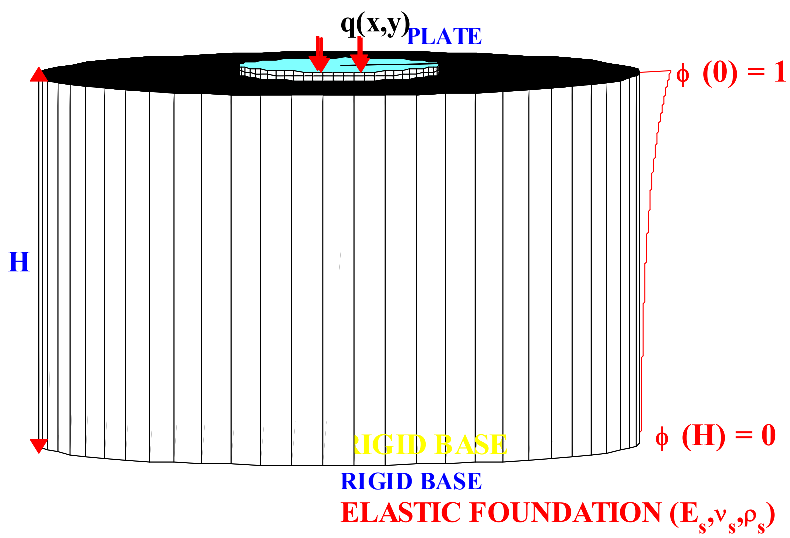

Fig. 3.6 Finite circular plates resting on two-parameter Elastic foundation

Vlasov made the following assumptions to simplify the derivation of the governing equations.

- The first assumption that he employed was to keep

$u(r,\theta,z) = 0$; $v(r,\theta,z) = 0$ in the soil.

- The second assumption that he made in his formulation is to select only a single term describing the w displacement function, that is,

  and $w(r,\theta,z) = w(r,\theta)\varphi(z)$ (Fig. 3.6) .

  Where $\varphi(z)$ is the function describing the variation of the function w from the top of the soil to its bottom such that $\varphi(0) = 1$ and $\varphi(H) = 0$, it is further assumed that the displacements of the surface of the soil are equal to the displacements of the middle surface of the plate, $w(r,\theta,0) = w(r,\theta)$ and the strain components $\boldsymbol{\varepsilon}_{rr}$, $\boldsymbol{\varepsilon}_{\theta\theta}$ and $\gamma_{r\theta}$ will therefore vanish.

Strain field $\varepsilon_{rr} = \frac{\partial u}{\partial r} = 0;\ \varepsilon_{\theta\theta} = \frac{\partial v}{\partial \theta} = 0;\ \varepsilon_{zz} = w\frac{\partial \varphi}{\partial z};\ \gamma_{r\theta} = \frac{\partial u}{\partial \theta} + \frac{\partial v}{\partial r} = 0;$

$\gamma_{\theta z} = \frac{\partial w}{\partial \theta} + \frac{\partial v}{\partial z} = 0;\ \gamma_{rz} = \frac{\partial u}{\partial z} + \frac{\partial w}{\partial r} = \frac{\partial w}{\partial r}\varphi$

$$\begin{Bmatrix} \varepsilon_{rr} \\ \varepsilon_{\theta\theta} \\ \varepsilon_{zz} \\ \gamma_{r\theta} \\ \gamma_{\theta z} \\ \gamma_{zr} \end{Bmatrix} = \begin{bmatrix} 0 \\ 0 \\ w\frac{\partial \varphi}{\partial z} \\ 0 \\ 0 \\ \varphi\frac{\partial w}{\partial r} \end{bmatrix};$$

$$\begin{bmatrix} \sigma_{rr} \\ \sigma_{\theta\theta} \\ \sigma_{zz} \\ \tau_{r\theta} \\ \tau_{\theta z} \\ \tau_{rz} \end{bmatrix} = \frac{E_s}{(1+v_s)(1-2v_s)} \begin{bmatrix} 1-v_s & v_s & v_s & 0 & 0 & 0 \\ v_s & 1-v_s & v_s & 0 & 0 & 0 \\ v_s & v_s & 1-v_s & 0 & 0 & 0 \\ 0 & 0 & 0 & \frac{1-2v_s}{2} & 0 & 0 \\ 0 & 0 & 0 & 0 & \frac{1-2v_s}{2} & 0 \\ 0 & 0 & 0 & 0 & 0 & \frac{1-2v_s}{2} \end{bmatrix} \begin{bmatrix} 0 \\ 0 \\ w\frac{\partial \varphi}{\partial z} \\ 0 \\ 0 \\ \varphi\frac{\partial w}{\partial r} \end{bmatrix}$$

$$\therefore \begin{bmatrix} \sigma_{zz} \\ \tau_{\theta z} \\ \tau_{rz} \end{bmatrix} = \frac{E_s}{(1+v_s)(1-2v_s)} \begin{bmatrix} 1-v_s & 0 & 0 \\ 0 & \frac{1-2v_s}{2} & 0 \\ 0 & 0 & \frac{1-2v_s}{2} \end{bmatrix} \begin{bmatrix} \varepsilon_{zz} \\ \gamma_{\theta z} \\ \gamma_{rz} \end{bmatrix};$$

$\overline{E} = \frac{E_s(1-v_s)}{(1+v_s)(1-2v_s)};\ G_s = \frac{E_s}{2(1+v_s)};\ \therefore \sigma_z = \overline{E}\varepsilon_{zz} = \overline{E}w\frac{\partial \varphi}{\partial z};\ \tau_{\theta z} = G_s \times 0$ and $\tau_{rz} = G_s\frac{\partial w}{\partial r}\varphi$

Strain energy, $\Pi_s = \frac{1}{2}\sigma_{ij}\varepsilon_{ij}dV = \frac{1}{2}\sigma_{ij}\varepsilon_{ij}rdrd\theta dz = \frac{1}{2}\int\int\int(\sigma_z\varepsilon_z + \tau_{rz}\gamma_{rz})rdrd\theta dz$

$$\Pi_s = \frac{1}{2}\int_0^H\int_0^{2\pi}\int_{-\infty}^{\infty}\left[\overline{E}\left(w\frac{\partial \varphi}{\partial z}\right)^2 + G_s\left(\frac{\partial w}{\partial r}\varphi\right)^2\right]rdrd\theta dz$$

$$\Pi_s = \pi\int_0^H\int_{-\infty}^{\infty}\left[\overline{E}\left(w\frac{\partial \varphi}{\partial z}\right)^2 + G_s\left(\frac{\partial w}{\partial r}\varphi\right)^2\right]rdrdz$$

The strain energy deformation in a thin plate corresponds to bending. The strain energy deformation in thin plates corresponding to bending and transverse shear and thickness stretch or contraction is taken as negligible; hence, it is a plane stress condition.

Displacement variations, excluding the stretching of the plate, are written as

$$u(r,\theta,z) = -z\frac{\partial w}{\partial r};\ v(r,\theta,z) = -\frac{z}{r}\frac{\partial w}{\partial \theta} \text{ and } \ w(r,\theta,z) = w(r,\theta)$$

$$\frac{\partial u}{\partial \theta} = \frac{\partial\left(-z\frac{\partial w}{\partial r}\right)}{\partial \theta} = -z\frac{\partial^2 w}{\partial r\,\partial \theta};\frac{\partial v}{\partial \theta} = \frac{\partial\left(-\frac{z\partial w}{r\,\partial \theta}\right)}{\partial \theta} = -\frac{z}{r}\frac{\partial^2 w}{\partial \theta^2};$$

$$\frac{\partial v}{\partial r} = \frac{\partial\left(-\frac{z\partial w}{r\,\partial \theta}\right)}{\partial r} = -z\frac{\partial}{\partial r}\left(\frac{\frac{\partial w}{\partial \theta}}{r}\right) = -z\left[\frac{r\frac{\partial^2 w}{\partial r\,\partial \theta} - \frac{\partial w}{\partial \theta}}{r^2}\right] = -\frac{z}{r}\frac{\partial^2 w}{\partial r\,\partial \theta} + \frac{z}{r^2}\frac{\partial w}{\partial \theta}$$

$$\varepsilon_{rr} = \frac{\partial u}{\partial r} = -z\frac{\partial^2 w}{\partial r^2};\varepsilon_{\theta\theta} = \frac{u}{r} + \frac{1}{r}\frac{\partial v}{\partial \theta} = -\frac{z}{r}\frac{\partial w}{\partial r} - \frac{z}{r^2}\frac{\partial^2 w}{\partial \theta^2};$$

$$\gamma_{r\theta} = \frac{1}{r}\frac{\partial u}{\partial \theta} + \frac{\partial v}{\partial r} - \frac{v}{r} = -\frac{z}{r}\frac{\partial^2 w}{\partial r\,\partial \theta} + \left(-\frac{z}{r}\frac{\partial^2 w}{\partial r\,\partial \theta} + \frac{z}{r^2}\frac{\partial w}{\partial \theta}\right) + \frac{z}{r^2}\frac{\partial w}{\partial \theta} = -\frac{2z}{r}\frac{\partial^2 w}{\partial r\,\partial \theta} + \frac{2z}{r^2}\frac{\partial w}{\partial \theta}$$

$$\text{and } \varepsilon_{zz} = \gamma_{rz} = \gamma_{\theta z} = 0;\begin{Bmatrix}\varepsilon_{rr}\\ \varepsilon_{\theta\theta}\\ \gamma_{r\theta}\end{Bmatrix} = \begin{bmatrix}-z\frac{\partial^2 w}{\partial r^2}\\ -\frac{z}{r}\frac{\partial w}{\partial r} - \frac{z}{r^2}\frac{\partial^2 w}{\partial \theta^2}\\ -\frac{2z}{r}\frac{\partial^2 w}{\partial r\,\partial \theta} + \frac{2z}{r^2}\frac{\partial w}{\partial \theta}\end{bmatrix}$$

The constitutive law for plane stress conditions is

$$\begin{Bmatrix}\sigma_r\\ \sigma_\theta\\ \tau_{r\theta}\end{Bmatrix} = \frac{E}{(1-v^2)}\begin{bmatrix}1 & v & 0\\ v & 1 & 0\\ 0 & 0 & \frac{1-v}{2}\end{bmatrix}\begin{Bmatrix}\epsilon_r\\ \epsilon_\theta\\ \gamma_{r\theta}\end{Bmatrix} = -\frac{Ez}{(1-v^2)}\begin{bmatrix}1 & v & 0\\ v & 1 & 0\\ 0 & 0 & \frac{1-v}{2}\end{bmatrix}\begin{Bmatrix}\frac{\partial^2 w}{\partial r^2}\\ \frac{1}{r}\frac{\partial w}{\partial r} + \frac{1}{r^2}\frac{\partial^2 w}{\partial \theta^2}\\ \frac{2}{r}\frac{\partial^2 w}{\partial r\,\partial \theta} - \frac{2}{r^2}\frac{\partial w}{\partial \theta}\end{Bmatrix}$$

$$\therefore\ \sigma_r = -\frac{Ez}{(1-v^2)}\left[\frac{\partial^2 w}{\partial r^2} + v\left(\frac{1}{r}\frac{\partial w}{\partial r} + \frac{1}{r^2}\frac{\partial^2 w}{\partial \theta^2}\right)\right];$$

$$\sigma_\theta = -\frac{Ez}{(1-v^2)}\left(v\frac{\partial^2 w}{\partial r^2} + \frac{1}{r}\frac{\partial w}{\partial r} + \frac{1}{r^2}\frac{\partial^2 w}{\partial \theta^2}\right);\tau_{r\theta} = -\frac{Ez}{(1+v)}\left(\frac{1}{r}\frac{\partial^2 w}{\partial r\,\partial \theta} - \frac{1}{r^2}\frac{\partial w}{\partial \theta}\right)$$

$$\text{Strain energy},\Pi = \frac{1}{2}\sigma_{ij}\varepsilon_{ij}dV = \frac{1}{2}\sigma_{ij}\varepsilon_{ij}rdrd\theta dz = \frac{1}{2}\int\int\int(\sigma_r\varepsilon_r + \sigma_\theta\varepsilon_\theta + \tau_{r\theta}\gamma_{r\theta})rdrd\theta dz$$

$$\Pi_p = \frac{1}{2}\frac{E}{(1-v^2)}\int\int\int_{-\frac{h}{2}}^{\frac{h}{2}}\left[\left\{\frac{\partial^2 w}{\partial r^2} + v\left(\frac{1}{r}\frac{\partial w}{\partial r} + \frac{1}{r^2}\frac{\partial^2 w}{\partial \theta^2}\right)\right\}\frac{\partial^2 w}{\partial r^2} + \left(v\frac{\partial^2 w}{\partial r^2} + \frac{1}{r}\frac{\partial w}{\partial r} + \frac{1}{r^2}\frac{\partial^2 w}{\partial \theta^2}\right)\left(\frac{1}{r}\frac{\partial w}{\partial r} + \frac{1}{r^2}\frac{\partial^2 w}{\partial \theta^2}\right) + 2(1-v)\left(\frac{1}{r}\frac{\partial^2 w}{\partial r\,\partial \theta} - \frac{1}{r^2}\frac{\partial w}{\partial \theta}\right)^2\right]z^2 rdrd\theta dz$$

$$\Pi_p = \frac{D}{2}\int\int\left[\left(\frac{\partial^2 w}{\partial r^2}\right)^2 + \left(\frac{1}{r}\frac{\partial w}{\partial r} + \frac{1}{r^2}\frac{\partial^2 w}{\partial \theta^2}\right)^2 + v\left(\frac{1}{r}\frac{\partial w}{\partial r} + \frac{1}{r^2}\frac{\partial^2 w}{\partial \theta^2}\right)\frac{\partial^2 w}{\partial r^2} + v\frac{\partial^2 w}{\partial r^2}\left(\frac{1}{r}\frac{\partial w}{\partial r} + \frac{1}{r^2}\frac{\partial^2 w}{\partial \theta^2}\right) + 2(1-v)\left(\frac{1}{r}\frac{\partial^2 w}{\partial r\,\partial \theta} - \frac{1}{r^2}\frac{\partial w}{\partial \theta}\right)^2\right] r dr d\theta$$

$$\Pi_p = \frac{D}{2}\int\int\left[\left(\frac{\partial^2 w}{\partial r^2} + \frac{1}{r}\frac{\partial w}{\partial r} + \frac{1}{r^2}\frac{\partial^2 w}{\partial \theta^2}\right)^2 - 2\frac{\partial^2 w}{\partial r^2}\left(\frac{1}{r}\frac{\partial w}{\partial r} + \frac{1}{r^2}\frac{\partial^2 w}{\partial \theta^2}\right) + 2v\frac{\partial^2 w}{\partial r^2}\left(\frac{1}{r}\frac{\partial w}{\partial r} + \frac{1}{r^2}\frac{\partial^2 w}{\partial \theta^2}\right) + 2(1-v)\left(\frac{1}{r}\frac{\partial^2 w}{\partial r\,\partial \theta} - \frac{1}{r^2}\frac{\partial w}{\partial \theta}\right)^2\right] r dr d\theta$$

$$\Pi_p = \frac{D}{2}\int\int\left[\left(\frac{\partial^2 w}{\partial r^2} + \frac{1}{r}\frac{\partial w}{\partial r} + \frac{1}{r^2}\frac{\partial^2 w}{\partial \theta^2}\right)^2 - 2(1-v)\frac{\partial^2 w}{\partial r^2}\left(\frac{1}{r}\frac{\partial w}{\partial r} + \frac{1}{r^2}\frac{\partial^2 w}{\partial \theta^2}\right) + 2(1-v)\left(\frac{1}{r}\frac{\partial^2 w}{\partial r\,\partial \theta} - \frac{1}{r^2}\frac{\partial w}{\partial \theta}\right)^2\right] r dr d\theta$$

$$\Pi_p = \frac{D}{2}\int\int\left[(\nabla^2 w)^2 - 2(1-v)\left\{\frac{\partial^2 w}{\partial r^2}\left(\frac{1}{r}\frac{\partial w}{\partial r} + \frac{1}{r^2}\frac{\partial^2 w}{\partial \theta^2}\right) - \left(\frac{1}{r}\frac{\partial^2 w}{\partial r\,\partial \theta} - \frac{1}{r^2}\frac{\partial w}{\partial \theta}\right)^2\right\}\right] r dr d\theta$$

$$\Pi_p = \frac{D}{2}\int\int\left[(\nabla^2 w)^2 - 2(1-v)\left\{\frac{1}{r}\frac{\partial^2 w}{\partial r^2}\frac{\partial w}{\partial r} + \frac{1}{r^2}\frac{\partial^2 w}{\partial r^2}\frac{\partial^2 w}{\partial \theta^2} - \frac{1}{r^2}\left(\frac{\partial^2 w}{\partial r\,\partial \theta}\right)^2 + \frac{2}{r^3}\frac{\partial w}{\partial \theta}\frac{\partial^2 w}{\partial r\,\partial \theta} - \frac{1}{r^4}\left(\frac{\partial w}{\partial \theta}\right)^2\right\}\right] r dr d\theta$$

Where $\nabla^2 = \left(\frac{\partial^2}{\partial r^2} + \frac{1}{r}\frac{\partial}{\partial r} + \frac{1}{r^2}\frac{\partial^2}{\partial \theta^2}\right)$ is the Laplacian operator

and $D = \frac{Eh^3}{12(1-v^2)}$ is the flexural rigidity of the plate.

In the case of an axisymmetric problem, all quantities are functions of r and z only. The variation of all amounts regarding circumferential coordinate θ is absent. No point undergoes displacement in θ direction.

Hence, the strain energy of an axisymmetric circular plate is given by

$$\Pi_p = \frac{D}{2}\int\int\left[\left(\frac{\partial^2 w}{\partial r^2} + \frac{1}{r}\frac{\partial w}{\partial r}\right)^2 - \frac{2(1-v)}{r}\frac{\partial^2 w}{\partial r^2}\frac{\partial w}{\partial r}\right] r dr d\theta$$

The total potential energy of the soil-plate system subjected to a UDL of q is given by

$$\Pi = \Pi_p + \Pi_s + V$$

Now, the potential energy of the soil-plate system is

$$\Pi = \frac{D}{2}\int_0^{2\pi}\int_0^{r}\left[(\nabla^2 w)^2 - \frac{2(1-v)}{r}\frac{\partial^2 w}{\partial r^2}\frac{\partial w}{\partial r}\right] r dr d\theta + \frac{1}{2}\int_0^{H}\int_0^{2\pi}\int_0^{\infty}\left[\overline{E} w^2\left(\frac{\partial \varphi}{\partial z}\right)^2 + G_s\varphi^2\left\{\frac{1}{r^2}\left(\frac{\partial w}{\partial \theta}\right)^2 + \left(\frac{\partial w}{\partial r}\right)^2\right\}\right] r dr d\theta dz - \int_0^{2\pi}\int_0^{r} q w r dr d\theta$$

We can now use the calculus of variations to obtain the equilibrium equations. For a stable equilibrium state to be reached, the first variation of the potential energy must be zero ($\delta\Pi = 0$). First, we consider the plate soil system within the plate domain and take variations on w. Taking variations on w, we get the following

$$\Pi = \frac{D}{2}\int_0^{2\pi}\int_0^{r}\left(\frac{\partial^2 w}{\partial r^2}+\frac{1}{r}\frac{\partial w}{\partial r}+\frac{1}{r^2}\frac{\partial^2 w}{\partial \theta^2}\right)^2 - 2(1-v)\left[\left(\frac{\partial^2 w}{\partial r^2}\right)\left(\frac{\partial^2 w}{\partial \theta^2}\right)-\left(\frac{\partial^2 w}{\partial r\,\partial \theta}\right)^2\right] r dr d\theta +$$

$$\frac{1}{2}\int_0^{H}\int_0^{2\pi}\int_0^{\infty}\left[\bar{E}w^2\left(\frac{\partial \varphi}{\partial z}\right)^2 + G_s\varphi^2\left\{\frac{1}{r^2}\left(\frac{\partial w}{\partial \theta}\right)^2+\left(\frac{\partial w}{\partial r}\right)^2\right\}\right] r dr d\theta dz - \int_0^{2\pi}\int_0^{r} qwrdrd\theta$$

$$\Pi = \frac{D}{2}\int_0^{2\pi}\int_0^{r}\left(\frac{\partial^2 w}{\partial r^2}+\frac{1}{r}\frac{\partial w}{\partial r}+\frac{1}{r^2}\frac{\partial^2 w}{\partial \theta^2}\right)^2 - 2(1-v)\left[\left(\frac{\partial^2 w}{\partial r^2}\right)\left(\frac{\partial^2 w}{\partial \theta^2}\right)-\left(\frac{\partial^2 w}{\partial r\,\partial \theta}\right)^2\right] r dr d\theta +$$

$$\int_0^{2\pi}\int_0^{\infty}\left[Kw^2 + 2t\left\{\frac{1}{r^2}\left(\frac{\partial w}{\partial \theta}\right)^2+\left(\frac{\partial w}{\partial r}\right)^2\right\}\right] r dr d\theta - \int_0^{2\pi}\int_0^{r} qwrdrd\theta$$

$$K = \int_0^{H}\bar{E}\left(\frac{\partial \varphi}{\partial z}\right)^2 dz \text{ and } 2t = \int_0^{H} G_s\varphi^2 dz$$

The field equation in the domain, Ω, can be written as (Gunerathne et al., 2019).

$$D\nabla^4 w(r,\theta) - 2t\nabla^2 w(r,\theta) + Kw(r,\theta) = q(r,\theta) \qquad (3.3.1.1)$$

Where $\nabla^2 = \left(\frac{\partial^2}{\partial r^2}+\frac{1}{r}\frac{\partial}{\partial r}+\frac{1}{r^2}\frac{\partial^2}{\partial \theta^2}\right)$ is the Laplacian operator.

More details of the modified Vlasov model are available in (Turhan, 1992; Celik and Saygun, 1999b; Straughan, 1990; Özgan and Daloğlu, 2008; Ozgan and Daloglu, 2009).

Axial Stiffness on the Boundary, k_s. The effect of the surrounding soil can be obtained by writing the potential energy of the soil outside the plate domain.

The shear force along $r = R$ of the foundation onto the plate is given by,

$$N = 2t \times \frac{dw}{dr} = 2t\alpha W_a \frac{K_1(\alpha r)}{K_0(\alpha R)} = \sqrt{2Kt}\frac{K_1(\alpha r)}{K_0(\alpha R)} W_a$$

using, $\alpha = \sqrt{\frac{K}{2t}}$ and $w(x,y) = W_a \frac{K_0(\alpha r)}{K_0(\alpha R)}$; R is the radius of the plate. $\frac{dw}{dr} = -\alpha W_a \frac{K_1(\alpha r)}{K_0(\alpha R)}$;

Equivalent boundary forces at the boundary nodes due to the infinite soil domain on the plate boundary (Vallabhan and Das, 1991b) $Q = aw\sqrt{2tK}\frac{K_1(\alpha R)}{K_0(\alpha R)}$. Where w is the deflection of the respective boundary node, K_1 and K_0 modified Bessel functions of the second kind of first and zero orders, R is the radius of the plate/raft and $\alpha = \sqrt{\frac{K}{2t}}$. Stiffness for infinite soil domain on the plate boundary nodes is $a\sqrt{2tK}\frac{K_1(\alpha R)}{K_0(\alpha R)}$ where 'a' is the tributary length of the respective node. Thus, the effect at the boundary nodes of the soil region is modelled by adding $a\sqrt{2tK}\frac{K_1(\alpha R)}{K_0(\alpha R)}$ to the stiffness term.

Field equation for elastic foundation for 0 < z < H (Vallabhan and Das, 1991b)

$$m\frac{d^2\varphi}{dz^2} - n\varphi = 0 \tag{3.3.1.2}$$

Where $m = \frac{E_s(1-v_s)}{(1+v_s)(1-2v_s)}\int_0^\infty (w)^2 rdr$ and $n = \frac{E_s}{2(1+v_s)}\int_0^\infty \left(\frac{dw}{dr}\right)^2 rdr$ here, m and n are the additional parameters that describe the behaviour of the elastic foundations. Those derivations for m and n are due to (Jones and Xenophontos, 1977). The introduction of a new parameter γ gives $\left(\frac{\gamma}{H}\right)^2 = \frac{n}{m} = \frac{(1-2v_s)\int_0^\infty \left(\frac{dw}{dr}\right)^2 rdr}{2(1-v_s)\int_0^\infty (w)^2 rdr}$ (3.3.1.3)

Solution scheme and the iterative procedure

Therefore, for a circular plate solution resting on an elastic foundation using modified Vlasov model, the variables w, q, K, 2t, H and γ are all related to each other. Since the parameter γ is not known a priori, the exact solutions need to be obtained by an iterative method. The initial value of γ is first assumed, and then the decay function φ is determined, thus the basis parameters K and 2t of the equations (3.2.1.7) and (3.2.1.8). Using the higher order finite element formulation, the plate displacements are now determined using K and 2t. Then, using equation (3.3.1.3), the measured plate displacements are used to obtain γ, and the calculated new value of γ is compared with the assumed original value. The iterations are repeated until the discrepancy is below the prescribed convergence tolerance between the values of the dimensionless γ parameter obtained from two successive iterations. It is also noted/found that with tolerance limit 0.0001, number of iteration (NI) less than 7 gives the most reliable solution regardless of the initial value of γ assumed (Fig. 3.7).

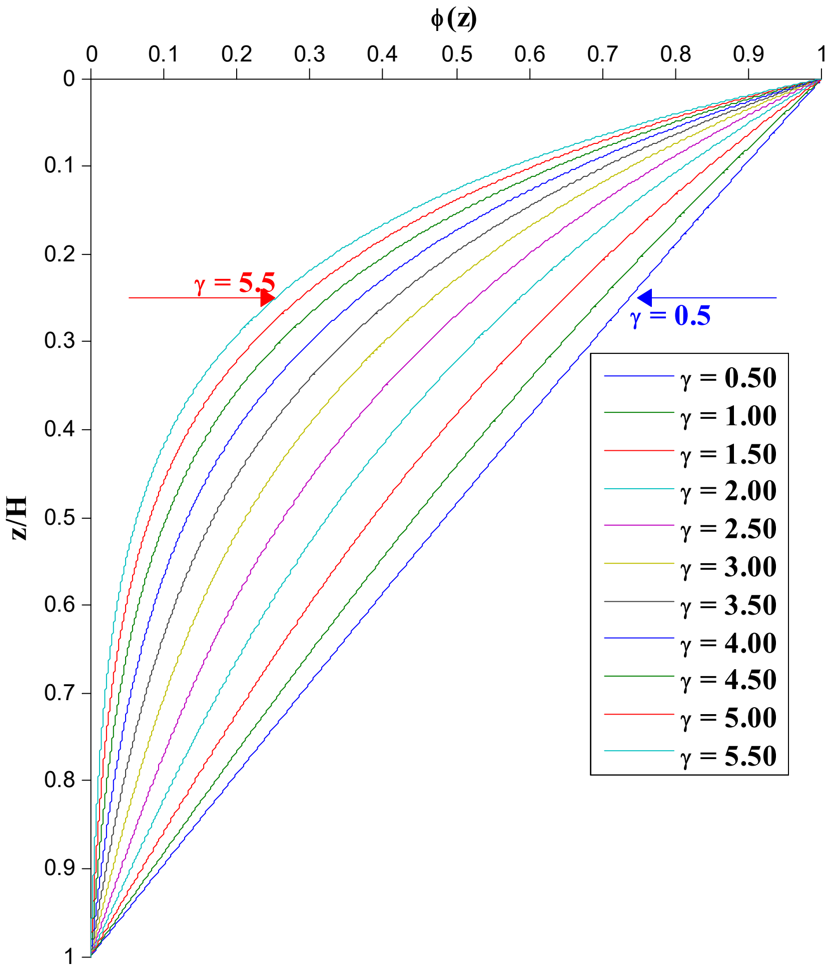

Fig. 3.7 Mode function φ (z) vs the value of γ

Displacement variations, excluding the stretching of the plate, are written as

$u(r,\theta,z) = z\beta_r + z^3\beta_r{}^*; v(r,\theta,z) = \frac{z}{r}\beta_\theta + \frac{z^3}{r}\beta_\theta{}^*$ and $w(r,\theta,z) = w(r,\theta) + z^2 w^*(r,\theta)$

$$\frac{\partial u}{\partial\theta} = \frac{\partial(z\beta_r + z^3\beta_r{}^*)}{\partial\theta} = z\frac{\partial\beta_r}{\partial\theta} + z^3\frac{\partial\beta_r{}^*}{\partial\theta}; \frac{\partial v}{\partial\theta} = \frac{\partial\left(\frac{z}{r}\beta_\theta + \frac{z^3}{r}\beta_\theta{}^*\right)}{\partial\theta} = \frac{z}{r}\frac{\partial\beta_\theta}{\partial\theta} + \frac{z^3}{r}\frac{\partial\beta_\theta{}^*}{\partial\theta};$$

$$\frac{\partial v}{\partial r} = \frac{\partial\left(\frac{z}{r}\beta_\theta + \frac{z^3}{r}\beta_\theta{}^*\right)}{\partial r} = z\frac{\partial}{\partial r}\left(\frac{\beta_\theta}{r}\right) + z^3\frac{\partial}{\partial r}\left(\frac{\beta_\theta{}^*}{r}\right)$$

$$\therefore \frac{\partial v}{\partial r} = z\left[\frac{r\frac{\partial\beta_\theta}{\partial r} - \beta_\theta}{r^2}\right] + z^3\left[\frac{r\frac{\partial\beta_\theta{}^*}{\partial r} - \beta_\theta{}^*}{r^2}\right] = \frac{z}{r}\frac{\partial\beta_\theta}{\partial r} + \frac{z^3}{r}\frac{\partial\beta_\theta{}^*}{\partial r} - \frac{z}{r^2}\beta_\theta - \frac{z^3\beta_\theta{}^*}{r^2}$$

$$\varepsilon_{rr} = \frac{\partial u}{\partial r} = z\frac{\partial\beta_r}{\partial r} + z^3\frac{\partial\beta_r{}^*}{\partial r};$$

$$\varepsilon_{\theta\theta} = \frac{u}{r} + \frac{1}{r}\frac{\partial v}{\partial \theta} = \frac{z}{r}\beta_r + \frac{z^3}{r}\beta_r{}^* + \frac{z}{r^2}\frac{\partial \beta_\theta}{\partial \theta} + \frac{z^3}{r^2}\frac{\partial \beta_\theta{}^*}{\partial \theta} \text{ and } \varepsilon_{zz} = \frac{\partial w}{\partial z} = 2zw^*$$

$$\gamma_{r\theta} = \frac{1}{r}\frac{\partial u}{\partial \theta} + \frac{\partial v}{\partial r} - \frac{v}{r} = \frac{z}{r}\frac{\partial \beta_r}{\partial \theta} + \frac{z^3}{r}\frac{\partial \beta_r{}^*}{\partial \theta} + \left(\frac{z}{r}\frac{\partial \beta_\theta}{\partial r} + \frac{z^3}{r}\frac{\partial \beta_\theta{}^*}{\partial r} - \frac{z}{r^2}\beta_\theta - \frac{z^3\beta_\theta{}^*}{r^2}\right) - \frac{z}{r^2}\beta_\theta - \frac{z^3}{r^2}\beta_\theta{}^*$$

$$\gamma_{r\theta} = \frac{z}{r}\left(\frac{\partial \beta_r}{\partial \theta} + \frac{\partial \beta_\theta}{\partial r}\right) + \frac{z^3}{r}\left(\frac{\partial \beta_r{}^*}{\partial \theta} + \frac{\partial \beta_\theta{}^*}{\partial r}\right) - \frac{2z}{r^2}\beta_\theta - \frac{2z^3}{r^2}\beta_\theta{}^*$$

$$\gamma_{rz} = \frac{\partial u}{\partial z} + \frac{\partial w}{\partial r} = \beta_r + 3z^2\beta_r{}^* + \frac{\partial w}{\partial r} + z^2\frac{\partial w^*}{\partial r} = \left(\beta_r + \frac{\partial w}{\partial r}\right) + z^2\left(3\beta_r{}^* + \frac{\partial w^*}{\partial r}\right);$$

$$\gamma_{\theta z} = \frac{\partial v}{\partial z} + \frac{1}{r}\frac{\partial w}{\partial \theta} = \frac{\beta_\theta}{r} + \frac{3z^2}{r}\beta_\theta{}^* + \frac{1}{r}\frac{\partial w}{\partial \theta} + \frac{z^2}{r}\frac{\partial w^*}{\partial \theta} = \frac{1}{r}\left(\beta_\theta + \frac{\partial w}{\partial \theta}\right) + \frac{z^2}{r}\left(3\beta_\theta{}^* + \frac{\partial w^*}{\partial \theta}\right)$$

$$\begin{bmatrix} \sigma_{rr} \\ \sigma_{\theta\theta} \\ \sigma_{zz} \\ \tau_{r\theta} \\ \tau_{\theta z} \\ \tau_{rz} \end{bmatrix} = \frac{E}{(1+v)(1-2v)} \begin{bmatrix} 1-v & v & v & 0 & 0 & 0 \\ v & 1-v & v & 0 & 0 & 0 \\ v & v & 1-v & 0 & 0 & 0 \\ 0 & 0 & 0 & \frac{1-2v}{2} & 0 & 0 \\ 0 & 0 & 0 & 0 & \frac{1-2v}{2} & 0 \\ 0 & 0 & 0 & 0 & 0 & \frac{1-2v}{2} \end{bmatrix} \begin{Bmatrix} \varepsilon_{rr} \\ \varepsilon_{\theta\theta} \\ \varepsilon_{zz} \\ \gamma_{r\theta} \\ \gamma_{rz} \\ \gamma_{\theta z} \end{Bmatrix}$$

$$\text{Lames constant}, \lambda = \frac{Ev}{(1+v)(1-2v)} \text{ and } G = \frac{E}{2(1+v)} \therefore \lambda + 2G = \frac{E(1-v)}{(1+v)(1-2v)}$$

$$\begin{bmatrix} \sigma_{rr} \\ \sigma_{\theta\theta} \\ \sigma_{zz} \\ \tau_{r\theta} \\ \tau_{rz} \\ \tau_{z\theta} \end{bmatrix} = \begin{bmatrix} \lambda+2G & \lambda & \lambda & 0 & 0 & 0 \\ \lambda & \lambda+2G & \lambda & 0 & 0 & 0 \\ \lambda & \lambda & \lambda+2G & 0 & 0 & 0 \\ 0 & 0 & 0 & G & 0 & 0 \\ 0 & 0 & 0 & 0 & G & 0 \\ 0 & 0 & 0 & 0 & 0 & G \end{bmatrix} \begin{Bmatrix} \varepsilon_{rr} \\ \varepsilon_{\theta\theta} \\ \varepsilon_{zz} \\ \gamma_{r\theta} \\ \gamma_{rz} \\ \gamma_{z\theta} \end{Bmatrix}$$

The total potential energy of the soil-plate system subjected to a UDL of q is given by

$\Pi = \Pi_p + \Pi_s + V$

The strain energy deformation in the HSDT plate corresponding to bending and shear deformation is

Strain energy, $\Pi_p = \frac{1}{2}\sigma_{ij}\varepsilon_{ij}dV = \frac{1}{2}\sigma_{ij}\varepsilon_{ij}rdrd\theta dz = \frac{1}{2}\int\int\int(\sigma_r\varepsilon_r + \sigma_\theta\varepsilon_\theta + \tau_{r\theta}\gamma_{r\theta})rdrd\theta dz$

$$\Pi_p = \frac{1}{2}\sigma_{ij}\varepsilon_{ij}dV = \frac{1}{2}\sigma_{ij}\varepsilon_{ij}rdrd\theta dz = \frac{1}{2}\int\int\int(\sigma_{rr}\varepsilon_{rr} + \sigma_{\theta\theta}\varepsilon_{\theta\theta} + \sigma_{zz}\varepsilon_{zz} + \tau_{r\theta}\gamma_{r\theta} + \tau_{rz}\gamma_{rz} + \tau_{z\theta}\gamma_{z\theta})rdrd\theta dz$$

$$\therefore \Pi_p = \frac{1}{2}\int\int\int(\{(\lambda+2G)\varepsilon_{rr} + \lambda\varepsilon_{\theta\theta} + \lambda\varepsilon_{zz}\}\varepsilon_{rr} + \{\lambda\varepsilon_{rr} + (\lambda+2G)\varepsilon_{\theta\theta} + \lambda\varepsilon_{zz}\}\varepsilon_{\theta\theta} + \{\lambda\varepsilon_{rr} + \lambda\varepsilon_{\theta\theta} + (\lambda+2G)\varepsilon_{zz}\}\varepsilon_{zz} + G\gamma_{r\theta}{}^2 + G\gamma_{rz}{}^2 + G\gamma_{z\theta}{}^2)rdrd\theta dz$$

$$\therefore \Pi_p = \frac{(\lambda+2G)}{2}\int_0^{2\pi}\int_0^r\int_{-h/2}^{h/2}({\varepsilon_{rr}}^2 + {\varepsilon_{\theta\theta}}^2 + {\varepsilon_{zz}}^2)rdrd\theta dz + \lambda\int_0^{2\pi}\int_0^r\int_{-h/2}^{h/2}(\varepsilon_{rr}\varepsilon_{\theta\theta} + \varepsilon_{rr}\varepsilon_{zz} + \varepsilon_{zz}\varepsilon_{\theta\theta})rdrd\theta dz + \frac{G}{2}\int_0^{2\pi}\int_0^r\int_{-h/2}^{h/2}({\gamma_{r\theta}}^2 + {\gamma_{rz}}^2 + \gamma_{z\theta})rdrd\theta dz$$

$$\varepsilon_{rr} = z\frac{\partial\beta_r}{\partial r} + z^3\frac{\partial{\beta_r}^*}{\partial r};\ \varepsilon_{\theta\theta} = \frac{z}{r}\beta_r + \frac{z^3}{r}{\beta_r}^* + \frac{z}{r^2}\frac{\partial\beta_\theta}{\partial\theta} + \frac{z^3}{r^2}\frac{\partial{\beta_\theta}^*}{\partial\theta} \text{ and } \varepsilon_{zz} = 2zw^*$$

$$\gamma_{r\theta} = \frac{z}{r}\left(\frac{\partial\beta_r}{\partial\theta} + \frac{\partial\beta_\theta}{\partial r}\right) + \frac{z^3}{r}\left(\frac{\partial{\beta_r}^*}{\partial\theta} + \frac{\partial{\beta_\theta}^*}{\partial r}\right) - \frac{2z}{r^2}\beta_\theta - \frac{2z^3}{r^2}{\beta_\theta}^*$$

$$\gamma_{rz} = \left(\beta_r + \frac{\partial w}{\partial r}\right) + z^2\left(3{\beta_r}^* + \frac{\partial w^*}{\partial r}\right);\ \gamma_{\theta z} = \frac{1}{r}\left(\beta_\theta + \frac{\partial w}{\partial\theta}\right) + \frac{z^2}{r}\left(3{\beta_\theta}^* + \frac{\partial w^*}{\partial\theta}\right)$$

In the case of an axisymmetric problem, all quantities are functions of r and z only. The variation of all quantities with reference to circumferential coordinate θ is absent. No point undergoes displacement in θ direction. Hence, the strain energy of an axisymmetric circular plate is given by

$$\varepsilon_{rr} = z\frac{\partial\beta_r}{\partial r} + z^3\frac{\partial{\beta_r}^*}{\partial r};\ \varepsilon_{\theta\theta} = \frac{z}{r}\beta_r + \frac{z^3}{r}{\beta_r}^* \text{ and } \varepsilon_{zz} = 2zw^*;$$

$$\gamma_{r\theta} = 0;\ \gamma_{rz} = \left(\beta_r + \frac{\partial w}{\partial r}\right) + z^2\left(3{\beta_r}^* + \frac{\partial w^*}{\partial r}\right);\ \gamma_{\theta z} = 0$$

$$\int_{-h/2}^{h/2}({\varepsilon_{rr}}^2 + {\varepsilon_{\theta\theta}}^2 + {\varepsilon_{zz}}^2)rdrd\theta dz = \frac{h^3}{12}\left(\frac{\partial\beta_r}{\partial r}\right)^2 + \frac{h^5}{40}\frac{\partial\beta_r}{\partial r}\frac{\partial{\beta_r}^*}{\partial r} + \frac{h^7}{448}\left(\frac{\partial{\beta_r}^*}{\partial r}\right)^2 + \frac{h^3}{12r^2}(\beta_r)^2 + \frac{h^5}{40r^2}\beta_r{\beta_r}^* + \frac{h^7}{448\ ^2}({\beta_r}^*)^2 + \frac{h^3}{3}w^*$$

$$\int_{-h/2}^{h/2}(\varepsilon_{rr}\varepsilon_{\theta\theta} + \varepsilon_{rr}\varepsilon_{zz} + \varepsilon_{zz}\varepsilon_{\theta\theta})rdrd\theta dz = \frac{h^3}{12r}\beta_r\frac{\partial\beta_r}{\partial r} + \frac{h^5}{80r}{\beta_r}^*\frac{\partial\beta_r}{\partial r} + \frac{h^5}{80r}\beta_r\frac{\partial{\beta_r}^*}{\partial r} + \frac{h^7}{448r}{\beta_r}^*\frac{\partial{\beta_r}^*}{\partial r} + \frac{h^3}{6}w^*\frac{\partial\beta_r}{\partial r} + \frac{h^5}{40}w^*\frac{\partial{\beta_r}^*}{\partial r} + \frac{h^3}{6}w^*\beta_r + \frac{h^5}{40}w^*{\beta_r}^*$$

$$\int_{-h/2}^{h/2}({\gamma_{r\theta}}^2 + {\gamma_{rz}}^2 + \gamma_{z\theta})rdrd\theta dz = h{\beta_r}^2 + 2h\beta_r\frac{\partial w}{\partial r} + \frac{h^3}{2}\beta_r{\beta_r}^* + \frac{h^3}{6}\beta_r\frac{\partial w^*}{\partial r} + h\left(\frac{\partial w}{\partial r}\right)^2 + \frac{h^3}{2}{\beta_r}^*\frac{\partial w}{\partial r} + \frac{h^3}{6}\frac{\partial w}{\partial r}\frac{\partial w^*}{\partial r} + \frac{9h^5}{80}{\beta_r}^{*2} + \frac{3h^5}{40}{\beta_r}^*\frac{\partial w^*}{\partial r} + \frac{h^5}{80}\left(\frac{\partial w^*}{\partial r}\right)^2$$

$$\Pi = \frac{(\lambda+2G)}{2}\int_0^{2\pi}\int_0^r\left[\frac{h^3}{12}\left(\frac{\partial\beta_r}{\partial r}\right)^2 + \frac{h^5}{40}\frac{\partial\beta_r}{\partial r}\frac{\partial{\beta_r}^*}{\partial r} + \frac{h^7}{448}\left(\frac{\partial{\beta_r}^*}{\partial r}\right)^2 + \frac{h^3}{12r^2}(\beta_r)^2 + \frac{h^5}{40r^2}\beta_r{\beta_r}^* + \frac{h^7}{448r^2}({\beta_r}^*)^2 + \frac{h^3}{3}w^*\right]rdrd\theta + \lambda\int_0^{2\pi}\int_0^r\left[\frac{h^3}{12r}\beta_r\frac{\partial\beta_r}{\partial r} + \frac{h^5}{80r}{\beta_r}^*\frac{\partial\beta_r}{\partial r} + \frac{h^5}{80}\beta_r\frac{\partial{\beta_r}^*}{\partial r} + \frac{h^7}{448r}{\beta_r}^*\frac{\partial{\beta_r}^*}{\partial r} + \frac{h^3}{6}w^*\frac{\partial\beta_r}{\partial r} + \frac{h^5}{40}w^*\frac{\partial{\beta_r}^*}{\partial r} + \frac{h^3}{6}w^*\beta_r + \frac{h^5}{40}w^*{\beta_r}^*\right]rdrd\theta + \frac{G}{2}\int_0^{2\pi}\int_0^r\left[h{\beta_r}^2 + 2h\beta_r\frac{\partial w}{\partial r} + \frac{h^3}{2}\beta_r{\beta_r}^* + \right.$$

$$\frac{h^3}{6}\beta_r\frac{\partial w^*}{\partial r}+h\left(\frac{\partial w}{\partial r}\right)^2+\frac{h^3}{2}\beta_r{}^*\frac{\partial w}{\partial r}+\frac{h^3}{6}\frac{\partial w}{\partial r}\frac{\partial w^*}{\partial r}+\frac{9h^5}{80}\beta_r{}^{*2}+\frac{3h^5}{40}\beta_r{}^*\frac{\partial w^*}{\partial r}+\frac{h^5}{80}\left(\frac{\partial w^*}{\partial r}\right)^2\Bigg]rdrd\theta+$$

$$\frac{1}{2}\int_0^{2\pi}\int_0^{\infty}\left[Kw^2+2t\left(\frac{\partial w}{\partial r}\right)^2\right]rdrd\theta-\int_0^{2\pi}\int_0^{r}qwrdrd\theta$$

$$K=\int_0^H\overline{E}\left(\frac{\partial\varphi}{\partial z}\right)^2dz \text{ and } 2t=\int_0^H G_s\varphi^2dz$$

We can now use the calculus of variations to obtain the equilibrium equations. For a stable equilibrium state to be reached, the first variation of the potential energy must be zero ($\delta\Pi = 0$). First, we consider the plate soil system within the plate domain and take variations on w. Taking variations on w, we get the following

$$F_1=\frac{(\lambda+2G)}{2}\left[\frac{h^3}{12}\left(\frac{\partial\beta_r}{\partial r}\right)^2+\frac{h^5}{40}\frac{\partial\beta_r}{\partial r}\frac{\partial\beta_r{}^*}{\partial r}+\frac{h^7}{448}\left(\frac{\partial\beta_r{}^*}{\partial r}\right)^2+\frac{h^3}{12r^2}(\beta_r)^2+\frac{h^5}{40r^2}\beta_r\beta_r{}^*+\frac{h^7}{448r^2}(\beta_r{}^*)^2+\right.$$

$$\left.\frac{h^3}{3}w^*\right]+\lambda\left[\frac{h^3}{12r}\beta_r\frac{\partial\beta_r}{\partial r}+\frac{h^5}{80}\beta_r{}^*\frac{\partial\beta_r}{\partial r}+\frac{h^5}{80r}\beta_r\frac{\partial\beta_r{}^*}{\partial r}+\frac{h^7}{448r}\beta_r{}^*\frac{\partial\beta_r{}^*}{\partial r}+\frac{h^3}{6}w^*\frac{\partial\beta_r}{\partial r}+\frac{h^5}{40}w^*\frac{\partial\beta_r{}^*}{\partial r}+\right.$$

$$\left.\frac{h^3}{6}w^*\beta_r+\frac{h^5}{40}w^*\beta_r{}^*\right]+\frac{G}{2}\left[h\beta_r{}^2+2h\beta_r\frac{\partial w}{\partial r}+\frac{h^3}{2}\beta_r\beta_r{}^*+\frac{h^3}{6}\beta_r\frac{\partial w^*}{\partial r}+h\left(\frac{\partial w}{\partial r}\right)^2+\frac{h^3}{2}\beta_r{}^*\frac{\partial w}{\partial r}+\right.$$

$$\left.\frac{h^3}{6}\frac{\partial w}{\partial r}\frac{\partial w^*}{\partial r}+\frac{9h^5}{80}\beta_r{}^{*2}+\frac{3h^5}{40}\beta_r{}^*\frac{\partial w^*}{\partial r}+\frac{h^5}{80}\left(\frac{\partial w^*}{\partial r}\right)^2\right]+\frac{2t}{2}\left(\frac{\partial w}{\partial r}\right)+\frac{1}{2}Kw^2-qw.$$

$$\frac{\partial F_1}{\partial w}-\frac{d}{dr}\left(\frac{\partial F_1}{\partial\left(\frac{\partial w}{\partial r}\right)}\right)=0 \tag{3.3.1.4}$$

$$\frac{\partial F_1}{\partial\beta_r}-\frac{d}{dr}\left(\frac{\partial F_1}{\partial\left(\frac{\partial\beta_r}{\partial r}\right)}\right)=0 \tag{3.3.1.5}$$

$$\frac{\partial F_1}{\partial w^*}-\frac{d}{dr}\left(\frac{\partial F_1}{\partial\left(\frac{dw^*}{dr}\right)}\right)=0 \tag{3.3.1.6}$$

$$\frac{\partial F_1}{\partial\beta_r{}^*}-\frac{d}{dr}\left(\frac{\partial F_1}{\partial\left(\frac{\partial\beta_r{}^*}{\partial r}\right)}\right)=0 \tag{3.3.1.7}$$

In the case of an axisymmetric problem there are only four governing PDE of the HSDT plate on a two-parameter Vlasov foundation.

It is known as the Euler-Lagrange equation and governing static equations of the equilibrium state of an elastic body.

Now, we obtain the governing differential equation for the foundation by taking the variation of φ and then equating it to zero.

3.4 Dynamic equation of plates on Vlasov foundation

$D\nabla^4 w + Kw - 2t\nabla^2 w = q$ is the static equation of a plate resting on a two-parameter elastic foundation.

After applying D'Alembert's principle, the unbalanced force equals the inertia force.

Unbalanced force $= q(x, y, t) - (D\nabla^4 w - 2t\nabla^2 w + Kw)$and inertia force $m\frac{\partial^2 w}{\partial t^2}$

$$\therefore m\frac{\partial^2 w}{\partial t^2} = q(x, y, t) - (D\nabla^4 w - 2t\nabla^2 w + Kw)$$

Considering the damping force $\left(c\frac{\partial w}{\partial t}\right)$ It also gets the following.

$$D\nabla^4 w - 2t\nabla^2 w + Kw + c\frac{\partial w}{\partial t} + (m_1 + m_0)\frac{\partial^2 w}{\partial t^2} = q(x, y, t) \quad (3.4.1)$$

is the dynamic equation of the plate resting on a two-parameter elastic foundation.

m_1 - Mass per unit plate area = ρh, ρ - mass density of plate material and c - Damping constant. m_0 - is the equivalent mass of soil participating in vibration.

Where D - is defined as the flexural rigidity of the plate and K, 2t, and m_0 are the soil parameters (Gibigaye et al., 2018; Vlasov and Leont'ev, 1966; Özgan and Daloğlu, 2012) defined as

$$\text{Activated soil mass, } m_0 = \rho_s \int_0^H \varphi^2(z)\, dz = \frac{\rho_s H}{\gamma}\left(\frac{\sinh\gamma\cosh\gamma - \gamma}{2\sinh^2\gamma}\right) \quad (3.4.2)$$

Where ρ_s is the mass density of soil.

For thin layer variation of φ may be assumed as $\varphi(z) = \left(1 - \frac{z}{H}\right)$

$$\therefore K = \frac{E_s(1 - v_s)}{H(1 + v_s)(1 - 2v_s)}, 2t = \frac{E_s H}{6(1 + v_s)} \text{ and } m_0 = \frac{\rho_s H}{3}$$

$D\nabla^4 w(r, \theta) - 2t\nabla^2 w(r, \theta) + Kw(r, \theta) = q(r, \theta)$ is the static equation of the plate on a two-parameter elastic foundation.

After applying D'Alembert's principle, the unbalanced force equals the inertia force.

Unbalanced force =

$q(r, \theta) - \left(D\nabla^4 w(r, \theta) - 2t\nabla^2 w(r, \theta) + Kw(r, \theta)\right)$and inertia force $m\frac{\partial^2 w}{\partial t^2}$

$$\therefore m\frac{\partial^2 w}{\partial t^2} = q(r, \theta, t) - (D\nabla^4 w(r, \theta) - 2t\nabla^2 w(r, \theta) + Kw(r, \theta))$$

Considering the damping force $\left(c\frac{\partial w}{\partial t}\right)$ also, it gets the following.

$D\nabla^4 w(r,\theta) - 2t\nabla^2 w(r,\theta) + Kw(r,\theta) + c\frac{\partial w}{\partial t} + (m_1 + m_0)\frac{\partial^2 w}{\partial t^2} = q(r,\theta,t)$ It is the plate's dynamic equation of plate on a two-parameter elastic foundation.

Now we can derive the dynamic equation of Mindlin and HSDT plate on a two-parameter elastic foundation after applying D'Alembert's principle, the unbalanced force equals the inertia force.

3.5 Solutions of Plate on Vlasov Foundation

A thin plate on an elastic foundation (Vlasov and Leont'ev, 1966) have presented such an analysis. The governing equation of a thin plate on a two-parameter elastic soil layer of thickness 'H' is

$$D\nabla^4 w - 2t\nabla^2 w + Kw = P(x,y) \tag{3.5.1}$$

In the Cartesian coordinate system

$$\nabla^2 = \text{Laplacian operator} = \frac{\partial^2}{\partial x^2} + \frac{\partial^2}{\partial y^2}$$

$$\nabla^4 = \text{Bi} - \text{harmonic operator} = \nabla^2\nabla^2 = \frac{\partial^4}{\partial x^4} + \frac{2\,\partial^4}{\partial x^2\,\partial y^2} + \frac{\partial^4}{\partial y^4}$$

and in a polar coordinate system

$$\nabla^2 = \left(\frac{\partial^2}{\partial r^2} + \frac{1}{r}\frac{\partial}{\partial r} + \frac{1}{r^2}\frac{\partial^2}{\partial \theta^2}\right)$$

$$\nabla^4 = \nabla^2\nabla^2 = \frac{\partial^4}{\partial r^4} + \frac{\partial^2}{r^2\,\partial r^2} + \frac{\partial^4}{r^4\,\partial \theta^4} + \frac{2\,\partial^3}{r\,\partial r^3} + \frac{2\,\partial^3}{r^3\,\partial \theta^2\,\partial r} + \frac{2\,\partial^4}{r^2\,\partial \theta^2\,\partial r^2}$$

From (3.5.1) $\nabla^4 w - \frac{2t}{D}\nabla^2 w + \frac{K}{D}w = \frac{P(x,y)}{D}$ and $\nabla^4 w - \frac{2t}{D}\nabla^2 w + \frac{K}{D}w = \frac{P(x,y)}{D}$

The bending moment can be expressed using thin plate theory as obtained by (Rao, 1998)

$$M_x = -D\left(\frac{\partial^2 w}{\partial x^2} + v_P\frac{\partial^2 w}{\partial y^2}\right); M_y = -D\left(\frac{\partial^2 w}{\partial y^2} + v_P\frac{\partial^2 w}{\partial x^2}\right); H = H_x = -H_Y = -D(1 - v_P)\frac{\partial^2 w}{\partial x\,\partial y}$$

$$N_x = -D\frac{\partial}{\partial x}\left(\frac{\partial^2 w}{\partial x^2} + \frac{\partial^2 w}{\partial y^2}\right) \text{and} N_y = -D\frac{\partial}{\partial y}\left(\frac{\partial^2 w}{\partial x^2} + \frac{\partial^2 w}{\partial y^2}\right)$$

$$Q_x = -D\left[\frac{\partial^3 w}{\partial x^3} + (2 - v_P)\frac{\partial^3 w}{\partial x\,\partial y^2}\right] \text{and } Q_y = -D\left[\frac{\partial^3 w}{\partial y^3} + (2 - v_P)\frac{\partial^3 w}{\partial y\,\partial x^2}\right]$$

For a simply supported rectangular plate of sides 'a' and 'b' the boundary condition on 'w' x, y = 0 and x = a and y = b

$$w(0,y) = 0 = w(a,y) = 0; \frac{\partial^2 w}{\partial x^2} + v_P\frac{\partial^2 w}{\partial y^2} = 0 \text{ at } x = 0 \text{ and } x = a$$

$$w(x,0) = 0 = w(x,b) = 0; \frac{\partial^2 w}{\partial y^2} + v_P\frac{\partial^2 w}{\partial x^2} = 0 \text{ at } y = 0 \text{ and } y = b$$

$f(x) = \sum_{n=1}^{\infty} f_m \sin\frac{n\pi x}{a} \therefore \int_0^a f(x)\sin\frac{n'\pi x}{a}dx = f_m\int_0^a \sin\frac{n\pi x}{a}\sin\frac{n'\pi x}{a}dx$

$\int_0^a f(x)\sin\frac{n'\pi x}{a}dx = \frac{f_m}{2}\int_0^a 2\sin\frac{n\pi x}{a}\sin\frac{n'\pi x}{a}dx$

$\int_0^a f(x)\sin\frac{n'\pi x}{a}dx = \frac{f_m}{2}\int_0^a \left[\cos\frac{\pi x}{a}(n-n') - \cos\frac{\pi x}{a}(n+n')\right]dx$

$\int_0^a f(x)\sin\frac{n'\pi x}{a}dx = \frac{f_m}{2}\left[\frac{\sin\frac{\pi x}{a}(n-n')}{\frac{\pi}{a}(n-n')} - \frac{\sin\frac{\pi x}{a}(n+n')}{\frac{\pi}{a}(n+n')}\right]_0^a$ When $n = n'$

$\int_0^a f(x)\sin\frac{n'\pi x}{a}dx = \frac{f_m}{2}\int_0^a 2\sin^2\frac{n\pi x}{a}dx = \frac{f_m}{2}\int_0^a \left(1-\cos\frac{2n\pi x}{a}\right)dx = \frac{f_m}{2}\left[x - \frac{\sin\frac{2n\pi x}{a}}{\frac{2n\pi}{a}}\right]_0^a$

$\int_0^a f(x)\sin\frac{n'\pi x}{a}dx = \frac{af_m}{2}$

When $n \neq n'$ and $\int_0^a f(x)\sin\frac{n'\pi x}{a}dx = 0$

$\therefore \int_0^a f(x)\sin\frac{n'\pi x}{a}dx = \frac{f_m a}{2}$ and $f_m = \frac{2}{a}\int_0^a f(x)\sin\frac{n\pi x}{a}dx$

$w(x,y) = \sum_{n=1}^{\infty}\sum_{m=1}^{\infty} W\sin\frac{n\pi x}{a}\sin\frac{m\pi y}{b}$

$$\text{Or} \int_{y=o}^{b}\int_{x=0}^{a} w(x,y)\sin\frac{n'\pi x}{a}\sin\frac{m'\pi y}{b}dxdy = \frac{ab}{4}\sum_{n=1}^{\infty}\sum_{m=1}^{\infty} W$$

$\therefore W = \frac{4}{ab}\int_{y=o}^{b}\int_{x=0}^{a} w(x,y)\sin\frac{n\pi x}{a}\sin\frac{m\pi y}{b}dxdy$

Assuming loading over the plate,

$$q = q(x,y) = \sum_{n=1}^{\infty}\sum_{m=1}^{\infty} q_{mn}\sin\frac{n\pi x}{a}\sin\frac{m\pi y}{b} \text{ for U.D.L} q(x,y) = q_0$$

$$\therefore q_{mn} = \frac{4}{ab}\int_{y=o}^{b}\int_{x=0}^{a} q_0\sin\frac{n\pi x}{a}\sin\frac{m\pi y}{b}dxdy = \frac{4q_0}{ab}\int_{y=o}^{b}\sin\frac{m\pi y}{b}dy\int_{x=0}^{a}\sin\frac{n\pi x}{a}dx$$

$\therefore q_{mn} = \frac{16q_0}{mn\pi^2}$

A patch load over an area u×v C.G (x_0, y_0) intensity q_0

$q(x,y) = \sum_{n=1}^{\infty}\sum_{m=1}^{\infty} q_{mn}\sin\frac{n\pi x}{a}\sin\frac{m\pi y}{b} \therefore q_{mn} = \frac{4q_0}{ab}\int_{y_0-\frac{v}{2}}^{y_0+\frac{v}{2}}\sin\frac{m\pi y}{b}dy\int_{x_0-\frac{u}{2}}^{x_0+\frac{u}{2}}\sin\frac{n\pi x}{a}dx$

$\therefore q_{mn} = \frac{4q_0}{ab}\times\frac{a}{n\pi}\times\frac{b}{m\pi}\left[\cos\frac{n\pi}{a}\left(x_0-\frac{u}{2}\right) - \cos\frac{n\pi}{a}\left(x_0+\frac{u}{2}\right)\right]\left[\cos\frac{m\pi}{b}\left(y_0-\frac{v}{2}\right) - \cos\frac{m\pi}{b}\left(y_0+\frac{v}{2}\right)\right]$

$\therefore q_{mn} = \frac{16q_0}{mn\pi^2}\sin\frac{n\pi x_0}{a}\sin\frac{n\pi u}{2a}\sin\frac{m\pi y_0}{b}\sin\frac{m\pi v}{2b}$

For point load

Assume the point load acts over an infinitesimal area $u \times v \therefore q_0 = \frac{P}{uv}$

$$\therefore q_{mn} = \frac{16}{mn\pi^2}\frac{P}{uv}\sin\frac{n\pi x_0}{a}\sin\frac{n\pi u}{2a}\sin\frac{m\pi y_0}{b}\sin\frac{m\pi v}{2b}$$

$$q_{mn} = \frac{4P}{ab}\sin\frac{n\pi x_0}{a}\sin\frac{m\pi y_0}{b}\lim_{u\to 0}\frac{\sin\frac{n\pi u}{2a}}{\frac{n\pi u}{2a}} \times \lim_{v\to 0}\frac{\sin\frac{m\pi v}{2b}}{\frac{m\pi v}{2b}}$$

$$\therefore q_{mn} = \frac{4P}{ab}\sin\frac{n\pi x_0}{a}\sin\frac{m\pi y_0}{b} \times 1 \times 1 = \frac{4P}{ab}\sin\frac{n\pi x_0}{a}\sin\frac{m\pi y_0}{b}$$

$$p(x,y) = \frac{4P}{ab}\sum_{n=1}^{\infty}\sum_{m=1}^{\infty}\sin\frac{n\pi x_0}{a}\sin\frac{m\pi y_0}{b}\sin\frac{n\pi x}{a}\sin\frac{m\pi y}{b}$$

Assume the line load acts over an infinitesimal area $u \times l$ $\therefore q_0 = \frac{P}{u}$

$$\therefore q_{mn} = \frac{16}{mn\pi^2}\frac{P}{u}\sin\frac{n\pi x_0}{a}\sin\frac{n\pi u}{2a}\sin\frac{m\pi y_0}{b}\sin\frac{m\pi l}{2b}$$

$$q_{mn} = \frac{8P}{m\pi a}\sin\frac{n\pi x_0}{a}\sin\frac{m\pi y_0}{b}\sin\frac{m\pi l}{2b}\lim_{u\to 0}\frac{\sin\frac{n\pi u}{2a}}{\frac{n\pi u}{2a}}$$

$$\therefore q_{mn} = \frac{8P}{m\pi a}\sin\frac{n\pi x_0}{a}\sin\frac{m\pi y_0}{b}\sin\frac{m\pi l}{2b} \times 1 = \frac{8P}{m\pi a}\sin\frac{n\pi x_0}{a}\sin\frac{m\pi y_0}{b}\sin\frac{m\pi l}{2b}$$

$$p(x,y) = \frac{8P}{m\pi a}\sum_{n=1}^{\infty}\sum_{m=1}^{\infty}\sin\frac{n\pi x_0}{a}\sin\frac{m\pi y_0}{b}\sin\frac{n\pi x}{a}\sin\frac{m\pi y}{b}\sin\frac{m\pi l}{2b}$$

For the boundary condition, using the two-dimensional Fourier sine integral transformations is convenient.

$$w(x,y) = \sum_{n=1}^{\infty}\sum_{m=1}^{\infty}\frac{4}{ab}W\sin\frac{n\pi x}{a}\sin\frac{m\pi y}{b}$$

$$\therefore \frac{\partial^4 w}{\partial x^4} = \left(\frac{n\pi}{a}\right)^4\sum_{n=1}^{\infty}\sum_{m=1}^{\infty}\frac{4}{ab}W\sin\frac{n\pi x}{a}\sin\frac{m\pi y}{b};$$

$$\therefore \frac{\partial^4 w}{\partial y^4} = \left(\frac{m\pi}{b}\right)^4\sum_{n=1}^{\infty}\sum_{m=1}^{\infty}\frac{4}{ab}W\sin\frac{n\pi x}{a}\sin\frac{m\pi y}{b}$$

$$\therefore \frac{\partial^4 w}{\partial x^2\,\partial y^2} = \left(\frac{nm\pi^2}{ab}\right)^2\sum_{n=1}^{\infty}\sum_{m=1}^{\infty}\frac{4}{ab}W\sin\frac{n\pi x}{a}\sin\frac{m\pi y}{b};$$

$$\frac{\partial^2 w}{\partial x^2} = -\left(\frac{n\pi}{a}\right)^2\sum_{n=1}^{\infty}\sum_{m=1}^{\infty}\frac{4}{ab}W\sin\frac{n\pi x}{a}\sin\frac{m\pi y}{b}$$

$$\frac{\partial^2 w}{\partial y^2} = -\left(\frac{m\pi}{b}\right)^2\sum_{n=1}^{\infty}\sum_{m=1}^{\infty}\frac{4}{ab}W\sin\frac{n\pi x}{a}\sin\frac{m\pi y}{b};$$

Plug in the governing equation

All ends are simply supported, and a point load 'P' at (x_0, y_0)

$$\nabla^4 w - \frac{2t}{D}\nabla^2 w + \frac{K}{D}w = \frac{P(x,y)}{D}$$

$$\left[\left(\frac{n\pi}{a}\right)^4 + 2\left(\frac{n\pi}{a}\right)^2\left(\frac{m\pi}{b}\right)^2 + \left(\frac{m\pi}{b}\right)^4 + \frac{2t}{D}\left\{\left(\frac{n\pi}{a}\right)^2 + \left(\frac{m\pi}{b}\right)^2\right\} + \frac{K}{D}\right]W = \frac{P}{D}\sin\frac{n\pi x_0}{a}\sin\frac{m\pi y_0}{b}$$

$$\text{Where, } J = \left[\left(\frac{n\pi}{a}\right)^4 + 2\left(\frac{n\pi}{a}\right)^2\left(\frac{m\pi}{b}\right)^2 + \left(\frac{m\pi}{b}\right)^4 + \frac{2t}{D}\left\{\left(\frac{n\pi}{a}\right)^2 + \left(\frac{m\pi}{b}\right)^2\right\} + \frac{K}{D}\right]$$

$$W = \frac{P}{JD}\sin\frac{n\pi x_0}{a}\sin\frac{m\pi y_0}{b}$$

$$w(x,y) = \sum_{n=1}^{\infty}\sum_{m=1}^{\infty}\frac{4}{ab}\frac{P}{JD}\sin\frac{n\pi x_0}{a}\sin\frac{m\pi y_0}{b}\sin\frac{n\pi x}{a}\sin\frac{m\pi y}{b}$$

All ends simply supported and a patch load of intensity q_0 over $(u \times v)$ centre at (x_0, y_0)

$$w(x,y) = \sum_{n=1}^{\infty}\sum_{m=1}^{\infty}\frac{16q_0}{JDmn\pi^2}\sin\frac{n\pi x_0}{a}\sin\frac{m\pi y_0}{b}\sin\frac{n\pi u}{2a}\sin\frac{m\pi v}{2b}\sin\frac{n\pi x}{a}\sin\frac{m\pi y}{b}$$

All ends are simply supported, and a UDL of intensity q_0 is on a full plate.

$$w(x,y) = \sum_{n=1}^{\infty}\sum_{m=1}^{\infty}\frac{16q_0}{JDmn\pi^2}\sin\frac{n\pi x}{a}\sin\frac{m\pi y}{b}$$

All ends are simply supported, and a line load of intensity q unit/meter on the plate.

$$w(x,y) = \sum_{n=1}^{\infty}\sum_{m=1}^{\infty}\frac{8q}{JDm\pi a}\sin\frac{n\pi x_0}{a}\sin\frac{m\pi y_0}{b}\sin\frac{n\pi x}{a}\sin\frac{m\pi y}{b}\sin\frac{m\pi l}{2b}$$

Dynamic response analysis of plate on vlasov foundation

$\nabla^4 w - \frac{2t}{D}\nabla^2 w + \frac{K}{D}w = \frac{P(x,y)}{D}$ It is the static equation of the plate on the Vlasov foundation.

A thin plate on elastic foundation (Vlasov and Leont'ev, 1966; Rao, 1998) have presented such an analysis. The governing equation of motion of a thin plate on a two-parameter elastic soil layer of thickness 'H' is

After applying D'Alembert's principle, unbalanced force is equal to inertia force.

Unbalanced force $= P(x,y,t) - (D\nabla^4 w - 2t\nabla^2 w + Kw)$ and inertia force $m\frac{\partial^2 w}{\partial t^2}$

$$\therefore m\frac{\partial^2 w}{\partial t^2} = P(x,y,t) - (D\nabla^4 w - 2t\nabla^2 w + Kw)$$

Considering the damping force $\left(c\frac{\partial w}{\partial t}\right)$ It also gets the following

$$D\nabla^4 w - 2t\nabla^2 w + Kw + c\frac{\partial w}{\partial t} + (m_1 + m_0)\frac{\partial^2 w}{\partial t^2} = P(x,y,t) \qquad (3.5.2)$$

Is the dynamic equation of the plate on the Vlasov foundation

$m_1 =$ mass per unit plate area $\frac{\gamma h}{g}$

C = Damping constant

$\gamma =$ unit weight of plate material

$g =$ accelaration due to graviy

p(x,y,t) = External load on plate

$m_0 =$ equivalent mass of soil participating in vibration.

Dynamic response of the plate on elastic foundation for suddenly applied load and moving load considering damping

Considering a rectangular isotropic plate with a moving mass exerting load (constant or harmonic) with simply supported edges parallel to x –the axis – a moving body with negligible inertia is moving parallel to the x-axis with the middle of y-axis, i.e. y = b/2 with constant velocity 'v'.

The governing equation for a system without damping neglects rotary moment of inertia and shear deformation. Kameswara Rao (1998) obtained the following.

For a simply supported rectangular plate of sides 'a' and 'b', the boundary condition on 'w' and the initial conditions, i.e. at t = 0 and x, y = 0 and x = a and y = b

$$w(x,y,0) = 0; \frac{\partial w(x,y,0)}{\partial t} = 0;$$

$$w(0,y,t) = 0 = w(a,y,t) = 0; \frac{\partial^2 w}{\partial x^2} + v_P \frac{\partial^2 w}{\partial y^2} = 0 \text{ at } x = 0 \text{ and } x = a$$

$$w(x,0,t) = 0 = w(x,b,t) = 0; \frac{\partial^2 w}{\partial y^2} + v_P \frac{\partial^2 w}{\partial x^2} = 0 \text{ at } y = 0 \text{ and } y = b$$

$$p(x,y,t) = \frac{4P}{ab} \sum_{n=1}^{\infty} \sum_{m=1}^{\infty} \sin\frac{n\pi x_0}{a} \sin\frac{m\pi y_0}{b} \sin\frac{n\pi x}{a} \sin\frac{m\pi y}{b} \text{ for point load } 'P'$$

For the boundary condition, using the two-dimensional Fourier sine integral transformations is convenient.

$$w(x,y,t) = \sum_{n=1}^{\infty} \sum_{m=1}^{\infty} \frac{4}{ab} W \sin\frac{n\pi x}{a} \sin\frac{m\pi y}{b}$$

$$\therefore \frac{\partial^4 w}{\partial x^4} = \left(\frac{n\pi}{a}\right)^4 \sum_{n=1}^{\infty} \sum_{m=1}^{\infty} \frac{4}{ab} W \sin\frac{n\pi x}{a} \sin\frac{m\pi y}{b};$$

$$\frac{\partial^4 w}{\partial y^4} = \left(\frac{m\pi}{b}\right)^4 \sum_{n=1}^{\infty} \sum_{m=1}^{\infty} \frac{4}{ab} W \sin\frac{n\pi x}{a} \sin\frac{m\pi y}{b}$$

$$\therefore \frac{\partial^4 w}{\partial x^2 \partial y^2} = \left(\frac{nm\pi^2}{ab}\right)^2 \sum_{n=1}^{\infty} \sum_{m=1}^{\infty} \frac{4}{ab} W \sin\frac{n\pi x}{a} \sin\frac{m\pi y}{b};$$

$$\frac{\partial^2 w}{\partial x^2} = -\left(\frac{n\pi}{a}\right)^2 \sum_{n=1}^{\infty} \sum_{m=1}^{\infty} \frac{4}{ab} W \sin\frac{n\pi x}{a} \sin\frac{m\pi y}{b}$$

$$\frac{\partial^2 w}{\partial y^2} = -\left(\frac{m\pi}{b}\right)^2 \sum_{n=1}^{\infty} \sum_{m=1}^{\infty} \frac{4}{ab} W \sin\frac{n\pi x}{a} \sin\frac{m\pi y}{b}; \frac{\partial w}{\partial t} = \sum_{n=1}^{\infty} \sum_{m=1}^{\infty} \frac{4}{ab} \frac{\partial W}{\partial t} \sin\frac{n\pi x}{a} \sin\frac{m\pi y}{b}$$

$$\text{and } \frac{\partial^2 w}{\partial t^2} = \sum_{n=1}^{\infty} \sum_{m=1}^{\infty} \frac{4}{ab} \frac{\partial^2 W}{\partial t^2} \sin\frac{n\pi x}{a} \sin\frac{m\pi y}{b}$$

Plug in the governing equation

$$\nabla^4 w - \frac{2t}{D} \nabla^2 w + \frac{K}{D} w + \frac{c}{D}\frac{\partial w}{\partial t} + m' \frac{\partial^2 w}{\partial t^2} = \frac{P(x,y,t)}{D}$$

$$m' \frac{\partial^2 W}{\partial t^2} + \frac{c}{D}\frac{\partial w}{\partial t} + \left[\left(\frac{n\pi}{a}\right)^4 + 2\left(\frac{n\pi}{a}\right)^2\left(\frac{m\pi}{b}\right)^2 + \left(\frac{m\pi}{b}\right)^4 + \frac{2t}{D}\left\{\left(\frac{n\pi}{a}\right)^2 + \left(\frac{m\pi}{b}\right)^2\right\} + s^4\right] W = \frac{P}{D} \sin\frac{n\pi x_0}{a} \sin\frac{m\pi y_0}{b}$$

For suddenly applied load

$x_0 = d$ and if $y_0 = b/2$ d is the distance of the applied load on the plate in the horizontal direction, i.e. , in the x-direction.

$$\text{Where } J = \left[\left(\frac{n\pi}{a}\right)^4 + 2\left(\frac{n\pi}{a}\right)^2\left(\frac{m\pi}{b}\right)^2 + \left(\frac{m\pi}{b}\right)^4 + \frac{2t}{D}\left\{\left(\frac{n\pi}{a}\right)^2 + \left(\frac{m\pi}{b}\right)^2\right\} + \frac{k}{D}\right]$$

$$\frac{d^2 W}{dt^2} + \frac{c}{Dm'}\frac{dW}{dt} + \frac{J}{m'} W = \frac{P}{Dm'} \sin\frac{n\pi d}{a}; \text{For C. F} \left(D^2 + \frac{c}{Dm'} D + \frac{J}{m'}\right) W = 0$$

$$\therefore D = \frac{-c}{2Dm\prime} \pm \frac{\sqrt{\left(\frac{c}{Dm\prime}\right)^2 - 4m\prime J}}{2m\prime}$$

When $\left(\frac{c}{Dm'}\right)^2 - 4m'J = 0$ critical damping $\therefore \left(\frac{c}{Dm'}\right)_{cr} = 2\sqrt{m'J}$

$\frac{c}{\frac{c}{Dm'}} = \xi \therefore c = 2\xi\sqrt{m'J};\ \omega_{mn}{}^2 = \frac{J}{m'}$ and $\frac{\frac{c}{Dm'}}{m'} = 2\xi\omega_{mn}$

$\therefore D = \frac{-2\xi\sqrt{m'J}}{2m'} \pm \frac{\sqrt{\left(2\xi\sqrt{m'J}\right)^2 - 4m'J}}{2m'} = -\xi\omega_{mn} \pm \sqrt{\xi^2\omega_{mn}{}^2 - \omega_{mn}{}^2}$

$\therefore D = -\xi\omega_{mn} \pm i\sqrt{\omega_{mn}{}^2(1-\xi^2)} = -\xi\omega_{mn} \pm i\omega_d$

$C.F = e^{-\omega_{mn}\xi t}(A\cos\omega_d t + B\sin\omega_d t);\ \omega_d = \omega_{mn}\sqrt{(1-\xi^2)}$

$\frac{d^2W}{dt^2} + \frac{c}{Dm'}\frac{dW}{dt} + \frac{J}{m'}W = \frac{P}{Dm'}\sin\frac{n\pi d}{a}\ \therefore P.I = \frac{P}{DJ}\sin\frac{n\pi d}{a}$

$\therefore W = C.F + P.I = e^{-\omega_{mn}\xi t}(A\cos\omega_d t + B\sin\omega_d t) + \frac{P}{DJ}\sin\frac{n\pi d}{a};$

After applying the initial condition $w = u_0; \frac{dw}{dt} = v_0$ at $t = 0$ solve for A and B;

For own computer program

$w(x,y,t) = \sum_{n=1,3,5}^{\infty}\sum_{m=1,3,5}^{\infty}\left[\frac{4}{ab}\sin\frac{n\pi x}{a}\sin\frac{m\pi y}{b}\left\{e^{-\omega_{mn}\xi t}(A\cos\omega_d t + B\sin\omega_d t) + \frac{P}{DJ}\sin\frac{n\pi d}{a}\right\}\right]$

Hence, velocity, acceleration and other responses.

For moving load case

For constant velocity 'v' $x_0 = vt$ and the load moves along the centre line ($y_0 = b/2$)

For constant point load

$\therefore m'\frac{\partial^2W}{\partial t^2} + q\frac{\partial W}{\partial t} + JW = \frac{P}{D}\sin\frac{n\pi vt}{a}\sin\frac{m\pi b}{2b}$ or $Dm'\frac{\partial^2W}{\partial t^2} + qD\frac{\partial W}{\partial t} + JDW = P\sin\frac{n\pi vt}{a}$

Where $J = \left[\left(\frac{n\pi}{a}\right)^4 + 2\left(\frac{n\pi}{a}\right)^2\left(\frac{m\pi}{b}\right)^2 + \left(\frac{m\pi}{b}\right)^4 + \frac{2t}{D}\left\{\left(\frac{n\pi}{a}\right)^2 + \left(\frac{m\pi}{b}\right)^2\right\} + \frac{k}{D}\right]$

$\frac{d^2W}{dt^2} + \frac{c}{Dm'}\frac{dW}{dt} + \frac{J}{m'}W = \frac{P}{Dm'}\sin\frac{n\pi vt}{a}$; For $C.F\left(D^2 + \frac{c}{Dm'}D + \frac{J}{m'}\right)W = 0$

$\therefore D = \frac{-c}{2Dm'} \pm \frac{\sqrt{\left(\frac{c}{Dm'}\right)^2 - 4m'J}}{2m'}$

When $\left(\frac{c}{Dm'}\right)^2 - 4m'J = 0$ critical damping $\therefore \left(\frac{c}{Dm'}\right)_{cr} = 2\sqrt{m'J}$

$\frac{c}{\frac{c}{Dm'}} = \xi \therefore c = 2\xi\sqrt{m'J};\ \omega_{mn}{}^2 = \frac{J}{m'}$ and $\frac{\frac{c}{Dm'}}{m'} = 2\xi\omega_{mn}$

$\therefore D = \frac{-2\xi\sqrt{m'J}}{2m'} \pm \frac{\sqrt{\left(2\xi\sqrt{m'J}\right)^2 - 4m'J}}{2m'} = -\xi\omega_{mn} \pm \sqrt{\xi^2\omega_{mn}{}^2 - \omega_{mn}{}^2}$

$\therefore D = -\xi\omega_{mn} \pm i\sqrt{\omega_{mn}{}^2(1-\xi^2)} = -\xi\omega_{mn} \pm i\omega_d$

$C.F = e^{-\omega_{mn}\xi t}(A\cos\omega_d t + B\sin\omega_d t);\ \omega_d = \omega_{mn}\sqrt{(1-\xi^2)}$

For P.I Assume $W_p = C\cos\frac{n\pi vt}{a} + D\sin\frac{n\pi vt}{a} = C\cos\omega_k t + D\sin\omega_k t$ Where $\frac{n\pi v}{a} = \omega_k$

$\frac{dW}{dt} = \omega_k(-C\sin\omega_k t + D\cos\omega_k t)$ and $\frac{d^2W}{dt^2} = -\omega_k{}^2(C\cos\omega_k t + D\sin\omega_k t)$

Plug in equition $\frac{d^2W}{dt^2} + 2\xi\omega_{mn}\frac{dW}{dt} + \omega_{mn}{}^2 W = \frac{P}{Dm'}\sin\frac{n\pi vt}{a}$

$[C(\omega_{mn}{}^2 - \omega_k{}^2) + 2\xi D\omega_{mn}\omega_k]\cos\omega_k t + [D(\omega_{mn}{}^2 - \omega_k{}^2) - 2\xi C\omega_{mn}\omega_k]\sin\omega_k t = \frac{P}{Dm'}\sin\omega_k t$

Above equation shall be valid for all times't' and for all constant C, D

$\therefore [C(\omega_{mn}{}^2 - \omega_k{}^2) + 2\xi D\omega_{mn}\omega_k] = 0$ and $[D(\omega_{mn}{}^2 - \omega_k{}^2) - 2\xi C\omega_{mn}\omega_k] = \frac{P}{Dm'}$

After solving $C = \frac{-2P\xi\omega_{mn}\omega_k}{Dm'[(\omega_{mn}{}^2-\omega_k{}^2)^2+(2\xi\omega_{mn}\omega_k)^2]}$ and $D = \frac{P(\omega_{mn}{}^2-\omega_k{}^2)}{Dm'[(\omega_{mn}{}^2-\omega_k{}^2)^2+(2\xi\omega_{mn}\omega_k)^2]}$

$\therefore W = e^{-\omega_{mn}\xi t}(A\cos\omega_d t + B\sin\omega_d t) + \frac{P}{Dm'[(\omega_{mn}{}^2-\omega_k{}^2)^2+(2\xi\omega_{mn}\omega_k)^2]}\{-2\xi\omega_{mn}\omega_k\cos\omega_k t + (\omega_{mn}{}^2 - \omega_k{}^2)\sin\omega_k t\}$

After applying the initial condition $w = u_0; \frac{dw}{dt} = v_0$ at $t = 0$; solve for A and B

For own computer program

$w(x,y,t) = \sum_{n=1,3,5}^{\infty}\sum_{m=1,3,5}^{\infty}\left[\frac{4}{ab}\sin\frac{n\pi x}{a}\sin\frac{m\pi y}{b}\{e^{-\omega_{mn}\xi t}(A\cos\omega_d t + B\sin\omega_d t) + (C\cos\omega_k t + D\sin\omega_k t)\}\right]$

Hence, velocity, acceleration and other responses.

Dynamic response of the plate on elastic foundation under suddenly applied and moving load without damping

$\nabla^4 w - \frac{2t}{D}\nabla^2 w + \frac{K}{D}w + m'\frac{\partial^2 w}{\partial t^2} = \frac{P(x,y,t)}{D}$

$m'\frac{\partial^2 W}{\partial t^2} + \left[\left(\frac{n\pi}{a}\right)^4 + 2\left(\frac{n\pi}{a}\right)^2\left(\frac{m\pi}{b}\right)^2 + \left(\frac{m\pi}{b}\right)^4 + \frac{2t}{D}\left\{\left(\frac{n\pi}{a}\right)^2 + \left(\frac{m\pi}{b}\right)^2\right\} + \frac{K}{D}\right]W = \frac{P}{D}\sin\frac{n\pi x_0}{a}\sin\frac{m\pi y_0}{b}$

For suddenly applied load

$x_0 = d$ and if $y_0 = b/2$

$\therefore m'\frac{\partial^2 W}{\partial t^2} + JW = \frac{P}{D}\sin\frac{n\pi vt}{a}\sin\frac{m\pi b}{2b}$ or $Dm'\frac{\partial^2 W}{\partial t^2} + JDW = P\sin\frac{n\pi d}{a}$ for constant point load.

$Dm'\frac{\partial^2 W}{\partial t^2} + JDW = P\cos\omega t\sin\frac{n\pi vt}{a}$ For the Harmonic point load of $P\cos\omega t$

Where $J = \left[\left(\frac{n\pi}{a}\right)^4 + 2\left(\frac{n\pi}{a}\right)^2\left(\frac{m\pi}{b}\right)^2 + \left(\frac{m\pi}{b}\right)^4 + \frac{2t}{D}\left\{\left(\frac{n\pi}{a}\right)^2 + \left(\frac{m\pi}{b}\right)^2\right\} + \frac{k}{D}\right] \therefore \omega_{mn}{}^2 = \frac{J}{m'}$

$\frac{d^2W}{dt^2} + \omega_{mn}{}^2 W = \frac{P}{Dm'}\sin\frac{n\pi d}{a}$ $C.F = A\cos\omega_{mn}t + B\sin\omega_{mn}t$

$\therefore P.I = \frac{1}{D^2+\omega_{mn}{}^2}\frac{P}{Dm'}\sin\frac{n\pi d}{a} = \frac{P}{Dm'}\frac{\sin\frac{n\pi d}{a}}{\omega_{mn}{}^2}$

$\therefore W = C.F + P.I = A\cos\omega_{mn}t + B\sin\omega_{mn}t + \frac{P}{Dm'}\frac{\sin\frac{n\pi d}{a}}{\omega_{mn}{}^2};$

After applying the initial condition $w = u_0; \frac{dw}{dt} = v_0$ at $t = 0$; solve for A and B

For own computer program

$$w(x,y,t) = \sum_{n=1,3,5}^{\infty}\sum_{m=1,3,5}^{\infty}\left[\frac{4}{ab}\sin\frac{n\pi x}{a}\sin\frac{m\pi y}{b}\left\{A\cos\omega_{mn}t + B\sin\omega_{mn}t + \frac{P}{Dm'}\frac{\sin\frac{n\pi d}{a}}{\omega_{mn}{}^2}\right\}\right]$$

Hence, velocity, acceleration and other responses.

For moving load case

For constant velocity 'v' $x_0 = vt$ and the load moves along the centre line ($y_0 = b/2$)

$\therefore m'\frac{\partial^2 W}{\partial t^2} + JW = \frac{P}{D}\sin\frac{n\pi vt}{a}\sin\frac{m\pi b}{2b}$

or $Dm'\frac{\partial^2 W}{\partial t^2} + JDW = P\sin\frac{n\pi vt}{a}$ For constant point load

$Dm'\frac{\partial^2 W}{\partial t^2} + JDW = P\cos\omega t\sin\frac{n\pi vt}{a}$ For the Harmonic point load of $P\cos\omega t$

Where $J = \left[\left(\frac{n\pi}{a}\right)^4 + 2\left(\frac{n\pi}{a}\right)^2\left(\frac{m\pi}{b}\right)^2 + \left(\frac{m\pi}{b}\right)^4 + \frac{2t}{D}\left\{\left(\frac{n\pi}{a}\right)^2 + \left(\frac{m\pi}{b}\right)^2\right\} + \frac{k}{D}\right] \therefore \omega_{mn}{}^2 = \frac{J}{m'}$

$\frac{d^2W}{dt^2} + \omega_{mn}{}^2 W = \frac{P}{Dm'}\sin\frac{n\pi vt}{a}$

$C.F = A\cos\omega_{mn}t + B\sin\omega_{mn}t$ and for P.I Assume $W = a_n\sin\frac{n\pi v}{a}$

$\frac{d^2W}{dt^2} = -\left(\frac{n\pi v}{a}\right)^2 a_n\sin\frac{n\pi vt}{a}$ Plug in equition $\frac{d^2W}{dt^2} + \omega_{mn}{}^2 W = \frac{P}{Dm'}\sin\frac{n\pi vt}{a}$

$-\left(\frac{n\pi v}{a}\right)^2 a_n\sin\frac{n\pi vt}{a} + \omega_{mn}{}^2 a_n\sin\frac{n\pi vt}{a} = \frac{P}{Dm'}\sin\frac{n\pi vt}{a} \therefore a_n = \frac{\frac{P}{Dm'}}{-\left(\frac{n\pi v}{a}\right)^2 + \omega_{mn}{}^2}$

$\therefore P.I = \frac{\frac{P}{Dm'}}{\omega_{mn}{}^2 - \left(\frac{n\pi v}{a}\right)^2}\sin\frac{n\pi vt}{a}$

$\therefore W = C.F + P.I = A\cos\omega_{mn}t + B\sin\omega_{mn}t + \frac{\frac{P}{Dm'}}{\omega_{mn}{}^2 - \left(\frac{n\pi v}{a}\right)^2}\sin\frac{n\pi vt}{a}$

After applying the initial condition $w = u_0; \frac{dw}{dt} = v_0$ at $t = 0$; solve for A and B

For own computer program

$w(x,y,t) =$

$$\sum_{n=1,3,5}^{\infty}\sum_{m=1,3,5}^{\infty}\left[\frac{4}{ab}\sin\frac{n\pi x}{a}\sin\frac{m\pi y}{b}\left(A\cos\omega_{mn}t + B\sin\omega_{mn}t + \frac{\frac{P}{Dm'}}{\omega_{mn}{}^2-\left(\frac{n\pi v}{a}\right)^2}\sin\frac{n\pi vt}{a}\right)\right]$$

Hence velocity, acceleration and other responses.

For moving harmonic point load Pcosωt

$$\frac{d^2W}{dt^2} + \omega_{mn}{}^2W = \frac{P\cos\omega}{Dm'}\sin\frac{n\pi vt}{a} = \frac{P}{2Dm'}[\sin(\omega_k+\omega)\,t + \sin(\omega_k-\omega)\,t] \;\text{ where } \frac{n\pi v}{a} = \omega_k$$

$$C.F = A\cos\omega_{mn}t + B\sin\omega_{mn}t \text{ and } P.I = \frac{P}{2D\ '}\left[\frac{\sin(\omega_k+\omega)t}{\omega_{mn}{}^2-(\omega_k+\omega)^2} + \frac{\sin(\omega_k-\omega)t}{\omega_{mn}{}^2-(\omega_k-\omega)^2}\right]$$

$$W = A\cos\omega_{mn}t + B\sin\omega_{mn}t + \frac{P}{2Dm'}\left(\frac{\sin(\omega_k+\omega)t}{\omega_{mn}{}^2-(\omega_k+\omega)^2} + \frac{\sin(\omega_k-\omega)t}{\omega_{mn}{}^2-(\omega_k-\omega)^2}\right)$$

After applying the initial condition $w = u_0; \frac{dw}{dt} = v_0$ at $t = 0$; solve for A and B

For own computer program

$w(x,y,t) =$

$$\sum_{n=1,3,5}^{\infty}\sum_{m=1,3,5}^{\infty}\left[\frac{4}{ab}\sin\frac{n\pi x}{a}\sin\frac{m\pi y}{b}\left\{A\cos\omega_{mn}t + B\sin\omega_{mn}t + \frac{P}{2Dm'}\left(\frac{\sin(\omega_k+\omega)t}{\omega_{mn}{}^2-(\omega_k+\omega)^2} + \frac{\sin(\omega_k-\omega)t}{\omega_{mn}{}^2-(\omega_k-\omega)^2}\right)\right\}\right]$$

Hence, velocity, acceleration and other responses.

Chapter 4

Finite Element Formulation

4.1 FEM of rectangular plate bending element

It has four corner nodes, each associated with four degrees of freedom. This element has a total of sixteen degrees of freedom. This compatible element was developed by (Bogner et al., 1966).

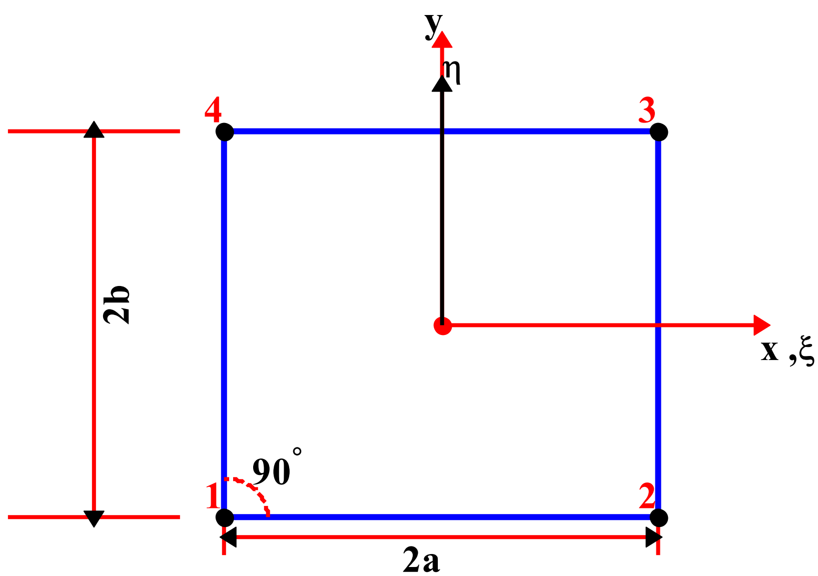

Fig. 4.1 PBR4 plate elements

Considered $\frac{\partial^2 w}{\partial x\, \partial y}$ also, a nodal unknown to overcome non-conformity in the case of four nodded twelve degrees of freedom element.

$u(x, y, z) = -z\frac{\partial w_0}{\partial x}; v(x, y, z) = -z\frac{\partial w_0}{\partial y}$ and $w(x, y, z) = w_0(x, y)$.

It is further assumed that as, w(x, y, 0) = w(x, y).

The displacements of the surface of the soil are equal to the displacements of the middle surface of the plate.

The nodal displacement at the ith node $\{\delta_i\} = \left\{w_i \quad \left(\frac{\partial w}{\partial x}\right)_i \quad \left(\frac{\partial w}{\partial y}\right)_i \quad \left(\frac{\partial^2 w}{\partial x\, \partial y}\right)_i\right\}^T$ (Fig. 4.1)

The element displacement vector is defined as $\{d_e\} = \{d_1\ d_2\ d_3\ d_4\}^T$ For four nodded elements.

The element is based on the thin plate theory. Hence, it is sufficient to prescribe a variation of transverse displacement within the element region. A complete product of cubic polynomial in x and y direction as $(1+x+x^2+x^3)(1+y+y^2+y^3)$.A 16 DOF rectangular plate element. Proper first-order cubic Hermitian function multiplications derive shape function in the x and y directions.

$$n_1x = \frac{1}{2} - \frac{3x}{4a} + \frac{x^3}{4a^3}; n_2x = \frac{a}{4} - \frac{x}{4} - \frac{x^2}{4a} + \frac{x^3}{4a^2};$$

$$n_3x = \frac{1}{2} + \frac{3x}{4a} - \frac{x^3}{4a^3}; n_4x = \frac{x^3}{4a^2} - \frac{a}{4} - \frac{x}{4} + \frac{x^2}{4a};$$

$$n_1y = \frac{1}{2} - \frac{3y}{4b} + \frac{y^3}{4b^3}; n_2y = \frac{b}{4} - \frac{y}{4} - \frac{y^2}{4b} + \frac{y^3}{4b^2};$$

$$n_3y = \frac{1}{2} + \frac{3y}{4b} - \frac{y^3}{4b^3}; n_4y = \frac{y^3}{4b^2} - \frac{b}{4} - \frac{y}{4} + \frac{y^2}{4b};$$

The shape functions for displacement parameters at node one are written as $N_1 = n_1x \times n_1y$;

$$N_1 = \frac{x^3}{8a^3} - \frac{3y}{8b} - \frac{3x}{8a} + \frac{y^3}{8b^3} - \frac{3xy^3}{16ab^3} - \frac{3x^3y}{16a^3b} + \frac{x^3y^3}{16a^3b^3} + \frac{9xy}{16ab} + \frac{1}{4};$$

$N_2 = n_1x \times n_2y$; $N_3 = n_2x \times n_1y$; $N_4 = n_2x \times n_2y$;

$N_5 = n_3x \times n_1y$; $N_6 = n_3x \times n_2y$; $N_7 = n_4x \times n_1y$;

$N_8 = n_4x \times n_2y$; $N_9 = n_3x \times n_3y$; $N_{10} = n_3x \times n_4y$;

$N_{11} = n_4x \times n_3y$; $N_{12} = n_4x \times n_4y$; $N_{13} = n_1x \times n_3y$;

$N_{14} = n_1x \times n_4y$; $N_{15} = n_2x \times n_3y$; $N_{16} = n_2x \times n_4y$;

$$\varepsilon_{xx} = \frac{\partial u}{\partial x} = -z\frac{\partial^2 w_0}{\partial x^2} = -z\chi_x; \varepsilon_{yy} = \frac{\partial v}{\partial y} = -z\frac{\partial^2 w_0}{\partial y^2} = -z\chi_y; \gamma_{xy} = \frac{\partial v}{\partial x} + \frac{\partial u}{\partial y}$$

$$\gamma_{xy} = -z\left(\frac{\partial^2 w_0}{\partial xdy} + \frac{\partial^2 w_0}{\partial xdy}\right) = -2z\frac{\partial^2 w_0}{\partial xdy} = -z\chi_{xy}; \varepsilon_{zz} = \gamma_{xz} = \gamma_{yz} = 0$$

$$\begin{Bmatrix} \chi_x \\ \chi_y \\ \chi_{xy} \end{Bmatrix} = \begin{bmatrix} \frac{\partial^2 w_0}{\partial x^2} \\ \frac{\partial^2 w_0}{\partial y^2} \\ 2\frac{\partial^2 w_0}{\partial xdy} \end{bmatrix} = \begin{bmatrix} \frac{\partial^2 N}{\partial x^2} \\ \frac{\partial^2 N}{\partial y^2} \\ 2\frac{\partial^2 N}{\partial xdy} \end{bmatrix}\{w_0\} \therefore [B_{bi}] = \begin{bmatrix} \frac{\partial^2 N}{\partial x^2} \\ \frac{\partial^2 N}{\partial y^2} \\ 2\frac{\partial^2 N}{\partial xdy} \end{bmatrix};$$

$[B_b] = [B_{b1}\ B_{b2} \ldots \ldots \ldots B_{b16}]$for four nodded elements.

$C_{11} = \frac{E}{(1-\nu^2)}$ and $G = \frac{E}{2(1+\nu)}$; $C_{22} = C_{11}$; $C_{33} = C_{11}$; $C_{12} = \nu C_{11}$; $C_{13} = C_{12}$;

$C_{21} = C_{12}$; $C_{23} = C_{12}$; $C_{31} = C_{12}$; $C_{32} = C_{12}$; $C_{44} = G$;

$$\therefore [C_b] = \begin{bmatrix} C_{11} & C_{12} & 0 \\ C_{21} & C_{22} & 0 \\ 0 & 0 & C_{44} \end{bmatrix}; [D] = \int_{-\frac{h}{2}}^{\frac{h}{2}} z[C_b]\, dz = \frac{Eh^3}{12(1-\nu^2)} \begin{bmatrix} 1 & \nu & 0 \\ \nu & 1 & 0 \\ 0 & 0 & \frac{1-\nu}{2} \end{bmatrix}$$

Hence, the bending stiffness matrix, $[K_b] = [B]^T[D][B]$;

$$[K_b] = \int_{-1}^{1} \int_{-1}^{1} [B_b]^T[D][B_b]|J|dsdt$$

Following the usual steps, the bending is expressed as

$$[K_b] = \sum_{j=1}^{5} \sum_{i=1}^{5} W_i W_j |J| [B_b]^T[D][B_b]$$

These equations show that a full 5 ×5 Point Gauss-Lobatto-type quadrature is adopted for bending stiffness.

Considering a structural element which has a differential area ‘dA’ in contact with the foundation, the lateral deflection of area ‘dA’ normal to the foundation is $w = [N_f]\{d\}$

The strain energy U_r in a linear spring is given by eq. $= \frac{1}{2}Kw^2$

$U_r = \frac{1}{2}\int Kw^2\, dA$; K is the soil first/vertical/Winkler parameter.

As ‘w’ is a scalar, so $w^2 = w^T w$ and $w^2 = \{d\}^T[N_f]^T[N_f]\{d\}$

Strain energy $U_r = \frac{1}{2}\int K\{d\}^T[N_f]^T[N_f]\{d\}\, dA = \frac{1}{2}\{d\}^T[K_f]\{d\}$

In which the foundation stiffness matrix for the element is, $[K_f] = \int K[N_f]^T[N_f]\, dA$

$$[K_f] = Kab \int_{-1}^{1} \int_{-1}^{1} [N_f]^T[N_f]\, dsdt = K \int_{-1}^{1} \int_{-1}^{1} [N_f]^T[N_f]\, |J|dsdt$$

If the problem deals with a plate on an elastic foundation, $[N_f]$ is identical to the plate's shape function matrix [N].

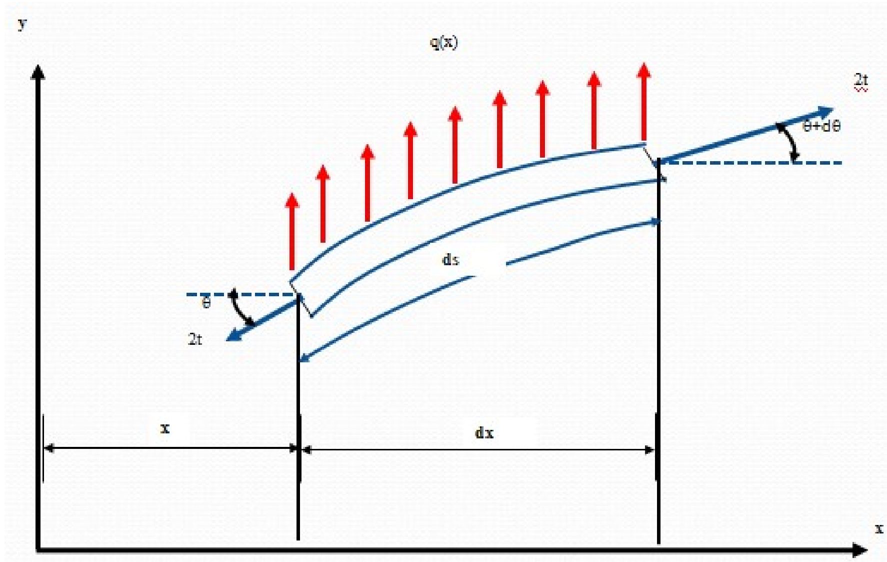

Fig. 4.2 the length of a differential element

The length of a differential element 'dx'in the deformed position, 'ds', can be expressed as

$$ds = \sqrt{(dx)^2 + (dw)^2} = dx\sqrt{1 + \left(\frac{dw}{dx}\right)^2} = dx\left[1 + \left(\frac{dw}{dx}\right)^2\right]^{\frac{1}{2}} = dx\left[1 + \frac{1}{2}\left(\frac{dw}{dx}\right)^2\right]$$

$$\therefore ds - dx = \frac{1}{2}\left(\frac{dw}{dx}\right)^2 dx$$

Strain energy stored by foundation parameter '2t' in x- direction is given by (Fig. 4.2.)

$$U = \frac{1}{2}\int_{-a}^{a} 2t\left(\frac{\partial w}{\partial x}\right)^2 dx = \frac{1}{2}\int_{-a}^{a} 2t\{d\}^T\left[\frac{\partial N_f}{\partial x}\right]^T\left[\frac{\partial N_f}{\partial x}\right]\{d\}\,dx = \frac{1}{2}\{d\}^T[K_{ex}]\{d\}$$

where $[K_{ex}] = \int_{-a}^{a} 2t\left[\frac{\partial N_f}{\partial x}\right]^T\left[\frac{\partial N_f}{\partial x}\right]dx$

and Similarly for y-direction $[K_{ey}] = \int_{-b}^{b} 2t\left[\frac{\partial N_f}{\partial y}\right]^T\left[\frac{\partial N_f}{\partial y}\right]dy$

So, the stiffness for the shear parameter, 2t, is $[K_e] = 2t\iint[S^TS + R^TR]dA$ where $R = \left[\frac{\partial N_f}{\partial x}\right]$ and $S = \left[\frac{\partial N_f}{\partial y}\right]$

$$[K_e] = 2tab\int_{-1}^{1}\int_{-1}^{1}\left(\frac{1}{a^2}\left[\frac{\partial N}{\partial s}\right]^T\left[\frac{\partial N}{\partial s}\right] + \frac{1}{b^2}\left[\frac{\partial N}{\partial t}\right]^T\left[\frac{\partial N}{\partial t}\right]\right)dsdt$$

$$[K_e] = 2t\int_{-1}^{1}\int_{-1}^{1}\left(\frac{1}{a^2}\left[\frac{\partial N}{\partial s}\right]^T\left[\frac{\partial N}{\partial s}\right] + \frac{1}{b^2}\left[\frac{\partial N}{\partial t}\right]^T\left[\frac{\partial N}{\partial t}\right]\right)|J|dsdt$$

The element load vector for a plate resulting from transverse distributed load acting on top of the plate is q per unit area.

$$\{f_q\} = q\int_{-1}^{1}\int_{-1}^{1}[N]^T\,|J|dsdt.$$

Force vector for point load $\{f_F\} = [N]^T[F]$

The element load vector $\{f\} = \{f_q\} + \{f_F\}$

The global load vector is generated by using the conventional finite element method.

$\therefore \{f_S\} = \sum_1^n(\{f_q\} + \{f_F\})$

The element load matrix for n nodded plate is due to the transversely distributed load of q per unit area acting on top of the plate.

$$\{q_i\} = q\sum_{i=1}^{5}\sum_{j=1}^{5} W_i W_j |J| N_i$$

Integration is carried out using 5 × 5 Gauss-Lobatto integration.

$\{f\} = \{q_1\ q_2 \dots\dots\dots\dots q_{16}\}^T$ For four nodded elements.

Similarly, a typical sub-matrix for the foundation parameter corresponding to i^{th} node is

$$[K_{fi}] = K\sum_{i=1}^{5}\sum_{j=1}^{5} W_i W_j |J| N_i^T N_j$$

$\{K_f\} = \{K_{f1}\ K_{f2} \dots\dots\dots\dots K_{f16}\}^T$ For four nodded elements.

A typical sub-matrix for the foundation second parameter corresponding to i^{th} node is

$$[K_{e_i}] = 2t\left(\sum_{i=1}^{5}\sum_{j=1}^{5} W_i W_j |J| \frac{dN}{dx_i} + \sum_{i=1}^{5}\sum_{j=1}^{5} W_i W_j |J| \frac{dN}{dy_i}\right)$$

A stiffness matrix of four nodded elements.

$$[K_e] = [K_{e1}\ K_{e2} \dots\dots\dots K_{e1}\ ]$$

Matrix of the elements' stiffness $[K] = [K_b] + [K_f] + [K_e]$

The traditional finite element approach is used to construct the global stiffness matrix.

$$\therefore [K_S] = \sum_1^n([K_b] + [K_f] + [K_e])$$

Hence obtain $[x] = [K_S]^{-1}\{f_S\}$

4.2 Application of Annular Sector Element

Displacement variations of thin circular plate written as (Figure 4.3).

$$u(r,\theta,z) = -z\frac{\partial w}{\partial r}; v(r,\theta,z) = -\frac{z}{r}\frac{\partial w}{\partial \theta} \text{ and } w(r,\theta,z) = w(r,\theta)$$

$$\frac{\partial u}{\partial \theta} = \frac{\partial\left(-z\frac{\partial w}{\partial r}\right)}{\partial \theta} = -z\frac{\partial^2 w}{\partial r\,\partial \theta}; \frac{\partial v}{\partial \theta} = \frac{\partial\left(-\frac{z\partial w}{r\partial \theta}\right)}{\partial \theta} = -\frac{z}{r}\frac{\partial^2 w}{\partial \theta^2}; \frac{\partial v}{\partial r} = \frac{\partial\left(-\frac{z\partial w}{r\partial \theta}\right)}{\partial r} = -z\frac{\partial}{\partial r}\left(\frac{\frac{\partial w}{\partial \theta}}{r}\right) = -z\left[\frac{r\frac{\partial^2 w}{\partial r\,\partial \theta} - \frac{\partial w}{\partial \theta}}{r^2}\right]$$

$$\frac{\partial v}{\partial r} = -\frac{z}{r}\frac{\partial^2 w}{\partial r\,\partial\theta} + \frac{z}{r^2}\frac{\partial w}{\partial\theta};\ \varepsilon_{rr} = \frac{\partial u}{\partial r} = -z\frac{\partial^2 w}{\partial r^2};\ \varepsilon_{\theta\theta} = \frac{u}{r} + \frac{1}{r}\frac{\partial v}{\partial\theta} = -\frac{z}{r}\frac{\partial w}{\partial r} - \frac{z}{r^2}\frac{\partial^2 w}{\partial\theta^2};$$

$$\gamma_{r\theta} = \frac{1}{r}\frac{\partial u}{\partial\theta} + \frac{\partial v}{\partial r} - \frac{v}{r} = -\frac{z}{r}\frac{\partial^2 w}{\partial r\,\partial\theta} + \left(-\frac{z}{r}\frac{\partial^2 w}{\partial r\,\partial\theta} + \frac{z}{r^2}\frac{\partial w}{\partial\theta}\right) + \frac{z}{r^2}\frac{\partial w}{\partial\theta} = -\frac{2z}{r}\frac{\partial^2 w}{\partial r\,\partial\theta} + \frac{2z}{r^2}\frac{\partial w}{\partial\theta}$$

and $\varepsilon_{zz} = \gamma_{rz} = \gamma_{\theta z} = 0$

$$\begin{Bmatrix}\varepsilon_{rr}\\ \varepsilon_{\theta\theta}\\ \gamma_{r\theta}\end{Bmatrix} = \begin{bmatrix} -z\frac{\partial^2 w}{\partial r^2} \\ -\frac{z}{r}\frac{\partial w}{\partial r} - \frac{z}{r^2}\frac{\partial^2 w}{\partial\theta^2} \\ -\frac{2z}{r}\frac{\partial^2 w}{\partial r\,\partial\theta} + \frac{2z}{r^2}\frac{\partial w}{\partial\theta}\end{bmatrix} = -z\begin{bmatrix}\frac{\partial^2 N}{\partial r^2} \\ \frac{1}{r}\frac{\partial N}{\partial r} + \frac{1}{r^2}\frac{\partial^2 N}{\partial\theta^2} \\ \frac{2}{r}\frac{\partial^2 N}{\partial r\,\partial\theta} - \frac{2}{r^2}\frac{\partial N}{\partial\theta}\end{bmatrix}\{w\} \therefore [B_{bi}] = \begin{bmatrix}\frac{\partial^2 N}{\partial r^2} \\ \frac{1}{r}\frac{\partial N}{\partial r} + \frac{1}{r^2}\frac{\partial^2 N}{\partial\theta^2} \\ \frac{2}{r}\frac{\partial^2 N}{\partial r\,\partial\theta} - \frac{2}{r^2}\frac{\partial N}{\partial\theta}\end{bmatrix};$$

$[B_b] = [B_{b1}\ B_{b2} \ldots\ldots\ldots B_{b16}]$ For four nodded elements.

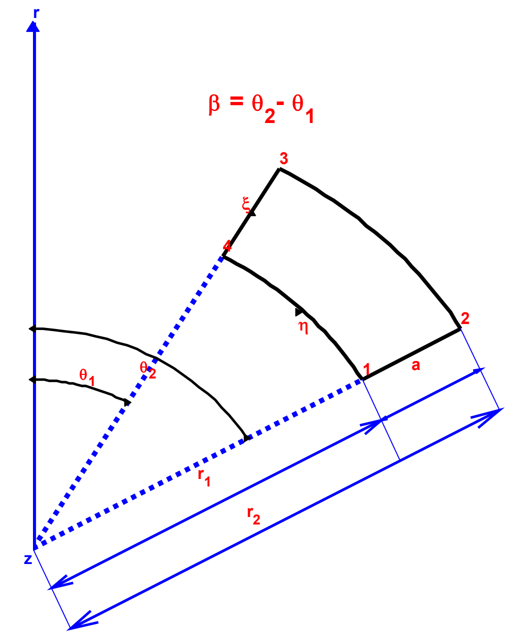

Fig. 4.3 Annular sector elements

For the plane stress condition, the relationship between stresses and strain is given by,

$D_{11} = \frac{E}{(1-\nu^2)}$ and $G = \frac{E}{2(1+\nu)}$; $D_{22} = D_{11}$; $D_{33} = D_{11}$; $D_{12} = \nu D_{11}$; $D_{13} = D_{12}$

$D_{21} = D_{12}$; $D_{23} = D_{12}$; $D_{31} = D_{12}$; $D_{32} = D_{12}$; $D_{44} = G$;

$$\therefore [C_b] = \begin{bmatrix} D_{11} & D_{12} & 0 \\ D_{21} & D_{22} & 0 \\ 0 & 0 & D_{44}\end{bmatrix};\ [D] = \int_{-\frac{h}{2}}^{\frac{h}{2}} z^2 [C_b]\,dz = \frac{Eh^3}{12(1-\nu^2)}\begin{bmatrix} 1 & \nu & 0 \\ \nu & 1 & 0 \\ 0 & 0 & \frac{1-\nu}{2}\end{bmatrix}.$$

Where [D] is the plate rigidity matrix.

4.2.1 FEM of circular plate bending element

Figure 4.4 shows the four nodded annular plate bending (A.P.B.) elements. Each node has four degrees of freedom (D.O.F.). For example, this element has 16 D.O.F. This compatible element was designed by (Bogner et al., 1966).

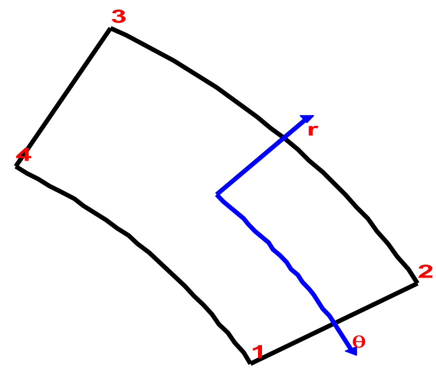

Fig. 4.4 4 A.P.B. element

The plate's length and subtended angles are r and β.

Nodes 1, 2, 3 and 4 have coordinates in polar systems of (r_1, 0), (r_2, 0), (r_2, β), (r_1, β) respectively. Where $a = r_2 - r_1$.

Considered w, $\frac{\partial w}{\partial r}, \frac{\partial w}{\partial \theta}, \frac{\partial^2 w}{\partial r\, \partial \theta}$ nodal unknown.

The displacement function for this type of element is assumed as follows

$$: w(r,\theta) = a_1 + a_2 r + a_3\theta + a_4 r^2 \ldots\ldots\ldots\ldots + a_{16} r^3 \theta^3 \quad (4.1.1)$$

The shape function can now be calculated from equation (4.1.1) by evaluating the sixteen corner displacements. Consequently, the stiffness matrix for bending,

$[K_b] = \int_{-1}^{1}\int_{-1}^{1}[B_b]^T[D][B_b]|J|\,dr\,d\theta$ and $|J| = ar\beta$.

The bending is described by the usual steps as follows

$[K_b] = \frac{1}{4}\sum_{j=1}^{4}\sum_{i=1}^{4} W_i W_j |J| [B_b]^T[D][B_b]$.

These equations demonstrate adopting a full 4 × 4 point Gauss-Legendre quadrature for bending stiffness.

The lateral displacement of an area 'dA' normal to the foundation for a structural member with a differential area 'dA' in contact with the foundation is given by w = [N] d. For example, in a linear spring, the strain energy Ur is given by ½Kw^2.

$\therefore U_r = \frac{1}{2}\int Kw^2\, dA = \frac{1}{2}\int K\{d\}^T[N]^T[N]\{d\}\, dA$; K is also known as the subgrade reaction modulus.$U_r = \frac{1}{2}\{d\}^T[K_f]\{d\}$.When the element's foundation stiffness matrix is,

$$[K_f] = \int K[N]^T[N]\, dA = \frac{Kar\beta}{4}\int_{-1}^{1}\int_{-1}^{1}[N]^T[N]\, drd\theta = \frac{Kar\beta}{4}\int_{-1}^{1}\int_{-1}^{1}[N]^T[N]\, drd\theta$$

$[K_f] = \frac{K}{4}\int_{-1}^{1}\int_{-1}^{1}[N]^T[N]\, |J| drd\theta$; [N] is the same as the plate's shape function matrix.

The foundation parameter corresponding to the i^{th} node's typical sub-matrix is

$$[K_{fi}] = \frac{K}{4}\sum_{i=1}^{4}\sum_{j=1}^{4} W_i W_j |J| N_i{}^T N_j$$

$[K_f] = \{K_{f1}\ K_{f2} \ldots\ldots\ldots\ldots K_{f16}\}^T$ for four nodded elements.

The strain energy is given by the foundation parameter '2t.'$\int 2t\left\{\frac{1}{r^2}\left(\frac{\partial w}{\partial \theta}\right)^2 + \left(\frac{\partial w}{\partial r}\right)^2\right\} dA$

$$[K_e] = 2t\int_{-1}^{1}\int_{-1}^{1}\left(\frac{1}{r^2}\left[\frac{\partial N}{\partial \theta}\right]^T\left[\frac{\partial N}{\partial \theta}\right] + \left[\frac{\partial N}{\partial r}\right]^T\left[\frac{\partial N}{\partial r}\right]\right)|J| drd\theta$$

Additionally, a typical sub-matrix for the i^{th} nodes for the second foundation parameter is

$$[K_{e_i}] = 2t\left(\sum_{i=1}^{4}\sum_{j=1}^{4} W_i W_j |J| \frac{dN}{dr}_i + \sum_{i=1}^{4}\sum_{j=1}^{4} W_i W_j |J| \frac{dN}{d\theta}_i\right)$$

To four nodded elements $[K_e] = [K_{e1}\ K_{e2} \ldots\ldots K_{e1}\ ]$.

Matrix of the elements' stiffness $[K] = [K_b] + [K_f] + [K_e]$.

The traditional finite element approach is used to construct the global stiffness matrix.

$$\therefore [K_S] = \sum_1^n([K_b] + [K_f] + [K_e])$$

The element load vector for a plate as a result of a transverse distributed load applied on top of the plate is q per unit area.

$\{f_1\} = q\int_{-1}^{1}\int_{-1}^{1}[N]^T |J| dsdt$ and $\{q_i\} = \frac{q}{4}\sum_{i=1}^{4}\sum_{j=1}^{4} W_i W_j |J| N_i$

4×4 Gauss-Legendre integration is used to complete the integration.

$\{f_1\} = \{q_1\ q_2 \dots \dots \dots \dots . q_{16}\}^T$ to four nodded components.

For a point load, the force vector $\{f_2\} = [N]^T[F]$ Where $[N]^T$ is the shape function assessed at the applied load (F). The global force vector is calculated using the conventional finite element method.$\therefore$ $\{f\} = \sum_1^n(\{f_1\} + \{f_2\})$.

Hence obtain $[x] = [K_S]^{-1}\{f\}$.

4.3 FEM of skews plate bending element

It shows four corner nodes, and Fig. 4.5 shows that each node corresponds to four degrees of freedom. As a result, the element has sixteen degrees of freedom altogether.

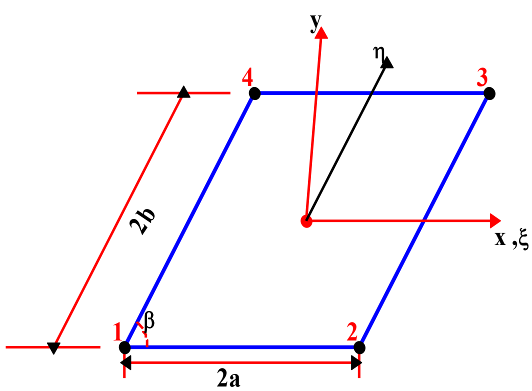

Fig. 4.5 PBS4 in oblique coordinate system

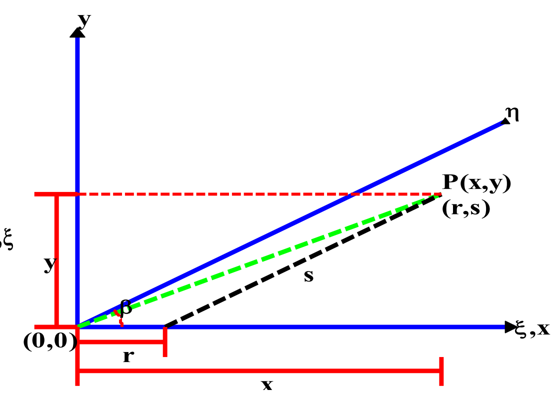

Fig. 4.6 Point in global and local coordinate system

x = r + scosβ and y = ssinβ or s = ycosecβ and r = x - ycotβ (Fig. 4.6) where β is the skew angle with the horizontal (Fig. 4.5, 4.6).

$$u(x, y, z) = -z\frac{\partial w_0}{\partial x}; v(x, y, z) = -z\frac{\partial w_0}{\partial y} \text{ and } w(x, y, z) = w_0(x, y).$$

Furthermore, it is assumed that w(x, y, 0) = w(x,y). The displacements of the soil's surface are the same as those of the plate's middle surface.

The nodal displacement at ith node $\{\delta_i\} = \left\{w_i \quad \left(\frac{\partial w}{\partial x}\right)_i \quad \left(\frac{\partial w}{\partial y}\right)_i \quad \left(\frac{\partial^2 w}{\partial x\,\partial y}\right)_i\right\}^T$.

For four nodded elements, the element displacement vector is defined as $\{d_e\} = \{d_1\ d_2\ d_3\ d_4\}^T$. The thin plate idea is the foundation of the element. Therefore, prescribing a variation in transverse displacement depending on the element region is sufficient. A cubic polynomial with the complete products $(1+x+x^2+x^3)(1+y+y^2+y^3)$ in the x and y directions.

For the plane stress condition, the relationship between stresses and strain is given by,

$$\frac{\partial r}{\partial x} = 1, \frac{\partial r}{\partial y} = -\cot\beta, \frac{\partial s}{\partial x} = 0, \frac{\partial s}{\partial y} = \mathrm{cosec}\beta$$

$$\frac{\partial w_0}{\partial x} = \frac{\partial w_0}{\partial r}\frac{\partial r}{\partial x} + \frac{\partial w_0}{\partial s}\frac{\partial s}{\partial x} = \frac{\partial w_0}{\partial r} \times 1 + \frac{\partial w_0}{\partial s} \times 0 = \frac{\partial w_0}{\partial r} \therefore \frac{\partial}{\partial x} = \frac{\partial}{\partial r} \text{ and } \frac{\partial^2 w_0}{\partial x^2} = \frac{\partial^2 w_0}{\partial r^2}$$

$$\frac{\partial w_0}{\partial y} = \frac{\partial w_0}{\partial r}\frac{\partial r}{\partial y} + \frac{\partial w_0}{\partial s}\frac{\partial s}{\partial y} = \frac{\partial w_0}{\partial r} \times (-\cot\beta) + \frac{\partial w_0}{\partial s} \times \mathrm{cosec}\beta = -\cot\beta\frac{\partial w_0}{\partial r} + \mathrm{cosec}\beta\frac{\partial w_0}{\partial s}$$

$$\therefore \frac{\partial}{\partial y} = -\cot\beta\frac{\partial}{\partial r} + \mathrm{cosec}\beta\frac{\partial}{\partial s} \text{ and } \frac{\partial^2 w_0}{\partial y^2} = \frac{\partial}{\partial y}\left(-\cot\beta\frac{\partial w_0}{\partial r} + \mathrm{cosec}\beta\frac{\partial w_0}{\partial s}\right)$$

$$\therefore \frac{\partial^2 w_0}{\partial y^2} = \cot^2\beta\frac{\partial^2 w_0}{\partial r^2} - 2\mathrm{cosec}\beta\cot\beta\frac{\partial^2 w_0}{\partial r\,\partial s} + \mathrm{cosec}^2\beta\frac{\partial^2 w_0}{\partial s^2}$$

$$\text{and } \frac{\partial^2 w_0}{\partial x\,\partial y} = -\cot\beta\frac{\partial^2 w_0}{\partial r^2} + \mathrm{cosec}\beta\frac{\partial^2 w_0}{\partial r\,\partial s}$$

Hence, generalized curvatures are written.

$$\begin{Bmatrix} \chi_x \\ \chi_y \\ \chi_{xy} \end{Bmatrix} = \begin{bmatrix} \frac{\partial^2 w_0}{\partial x^2} \\ \frac{\partial^2 w_0}{\partial y^2} \\ 2\frac{\partial^2 w_0}{\partial xdy} \end{bmatrix} = \begin{bmatrix} 1 & 0 & 0 \\ \cot^2\beta & \mathrm{cosec}^2\beta & -2\mathrm{cosec}\beta\cot\beta \\ -2\cot\beta & 0 & 2\mathrm{cosec}\beta \end{bmatrix} \begin{bmatrix} \frac{\partial^2 w_0}{\partial r^2} \\ \frac{\partial^2 w_0}{\partial s^2} \\ \frac{\partial^2 w_0}{\partial r\,\partial s} \end{bmatrix}$$

$$\begin{Bmatrix} \chi_x \\ \chi_y \\ \chi_{xy} \end{Bmatrix} = \begin{bmatrix} \frac{\partial^2 N}{\partial r^2} & 0 & 0 \\ \cot^2\beta\frac{\partial^2 N}{\partial r^2} & \mathrm{cosec}^2\beta\frac{\partial^2 N}{\partial s^2} & -2\mathrm{cosec}\beta\cot\beta\frac{\partial^2 N}{\partial r\,\partial s} \\ -2\cot\beta\frac{\partial^2 N}{\partial r^2} & 0 & 2\mathrm{cosec}\beta\frac{\partial^2 N}{\partial r\,\partial s} \end{bmatrix} \{w\}$$

$$\therefore [B_{bi}] = \begin{bmatrix} \frac{\partial^2 N}{\partial r^2} & 0 & 0 \\ \cot^2\beta\frac{\partial^2 N}{\partial r^2} & \mathrm{cosec}^2\beta\frac{\partial^2 N}{\partial s^2} & -2\mathrm{cosec}\beta\cot\beta\frac{\partial^2 N}{\partial r\,\partial s} \\ -2\cot\beta\frac{\partial^2 N}{\partial r^2} & 0 & 2\mathrm{cosec}\beta\frac{\partial^2 N}{\partial r\,\partial s} \end{bmatrix}$$

$[B_{bi}] = [B_{b1}\ B_{b2} \dots \dots \dots B_{b16}]$ For four nodded elements.

Hence, the bending stiffness matrix,

$[K_b] = [B]^T[D][B] = \int_{-1}^{1}\int_{-1}^{1}[B_b]^T[D][B_b]|J|dsdt$ and $|J| = ab\sin\beta$. Following the usual steps, the bending is expressed as $[K_b] = \sum_{j=1}^{4}\sum_{i=1}^{4} W_iW_j|J|[B_b]^T[D][B_b]$.

These equations show that a full 4 × 4 Point Gauss-Legendre type quadrature is adopted for bending stiffness.

The lateral displacement of an area 'dA' normal to the foundation for a structural member with a differential area 'dA' in contact with the foundation is given by w = [N]d. For example, in a linear spring, the strain energy Ur is given by $½Kw^2$.

$U_r = \frac{1}{2}\int Kw^2\, dA = \frac{1}{2}\int K\{d\}^T[N]^T[N]\{d\}\, dA$; K is also referred to as the modulus of subgrade reaction. $U_r = \frac{1}{2}\{d\}^T[K_f]\{d\}$ .When the element's foundation stiffness matrix is, $[K_f] = \int K[N]^T[N]\, dA$

$[K_f] = Kab\sin\beta \int_{-1}^{1}\int_{-1}^{1}[N]^T[N]\, dsdt = K\int_{-1}^{1}\int_{-1}^{1}[N]^T[N]\,|J|dsdt$.[N] is the same as the shape function matrix of the plate.

For the i^{th} node's related foundation parameter, a typical sub-matrix is

$[K_{fi}] = \frac{K}{4}\sum_{i=1}^{4}\sum_{j=1}^{4} W_iW_j|J|{N_i}^TN_j$ and $[K_f] = \{K_{f1}\ K_{f2} \ldots\ldots\ldots\ldots K_{f16}\}^T$ for four nodded elements.

$$U = \frac{1}{2}\int_{-a}^{a} 2t\left(\frac{\partial w}{\partial x}\right)^2 dx = \frac{1}{2}\int_{-a}^{a} 2t\{d\}^T\left[\frac{\partial N}{\partial x}\right]^T\left[\frac{\partial N}{\partial x}\right]\{d\}\, dx = \frac{1}{2}\{d\}^T[K_{ex}]\{d\}$$

where $[K_{ex}] = \int_{-a}^{a} 2t\left[\frac{\partial N}{\partial x}\right]^T\left[\frac{\partial N}{\partial x}\right] dx$

Similarly, for y-direction, $[K_{ey}] = \int_{-b}^{b} 2t\left[\frac{\partial N}{\partial y}\right]^T\left[\frac{\partial N}{\partial y}\right] dy$ Now $R = \frac{\partial N}{\partial x}$ and $S = \frac{\partial N}{\partial y}$.

So, the stiffness for the shear parameter, 2t, is $[K_e] = 2t\iint[S^TS + R^TR]dA$

$$[K_e] = 2t\int_{-1}^{1}\int_{-1}^{1}\left(\frac{1}{a^2}\left[\frac{\partial N}{\partial s}\right]^T\left[\frac{\partial N}{\partial s}\right] + \frac{1}{b^2}\left[\frac{\partial N}{\partial t}\right]^T\left[\frac{\partial N}{\partial t}\right]\right)|J|dsdt$$

$$[K_e] = 2tab\sin\beta\int_{-1}^{1}\int_{-1}^{1}\left(\frac{1}{a^2}\left[\frac{\partial N}{\partial s}\right]^T\left[\frac{\partial N}{\partial s}\right] + \frac{1}{b^2}\left[\frac{\partial N}{\partial t}\right]^T\left[\frac{\partial N}{\partial t}\right]\right) dsdt$$

Additionally, a typical sub-matrix for the i^{th} nodes for the second foundation parameter is

$$[K_{e_i}] = 2t\left(\sum_{i=1}^{4}\sum_{j=1}^{4} W_iW_j|J|\frac{dN}{dx_i} + \sum_{i=1}^{4}\sum_{j=1}^{4} W_iW_j|J|\frac{dN}{dy_i}\right)$$

When it comes to elements with four nodes, $[K_e] = [K_{e1}\ K_{e2} \ldots\ldots\ldots K_{e16}]$.

Element’s stiffness matrix is $[K] = [K_b] + [K_f] + [K_e]$

The global stiffness matrix is generated by using the conventional finite element method. $\therefore [K_S] = \sum_1^n([K_b] + [K_f] + [K_e])$

The element load vector for a plate resulting from transverse distributed load acting on top of the plate is q per unit area.

$\{f_q\} = q\int_{-1}^{1}\int_{-1}^{1}[N]^T\,|J|dsdt.$

Force vector for point load $\{f_F\} = [N]^T[F]$

The element load vector $\{f\} = \{f_q\} + \{f_F\}$

The global load vector is generated by using the conventional finite element method.

$\therefore \{f_S\} = \sum_1^n(\{f_q\} + \{f_F\})$

Due to the plate being subjected to a transverse distributed load of q per unit area, the element load vector for an n-nodded plate is $\{q_i\} = q\sum_{i=1}^{4}\sum_{j=1}^{4}W_iW_j|J|N_i$

4×4 Gauss-Legendre integration is used to complete the integration.

$\{f_q\} = \{q_1\ q_2 \ldots\ldots\ldots\ldots q_{16}\}^T$

Hence obtain $[x] = [K_S]^{-1}\{f_S\}$

Before attempting to solve the system equation, boundary conditions must be added.

4.4 FEM of rectangular HSDT plate

In this study, Higher-order displacement variations of each node written by (Kant, 1982),

$u(x,y,z) = z\theta_x(x,y) + z^3\theta_x{}^*(x,y); v(x,y,z) = z\theta_y(x,y) + z^3\theta_y{}^*(x,y)$

and $w(x,y,z) = w(x,y) + z^2w^*(x,y)$

$$\varepsilon_{xx} = \frac{\partial u}{\partial x} = z\frac{\partial\theta_x}{\partial x} + z^3\frac{\partial\theta_x{}^*}{\partial x} = z\chi_x + z^3\chi_x{}^*; \varepsilon_{yy} = \frac{\partial v}{\partial y} = z\frac{\partial\theta_y}{\partial y} + z^3\frac{\partial\theta_y{}^*}{\partial x} = z\chi_y + z^3\chi_y{}^*$$

$$\gamma_{xy} = \frac{\partial v}{\partial x} + \frac{\partial u}{\partial y} = z\left(\frac{\partial\theta_x}{\partial y} + \frac{\partial\theta_y}{\partial x}\right) + z^3\left(\frac{\partial\theta_x{}^*}{\partial y} + \frac{\partial\theta_y{}^*}{\partial x}\right) = z\chi_{xy} + z^3\chi_{xy}{}^*$$

and $\varepsilon_{zz} = \frac{\partial w}{\partial z} = 2zw^*(x,y) = z\chi_z$

$$\gamma_{xz} = \frac{\partial u}{\partial z} + \frac{\partial w}{\partial x} = \theta_x + 3z^2\theta_x{}^* + \frac{\partial w}{\partial x} + z^2\frac{\partial w^*}{\partial x} = \left(\theta_x + \frac{\partial w}{\partial x}\right) + z^2\left(3\theta_x{}^* + \frac{\partial w^*}{\partial x}\right)$$

$$\gamma_{xz} = \varphi_x + z^2\varphi_x{}^*$$

$$\gamma_{yz} = \frac{\partial v}{\partial z} + \frac{\partial w}{\partial y} = \theta_y + 3z^2\theta_y{}^* + \frac{\partial w}{\partial y} + z^2\frac{\partial w^*}{\partial y} = \left(\theta_y + \frac{\partial w}{\partial y}\right) + z^2\left(3\theta_y{}^* + \frac{\partial w^*}{\partial y}\right)$$

$$\gamma_{yz} = \varphi_y + z^2\varphi_y{}^*$$

$$\chi_x = \frac{\partial\theta_x}{\partial x}; \chi_x{}^* = \frac{\partial\theta_x{}^*}{\partial x}; \chi_y = \frac{\partial\theta_y}{\partial y}; \chi_y{}^* = \frac{\partial\theta_y{}^*}{\partial x}; \chi_z = 2w^*; \chi_{xy} = \frac{\partial\theta_x}{\partial y} + \frac{\partial\theta_y}{\partial x}$$

$\chi_y{}^* = \frac{\partial \theta_y{}^*}{\partial x}; \chi_z = 2w^*$

$\chi_{xy} = \frac{\partial \theta_x}{\partial y} + \frac{\partial \theta_y}{\partial x}; \chi_{xy}{}^* = \frac{\partial \theta_x{}^*}{\partial y} + \frac{\partial \theta_y{}^*}{\partial x}; \varphi_x = \theta_x + \frac{\partial \omega}{\partial x}; \varphi_y = \theta_y + \frac{\partial \omega}{\partial y};$

$\varphi_x{}^* = 3\theta_x{}^* + \frac{\partial w^*}{\partial x}; \varphi_y{}^* = 3\theta_y{}^* + \frac{\partial w^*}{\partial y}$

$$\begin{Bmatrix} \varepsilon_{xx} \\ \varepsilon_{yy} \\ \varepsilon_{zz} \\ \gamma_{xy} \end{Bmatrix} = \begin{bmatrix} z & 0 & 0 & 0 & z^3 & 0 & 0 \\ 0 & z & 0 & 0 & 0 & z^3 & 0 \\ 0 & 0 & z & 0 & 0 & 0 & 0 \\ 0 & 0 & 0 & z & 0 & 0 & z^3 \end{bmatrix} \begin{Bmatrix} \chi_x \\ \chi_y \\ \chi_z \\ \chi_{xy} \\ \chi_x{}^* \\ \chi_y{}^* \\ \chi_{xy}{}^* \end{Bmatrix} and \ \{\gamma\} = \begin{Bmatrix} \gamma_{xz} \\ \gamma_{yz} \end{Bmatrix} = \begin{bmatrix} 1 & 0 & z^2 & 0 \\ 0 & 1 & 0 & z^2 \end{bmatrix} \begin{Bmatrix} \varphi_x \\ \varphi_y \\ \varphi_x{}^* \\ \varphi_y{}^* \end{Bmatrix}$$

$$Z_b = \begin{bmatrix} z & 0 & 0 & 0 & z^3 & 0 & 0 \\ 0 & z & 0 & 0 & 0 & z^3 & 0 \\ 0 & 0 & z & 0 & 0 & 0 & 0 \\ 0 & 0 & 0 & z & 0 & 0 & z^3 \end{bmatrix} and \ Z_s = \begin{bmatrix} 1 & 0 & z^2 & 0 \\ 0 & 1 & 0 & z^2 \end{bmatrix};$$

$\mathrm{LC} = \frac{\mathrm{Ev}}{(1+\mathrm{v})(1-2\mathrm{v})}$ and $\mathrm{G} = \frac{\mathrm{E}}{2(1+\mathrm{v})}$

$\mathrm{D}_{11} = \mathrm{LC} + 2\mathrm{G}; \mathrm{D}_{22} = \mathrm{D}_{11}; \mathrm{D}_{33} = \mathrm{D}_{11}; \mathrm{D}_{12} = \mathrm{LC}; \mathrm{D}_{13} = \mathrm{D}_{12}; \mathrm{D}_{21} = \mathrm{D}_{12}; \mathrm{D}_{23} = \mathrm{D}_{12}$

$\mathrm{D}_{31} = \mathrm{D}_{12}; \mathrm{D}_{32} = \mathrm{D}_{12}; \mathrm{D}_{44} = \mathrm{G};$

$$\mathrm{C_b} = \begin{bmatrix} \mathrm{D}_{11} & \mathrm{D}_{12} & \mathrm{D}_{13} & 0 \\ \mathrm{D}_{21} & \mathrm{D}_{22} & \mathrm{D}_{23} & 0 \\ \mathrm{D}_{31} & \mathrm{D}_{32} & \mathrm{D}_{33} & 0 \\ 0 & 0 & 0 & \mathrm{D}_{44} \end{bmatrix}; \mathrm{C_s} = \begin{bmatrix} \mathrm{D}_{44} & 0 \\ 0 & \mathrm{D}_{44} \end{bmatrix}$$

$$\mathrm{D_b} = \int_{-\frac{h}{2}}^{\frac{h}{2}} [\mathrm{Z_b}]^{\mathrm{T}} [\mathrm{C_b}] [\mathrm{Z_b}]\, \mathrm{dzand}\ \mathrm{D_s} = \int_{-\frac{h}{2}}^{\frac{h}{2}} [\mathrm{Z_s}]^{\mathrm{T}} [\mathrm{C_s}] [\mathrm{Z_s}]\, \mathrm{dz}$$

$$\therefore \begin{Bmatrix} \chi_x \\ \chi_y \\ \chi_z \\ \chi_{xy} \\ \chi_x{}^* \\ \chi_y{}^* \\ \chi_{xy}{}^* \end{Bmatrix} = \begin{bmatrix} 0 & \frac{\partial N}{\partial x} & 0 & 0 & 0 & 0 \\ 0 & 0 & \frac{\partial N}{\partial x} & 0 & 0 & 0 \\ 0 & 0 & 0 & 2N & 0 & 0 \\ 0 & \frac{\partial N}{\partial y} & \frac{\partial N}{\partial x} & 0 & 0 & 0 \\ 0 & 0 & 0 & 0 & \frac{\partial N}{\partial x} & 0 \\ 0 & 0 & 0 & 0 & 0 & \frac{\partial N}{\partial y} \\ 0 & 0 & 0 & 0 & \frac{\partial N}{\partial y} & \frac{\partial N}{\partial x} \end{bmatrix} \begin{Bmatrix} w \\ \theta_x \\ \theta_y \\ w^* \\ \theta_x{}^* \\ \theta_y{}^* \end{Bmatrix}$$

$$\begin{Bmatrix} \varphi_x \\ \varphi_y \\ \varphi_x{}^* \\ \varphi_y{}^* \end{Bmatrix} = \begin{bmatrix} \frac{\partial N}{\partial x} & N & 0 & 0 & 0 & 0 \\ \frac{\partial N}{\partial y} & 0 & N & 0 & 0 & 0 \\ 0 & 0 & 0 & \frac{\partial N}{\partial x} & 3N & 0 \\ 0 & 0 & 0 & \frac{\partial N}{\partial y} & 0 & 3N \end{bmatrix} \begin{Bmatrix} w \\ \theta_x \\ \theta_y \\ w^* \\ \theta_x{}^* \\ \theta_y{}^* \end{Bmatrix};$$

$$[B_{bi}] = \begin{bmatrix} 0 & \frac{\partial N}{\partial x} & 0 & 0 & 0 & 0 \\ 0 & 0 & \frac{\partial N}{\partial x} & 0 & 0 & 0 \\ 0 & 0 & 0 & 2N & 0 & 0 \\ 0 & \frac{\partial N}{\partial y} & \frac{\partial N}{\partial x} & 0 & 0 & 0 \\ 0 & 0 & 0 & 0 & \frac{\partial N}{\partial x} & 0 \\ 0 & 0 & 0 & 0 & 0 & \frac{\partial N}{\partial y} \\ 0 & 0 & 0 & 0 & \frac{\partial N}{\partial y} & \frac{\partial N}{\partial x} \end{bmatrix}; [B_{si}] = \begin{bmatrix} \frac{\partial N}{\partial x} & N & 0 & 0 & 0 & 0 \\ \frac{\partial N}{\partial y} & 0 & N & 0 & 0 & 0 \\ 0 & 0 & 0 & \frac{\partial N}{\partial x} & 3N & 0 \\ 0 & 0 & 0 & \frac{\partial N}{\partial y} & 0 & 3N \end{bmatrix}$$

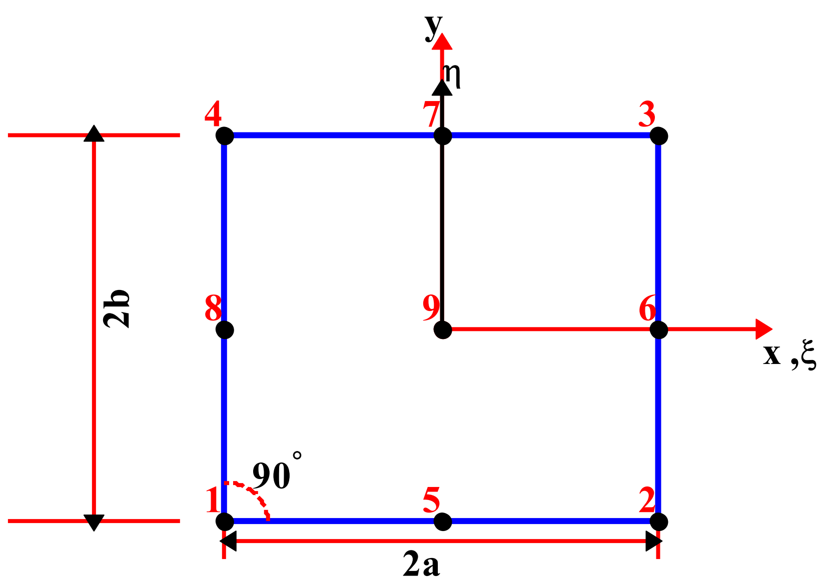

Fig. 4.7 PBQ9 plate elements

$[B_b] = [B_{b1}\ B_{b2} \dots \dots \dots B_{bn}]\ and\ [B_s] = [B_{s1}\ B_{s2} \dots \dots \dots B_{sn}]\ for\ n\ nodded\ element$

$[K_b] = \int_{-1}^{1}\int_{-1}^{1}[B_b]^T[D_b][B_b]|J|dsdt\ and\ [K_s] = \int_{-1}^{1}\int_{-1}^{1}[B_s]^T[D_s][B_s]|J|dsdt$

The bending and shear stiffness matrices are expressed after the standard processes.

$[K_b] = \sum_{j=1}^{n}\sum_{i=1}^{n} W_i W_j |J| [B_b]^T[D_b][B_b]\ and\ [K_s] = \sum_{j=1}^{n}\sum_{i=1}^{n} W_i W_j |J| [B_s]^T[D_s][B_s]$

A full 3 × 3 point Gauss Quadrature is adopted for the present 9 - nodded elements for both bending stiffness and shear stiffness, respectively.

The lateral displacement of an area 'dA' normal to the foundation for a structural member with a differential area 'dA' in contact with the foundation is given by w = [N]d. For example, in a linear spring, the strain energy Ur is given by ½Kw^2.

$U_r = \frac{1}{2}\int Kw^2\, dA = \frac{1}{2}\int K\{d\}^T[N]^T[N]\{d\}\, dA$; K is also referred to as the modulus of subgrade reaction.$U_r = \frac{1}{2}\{d\}^T[K_f]\{d\}$.When the element's foundation stiffness matrix is,

$$[K_f] = \int K[N]^T[N]\, dA$$

Where the element's foundation stiffness matrix is

$$[K_f] = \int K[N_f]^T[N_f]\, dA = Kab\int_{-1}^{1}\int_{-1}^{1}[N_f]^T[N_f]\, dsdt = K\int_{-1}^{1}\int_{-1}^{1}[N_f]^T[N_f]\, |J|dsdt$$

$[N_f]$ is the same as the shape function matrix of the plate, [N].

For the i[th] node's related foundation parameter, a typical sub-matrix is

$$[K_{fi}] = \frac{K}{4}\sum_{i=1}^{4}\sum_{j=1}^{4} W_iW_j|J|N_i^TN_j$$

$[K_f] = \{K_{f1}\ K_{f2} \ldots\ldots\ldots\ldots K_{f54}\}^T$ for nine nodded elements.$R = \frac{\partial N}{\partial x}$ and $S = \frac{\partial N}{\partial y}$

$\therefore$ Stiffness for shear parameter, 2t is $[K_e] = 2t\int[S^TS + R^TR]dA$

$$[K_e] = 2t\int_{-1}^{1}\int_{-1}^{1}\left(\frac{1}{a^2}\left[\frac{\partial N}{\partial s}\right]^T\left[\frac{\partial N}{\partial s}\right] + \frac{1}{b^2}\left[\frac{\partial N}{\partial t}\right]^T\left[\frac{\partial N}{\partial t}\right]\right)|J|dsdt$$

$$[K_e] = 2tab\int_{-1}^{1}\int_{-1}^{1}\left(\frac{1}{a^2}\left[\frac{\partial N}{\partial s}\right]^T\left[\frac{\partial N}{\partial s}\right] + \frac{1}{b^2}\left[\frac{\partial N}{\partial t}\right]^T\left[\frac{\partial N}{\partial t}\right]\right)dsdt$$

The element load vector for a plate as a function of a q per unit area transverse distributed load applied on the plate

$$\{f_q\} = q\int_{-1}^{1}\int_{-1}^{1}[N]^T\, |J|dsdt.$$

The load vector for a concentrated load (PL) is $\{f_F\} = [N]^T[F]$

The element load vector for the n-nodded plate is due to the q per unit area acting on top of the plate.

$$\{q_i\} = q\sum_{i=1}^{4}\sum_{j=1}^{4} W_iW_j|J|N_i$$

Integration is carried out using 3 × 3 Gauss-Legendre integration.

$$\{f_q\} = \{q_1\ q_2 \ldots\ldots\ldots\ldots q_{54}\}^T$$

The element load vector, $\{f\} = \{f_q\} + \{f_F\}$

Transversely distributed load of q/unit area on the n-nodded plate gives load vector 6n. $\{q_e\} = \{q_1 \quad \dots \dots \dots . \quad q_n\}^T$

Typical i^{th}-node sub matrix is $\{q_i\} = q \sum \sum W_i W_j |J| N_i \begin{Bmatrix} 1 \\ 0 \\ 0 \\ \frac{h^2}{4} \\ 0 \\ 0 \end{Bmatrix}$

The load vector for elements with 'n' nodes is $\{f_u\} = \{q_1\; q_2 \dots \dots \dots \dots . \, q_n\}^T$

A typical sub-matrix for the foundation's first parameter, K, is

$$[K_{fi}] = K \sum \sum W_i W_j |J| N_i^T N_j \begin{Bmatrix} 1 \\ 0 \\ 0 \\ \frac{h^2}{4} \\ 0 \\ 0 \end{Bmatrix}$$

For 'n' nodded elements, $[K_f] = [K_{f1}\; K_{f2} \dots \dots \dots \dots . \, K_{fn}]^T$

A typical foundation second parameter sub-matrix for the i^{th} node is

$$[K_{ei}] = 2t \left(\sum \sum W_i W_j |J| \frac{dN}{dx}_i \begin{Bmatrix} 1 \\ 0 \\ 0 \\ \frac{h^2}{4} \\ 0 \\ 0 \end{Bmatrix} + \sum \sum W_i W_j |J| \frac{dN}{dy}_i \begin{Bmatrix} 1 \\ 0 \\ 0 \\ \frac{h^2}{4} \\ 0 \\ 0 \end{Bmatrix} \right)$$

For 'n' nodded elements, $[K_e] = [\{K_{e1}\; K_{e2} \dots \dots \dots .. \, K_{en}\}]$

When it comes to elements with nine-nodes. $[K_e] = [K_{e1}\; K_{e2} \dots \dots .. \, K_{e54}]$.

The element's stiffness matrix is $[\mathrm{K_E}] = [\mathrm{K_b}] + [\mathrm{K_s}] + [\mathrm{K_f}] + [\mathrm{K_e}]$

The traditional finite element approach is used to construct the global stiffness matrix.

$\therefore [\mathrm{KK}] = \sum_1^n([\mathrm{K_b}] + [K_s] + [\mathrm{K_f}] + [\mathrm{K_e}])$

The element load vector $\{f\} = \{\mathrm{f_q}\} + \{\mathrm{f_F}\}$

The global load vector is generated by using the conventional finite element method.

$\therefore \{\mathrm{f_S}\} = \sum_1^n(\{\mathrm{f_q}\} + \{\mathrm{f_F}\})$

Hence obtain $[x] = [KK]^{-1}\{f_S\}$ Before attempting to solve the system equation, boundary conditions must be added.

Why the Lagrangian plate element?

The choosing of thick or thin formulations is fundamental to the plate-bending problem. The ratio of thickness h to span B has a significant impact on the performance of thick plate elements. The results for the serendipity (quadratic) completely integrated thick elements clearly deviate significantly from the exact Kirchhoff plate solution for small h/B ratios (Zienkiewicz and Taylor, 1991; Hughes, 1987). Starting at B/h = 100, the serendipity element diverges quickly for relatively modest values. The phenomena of shear locking can appear when this ratio approaches a tiny value. Numerical integration, either reduced or selective, can be used to remove locking. Nevertheless, as the plate thickness h goes to zero, the eight serendipity element nodes that used reduced 2×2 integration behave poorly in the thin plate limit. Clamped-edge linear quadrilateral elements produce a notable gain in performance. In quadratic interpolation, Lagrangian elements perform noticeably better, even in the absence of a reduction in integration order. However, we observe that when numerical integration is lowered in cubic elements, essentially no change happens (Zienkiewicz and Taylor, 1991), and again, Lagrangian-type elements perform significantly better. For Lagrangian elements, the numerical degradation starts at the ratios, not before B/h = 10^6. The Lagrange nine-node elements have a steady convergence characteristic for large B/h ratios, according to Hughes (Hughes, 1987). Using the heterosis element is an alternate option. The shape function of the Lagrange type interpolates rotations in such an element, while the shape function of the serendipity family describes displacements (Hughes and Cohen, 1978)..
In summary, the thick plate components should be used with caution because some of them have the potential to malfunction occasionally, locking or behaving singularly when applied to linear quadrilaterals where lower integration on all terms was selected. Lagrangian quadratic elements appear to be a good option when simulating the interaction of thick plates with non-homogeneous soil foundations.

4.5 FEM of circular HSDT plate

Displacement variations, excluding the stretching of the plate written as

$u(r,\theta,z) = z\beta_r + z^3\beta_r^{*}; v(r,\theta,z) = \frac{z}{r}\beta_\theta + \frac{z^3}{r}\beta_\theta^{*}$ and $w(r,\theta,z) = w(r,\theta) + z^2 w^{*}(r,\theta)$

$$\frac{\partial u}{\partial \theta}=\frac{\partial\left(z\beta_r+z^3{\beta_r}^*\right)}{\partial \theta}=z\frac{\partial \beta_r}{\partial \theta}+z^3\frac{\partial {\beta_r}^*}{\partial \theta};\frac{\partial v}{\partial \theta}=\frac{\partial\left(\frac{z}{r}\beta_\theta+\frac{z^3}{r}{\beta_\theta}^*\right)}{\partial \theta}=\frac{z}{r}\frac{\partial \beta_\theta}{\partial \theta}+\frac{z^3}{r}\frac{\partial {\beta_\theta}^*}{\partial \theta};$$

$$\frac{\partial \mathrm{v}}{\partial \mathrm{r}}=\frac{\partial\left(\frac{\mathrm{z}}{\mathrm{r}}\beta_\theta+\frac{\mathrm{z}^3}{\mathrm{r}}{\beta_\theta}^*\right)}{\partial \mathrm{r}}=\mathrm{z}\frac{\partial}{\partial \mathrm{r}}\left(\frac{\beta_\theta}{\mathrm{r}}\right)+\mathrm{z}^3\frac{\partial}{\partial \mathrm{r}}\left(\frac{{\beta_\theta}^*}{\mathrm{r}}\right)$$

$$\therefore \frac{\partial v}{\partial r}=z\left[\frac{r\frac{\partial \beta_\theta}{\partial r}-\beta_\theta}{r^2}\right]+z^3\left[\frac{r\frac{\partial {\beta_\theta}^*}{\partial r}-{\beta_\theta}^*}{r^2}\right]=\frac{z}{r}\frac{\partial \beta_\theta}{\partial r}+\frac{z^3}{r}\frac{\partial {\beta_\theta}^*}{\partial r}-\frac{z}{r^2}\beta_\theta-\frac{z^3{\beta_\theta}^*}{r^2}$$

$$\varepsilon_{rr}=\frac{\partial u}{\partial r}=z\frac{\partial \beta_r}{\partial r}+z^3\frac{\partial {\beta_r}^*}{\partial r};\varepsilon_{\theta\theta}=\frac{u}{r}+\frac{1}{r}\frac{\partial v}{\partial \theta}=\frac{z}{r}\beta_r+\frac{z^3}{r}{\beta_r}^*+\frac{z}{r^2}\frac{\partial \beta_\theta}{\partial \theta}+\frac{z^3}{r^2}\frac{\partial {\beta_\theta}^*}{\partial \theta}$$

$$and\ \varepsilon_{zz}=\frac{\partial w}{\partial z}=2zw^*$$

$$\gamma_{r\theta}=\frac{1}{r}\frac{\partial u}{\partial \theta}+\frac{\partial v}{\partial r}-\frac{v}{r}=\frac{z}{r}\frac{\partial \beta_r}{\partial \theta}+\frac{z^3}{r}\frac{\partial {\beta_r}^*}{\partial \theta}+\left(\frac{z}{r}\frac{\partial \beta_\theta}{\partial r}+\frac{z^3}{r}\frac{\partial {\beta_\theta}^*}{\partial r}-\frac{z}{r^2}\beta_\theta-\frac{z^3{\beta_\theta}^*}{r^2}\right)-\frac{z}{r^2}\beta_\theta-\frac{z^3}{r^2}{\beta_\theta}^*$$

$$\gamma_{r\mathrm{\theta}}=\frac{z}{r}\left(\frac{\partial \beta_r}{\partial \theta}+\frac{\partial \beta_\theta}{\partial r}\right)+\frac{z^3}{r}\left(\frac{\partial {\beta_r}^*}{\partial \theta}+\frac{\partial {\beta_\theta}^*}{\partial r}\right)-\frac{2z}{r^2}\beta_\theta-\frac{2z^3}{r^2}{\beta_\theta}^*$$

$$\gamma_{rz}=\frac{\partial u}{\partial z}+\frac{\partial w}{\partial r}=\beta_r+3z^2{\beta_r}^*+\frac{\partial w}{\partial r}+z^2\frac{\partial w^*}{\partial r}=\left(\beta_r+\frac{\partial w}{\partial r}\right)+z^2\left(3{\beta_r}^*+\frac{\partial w^*}{\partial r}\right);$$

$$\gamma_{\theta z}=\frac{\partial v}{\partial z}+\frac{1}{r}\frac{\partial w}{\partial \theta}=\frac{\beta_\theta}{r}+\frac{3z^2}{r}{\beta_\theta}^*+\frac{1}{r}\frac{\partial w}{\partial \theta}+\frac{z^2}{r}\frac{\partial w^*}{\partial \theta}=\frac{1}{r}\left(\beta_\mathrm{\theta}+\frac{\partial w}{\partial \theta}\right)+\frac{z^2}{r}\left(3{\beta_\theta}^*+\frac{\partial w^*}{\partial \theta}\right)$$

$$\chi_x=\frac{\partial \beta_r}{\partial r};{\chi_x}^*=\frac{\partial {\beta_r}^*}{\partial r};\chi_y=\beta_r;{\chi_y}^*={\beta_r}^*;{\chi_y}^{**}=\frac{\partial \beta_\theta}{\partial \theta};{\chi_y}^{***}=\frac{\partial {\beta_\theta}^*}{\partial \theta};$$

$$\chi_z=2w^*;\chi_{xy}=\left(\frac{\partial \beta_r}{\partial \theta}+\frac{\partial \beta_\theta}{\partial r}\right);{\chi_{xy}}^*=\left(\frac{\partial {\beta_r}^*}{\partial \theta}+\frac{\partial {\beta_\theta}^*}{\partial r}\right);{\chi_{xy}}^{**}=\beta_\theta;{\chi_{xy}}^{***}={\beta_\theta}^*$$

$$\varphi_x=\beta_r+\frac{\partial w}{\partial r};{\varphi_x}^*=3{\beta_r}^*+\frac{\partial w^*}{\partial r};\varphi_y=\beta_\theta+\frac{\partial w}{\partial \theta};{\varphi_y}^*=3{\beta_\theta}^*+\frac{\partial w^*}{\partial \theta}$$

$$\begin{Bmatrix}\chi_x\\ \chi_y\\ \chi_z\\ \chi_{xy}\\ {\chi_x}^*\\ {\chi_y}^*\\ {\chi_{xy}}^*\\ {\chi_y}^{**}\\ {\chi_{xy}}^{**}\\ {\chi_y}^{***}\\ {\chi_{xy}}^{***}\end{Bmatrix}=\begin{bmatrix}0&\frac{\partial N}{\partial r}&0&0&0&0\\ 0&N&0&0&0&0\\ 0&0&0&2N&0&0\\ 0&\frac{\partial N}{\partial \theta}&\frac{\partial N}{\partial r}&0&0&0\\ 0&0&0&0&\frac{\partial N}{\partial r}&0\\ 0&0&0&0&N&0\\ 0&0&0&0&\frac{\partial N}{\partial \theta}&\frac{\partial N}{\partial r}\\ 0&0&\frac{\partial N}{\partial \theta}&0&0&0\\ 0&0&N&0&0&0\\ 0&0&0&0&0&\frac{\partial N}{\partial \theta}\\ 0&0&0&0&0&N\end{bmatrix}\begin{Bmatrix}w\\ \beta_r\\ \beta_\theta\\ w^*\\ {\beta_r}^*\\ {\beta_\theta}^*\end{Bmatrix}\therefore [B_{b\mathrm{i}}]=\begin{bmatrix}0&\frac{\partial N}{\partial r}&0&0&0&0\\ 0&N&0&0&0&0\\ 0&0&0&2N&0&0\\ 0&\frac{\partial N}{\partial \theta}&\frac{\partial N}{\partial r}&0&0&0\\ 0&0&0&0&\frac{\partial N}{\partial r}&0\\ 0&0&0&0&N&0\\ 0&0&0&0&\frac{\partial N}{\partial \theta}&\frac{\partial N}{\partial r}\\ 0&0&\frac{\partial N}{\partial \theta}&0&0&0\\ 0&0&N&0&0&0\\ 0&0&0&0&0&\frac{\partial N}{\partial \theta}\\ 0&0&0&0&0&N\end{bmatrix}$$

$$and\begin{Bmatrix}\varphi_x\\ \varphi_y\\ \varphi_x{}^*\\ \varphi_y{}^*\end{Bmatrix}=\begin{bmatrix}\frac{\partial N}{\partial r} & N & 0 & 0 & 0 & 0\\ \frac{\partial N}{\partial \theta} & 0 & N & 0 & 0 & 0\\ 0 & 0 & 0 & \frac{\partial N}{\partial r} & 3N & 0\\ 0 & 0 & 0 & \frac{\partial N}{\partial \theta} & 0 & 3N\end{bmatrix}\begin{Bmatrix}w\\ \beta_r\\ \beta_\theta\\ w^*\\ \beta_r{}^*\\ \beta_\theta{}^*\end{Bmatrix}\therefore [B_{si}]=\begin{bmatrix}\frac{\partial N}{\partial r} & N & 0 & 0 & 0 & 0\\ \frac{\partial N}{\partial \theta} & 0 & N & 0 & 0 & 0\\ 0 & 0 & 0 & \frac{\partial N}{\partial r} & 3N & 0\\ 0 & 0 & 0 & \frac{\partial N}{\partial \theta} & 0 & 3N\end{bmatrix}$$

$$\begin{Bmatrix}\varepsilon_{rr}\\ \varepsilon_{\theta\theta}\\ \varepsilon_{zz}\\ \gamma_{r\theta}\end{Bmatrix}=\begin{bmatrix}z & 0 & 0 & 0 & z^3 & 0 & 0 & 0 & 0 & 0 & 0\\ 0 & \frac{z}{r} & 0 & 0 & \frac{z^3}{r} & 0 & 0 & \frac{z}{r^2} & 0 & \frac{z^3}{r^2} & 0\\ 0 & 0 & 2z & 0 & 0 & 0 & 0 & 0 & 0 & 0 & 0\\ 0 & 0 & 0 & \frac{z}{r} & 0 & 0 & \frac{z^3}{r} & 0 & \frac{-2z}{r^2} & 0 & \frac{-2z^3}{r^2}\end{bmatrix}\begin{Bmatrix}\chi_x\\ \chi_y\\ \chi_z\\ \chi_{xy}\\ \chi_x{}^*\\ \chi_y{}^*\\ \chi_{xy}{}^*\\ \chi_y{}^{**}\\ \chi_{xy}{}^{**}\\ \chi_y{}^{***}\\ \chi_{xy}{}^{***}\end{Bmatrix} and$$

$$\{\gamma\}=\begin{Bmatrix}\gamma_{xz}\\ \gamma_{yz}\end{Bmatrix}=\begin{bmatrix}1 & 0 & z^2 & 0\\ 0 & \frac{1}{r} & 0 & \frac{z^2}{r}\end{bmatrix}\begin{Bmatrix}\varphi_x\\ \varphi_y\\ \varphi_x{}^*\\ \varphi_y{}^*\end{Bmatrix};$$

$$Z_b=\begin{bmatrix}z & 0 & 0 & 0 & z^3 & 0 & 0 & 0 & 0 & 0 & 0\\ 0 & \frac{z}{r} & 0 & 0 & \frac{z^3}{r} & 0 & 0 & \frac{z}{r^2} & 0 & \frac{z^3}{r^2} & 0\\ 0 & 0 & 2z & 0 & 0 & 0 & 0 & 0 & 0 & 0 & 0\\ 0 & 0 & 0 & \frac{z}{r} & 0 & 0 & \frac{z^3}{r} & 0 & \frac{-2z}{r^2} & 0 & \frac{-2z^3}{r^2}\end{bmatrix} and$$

$$\mathrm{Z_s}=\begin{bmatrix}1 & 0 & \mathrm{z}^2 & 0\\ 0 & \frac{1}{\mathrm{r}} & 0 & \frac{\mathrm{z}^2}{\mathrm{r}}\end{bmatrix};\mathrm{LC}=\frac{\mathrm{Ev}}{(1+\mathrm{v})(1-2\mathrm{v})}\text{ and }\mathrm{G}=\frac{\mathrm{E}}{2(1+\mathrm{v})};$$

$$\mathrm{C_{22}}=\mathrm{LC}+2\mathrm{G};\mathrm{C_{22}}=\mathrm{C_{11}};\mathrm{C_{33}}=\mathrm{C_{11}};\mathrm{C_{12}}=\mathrm{LC};\mathrm{C_{13}}=\mathrm{C_{12}};\mathrm{C_{21}}=\mathrm{C_{12}};$$

$$C_{23}=C_{12};C_{31}=C_{12};C_{32}=C_{12};C_{44}=G;$$

$$\mathrm{C_b}=\begin{bmatrix}\mathrm{C_{11}} & \mathrm{C_{12}} & \mathrm{C_{13}} & 0\\ \mathrm{C_{21}} & \mathrm{C_{22}} & \mathrm{C_{23}} & 0\\ \mathrm{C_{31}} & \mathrm{C_{32}} & \mathrm{C_{33}} & 0\\ 0 & 0 & 0 & \mathrm{C_{44}}\end{bmatrix}\text{ and }\mathrm{C_s}=\begin{bmatrix}\mathrm{C_{44}} & 0\\ 0 & \mathrm{C_{44}}\end{bmatrix}$$

$$\mathrm{D_b}=\int_{-\frac{h}{2}}^{\frac{h}{2}}[\mathrm{Z_b}]^{\mathrm{T}}[\mathrm{C_b}][\mathrm{Z_b}]\,\mathrm{dz}\text{ and }\mathrm{D_s}=\int_{-\frac{h}{2}}^{\frac{h}{2}}[\mathrm{Z_s}]^{\mathrm{T}}[\mathrm{C_s}][\mathrm{Z_s}]\,\mathrm{dz}$$

Using an annular sector element proves convenient in some situations. The element comprises 'n' nodes, with each node having a corresponding displacement in the r and θ directions.

Utilizing this element has the advantage of referring to the displacements and stresses as polar coordinates, r and θ (Fig. 4.4).

Taking the natural coordinates of nodes 1, 2, 3 , and 4 are (-1, 1), (1, 1), (1, -1), and (-1, -1) respectively , and in polar coordinate systems of (r_1, 0), (r_2, 0), (r_2, θ), and (r_1, θ) respectively.

Using the Lagrange formula, we can derive the shape function.

$\therefore \mathrm{N}_1 = \frac{(r-r_2)(\theta-\theta_4)}{(r_1-r_2)(\theta_1-\theta_4)} = \frac{(r-1)(\theta+1)}{(-1-1)(1+1)} = \frac{(1-r)(1+\theta)}{4}$

Similarly, we can obtain $\mathrm{N}_2 = \frac{(r-r_1)(\theta-\theta_3)}{(r_2-r_1)(\theta_2-\theta_3)} = \frac{(1+r)(1+\theta)}{4}$ and

$\mathrm{N}_3 = \frac{(r-r_4)(\theta-\theta_2)}{(r_3-r_4)(\theta_3-\theta_2)} = \frac{(1+r)(1-\theta)}{4}; \mathrm{N}_4 = \frac{(r-r_3)(\theta-\theta_1)}{(r_4-r_3)(\theta_4-\theta_1)} = \frac{(1-r)(1-\theta)}{4}$

We can use the serendipity concept to derive the same shape function.

For N_1, the equation of lines 2-3 is (1-r) and line 3-4 is (1+θ).

$\therefore \mathrm{N}_1 = \mathrm{C}(1-r)(1+\theta)$ at Node 1 $\mathrm{N}_1 = 1$ and $r = -1; \theta = 1$

$\therefore 1 = \mathrm{C}(1+1)(1+1) \therefore \mathrm{C} = \frac{1}{4} \therefore \mathrm{N}_1 = \frac{(1-r)(1+\theta)}{4}$

In a similar manner, we can get

$\mathrm{N}_2 = \frac{(1+r)(1+\theta)}{4}; \mathrm{N}_3 = \frac{(1+r)(1-\theta)}{4}; \mathrm{N}_4 = \frac{(1-r)(1-\theta)}{4}$

$[K_b] = \int_{-1}^{1}\int_{-1}^{1}[B_b]^T[D_b][B_b]|\mathrm{J}|\mathrm{d}r\mathrm{d}\theta \; and \; [K_s] = \int_{-1}^{1}\int_{-1}^{1}[B_s]^T[D_s][B_s]|\mathrm{J}|\mathrm{d}r\mathrm{d}\theta$ and $|J| = ar\beta$

The lateral displacement of an area 'dA' normal to the foundation for a structural member with a differential area 'dA' in contact with the foundation is given by w = [N]d. For example, in a linear spring, the strain energy Ur is given by $\frac{1}{2}Kw^2$.

$U_r = \frac{1}{2}\int Kw^2\, dA = \frac{1}{2}\int K\{d\}^T[N]^T[N]\{d\}\, dA$; K is also referred to as the modulus of subgrade reaction. $U_r = \frac{1}{2}\{d\}^T[K_f]\{d\}$ .When the element's foundation stiffness matrix is,$[K_f] = \int K[N]^T[N]\, dA$

Where the element's foundation stiffness matrix is

$[\mathrm{K_f}] = \int \mathrm{K}[\mathrm{N}]^{\mathrm{T}}[\mathrm{N}]\,\mathrm{dA} = \frac{\mathrm{K}ar\beta}{4}\int_{-1}^{1}\int_{-1}^{1}[\mathrm{N}]^{\mathrm{T}}[\mathrm{N}]\,\mathrm{d}r\mathrm{d}\theta = \frac{\mathrm{K}ar\beta}{4}\int_{-1}^{1}\int_{-1}^{1}[\mathrm{N}]^{\mathrm{T}}[\mathrm{N}]\,\mathrm{d}r\mathrm{d}\theta$

$[\mathrm{K_f}] = \frac{\mathrm{K}}{4}\int_{-1}^{1}\int_{-1}^{1}[\mathrm{N}]^{\mathrm{T}}[\mathrm{N}]\,|\mathrm{J}|\mathrm{d}r\mathrm{d}\theta$; [N] is the same as the plate's shape function matrix.

The foundation parameter corresponding to the i^{th} node's typical sub-matrix is

$[\mathrm{K_{fi}}] = \frac{\mathrm{K}}{4}\sum_{i=1}^{4}\sum_{j=1}^{4}\mathrm{W_i W_j}|\mathrm{J}|\mathrm{N_i}^{\mathrm{T}}\mathrm{N_j}$

$[\mathrm{K_f}] = \{\mathrm{K_{f1}}\;\mathrm{K_{f2}} \ldots\ldots\ldots\ldots\mathrm{K_{f1}}\;\}^{\mathrm{T}}$ for four nodded elements.

The strain energy is given by the foundation parameter '2t.' $\int 2t\left\{\frac{1}{r^2}\left(\frac{\partial w}{\partial \theta}\right)^2+\left(\frac{\partial w}{\partial r}\right)^2\right\}dA$

$[K_e]=2t\int_{-1}^{1}\int_{-1}^{1}\left(\frac{1}{r^2}\left[\frac{\partial N}{\partial \theta}\right]^T\left[\frac{\partial N}{\partial \theta}\right]+\left[\frac{\partial N}{\partial r}\right]^T\left[\frac{\partial N}{\partial r}\right]\right)|J|dr d\theta$

Additionally, a typical sub-matrix for the i^{th} nodes for the second foundation parameter is

$[K_{e_i}]=2t\left(\sum_{i=1}^{4}\sum_{j=1}^{4}W_iW_j|J|\frac{dN}{dr}_i+\sum_{i=1}^{4}\sum_{j=1}^{4}W_iW_j|J|\frac{dN}{d\theta}_i\right)$

To four nodded elements $[K_e]=[K_{e1}\ K_{e2}\ \ldots\ldots.\ K_{e16}]$.

Matrix of the elements' stiffness $[K_E]=[K_b]+[K_s]+[K_f]+[K_e]$.

The traditional finite element approach is used to construct the global stiffness matrix.

$\therefore [KK]=\sum_1^n([K_b]+[K_s]+[K_f]+[K_e])$

The element load vector for a plate as a result of a transverse distributed load applied on top of the plate is q per unit area.

$\{f_1\}=q\int_{-1}^{1}\int_{-1}^{1}[N]^T|J|dsdt$ and $\{q_i\}=\frac{q}{4}\sum_{i=1}^{4}\sum_{j=1}^{4}W_iW_j|J|N_i$

4×4 Gauss-Legendre integration is used to complete the integration.

$\{f_1\}=\{q_1\ q_2\ \ldots\ldots\ldots\ldots.\ q_{16}\}^T$ to four nodded components.

For a point load, the force vector $\{f_2\}=[N]^T[F]$ Where $[N]^T$ is the shape function assessed at the applied load (F). The global force vector is calculated using the conventional finite element method. $\therefore \{f\}=\sum_1^n(\{f_1\}+\{f_2\})$.

Hence obtain $[x]=[KK]^{-1}\{f\}$.

Another form

Theoretically, we can use an isoparametrie nine-noded thick plate element to analyze general plates, including circular ones. However, in order to apply boundary conditions, displacement transformations are required at nodes on a simply supported, curved boundary. Cartesian coordinates refer to the stress-resultants. Thus, the analysis of circular plates subjected to an axisymmetric load using nine node elements is inconvenient. Here, we used three-noded ring-type elements for the analysis of thick circular plates. In an axisymmetric situation, the problem becomes one-dimensional. All quantities are functions of only the radial coordinate r. We can express the displacements of a point at distance z from the mid-plane, known as the mid-plane point, in terms of generalized displacement parameters for a higher-order thick circular plate subjected to axisymmetric loads.

$u(r,\theta,z)=z\beta_r+z^3\beta_r{}^*; v(r,\theta,z)=0$ and $w(r,\theta,z)=w(r)+z^2w^*(r)$

$$\frac{\partial u}{\partial \theta}=\frac{\partial\left(z\beta_r+z^3\beta_r{}^*\right)}{\partial \theta}=z\frac{\partial \beta_r}{\partial \theta}+z^3\frac{\partial \beta_r{}^*}{\partial \theta};\frac{\partial v}{\partial \theta}=0;\frac{\partial v}{\partial r}=\frac{\partial\left(\frac{z}{r}\beta_\theta+\frac{z^3}{r}\beta_\theta{}^*\right)}{\partial r}=0$$

$$\varepsilon_{rr}=\frac{\partial u}{\partial r}=z\frac{\partial \beta_r}{\partial r}+z^3\frac{\partial \beta_r{}^*}{\partial r}=z\chi_r+z^3\chi_r{}^*;\varepsilon_{\theta\theta}=\frac{u}{r}+\frac{1}{r}\frac{\partial v}{\partial \theta}=\frac{z}{r}\beta_r+\frac{z^3}{r}\beta_r{}^*=z\chi_\theta+z^3\chi_\theta{}^*$$

$$\varepsilon_{zz}=\frac{\partial w}{\partial z}=2zw^*=z\chi_z;\gamma_{rz}=\frac{\partial u}{\partial z}+\frac{\partial w}{\partial r}=\beta_r+3z^2\beta_r{}^*+\frac{\partial w}{\partial r}+z^2\frac{\partial w^*}{\partial r}$$

$$\gamma_{rz}=\left(\beta_r+\frac{\partial w}{\partial r}\right)+z^2\left(3\beta_r{}^*+\frac{\partial w^*}{\partial r}\right)$$

$$\chi_r=\frac{\partial \beta_r}{\partial r};\chi_r{}^*=\frac{\partial \beta_r{}^*}{\partial r};\chi_\theta=\frac{\beta_r}{r};\chi_\theta{}^*=\frac{\beta_r{}^*}{r};\chi_z=2w^*;\varphi_r=\beta_r+\frac{\partial w}{\partial r};\varphi_\theta=3\beta_r{}^*+\frac{\partial w^*}{\partial r}$$

$$\{\varepsilon\}=\begin{Bmatrix}\varepsilon_{rr}\\ \varepsilon_{\theta\theta}\\ \varepsilon_{zz}\\ \gamma_{rz}\end{Bmatrix}=\begin{bmatrix}z&0&0&z^3&0&0&0\\0&z&0&0&z^3&0&0\\0&0&z&0&0&0&0\\0&0&0&0&0&1&z^2\end{bmatrix}\begin{Bmatrix}\chi_r\\ \chi_\theta\\ \chi_z\\ \chi_r{}^*\\ \chi_\theta{}^*\\ \varphi_r\\ \varphi_\theta\end{Bmatrix}\text{ and}$$

$$\begin{Bmatrix}\chi_r\\ \chi_\theta\\ \chi_z\\ \chi_r{}^*\\ \chi_\theta{}^*\\ \varphi_r\\ \varphi_\theta\end{Bmatrix}=\begin{bmatrix}\frac{\partial \beta_r}{\partial r}\\ \frac{\beta_r}{r}\\ 2w^*\\ \frac{\partial \beta_r{}^*}{\partial r}\\ \frac{\beta_r{}^*}{r}\\ \beta_r+\frac{\partial w}{\partial r}\\ 3\beta_r{}^*+\frac{\partial w^*}{\partial r}\end{bmatrix}=\begin{bmatrix}0&\frac{\partial N}{\partial r}&0&0\\0&\frac{N}{r}&0&0\\0&0&2N&0\\0&0&0&\frac{\partial N}{\partial r}\\0&0&0&\frac{N}{r}\\ \frac{\partial N}{\partial r}&N&0&0\\0&0&\frac{\partial N}{\partial r}&3N\end{bmatrix}\begin{Bmatrix}w\\ \beta_r\\ w^*\\ \beta_r{}^*\end{Bmatrix}\therefore[B_{bi}]=\begin{bmatrix}0&\frac{\partial N}{\partial r}&0&0\\0&\frac{N}{r}&0&0\\0&0&2N&0\\0&0&0&\frac{\partial N}{\partial r}\\0&0&0&\frac{N}{r}\\ \frac{\partial N}{\partial r}&N&0&0\\0&0&\frac{\partial N}{\partial r}&3N\end{bmatrix}$$

$$Z_b=\begin{bmatrix}z&0&0&z^3&0&0&0\\0&z&0&0&z^3&0&0\\0&0&z&0&0&0&0\\0&0&0&0&0&1&z^2\end{bmatrix}\text{and }LC=\frac{Ev}{(1+v)(1-2v)}\text{ and }G=\frac{E}{2(1+v)};$$

$$C_{22}=LC+2G;C_{22}=C_{11};C_{33}=C_{11};C_{12}=LC;C_{13}=C_{12};C_{21}=C_{12};$$

$$C_{23}=C_{12};C_{31}=C_{12};C_{32}=C_{12};C_{44}=G;$$

$$C_b=\begin{bmatrix}C_{11}&C_{12}&C_{13}&0\\C_{21}&C_{22}&C_{23}&0\\C_{31}&C_{32}&C_{33}&0\\0&0&0&C_{44}\end{bmatrix}\text{and }D_b=\int_{-\frac{h}{2}}^{\frac{h}{2}}[Z_b]^T[C_b][Z_b]\,dz$$

4.6 Mass Matrix

Subsoil parameters are calculated according to the subsoil surface deformations due to the dead loads of the structure, and they are taken as constant during the analyses. It is also assumed that the mass of the subsoil does not change with depth. Plate finite elements idealize the mat foundation and the subsoil zone under and outside the mat foundation is idealized as a shear layer by quadrilateral subsoil shear elements.

Kinetic energy is the accumulation of the three velocity components that each particle in the plate's whole domain contributes to in the x, y, and z dimensions.

Case-1 for Love- Kirchhoff's Plate

$$T_e = \frac{1}{2}\rho \int_{A_e}\left(\int_{\frac{-h}{2}}^{\frac{h}{2}} \dot{w}^2 dz\right) dA = \frac{1}{2}\rho \int_{A_e} h\dot{w}^2\, dA = \frac{1}{2}\{d'\}^T \rho h \int_0^l [N]^T\, [N] dA \{d'\}$$

$\therefore [M] = \rho h \int_{A_e} [N]^T [N] dA$ including soil ρh replace with $\rho h + m_0$;

Case-2 for Mindlin's Plate

$$T_e = \frac{1}{2}\rho \int_{A_e}\left[\int_{\frac{-h}{2}}^{\frac{h}{2}} \left(\dot{w}^2 + z^2\dot{\theta}_x^{\ 2} + z^2\dot{\theta}_y^{\ 2}\right) dz\right] dA = \frac{1}{2}\rho \int_{A_e}\left(h\dot{w}^2 + \frac{h^3}{12}\dot{\theta}_x^{\ 2} + \frac{h^3}{12}\dot{\theta}_y^{\ 2}\right) dA$$

$$T_e = \frac{1}{2}\{d'\}^T \rho \int_0^l [N]^T [I]\, [N] dA \{d'\} \therefore [M] = \rho \int_{A_e} [N]^T [I][N] dA$$

$$\text{Here, } d = \begin{bmatrix} N_w & 0 & 0 \\ 0 & N_{\theta_x} & 0 \\ 0 & 0 & N_{\theta_y} \end{bmatrix} \begin{Bmatrix} w \\ \theta_x \\ \theta_y \end{Bmatrix}; I = \begin{bmatrix} \rho h + m_0 & 0 & 0 \\ 0 & \frac{\rho h^3}{12} & 0 \\ 0 & 0 & \frac{\rho h^3}{12} \end{bmatrix} \text{and } N = \begin{bmatrix} N_w & 0 & 0 \\ 0 & N_{\theta_x} & 0 \\ 0 & 0 & N_{\theta_y} \end{bmatrix};$$

$m_0 = \frac{\rho_s H}{\gamma}\left(\frac{\sinh\gamma \cosh\gamma - \gamma}{2\sinh^2\gamma}\right)$ Here, H is the depth from the ground surface to the top of the assumed rigid base.

Case-3 for Thick HSDT Plate

$u(x, y, z) = z\theta_x(x, y) + z^3\theta_x^{\ *}(x, y)\}; v(x, y, z) = z\theta_y(x, y) + z^3\theta_y^{\ *}(x, y)$

and $w(x, y, z) = w(x, y) + z^2 w^*(x, y)$

$$T_e = \frac{1}{2}\rho \int_{A_e}\left[\int_{\frac{-h}{2}}^{\frac{h}{2}} \left(\dot{w}^2 + z^2\dot{\theta}_x^{\ 2} + z^2\dot{\theta}_y^{\ 2} + z^4\dot{w}^{*2} + z^6\dot{\theta}_x^{\ *2} + z^6\dot{\theta}_y^{\ *2}\right) dz\right] dA$$

$$T_e = \frac{1}{2}\rho \int_{A_e}\left(h\dot{w}^2 + \frac{h^3}{12}\dot{\theta}_x^{\ 2} + \frac{h^3}{12}\dot{\theta}_y^{\ 2} + \frac{h^5}{80} w^x + \frac{h^7}{896}\dot{\theta}_x^{\ \dot{*}2} + \frac{h^7}{896}\dot{\theta}_y^{\ *2}\right) dA$$

$$T_e = \frac{1}{2}\{d'\}^T \rho \int_0^l [N]^T [I]\, [N] dA \{d'\} \therefore [M] = \rho \int_{A_e} [N]^T [I][N] dA$$

$$\text{Here, } d = \begin{bmatrix} N_w & 0 & 0 & 0 & 0 & 0 \\ 0 & N_{\theta_x} & 0 & 0 & 0 & 0 \\ 0 & 0 & N_{\theta_y} & 0 & 0 & 0 \\ 0 & 0 & 0 & N_{w^*} & 0 & 0 \\ 0 & 0 & 0 & 0 & N_{\theta_x{}^*} & 0 \\ 0 & 0 & 0 & 0 & 0 & N_{\theta_y{}^*} \end{bmatrix} \begin{Bmatrix} w \\ \theta_x \\ \theta_y \\ w^* \\ \theta_x{}^* \\ \theta_y{}^* \end{Bmatrix}$$

$$\therefore I = \begin{bmatrix} \rho h + m_0 & 0 & 0 & 0 & 0 & 0 \\ 0 & \frac{\rho h^3}{12} & 0 & 0 & 0 & 0 \\ 0 & 0 & \frac{\rho h^3}{12} & 0 & 0 & 0 \\ 0 & 0 & 0 & \frac{\rho h^5}{80} & 0 & 0 \\ 0 & 0 & 0 & 0 & \frac{\rho h^7}{896} & 0 \\ 0 & 0 & 0 & 0 & 0 & \frac{\rho h^7}{896} \end{bmatrix} \text{and } N = \begin{bmatrix} N_w & 0 & 0 & 0 & 0 & 0 \\ 0 & N_{\theta_x} & 0 & 0 & 0 & 0 \\ 0 & 0 & N_{\theta_y} & 0 & 0 & 0 \\ 0 & 0 & 0 & N_{w^*} & 0 & 0 \\ 0 & 0 & 0 & 0 & N_{\theta_x{}^*} & 0 \\ 0 & 0 & 0 & 0 & 0 & N_{\theta_y{}^*} \end{bmatrix}$$

4.7 Characteristic equation

Using the Hamilton principle (Petyt, 1990), plate-soil equations of motion for free vibration without damping are

$$[M]\{\ddot{w}\} + [KK]\{w\} = \{0\} \tag{4.7.1}$$

Where w is the plate's displacement and $\ddot{w}$ acceleration, respectively, and [KK] and [M] are the stiffness and mass matrices of the plate-soil system. One can get (Hinton, 1988) the natural frequencies and vibrational mode by resolving the generalized eigenvalue problems.

If a harmonic motion is assumed for free vibration analysis

$\{w\} = \{\overline{w}\}e^{i\omega t}$ and $\{\ddot{w}\} = -\omega^2\{\overline{w}\}e^{i\omega t}$

Where $\{\overline{w}\}$ is the amplitude of $\{w\}$.

When $\{w\}$ and $\{\ddot{w}\}$ are substituted in equation (4.7.1), one obtains

$$([KK] - \omega^2[M])\{\overline{w}\} = \{0\} \tag{4.7.2}$$

Equation (11)'s non-trivial approach implies that

$|([KK] - \omega^2[M])| = 0$ the determining equation.' ω' represents the natural frequency.

Chapter 5
Results and Discussions

5.1 Thin Rectangular Plate Using Higher-Order FEM

This study considers several boundary conditions, such as SSSS, CCCC, and FFFF, where S refers to a simply-supported edge, F to a free edge, and C to a clamped edge. Clamped edge, $w = \frac{\partial w}{\partial x} = \frac{\partial w}{\partial y} = \frac{\partial^2 w}{\partial x \partial y} = 0$, simply supported edge, w = 0 and free edge, $w \neq 0, \frac{\partial w}{\partial x} \neq 0, \frac{\partial w}{\partial y} \neq 0, \frac{\partial^2 w}{\partial x \partial y} \neq 0$.

For example, CFSC means that edge (Fig. 4.1): (ξ = - a) is clamped, edge: (η = - b) is free, edge: (ξ = a) is simply supported and edge (η = b) is clamped.

In the present element, stress at any position is determined by taking the weighted average of stress values at the nearest Gauss points for all the elements around the point and the relevant element area as weight. It is simple to calculate stresses at a point where concentrated loads act.

In the present study (P.S.), the tolerance limit of parameter γ set for the iterations is 0.0001.

5.1.1 Convergence study

For convergence study, first considered a square plate without foundation for the clamped (CCCC) and simply supported (SSSS) under uniformly distributed load (UDL),q and central concentrated load (PL), P for each boundary condition for the maximum non-dimensional displacement, $\overline{w}_{max} = \frac{wD}{qL^4} = \frac{wD}{PL^2}$ and bending moments, $\overline{M}_{max} = \frac{M}{qL^2} = \frac{M}{P}$ and mesh size of 12 × 12 is decided for a reasonable result compared to 20 × 20 of a 12 DOF rectangular element, hence less uses of computer memory and time. The results in Tables 5.1 and 5.2 are compared with (Timoshenko and Woinowsky-Krieger, 1970).

Table 5.1

Maximum non-dimensional displacement and bending moment of a SSSS plate with UDL

Mesh Size	$\overline{w}_{max}$	$\overline{M}_{max}$
2 × 2	0.0044895	0.05553
4 × 4	0.0040768	0.04916
6 × 6	0.0040644	0.04840
8 × 8	0.0040629	0.04816
10 × 10	0.0040625	0.04806

12 × 12	0.0040624	0.04800
14 × 14	0.0040624	0.04797
16 × 16	0.0040624	0.04795
18 × 18	0.0040624	0.04794
20 × 20	0.0040623	0.04793
(Timoshenko and Woinowsky-Krieger, 1970)	0.004062	0.04790

Table 5.2

Maximum non-dimensional displacement and bending moment of a CCCC plate with UDL

Mesh Size	$\overline{w}_{max}$	$\overline{M}_{max}$
2 × 2	0.001325	0.041333
4 × 4	0.001265	0.025102
6 × 6	0.001265	0.023735
8 × 8	0.001265	0.023344
10 × 10	0.001265	0.023178
12 × 12	0.001265	0.023091
14 × 14	0.001265	0.023041
16 × 16	0.001265	0.023008
18 × 18	0.001265	0.022986
20 × 20	0.001265	0.022971
(Timoshenko and Woinowsky-Krieger, 1970)	0.00126	0.0230

Tables 5.1 and 5.2 show the rapid convergence rate of the proposed plate bending element.

5.1.2 Validation work

An example has been chosen from the study by (Özgan and Daloğlu, 2008) to validate the present formulation in the thin to moderately thick plate limit. The properties of the plate-soil system are as follows. The modulus of elasticity of the subsoil is 68950 kN/m^2, the Poisson's ratio of the subsoil is 0.25, the modulus of elasticity of the plate is 20685000 kN/m^2, the Poisson's ratio of the plate equals to 0.20, and the thickness of the plate is considered as, i.e. L/h = 60, 20,10,6.67,5 is the thin plate to moderate thick plate limit where h is the thickness of plate, L is the shorter dimension of the plate. B is the longer dimension of the plate, and the plate dimensions are (L × B) 9.144 × 12.192 m. The uniformly distributed load on the plate is 23.94 kN/m^{2,} and the concentrated load is 133.34 kN. The analysis is performed for four depths of the soil stratum, H = 3.048, 6.096, 9.144 and 15.240 m, for all free plate edges.

From the convergence study, the plate is discretised into 10 × 12 elements. The results are tabulated in Tables 5.3 and 5.4 for uniformly distributed and concentrated load cases.

The same example is considered by (Buczkowski and Torbacki, 2001). Still, only subsoil depth H = 15.24 m is different for the B/h ratio from 2 to 10^6, i.e. thin to thick plate limit for uniformly distributed loading case only. The results are tabulated in Table 5.5.

Table 5.3

Maximum displacements (w) and Maximum moments (Mx) for free plate with uniformly distributed load

H(m)	h/L	w_{max} (mm)		M_{xmax} (KN-m/m)	
		(Özgan and Daloğlu, 2008)	PS	(Özgan and Daloğlu, 2008)	PS
3.048	0.0167	0.8740	0.8734	0.05	0.05
	0.0500	0.8983	0.8967	5.38	5.33
6.096	0.0167	1.5330	1.5360	0.28	0.28
	0.0500	1.5046	1.5135	10.36	10.18
9.144	0.0167	1.9180	1.9217	0.39	0.40
	0.0500	1.8414	1.8728	12.28	12.01
15.240	0.0167	2.2380	2.2778	0.43	0.45
	0.0500	2.1319	2.2124	12.78	12.37

Table 5.4

Maximum displacements (w) and Maximum moments (Mx) for a free plate with concentrated load at mid-point

H(m)	h/L	w_{max} (mm)		M_{xmax} (KN-m/m)	
		(Özgan and Daloğlu, 2008)	PS	(Özgan and Daloğlu, 2008)	PS
3.048	0.0167	0.8570	0.7977	17.63	15.29
	0.0500	0.2409	0.2210	32.26	30.17
6.096	0.0167	0.8840	0.8254	17.13	14.84
	0.0500	0.2883	0.2690	32.36	30.40
9.144	0.0167	0.8850	0.8265	17.07	13.10
	0.0500	0.3043	0.2861	31.97	30.13
15.240	0.0167	0.8850	0.8266	17.07	13.10
	0.0500	0.3118	0.2947	31.45	29.77

Table 5.5

Maximum displacements (w) for free plate with uniformly distributed load

B/h	w_{max} (mm)	
	(Buczkowski and Torbacki, 2001)	Present PBR4
20	1.9350	2.1230
80	2.2055	2.2778
100	2.2090	2.2811
500	2.2104	2.2937
1000	2.2104	2.2940
1000000	2.2104	2.2940

It is observed that displacements and bending moments from Tables 5.3 and 5.4 are in excellent agreement with the results given in (Özgan and Daloğlu, 2008) for any loading cases regardless of the subsoil depth. Furthermore, it is observed from table 5.5 is in reasonable conformity with the results given by (Buczkowski and Torbacki, 2001).

It is also observed from Tables 5.3, 5.4, and 5.5 that the present formulation is effectively used for thin and moderately thick plates.

5.1.3 The effectiveness of the formulation

With free boundary conditions, the preceding example is considered. The properties of the plate-soil system are the same as before. The ratio (h/L) between the plate's thickness and the plate's shorter side is 0.002, 0.001, 0.02 and 0.01. The example is solved by the rectangular plate bending element consistent with C^2 based on thin plate theory to demonstrate the effect of several subsoil depths, and the thickness of the plate is displayed in tabular and graphical forms on displacements and bending moments of the plate. For an increasing h/L ratio, the displacement of the plate often decreases with a constant value of subsoil depth (H) for all loading situations.

In contrast, the bending moment of the plate increases, as observed in Tables 5.6 and 5.7. As H increases with a constant value of h/L, the displacement and bending moment of the plate often increase in any loading situation. It is also observed from Figure 5.1-5.12 that as the value of h/L increases, the curves get somewhat closer to each other. After a certain subsoil depth (H) for particular conditions, the influence of H is negligible.

Table 5.6

Maximum displacements (w) and Maximum moments (M_x) for free plate with uniformly distributed load

H(m)	h/L	w_{max} (mm)	M_{xmax} (KN-m/m)	M_{ymax} (KN-m/m)	γ
3.048	0.02	0.8767	0.09	0.026000	0.5906
6.096		1.5378	0.50	0.265900	0.9226
9.144		1.9215	0.70	0.426600	1.1869
15.24		2.2750	0.77	0.534700	1.6036
3.048	0.01	0.8700	0.01	0.004100	0.6051
6.096		1.5339	0.06	0.031800	0.9348
9.144		1.9228	0.08	0.051800	1.1986
15.24		2.2852	0.10	0.065600	1.6203
3.048	0.002	0.8691	0.0001	0.000035	0.6112
6.096		1.5341	0.0005	0.000253	0.9429
9.144		1.9259	0.0007	0.000411	1.2090
15.24		2.2939	0.0008	0.000520	1.6369
3.048	0.001	0.8691	0.000011	0.000004	0.6114
6.096		1.5341	0.000059	0.000031	0.9431
9.144		1.9259	0.000084	0.000051	1.2092
15.24		2.2940	0.000096	0.000065	1.6371

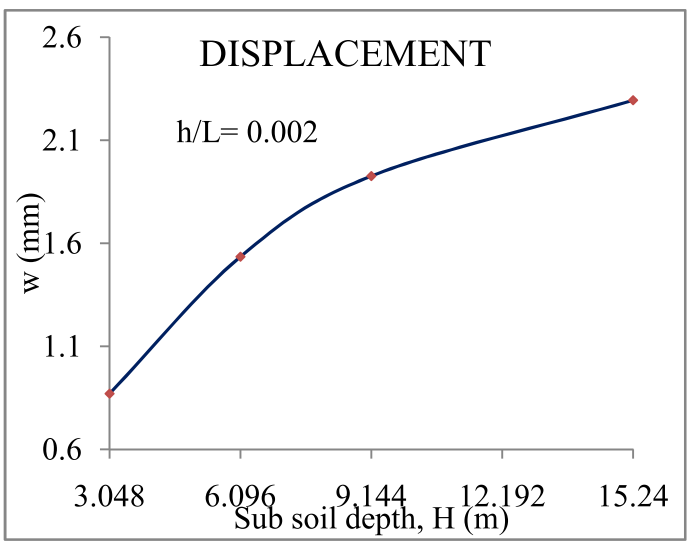

Fig. 5.1 Changes of deflection, w of a free plate with uniformly distributed load

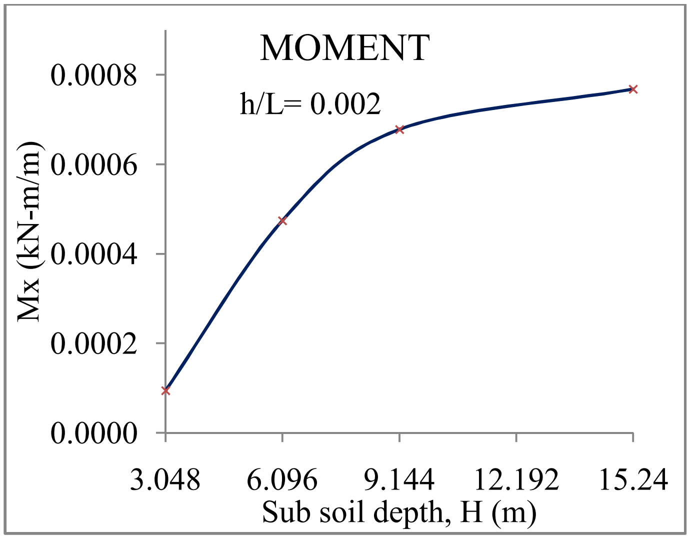

Fig. 5.2 Changes of bending moment Mx of a free plate with uniformly distributed load

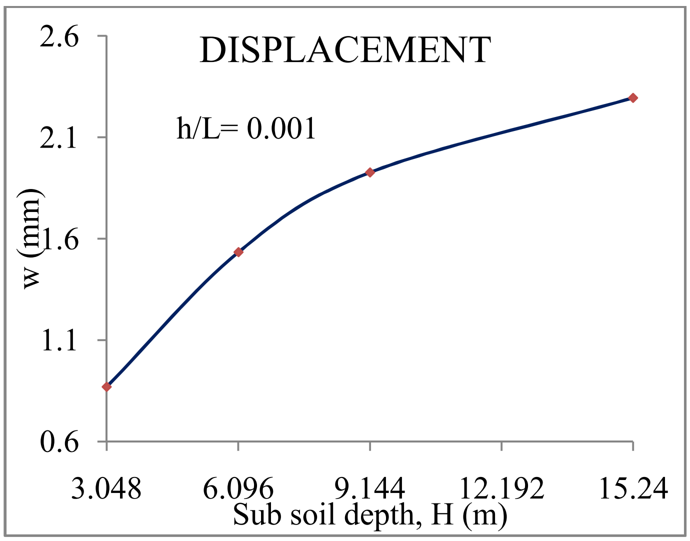

Fig. 5.3 Changes of deflection, w of a free plate with uniformly distributed load

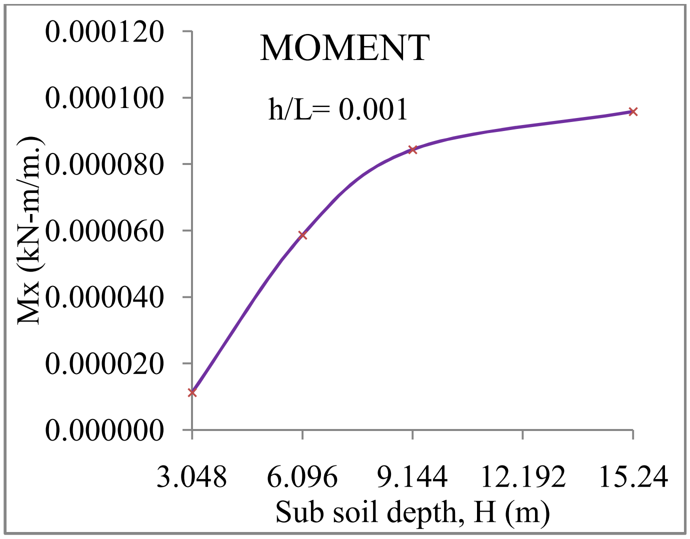

Fig. 5.4 Changes of bending moment Mx of a free plate with uniformly distributed load

Table 5.7

Maximum displacements (w) and Maximum moments (M_x) for free plate with concentrated load

H(m)	h/L	w_{max} (mm)	M_{xmax} (KN-m/m)	M_{ymax} (KN-m/m)	γ
3.048	0.02	0.6605	17.9	17.3086	1.6978
6.096		0.6971	17.38	16.8008	3.0263
9.144		0.6998	17.28	16.6998	4.4659
15.24		0.6999	17.27	16.6899	7.4323
3.048	0.01	1.2488	8.454	7.9942	2.5555
6.096		1.2555	8.288	7.8385	4.9552
9.144		1.2555	8.285	7.8355	7.4290
15.24		1.2555	8.285	7.8355	12.3815
3.048	0.002	2.0229	0.189	0.1719	3.2271
6.096		2.0152	0.186	0.1696	6.4129
9.144		2.0152	0.186	0.1696	9.6192
15.24		2.0152	0.186	0.1696	16.0320
3.048	0.001	2.0413	0.024	0.0219	3.2351
6.096		2.0333	0.024	0.0216	6.4300
9.144		2.0333	0.024	0.0216	9.6447
15.24		2.0333	0.024	0.0216	16.0744

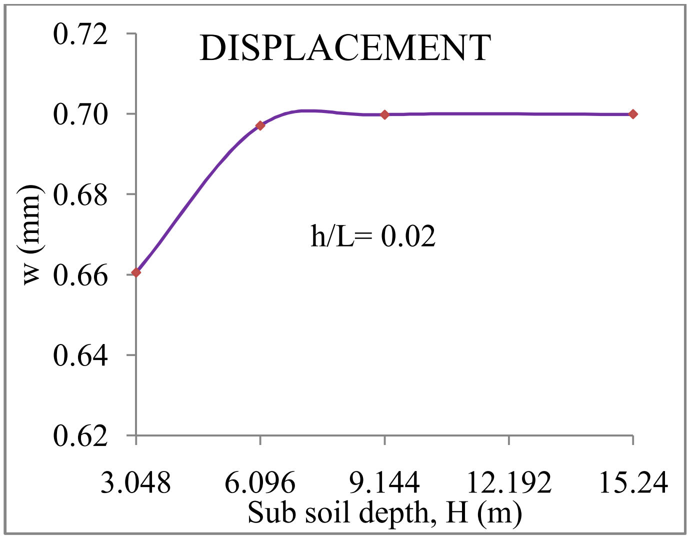

Fig. 5.5 Changes of deflection, w of a free plate with concentrated load

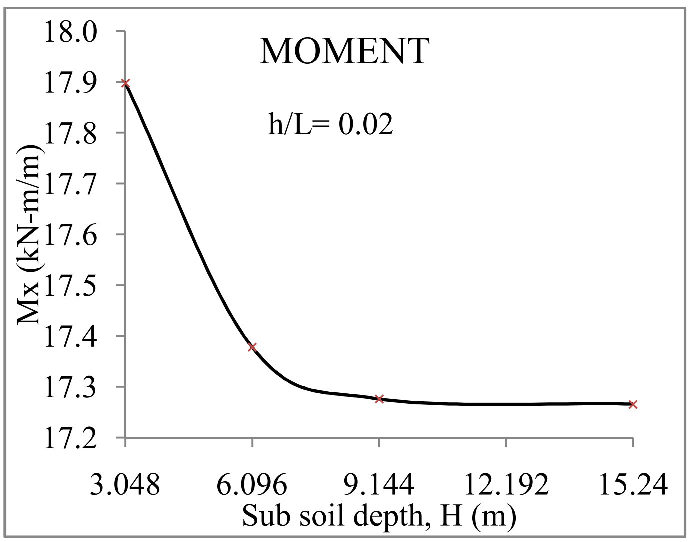

Fig. 5.6 Changes of bending moment Mx of a free plate with a concentrated load

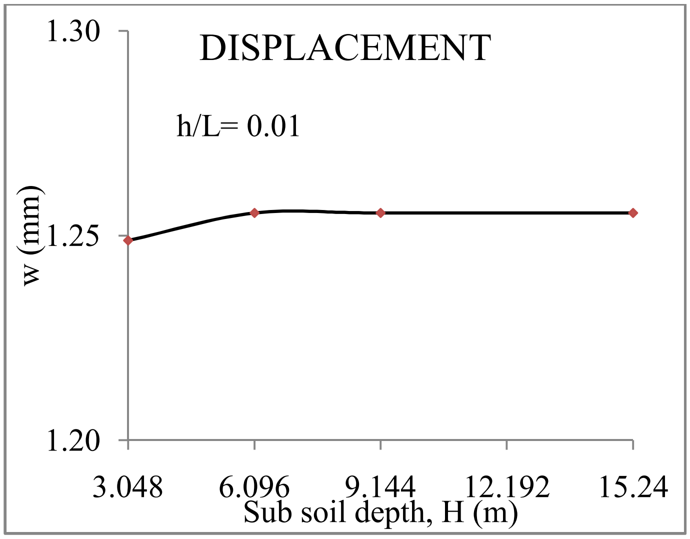

Fig. 5.7 Changes of deflection, w of a free plate with a concentrated load

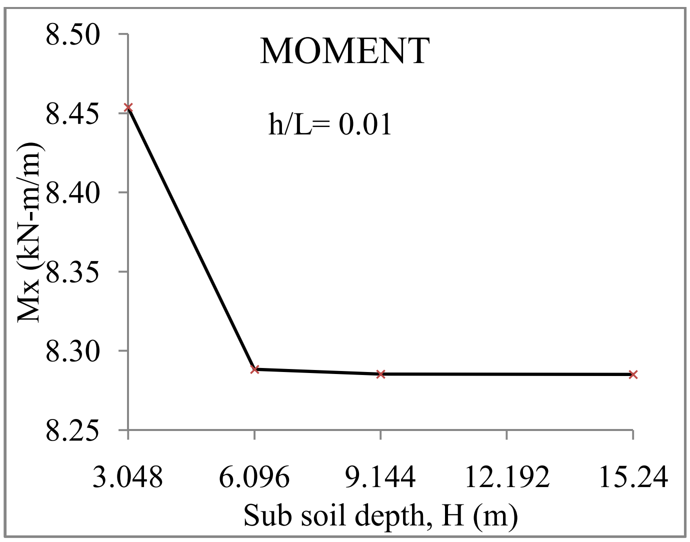

Fig. 5.8 Changes of bending moment Mx of a free plate with a concentrated load

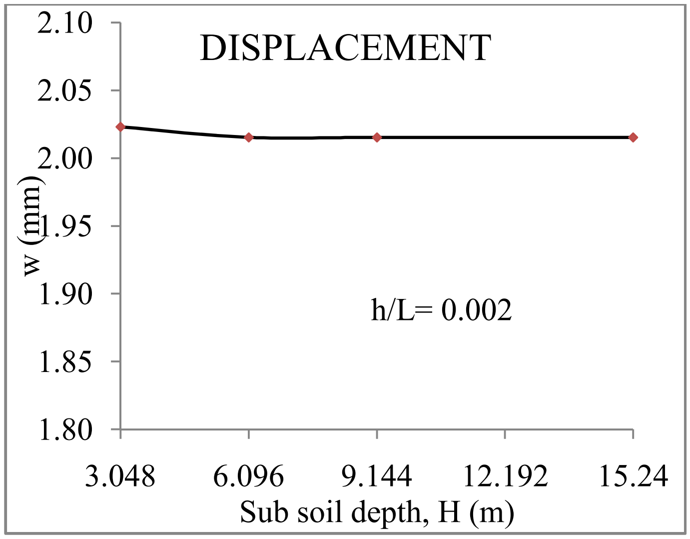

Fig. 5.9 Changes of deflection, w of a free plate with concentrated load

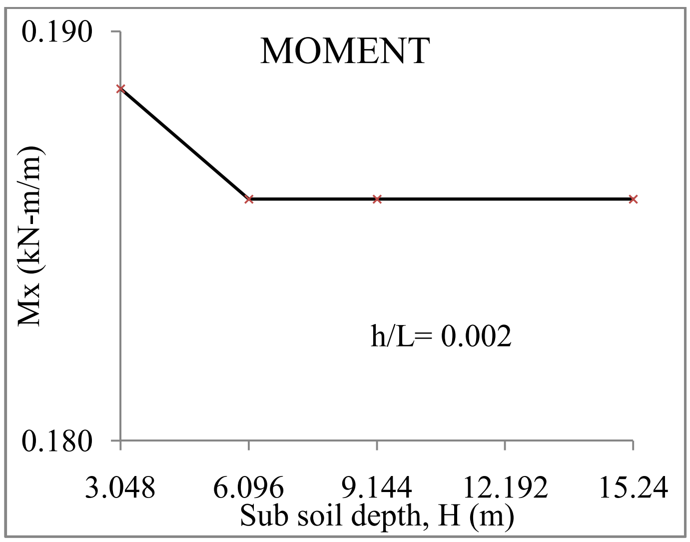

Fig. 5.10 Changes of bending moment Mx of a free plate with a concentrated load

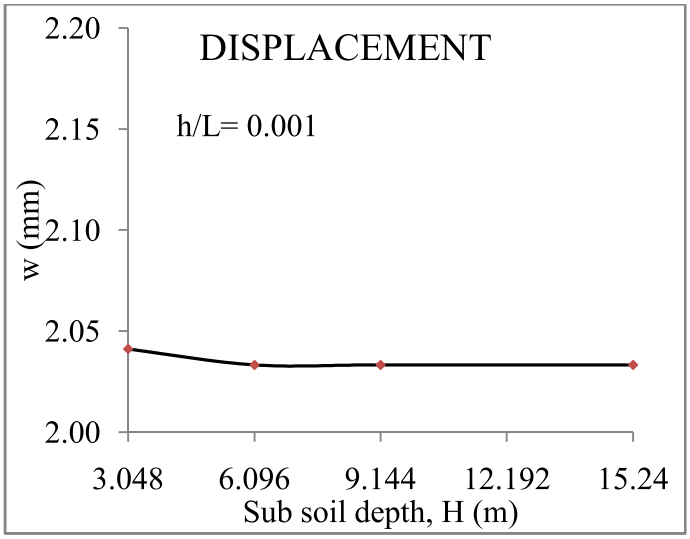

Fig. 5.11 Changes of deflection, w of a free plate with concentrated load

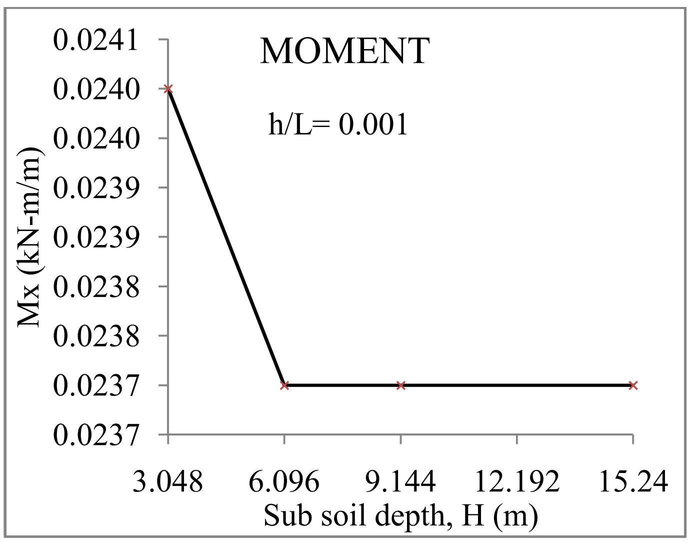

Fig. 5.12 Changes of bending moment Mx of a free plate with concentrated load

The effect of subsoil depth and thickness of the plate on the displacement is more significant for the concentrated load case than for the distributed load case, and this effect increases as the h/L ratio increases for any subsoil depth. The observations indicate that the impact of the thickness of the plate on the behaviour of the plate bending is always negligible for free plates.

5.2 Thin Circular Plate Using Higher-Order FEM

This study considers several boundary conditions, such as S.S., C, and F, where S.S. refers to a simply supported edge, F to a free edge, and C to a clamped edge. Clamped edge,

$w = \frac{\partial w}{\partial r} = \frac{\partial w}{\partial \theta} = \frac{\partial^2 w}{\partial r\, \partial \theta} = 0$, simply supported edge, $w = \frac{\partial^2 w}{\partial r\, \partial \theta} = 0$ and free edge,

$w \neq 0, \frac{\partial w}{\partial r} \neq 0, \frac{\partial w}{\partial \theta} \neq 0, \frac{\partial^2 w}{\partial r\, \partial \theta} \neq 0.$

In this element, the stress at any position is determined by taking the weighted average of the stress at the centre points of all the surrounding elements and the relevant element area as weight. Even for determining stresses at a point where a concentrated load is applied, no difficulty arises.

5.2.1 Convergence Study

For the convergence study for a C and S.S. plate under an entirely uniform distributed load (q) and a central concentrated load (P), a circular plate (ν = 0.25) without foundation is first taken into consideration. Compared to 15×90, or 1350 elements, of a 12 D.O.F. element, this mesh size of 10×60, or 600 elements, produces an excellent output using less computer memory. Table 5.8 presents the results and a comparison with (Timoshenko and Woinowsky-Krieger, 1970).

Table 5.8

Central non-dimensional displacement for clamped (C) and simply supported (S.S.) plate under fully U.D.L. (q) and central concentrated load (P)

Mesh size (Ring × Annular sector)	For fully U.D.L., q		For central concentrated load, P	
	$\overline{w}$ (C)	$\overline{w}$ (S.S.)	$\overline{w}$ (C)	$\overline{w}$(S.S.)
2 × 12	11.285	45.007	901.0	240.20
3 × 20	10.772	44.006	937.2	251.34
4 × 24	10.514	43.403	959.5	255.69
6 × 36	10.282	42.809	981.2	258.85
8 × 40	10.182	42.536	990.3	259.85
10 × 60	10.129	42.387	994.8	260.23
(Timoshenko and Woinowsky-Krieger, 1970)	10.000	42.000	1000.0	260.00
Difference (%)	1.29	0.92	0.52	0.09

5.2.2 Validation

(Yue et al., 2019) studies were used as examples to validate the current formulation for uniform loading circumstances. A solid circular plate with a radius of 0.4 m is the same thickness throughout 0.05 m and has a uniformly distributed loading of 1000 kN/m² intensity. The plate's material characteristics are $E = 2.8\times10^4$ MN/m² and a Poisson's ratio of 0.15, and foundation characteristics are $E_s = 6.9 \times 10^4$ kN/m², $\nu_s = 0.3$ and H = 1 m.

Table 5.9 compares the present study's (P.S.) results with those of (Yue et al., 2019). The reference's findings can be regarded as having full conformity.

Table 5.9

Comparison of the Deflections (in mm) at the centre of the plate with the Reference Value

Deflections (in mm)		Difference (%)
PS	(Yue et al., 2019)	
5.083	5.083	0

(Yue et al., 2019) Studies were used as an example to validate the current formulation for the concentrated loading condition. A concentrated load of 98.1 kN is applied to the centre of a solid circular plate with a radius of 5 m and an elastic foundation. This plate has a uniform thickness of 0.5 m. The plate's material characteristics are $E = 1.7658\times10^4$ MN/m² and a Poisson's ratio of 0.17, and foundation characteristics are $E_s = 8.6 \times 10^3$ kN/m², $\nu_s = 0.2$ and H = 1 m.

Table 5.10 compares the P.S. with (Yue et al., 2019) and provides the results. Again, the reference's findings can be regarded as a solid agreement.

Table 5. 10

Comparison of the Deflections (in mm) at the centre of the plate with the Reference Value

Deflections (in mm)		Difference (%)
PS	(Yue et al., 2019)	
0.318	0.320	0.63

(Yue et al., 2019) Studies were used as an example to validate the current formulation for the patch loading condition. As shown in Table 5.11, the parameter of the solid circular plate with a radius of 1.35 m is supported by an elastic foundation. The plate's centre is subjected to a patch load with an intensity of 1000 kN/m² and a radius of 0.18 m. The plate's material characteristics are E = 2.45×10⁴ MN/m², thickness of the plate h = 0.25 m and a Poisson's ratio of 1/6 and foundation characteristics are $E_s = 62.5 \times 10^3$ kN/m², $\nu_s = 0.25$ and H = 2 m.

Table 5.11 compares the P.S. solution to (Yue et al., 2019). Again, the results concerning the reference can be accepted as a fair agreement.

Table 5.11

Comparison of the Deflections (in mm) at the centre of the plate with the Reference Value

Deflections (in mm)		Difference (%)
PS	(Yue et al., 2019)	
0.372	0.345	7.83

5.2.3 The effectiveness of the formulation

For this investigation, a solid circular plate of radius 3 m, Ep = 2.5×10^4 MN/m², ν = 0.2 and t or h = 200 mm, and elasticity modulus of the foundation soil E_s = 20 MN/m², 30 MN/m² and 40 MN/m², Poisson's ratio of the foundation ν_s = 0.2, 0.25, 0.3, depth of the foundation soil, H = 3 m, 5 m, 7 m, and The plate's uniformly distributed load is 40 kN/m², and its concentrated load is 300 kN. Tables 5.12, 5.13, and Figures 5.13-5.26 show the study's parametric results.

Table 5.12

Displacements (w_c) and radial bending moments (B.M.) (M_{cnn}) at the centre and other parameters of a free (F) plate with fully U.D.L

E_s (Mpa)	ν_s	H (m)	w_c (mm)	M_{cnn} (kN-m/m)	K (MN/m³)	2t (MN/m)	γ	N.I.
20	0.2	3	4.36	9.83	7.47	7.65	0.8188	5
		5	5.50	11.98	4.57	11.95	1.1113	5
		7	6.02	12.42	3.36	15.59	1.3766	6
30		3	3.01	6.98	11.20	11.55	0.7871	5
		5	3.78	8.53	6.83	18.06	1.0801	5
		7	4.12	8.78	5.02	23.58	1.3471	6
40		3	2.30	5.31	14.92	15.46	0.7679	5
		5	2.89	6.55	9.09	24.19	1.0619	5
		7	3.14	6.73	6.67	31.59	1.3303	6
20	0.25	3	4.15	9.35	8.06	7.39	0.7907	5
		5	5.30	11.66	4.91	11.59	1.0699	5
		7	5.85	12.22	3.60	15.19	1.3237	6

30		3	2.86	6.61	12.08	11.15	0.7594	5
		5	3.65	8.29	7.35	17.51	1.0387	5
		7	4.01	8.64	5.38	22.97	1.2943	6
40		3	2.18	5.01	16.10	14.92	0.7406	5
		5	2.78	6.35	9.79	23.45	1.0204	4
		7	3.05	6.62	7.16	30.76	1.2774	6
20		3	3.82	8.63	9.03	7.15	0.7548	5
		5	4.97	11.08	5.49	11.28	1.0170	4
		7	5.54	11.79	4.01	14.87	1.2568	6
30		3	2.63	6.04	13.54	10.79	0.7244	5
	0.3	5	3.42	7.85	8.22	17.04	0.9862	4
		7	3.80	8.32	5.99	22.48	1.2275	6
40		3	2.01	4.55	18.04	14.43	0.7061	5
		5	2.61	6.00	10.95	22.82	0.9681	5
		7	2.89	6.37	7.98	30.11	1.2107	6

Table 5.13

Displacements (w_c) and radial bending moments (B.M.) (M_{cnn}) at the centre of a C, S.S. and F plate with a concentrated load at the centre

E_s (Mpa)	v_s	H (m)	B.C.- C		B.C.- S.S.		B.C.- F	
			w_c (mm)	M_{cnn} (kN-m/m)	w_c (mm)	M_{cnn} (kN-m/m)	w_c (mm)	M_{cnn} (kN-m/m)
20		3	1.99	54.36	2.70	55.45	2.83	54.37
		5	1.91	52.43	2.61	53.78	3.07	52.98
		7	1.77	49.97	2.35	51.07	3.11	51.20
30		3	1.71	50.42	2.11	50.48	2.17	49.85
	0.20	5	1.62	48.08	2.02	48.45	2.31	48.01
		7	1.48	45.32	1.81	45.64	2.30	46.01
40		3	1.51	47.41	1.76	47.13	1.80	46.70
		5	1.41	44.79	1.67	44.81	1.88	44.56
		7	1.27	41.87	1.49	41.93	1.86	42.42
20		3	1.98	54.27	2.65	55.21	2.76	54.20
		5	1.91	52.58	2.61	53.90	3.01	53.01
	0.25	7	1.79	50.27	2.38	51.37	3.07	51.32
30		3	1.70	50.35	2.07	50.32	2.12	49.74
		5	1.63	48.27	2.02	48.60	2.27	48.09

		7	1.49	45.65	1.83	45.96	2.28	46.16
40		3	1.50	47.36	1.73	47.02	1.76	46.64
		5	1.42	45.00	1.68	44.99	1.85	44.68
		7	1.29	42.21	1.51	42.26	1.84	42.60
20	0.30	3	1.95	53.98	2.57	54.67	2.64	53.79
		5	1.91	52.61	2.58	53.80	2.91	52.86
		7	1.79	50.47	2.39	51.53	2.98	51.27
30		3	1.67	50.06	2.00	49.89	2.04	49.41
		5	1.62	48.33	2.00	48.57	2.20	48.01
		7	1.50	45.88	1.84	46.16	2.22	46.17
40		3	1.47	47.09	1.67	46.68	1.69	46.36
		5	1.42	45.08	1.66	45.01	1.80	44.64
		7	1.30	42.47	1.51	42.49	1.80	42.65

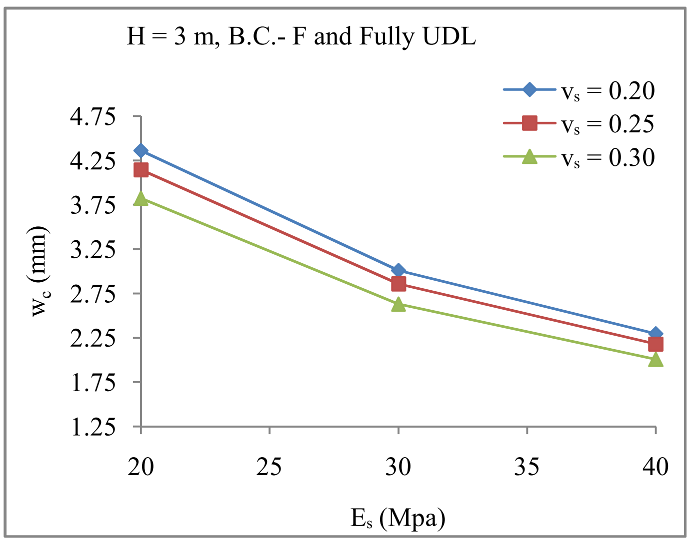

Fig. 5.13 Central deflection vs sub-soil elastic modulus

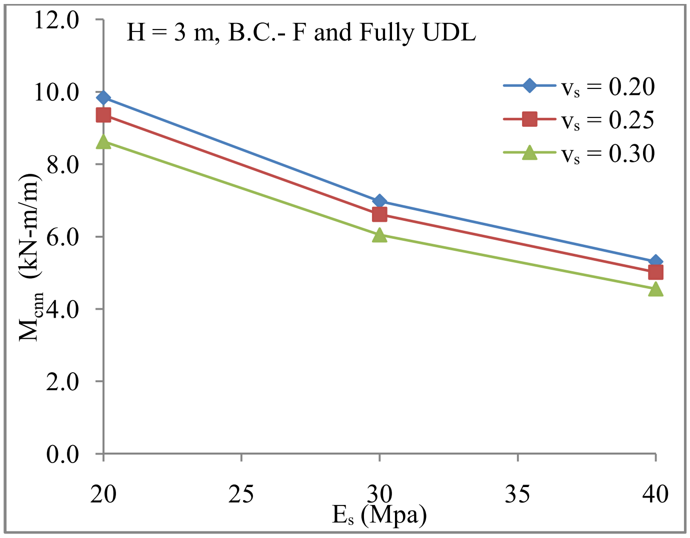

Fig. 5.14 Central radial B.M. vs sub-soil elastic modulus

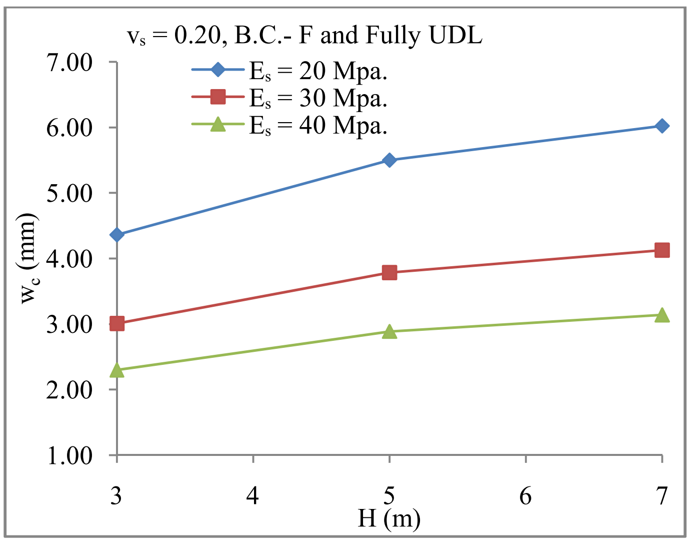

Fig. 5.15 Central deflection vs sub-soil depth

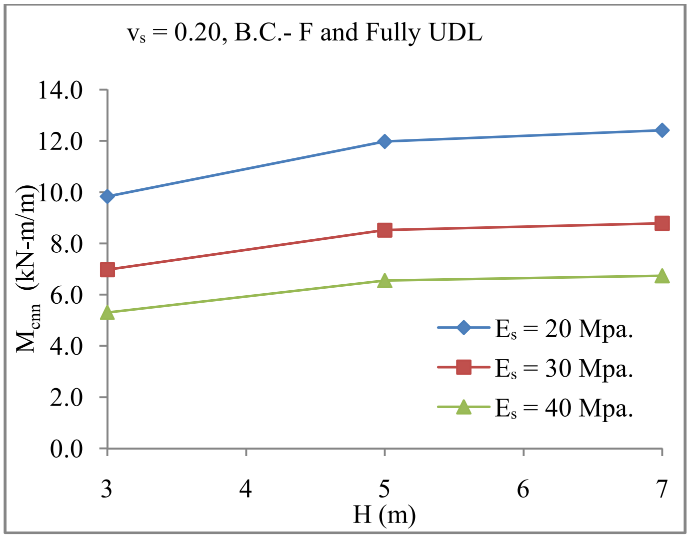

Fig. 5.16 Central radial B.M. vs sub-soil depth

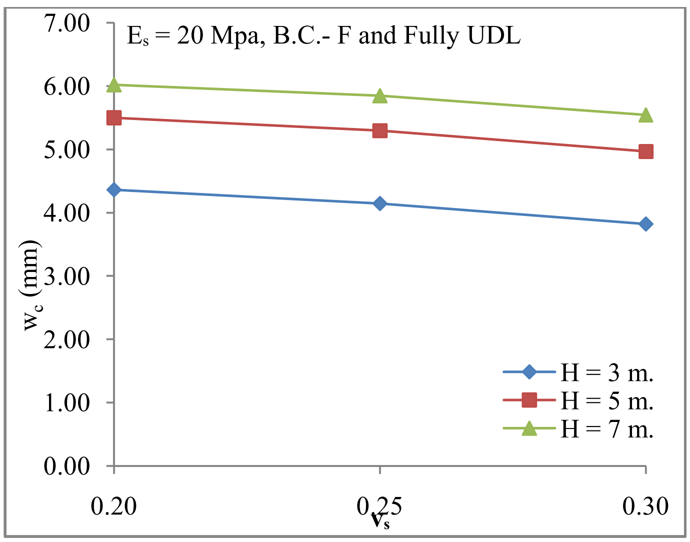

Fig. 5.17 Central deflection vs sub-soil Poisson's ratio

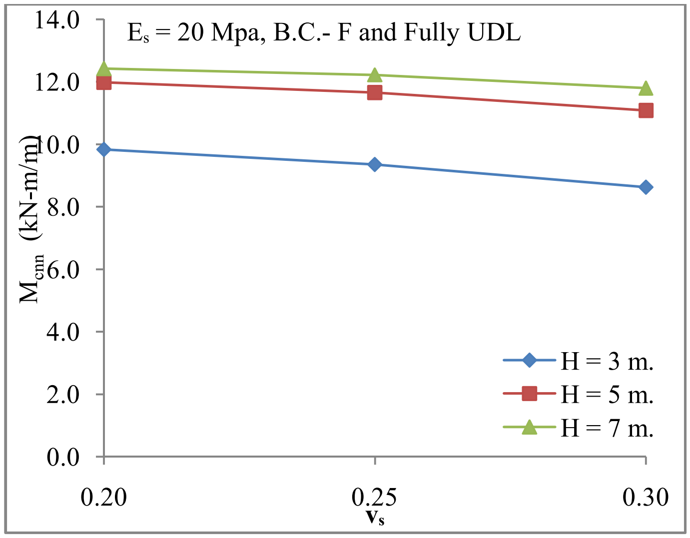

Fig. 5.18 Central radial B.M. vs sub-soil Poisson's ratio

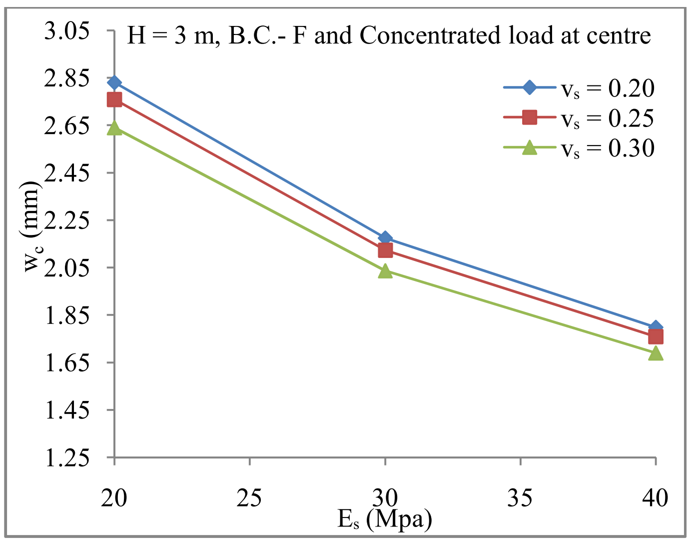

Fig. 5.19 Central deflection vs sub-soil elastic modulus

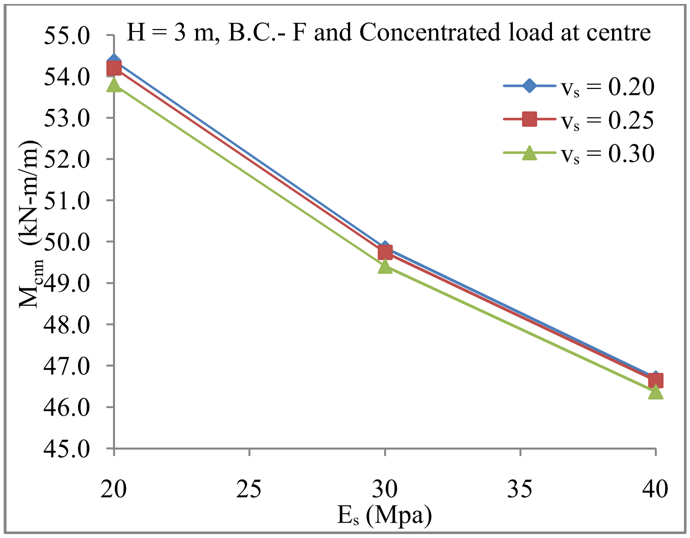

Fig. 5.20 Central radial B.M vs sub-soil elastic modulus

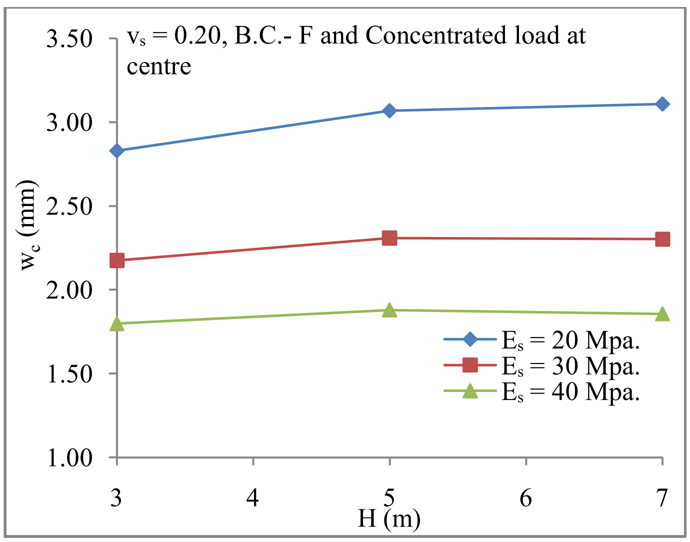

Fig. 5.21 Central deflection vs sub-soil depth

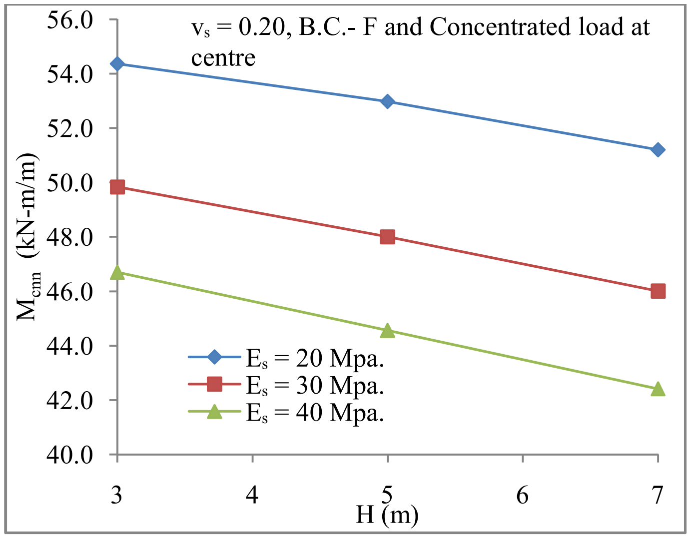

Fig. 5.22 Central radial B.M. vs sub-soil depth

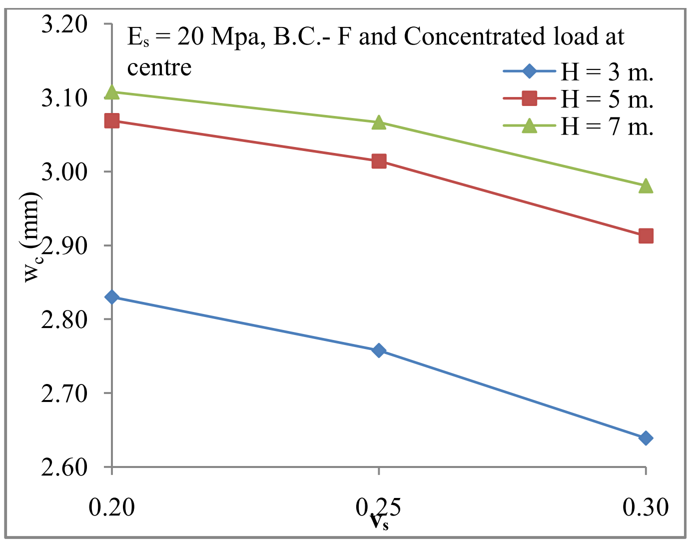

Fig. 5.23 Central deflection vs sub-soil Poisson's ratio

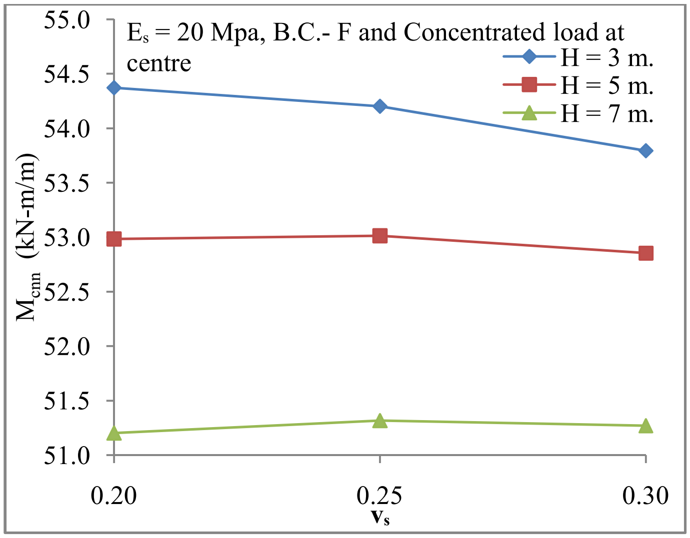

Fig. 5.24 Central radial B.M. vs sub-soil Poisson's ratio

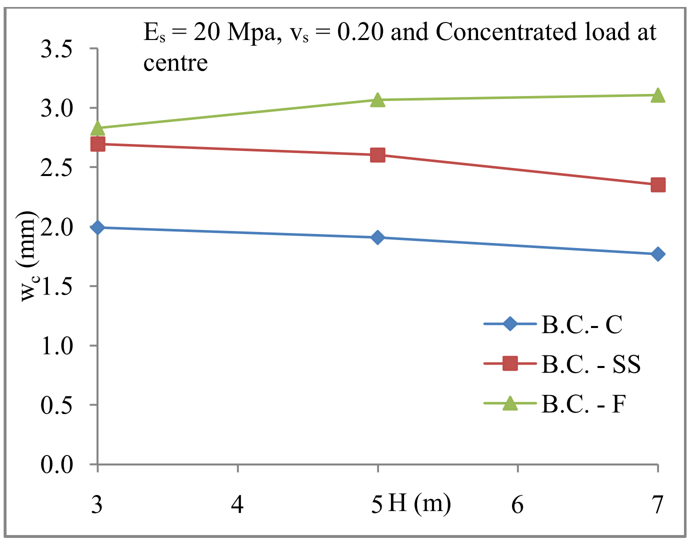

Fig. 5.25 Central deflection vs sub-soil depth

As sub-soil elastic modulus increases, for any loading conditions, the plate's central displacement and bending moment always decrease (Figures 5.13, 5.14, 5.19, and 5.20). As subsoil depth (H) increases, for uniform loading conditions, the plate's central displacement and bending moment often increase (Figures 5.15,5.16). However, the central displacement marginally increases in the case of concentrated loading at the centre. (Figure 5.21), and the bending moment of the plate decreases (Figure 5.22). It is also observed that sub-soil Poisson's ratio has a negligible effect on any loading conditions (Figures 5.17,5.18,5.23 and 5.24. Additionally, it is noted that the central bending moment and displacement drop as the edge constraints increase, indicating that an increase in edge constraints increases the plate's flexural rigidity and reduces displacement (Table 5.13 and Figures 5.25).

5.3 Thin Skew Plate Using Higher-Order FEM

The skew angle β is defined as the angle that the oblique edge of the plate makes with the horizontal, as shown in Fig. 4.5 and 4.6.

5.3.1 Validation

A mesh size of 20 × 20 nodes is applied throughout the article following the convergence study for a fair result. In this section, we begin with similarities to other researchers' studies. The present element allows static analyses of skew and rectangular plates under various loads and boundary conditions, including free-free.

According to the authors, no published works have examined skew plates supported by elastic foundations using the modified Vlasov model. The findings of the static analysis of the plate on the Vlasov foundation have been compared with rectangular results in the literature by setting a skew angle, $\beta = 90°$, because there is a lack of reliable data. The deflection and moment numbers indicate that the present results are surprisingly accurate.

A skew plate on Pasternak foundations is considered to validate the present formulation for a plate on a two-parameter elastic foundation.

An illustration from the study by (Özgan and Daloğlu, 2008) has been used to show the validity of the formulation in the context of a thin plate. The plate-soil system has the following characteristics.

The subsoil's modulus of elasticity is 68950 kN/m², and its Poisson ratio is 0.25. The plate's modulus of elasticity is 20685 MN/m², and its Poisson ratio is 0.20. The plate's thickness is 0.1524 m; thus, L/h = 60 is the thin plate limit. (L × B) 9.144 × 12.192 m. The plate's uniform load is 23.94 kN/m^2, and its concentrated load is 133.34 kN. All edge-free plates are analyzed at two soil levels, H = 3.048 and 6.096 m. The convergence study divides the plate into 20 × 24 pieces. Tables 5.14 and 5.15 show the uniformly distributed and concentrated load results.

Table 5.14

Maximum displacements (w) and Maximum moments (Mx) for a free plate with a uniformly distributed load

H (m)	Ref.	K kN/m³)	2t (kN/m)	γ	w (mm)	M_x (kN-m/m)
3.048	(Vallabhan et al., 1991)**	27206	26904	0.5724	0.872	0.0529
	(Celik and Saygun, 1999b)**	27192	26826	0.5766	0.853	0.0445
	(Özgan and Daloğlu, 2008)	27208	26841	0.5750	0.876	0.0465
	PS	27212	26800	0.5857	0.872	0.0606
6.096	(Vallabhan et al., 1991)**	13757	50282	0.9297	1.524	0.3113
	(Celik and Saygun, 1999b)**	13757	50410	0.9194	1.526	0.2880
	(Özgan and Daloğlu, 2008)	13744	50615	0.9010	1.541	0.2546
	PS	13744	50609	0.9012	1.521	0.3040

Table 5.15

Maximum displacements (w) and Maximum moments (M_x) for a free plate with a concentrated load at mid-point

H (m)	Ref.	K (kN/m³)	2t (kN/m)	γ	w (mm)	M_x (kN-m/m)
3.048	(Vallabhan et al., 1991)**	31610	19130	1.9018	0.480	12.5440
	(Celik and Saygun, 1999b)**	31898	18912	1.9478	0.818	15.0470
	(Özgan and Daloğlu, 2008)	31732	19050	1.9250	0.822	5.5600
	PS	32885	18158	2.0769	0.814	11.8480
6.096	(Vallabhan et al., 1991)**	23918	23918	3.4737	0.975	12.5440
	(Celik and Saygun, 1999b)**	24256	23596	3.5249	0.845	14.563
	(Özgan and Daloğlu, 2008)	23774	24089	3.4480	0.850	5.4460
	PS	26201	21814	3.8295	0.841	11.6170

** Taken from (Özgan and Daloğlu, 2008)

It is observed that displacements and bending moments from tables 5.14 and 5.15 results are in excellent agreement with the results given in (Özgan and Daloğlu, 2008; Celik and Saygun, 1999b; Vallabhan et al., 1991) for any loading cases regardless of the subsoil depth.

A skew plate on the Pasternak foundation is considered to validate the present formulation for different boundary conditions under uniformly distributed load. Properties of plate is, 2a = 1 m, 2b = 1.5 m, h = 0.01 m, $\upsilon = 0.3$, $\beta = 75°$, $K = 10^6$ Pa/m, $2t = 10^5$ N/m, $q = 10^4$ Pa, E = 70 Gpa. The results listed in Table 5.16 have been compared with (Joodaky and Joodaky, 2015) show good agreement.

Table 5.16

Comparison of central displacement of the skew plate different boundary conditions with uniformly distributed load

Reference	CCCC	SSSS	SCSC	CFCF
PS	0.001919	0.003808	0.003263	0.002151
(Joodaky and Joodaky, 2015)	0.001881	0.003734	0.003179	0.002172
Difference (%)	2.02	1.98	2.64	0.97

A skewed plate (a/b = 1) without foundation is considered for testing the present formulation for a concentrated load case. The results in Table 5.17, compared with those of (Sengupta, 1995) and (Butalia et al., 1990), show good agreement.

Table 5.17

Non-dimensional central displacement and maximum and minimum non-dimensional central bending moment of the plate with a concentrated load at the centre

β	References	B.C.	w_c	M_{cmax}	M_{cmin}
60°	PS	CCCC	1.7276	3.2171	2.9191
	(Sengupta, 1995)		1.7442	2.9334	2.4226
	(Butalia et al., 1990)		1.7030	3.1076	2.4052
45°	PS		1.1896	3.1186	2.6497
	(Sengupta, 1995)		1.2031	2.8234	2.3174
	(Butalia et al., 1990)		1.1481	2.8969	1.9720
30°	PS		0.6174	2.8475	2.1717
	(Sengupta, 1995)		0.6282	2.5981	2.1130
	(Butalia et al., 1990)		0.5635	2.5044	1.4437
60°	PS	SSSS	3.6035	3.7932	3.4234
	(Sengupta, 1995)		3.6442	3.4862	2.9637
	(Butalia et al., 1990)		3.5216	3.6722	2.8920
45°	PS		2.5229	3.7225	3.1438

	(Sengupta, 1995)		2.5685	3.4082	2.8579
	(Butalia et al., 1990)		2.3088	3.4467	2.3850
30°	PS		1.3269	3.4692	2.6368
	(Sengupta, 1995)		1.3777	3.2360	2.6293
	(Butalia et al., 1990)		1.0729	2.9839	1.7420

5.3.2 Parametric study

Plate-soil system features include. The modulus of elasticity of the subsoil was 68.95 MN/m², 103.425 MN/m², and 137.9 MN/m²; the Poisson's ratio of the subsoil was v_s = 0.2, 0.25, and 0.3; the depth of the soil stratum was H = 3.048 m, 6.096 m, and 9.144 m; the plate's modulus of elasticity is 20685 MN/m² Thin plate limit is L/h = 60, where h is the plate thickness, L is the shorter dimension. The plate dimensions are (L × B) 9.144 × 12.192 m, and the skew angle is 60°, 45°, and 30° with varied boundary conditions. The plate's uniform load is 23.94 kN/m², and its concentrated load is 133.34 kN. Tables 5.18-5.23 and Figures 5.26-5.41 show parametric study results.

Table 5.18

Central displacement and maximum and minimum central bending moment of the plate (β = 60°) with the uniformly distributed load.

Es (Mpa)	v_s	H (m)	B.C. - CCCC			B.C. - SSSS			B.C. - FFFF		
			w_c (mm)	M_{cmax} (kN-m/m)	M_{cmin} (kN-m/m)	w_c (mm)	M_{cmax} (kN-m/m)	M_{cmin} (kN-m/m)	w_c (mm)	M_{cmax} (kN-m/m)	M_{cmin} (kN-m/m)
68.950	0.30	3.048	0.7540	0.2612	0.0727	0.7608	0.1740	0.0476	0.7756	0.0903	0.0263
		6.096	1.0976	0.8022	0.3309	1.1256	0.7511	0.3126	1.3268	0.3813	0.1732
		9.144	1.0985	0.9141	0.4136	1.1218	0.8950	0.4074	1.6105	0.4819	0.2512
103.425		3.048	0.5017	0.1463	0.0425	0.5047	0.1080	0.0313	0.5160	0.0571	0.0175
		6.096	0.7405	0.5108	0.2122	0.7539	0.4870	0.2035	0.8857	0.2491	0.1135
		9.144	0.7444	0.5970	0.2715	0.7556	0.5881	0.2686	1.0772	0.3177	0.1658
137.900		3.048	0.3759	0.1008	0.0300	0.3776	0.0789	0.0235	0.3866	0.0421	0.0132
		6.096	0.5592	0.3735	0.1557	0.5671	0.3595	0.1506	0.6648	0.1847	0.0843

		9.144	0.5636	0.4426	0.2019	0.5702	0.4374	0.2001	0.8096	0.2368	0.1237
68.950	0.25	3.048	0.8306	0.3338	0.0988	0.8405	0.2358	0.0693	0.8639	0.1227	0.0384
		6.096	1.1586	0.8784	0.3692	1.1891	0.8299	0.3519	1.4410	0.4249	0.1987
		9.144	1.1272	0.9535	0.4357	1.1506	0.9366	0.4304	1.7181	0.5089	0.2707
103.425		3.048	0.5533	0.1900	0.0581	0.5578	0.1461	0.0447	0.5748	0.0775	0.0251
		6.096	0.7827	0.5618	0.2377	0.7973	0.5392	0.2295	0.9623	0.2780	0.1303
		9.144	0.7645	0.6241	0.2866	0.7757	0.6162	0.2841	1.1497	0.3358	0.1789
137.900		3.048	0.4148	0.1315	0.0410	0.4174	0.1063	0.0332	0.4307	0.0569	0.0188
		6.096	0.5915	0.4117	0.1748	0.6001	0.3985	0.1700	0.7225	0.2064	0.0969
		9.144	0.5790	0.4632	0.2134	0.5857	0.4586	0.2119	0.8642	0.2504	0.1335
68.950	0.20	3.048	0.8824	0.3888	0.1199	0.8948	0.2852	0.0878	0.9266	0.1491	0.0489
		6.096	1.1911	0.9240	0.3934	1.2227	0.8785	0.3774	1.5149	0.4527	0.2162
		9.144	1.1353	0.9699	0.4462	1.1581	0.9547	0.4416	1.7820	0.5220	0.2817
103.425		3.048	0.5884	0.2240	0.0709	0.5940	0.1771	0.0562	0.6167	0.0944	0.0319
		6.096	0.8055	0.5929	0.2541	0.8206	0.5717	0.2464	1.0120	0.2966	0.1419
		9.144	0.7703	0.6358	0.2940	0.7813	0.6287	0.2918	1.1928	0.3447	0.1863
137.900		3.048	0.4413	0.1557	0.0501	0.4445	0.1286	0.0415	0.4621	0.0692	0.0237
		6.096	0.6090	0.4353	0.1872	0.6180	0.4229	0.1827	0.7600	0.2203	0.1056
		9.144	0.5835	0.4723	0.2190	0.5901	0.4682	0.2177	0.8968	0.2571	0.1391

Table 5.19

Central displacement and maximum and minimum central bending moment of the plate (β = 45°) with the uniformly distributed load.

Es (Mpa)	v_s	H (m)	B.C. - CCCC			B.C. - SSSS			B.C. - FFFF		
			w_c (mm)	M_{cmax} (kN-m/m)	M_{cmin} (kN-m/m)	w_c (mm)	M_{cmax} (kN-m/m)	M_{cmin} (kN-m/m)	w_c (mm)	M_{cmax} (kN-m/m)	M_{cmin} (kN-m/m)
68.950	0.30	3.048	0.7119	0.6487	0.1702	0.7329	0.4264	0.1102	0.7619	0.2197	0.0600
		6.096	0.9226	1.1960	0.4173	0.9712	1.0983	0.3884	1.2281	0.5645	0.2196
		9.144	0.8669	1.1875	0.4485	0.9030	1.1534	0.4399	1.4353	0.6311	0.2777
103.425		3.048	0.4764	0.3607	0.0958	0.4859	0.2551	0.0675	0.5068	0.1354	0.0379
		6.096	0.6284	0.7595	0.2669	0.6519	0.7126	0.2528	0.8205	0.3688	0.1439
		9.144	0.5925	0.7747	0.2945	0.6100	0.7587	0.2903	0.9614	0.4160	0.1835
137.900		3.048	0.3578	0.2428	0.0653	0.3633	0.1813	0.0488	0.3796	0.0978	0.0278
		6.096	0.4769	0.5539	0.1955	0.4910	0.5262	0.1870	0.6162	0.2734	0.1069
		9.144	0.4507	0.5739	0.2189	0.4612	0.5646	0.2164	0.7231	0.3099	0.1369
68.950	0.25	3.048	0.7745	0.7607	0.2070	0.8015	0.5233	0.1412	0.8442	0.2719	0.0781
		6.096	0.9627	1.2746	0.4512	1.0145	1.1824	0.4243	1.3242	0.6119	0.2443
		9.144	0.8834	1.2217	0.4650	0.9194	1.1911	0.4577	1.5212	0.6556	0.2936
103.425		3.048	0.5195	0.4305	0.1183	0.5318	0.3164	0.0869	0.5618	0.1692	0.0495
		6.096	0.6568	0.8131	0.2899	0.6819	0.7689	0.2767	0.8852	0.4005	0.1603
		9.144	0.6043	0.7986	0.3060	0.6218	0.7844	0.3024	1.0195	0.4325	0.1942
137.900		3.048	0.3907	0.2925	0.0813	0.3977	0.2256	0.0628	0.4209	0.1225	0.0362
		6.096	0.4989	0.5945	0.2129	0.5140	0.5684	0.2050	0.6650	0.2972	0.1192
		9.144	0.4599	0.5923	0.2278	0.4704	0.5840	0.2256	0.7671	0.3223	0.1450

68.950	0.20	3.048	0.8149	0.8371	0.2336	0.8462	0.5942	0.1651	0.9017	0.3112	0.0926
		6.096	0.9821	1.3162	0.4707	1.0351	1.2297	0.4458	1.3846	0.6395	0.2601
		9.144	0.8863	1.2318	0.4714	0.9213	1.2039	0.4650	1.5703	0.6647	0.3014
103.425		3.048	0.5475	0.4796	0.1350	0.5618	0.3620	0.1020	0.6002	0.1950	0.0589
		6.096	0.6707	0.8424	0.3034	0.6964	0.8010	0.2912	0.9259	0.4191	0.1709
		9.144	0.6065	0.8064	0.3106	0.6235	0.7935	0.3075	1.0528	0.4387	0.1995
137.900		3.048	0.4120	0.3282	0.0933	0.4203	0.2588	0.0738	0.4497	0.1416	0.0432
		6.096	0.5098	0.6170	0.2232	0.5252	0.5927	0.2159	0.6958	0.3113	0.1271
		9.144	0.4617	0.5986	0.2314	0.4719	0.5911	0.2295	0.7923	0.3271	0.1490

Table 5.20

Central displacement and maximum and minimum central bending moment of the plate (β = 30°) with the uniformly distributed load.

Es (Mpa)	v_s	H (m)	B.C. - CCCC			B.C. - SSSS			B.C. - FFFF		
			w_c (mm)	M_{cmax} (kN-m/m)	M_{cmin} (kN-m/m)	w_c (mm)	M_{cmax} (kN-m/m)	M_{cmin} (kN-m/m)	w_c (mm)	M_{cmax} (kN-m/m)	M_{cmin} (kN-m/m)
68.950	0.30	3.048	0.5674	1.7986	0.4296	0.6413	1.2459	0.2946	0.7143	0.6314	0.1577
		6.096	0.6131	2.0167	0.5571	0.7093	1.8082	0.5128	1.0359	0.9295	0.3006
		9.144	0.5346	1.7147	0.4980	0.5994	1.6365	0.4863	1.1372	0.8904	0.3184
103.425		3.048	0.3928	1.0853	0.2558	0.4278	0.7551	0.1774	0.4763	0.3964	0.0989
		6.096	0.4308	1.3012	0.3609	0.4795	1.1838	0.3350	0.6933	0.6115	0.1979
		9.144	0.3747	1.1233	0.3288	0.4071	1.0825	0.3219	0.7632	0.5882	0.2113
137.900		3.048	0.2999	0.7477	0.1759	0.3205	0.5310	0.1249	0.3571	0.2857	0.0715
		6.096	0.3324	0.9502	0.2647	0.3623	0.8762	0.2480	0.5212	0.4542	0.1473
		9.144	0.2889	0.8315	0.2447	0.3087	0.8070	0.2403	0.5750	0.4383	0.1580

68.950	0.25	3.048	0.6017	1.9490	0.4725	0.6869	1.3873	0.3343	0.7831	0.7114	0.1834
		6.096	0.6309	2.0912	0.5818	0.7316	1.8923	0.5410	1.1041	0.9736	0.3216
		9.144	0.5426	1.7470	0.5094	0.6076	1.6731	0.4991	1.1924	0.9053	0.3283
103.425		3.048	0.4181	1.1887	0.2844	0.4589	0.8489	0.2031	0.5224	0.4508	0.1160
		6.096	0.4441	1.3541	0.3783	0.4951	1.2416	0.3542	0.7393	0.6415	0.2120
		9.144	0.3806	1.1462	0.3369	0.4131	1.1078	0.3308	0.8009	0.5983	0.2180
137.900		3.048	0.3199	0.8250	0.1970	0.3440	0.6005	0.1437	0.3918	0.3267	0.0843
		6.096	0.3430	0.9910	0.2782	0.3744	0.9202	0.2625	0.5560	0.4769	0.1580
		9.144	0.2936	0.8493	0.2510	0.3135	0.8263	0.2470	0.6036	0.4460	0.1632
68.950	0.20	3.048	0.6216	2.0370	0.4986	0.7141	1.4765	0.3604	0.8296	0.7649	0.2018
		6.096	0.6384	2.1229	0.5934	0.7405	1.9329	0.5555	1.1444	0.9935	0.3332
		9.144	0.5439	1.7530	0.5125	0.6078	1.6826	0.5032	1.2212	0.9042	0.3311
103.425		3.048	0.4329	1.2505	0.3022	0.4775	0.9092	0.2202	0.5536	0.4877	0.1284
		6.096	0.4498	1.3776	0.3868	0.5016	1.2701	0.3642	0.7666	0.6551	0.2199
		9.144	0.3816	1.1511	0.3393	0.4135	1.1148	0.3337	0.8206	0.5977	0.2201
137.900		3.048	0.3317	0.8720	0.2103	0.3581	0.6457	0.1563	0.4153	0.3548	0.0936
		6.096	0.3476	1.0097	0.2849	0.3795	0.9420	0.2702	0.5767	0.4873	0.1640
		9.144	0.2944	0.8535	0.2530	0.3139	0.8318	0.2493	0.6187	0.4456	0.1648

Table 5.21

Central displacement and maximum and minimum central bending moment of the plate (β = 60°) with a central concentrated load

Es (Mpa)	v_s	H (m)	B.C. - CCCC			B.C. - SSSS			B.C. - FFFF		
			w_c (mm)	M_{cmax} (kN-m/m)	M_{cmin} (kN-m/m)	w_c (mm)	M_{cmax} (kN-m/m)	M_{cmin} (kN-m/m)	w_c (mm)	M_{cmax} (kN-m/m)	M_{cmin} (kN-m/m)
68.950	0.30	3.048	0.7803	22.4682	18.8159	0.7804	22.4669	18.8149	0.7804	22.4673	18.8152
		6.096	0.7488	19.3219	15.9283	0.7491	19.2961	15.9063	0.7482	19.1510	15.7789
		9.144	0.6391	16.7981	13.6189	0.6396	16.7755	13.5995	0.6405	16.3410	13.2190
103.425		3.048	0.5968	20.4389	16.8623	0.5968	20.4386	16.8620	0.5968	20.4388	16.8622
		6.096	0.5560	16.9238	13.7110	0.5560	16.9058	13.6955	0.5544	16.7707	13.5775
		9.144	0.4648	14.3203	11.3887	0.4649	14.3044	11.3752	0.4622	13.8790	11.0081
137.900		3.048	0.4913	19.0028	15.4966	0.4913	19.0027	15.4965	0.4913	19.0027	15.4965
		6.096	0.4482	15.2617	12.2036	0.4481	15.2478	12.1917	0.4464	15.1208	12.0819
		9.144	0.3689	12.6379	9.9084	0.3689	12.6255	9.8980	0.3651	12.2108	9.5455
68.950	0.25	3.048	0.8069	22.6032	18.9533	0.8070	22.6008	18.9515	0.8070	22.6011	18.9517
		6.096	0.7632	19.3063	15.9170	0.7636	19.2759	15.8909	0.7620	19.0784	15.7165
		9.144	0.6445	16.7418	13.5690	0.6450	16.7169	13.5475	0.6442	16.1707	13.0674
103.425		3.048	0.6161	20.5755	16.9996	0.6161	20.5749	16.9991	0.6161	20.5750	16.9992
		6.096	0.5662	16.9041	13.6970	0.5662	16.8827	13.6786	0.5638	16.6979	13.5166
		9.144	0.4686	14.2658	11.3420	0.4687	14.2483	11.3270	0.4641	13.7126	10.8640
137.900		3.048	0.5068	19.1434	15.6359	0.5068	19.1432	15.6358	0.5068	19.1432	15.6358
		6.096	0.4562	15.2419	12.1900	0.4561	15.2253	12.1757	0.4537	15.0510	12.0246
		9.144	0.3719	12.5864	9.8655	0.3719	12.5728	9.8540	0.3661	12.0506	9.4096

68.950	0.20	3.048	0.8213	22.6520	19.0051	0.8214	22.6486	19.0025	0.8214	22.6487	19.0026
		6.096	0.7682	19.2367	15.8542	0.7684	19.2030	15.8251	0.7660	18.9569	15.6069
		9.144	0.6434	16.6422	13.4792	0.6438	16.6158	13.4564	0.6410	15.9707	12.8882
103.425		3.048	0.6263	20.6270	17.0534	0.6264	20.6261	17.0526	0.6264	20.6261	17.0527
		6.096	0.5695	16.8340	13.6356	0.5694	16.8101	13.6149	0.5662	16.5792	13.4120
		9.144	0.4676	14.1712	11.2592	0.4677	14.1523	11.2430	0.4611	13.5195	10.6956
137.900		3.048	0.5148	19.1991	15.6929	0.5148	19.1988	15.6927	0.5148	19.1989	15.6927
		6.096	0.4587	15.1739	12.1317	0.4585	15.1552	12.1156	0.4553	14.9372	11.9263
		9.144	0.3711	12.4969	9.7888	0.3710	12.4824	9.7765	0.3634	11.8658	9.2518

Table 5.22

Central displacement and maximum and minimum central bending moment of the plate (β = 45°) with a central concentrated load.

Es (Mpa)	v_s	H (m)	B.C. - CCCC			B.C. - SSSS			B.C. - FFFF		
			w_c (mm)	M_{cmax} (kN-m/m)	M_{cmin} (kN-m/m)	w_c (mm)	M_{cmax} (kN-m/m)	M_{cmin} (kN-m/m)	w_c (mm)	M_{cmax} (kN-m/m)	M_{cmin} (kN-m/m)
68.950	0.30	3.048	0.7652	23.7460	17.6574	0.7658	23.7312	17.6493	0.7658	23.7314	17.6495
		6.096	0.7451	20.9375	15.2378	0.7470	20.8642	15.1842	0.7472	20.5630	14.9463
		9.144	0.6353	18.5434	13.1774	0.6369	18.4833	13.1321	0.6394	17.7456	12.5448
103.425		3.048	0.5835	21.7807	15.8256	0.5837	21.7761	15.8228	0.5836	21.7765	15.8231
		6.096	0.5561	18.5880	13.1868	0.5565	18.5357	13.1474	0.5547	18.2547	12.9258
		9.144	0.4657	16.0866	11.1168	0.4661	16.0435	11.0842	0.4624	15.3138	10.5147
137.900		3.048	0.4792	20.3930	14.5549	0.4793	20.3914	14.5539	0.4793	20.3917	14.5542
		6.096	0.4498	16.9547	11.8000	0.4499	16.9134	11.7687	0.4474	16.6472	11.5615
		9.144	0.3717	14.4022	9.7502	0.3717	14.3682	9.7247	0.3659	13.6492	9.1753

		3.048	0.7909	23.8974	17.8076	0.7919	23.8777	17.7966	0.7919	23.8766	17.7960
68.950		6.096	0.7604	20.9762	15.2750	0.7624	20.8933	15.2135	0.7618	20.5076	14.9053
		9.144	0.6425	18.5460	13.1808	0.6439	18.4805	13.1309	0.6435	17.5837	12.4122
		3.048	0.6023	21.9314	15.9730	0.6025	21.9249	15.9690	0.6025	21.9250	15.9691
103.425	0.25	6.096	0.5676	18.6223	13.2209	0.5679	18.5625	13.1753	0.5649	18.2008	12.8879
		9.144	0.4712	16.0898	11.1214	0.4715	16.0425	11.0854	0.4647	15.1541	10.3892
		3.048	0.4942	20.5465	14.7019	0.4943	20.5441	14.7004	0.4943	20.5443	14.7005
137.900		6.096	0.4591	16.9882	11.8332	0.4590	16.9407	11.7970	0.4554	16.5975	11.5281
		9.144	0.3761	14.4067	9.7560	0.3761	14.3694	9.7279	0.3673	13.4935	9.0566
		3.048	0.8047	23.9610	17.8726	0.8059	23.9378	17.8594	0.8060	23.9354	17.8579
68.950		6.096	0.7664	20.9518	15.2553	0.7683	20.8621	15.1879	0.7666	20.4023	14.8177
		9.144	0.6432	18.4944	13.1376	0.6444	18.4252	13.0845	0.6406	17.3912	12.2523
		3.048	0.6121	21.9959	16.0378	0.6124	21.9879	16.0329	0.6124	21.9876	16.0327
103.425	0.20	6.096	0.5719	18.5970	13.2020	0.5722	18.5318	13.1520	0.5679	18.0991	12.8065
		9.144	0.4718	16.0413	11.0828	0.4719	15.9912	11.0445	0.4620	14.9663	10.2396
		3.048	0.5019	20.6138	14.7679	0.5020	20.6107	14.7660	0.5020	20.6109	14.7661
137.900		6.096	0.4626	16.9641	11.8163	0.4624	16.9122	11.7766	0.4577	16.5015	11.4536
		9.144	0.3766	14.3616	9.7214	0.3765	14.3221	9.6916	0.3649	13.3117	8.9164

Table 5.23

Central displacement and maximum and minimum central bending moment of the plate (β = 30°) with a central concentrated load

Es (Mpa)	v_s	H (m)	B.C. - CCCC			B.C. - SSSS			B.C. - FFFF		
			w_c (mm)	M_{cmax} (kN-m/m)	M_{cmin} (kN-m/m)	w_c (mm)	M_{cmax} (kN-m/m)	M_{cmin} (kN-m/m)	w_c (mm)	M_{cmax} (kN-m/m)	M_{cmin} (kN-m/m)
68.950	0.30	3.048	0.7085	24.3968	15.1839	0.7219	24.2490	15.1667	0.7234	24.2243	15.1642
		6.096	0.7155	22.6294	13.8226	0.7324	22.3441	13.6921	0.7430	21.6147	13.2346
		9.144	0.6194	20.6378	12.2894	0.6292	20.3911	12.1546	0.6349	18.9146	11.1606
103.425		3.048	0.5402	22.5078	13.5931	0.5447	22.4389	13.5814	0.5449	22.4340	13.5815
		6.096	0.5450	20.4279	12.1130	0.5513	20.2168	12.0016	0.5534	19.5630	11.5807
		9.144	0.4652	18.3318	10.5676	0.4685	18.1470	10.4592	0.4617	16.6960	9.4927
137.900		3.048	0.4422	21.2032	12.5009	0.4440	21.1691	12.4945	0.4440	21.1691	12.4951
		6.096	0.4459	18.9128	10.9606	0.4487	18.7437	10.8662	0.4479	18.1395	10.4778
		9.144	0.3768	16.7485	9.4218	0.3780	16.5986	9.3321	0.3670	15.1656	8.3960
68.950	0.25	3.048	0.7295	24.5796	15.3398	0.7453	24.4180	15.3212	0.7474	24.3857	15.3170
		6.096	0.7315	22.7710	13.9333	0.7495	22.4648	13.7898	0.7596	21.6080	13.2396
		9.144	0.6307	20.7573	12.3799	0.6404	20.4936	12.2332	0.6398	18.7861	11.0680
103.425		3.048	0.5563	22.6801	13.7416	0.5617	22.6025	13.7283	0.5620	22.5952	13.7279
		6.096	0.5579	20.5640	12.2194	0.5646	20.3355	12.0968	0.5657	19.5649	11.5926
		9.144	0.4744	18.4491	10.6546	0.4774	18.2508	10.5369	0.4649	16.5698	9.4069
137.900		3.048	0.4553	21.3708	12.6439	0.4575	21.3315	12.6364	0.4575	21.3308	12.6369
		6.096	0.4568	19.0462	11.0636	0.4598	18.8624	10.9596	0.4578	18.1503	10.4960
		9.144	0.3845	16.8645	9.5059	0.3856	16.7035	9.4085	0.3694	15.0428	8.3159

68.950	0.20	3.048	0.7402	24.6673	15.4147	0.7573	24.4981	15.3952	0.7599	24.4608	15.3896
		6.096	0.7389	22.8272	13.9771	0.7572	22.5076	13.8244	0.7661	21.5487	13.1982
		9.144	0.6353	20.7976	12.4104	0.6446	20.5228	12.2555	0.6378	18.6256	10.9491
103.425		3.048	0.5644	22.7622	13.8127	0.5703	22.6798	13.7985	0.5707	22.6709	13.7976
		6.096	0.5639	20.6185	12.2623	0.5706	20.3789	12.1322	0.5705	19.5156	11.5611
		9.144	0.4781	18.4898	10.6851	0.4809	18.2829	10.5612	0.4631	16.4135	9.2976
137.900		3.048	0.4618	21.4506	12.7123	0.4642	21.4085	12.7042	0.4643	21.4072	12.7046
		6.096	0.4618	19.1003	11.1059	0.4648	18.9071	10.9956	0.4618	18.1108	10.4728
		9.144	0.3878	16.9059	9.5362	0.3886	16.7378	9.4339	0.3677	14.8913	8.2143

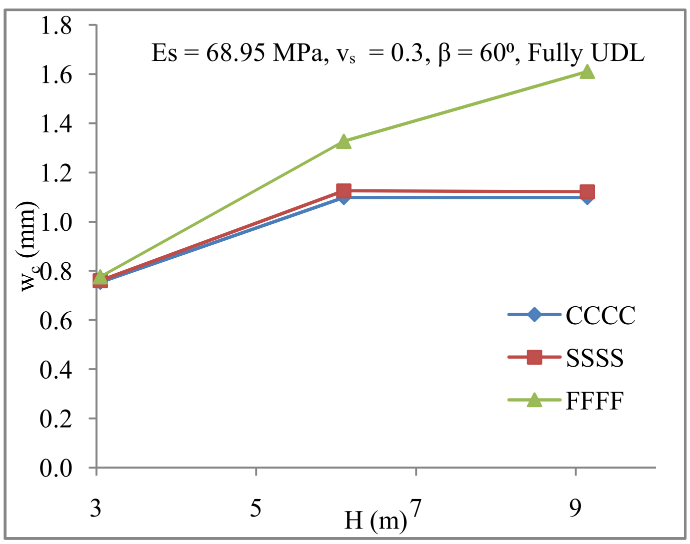

Fig. 5.26 Central deflection vs sub-soil depth

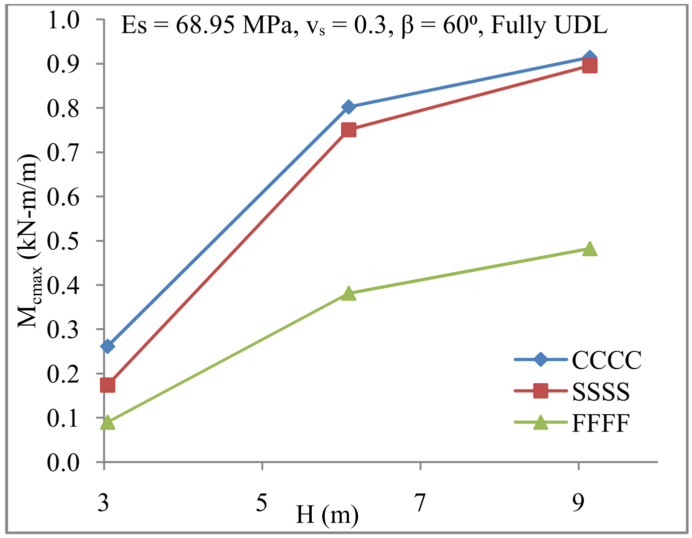

Fig. 5.27 Central maximum bending moment vs sub-soil depth

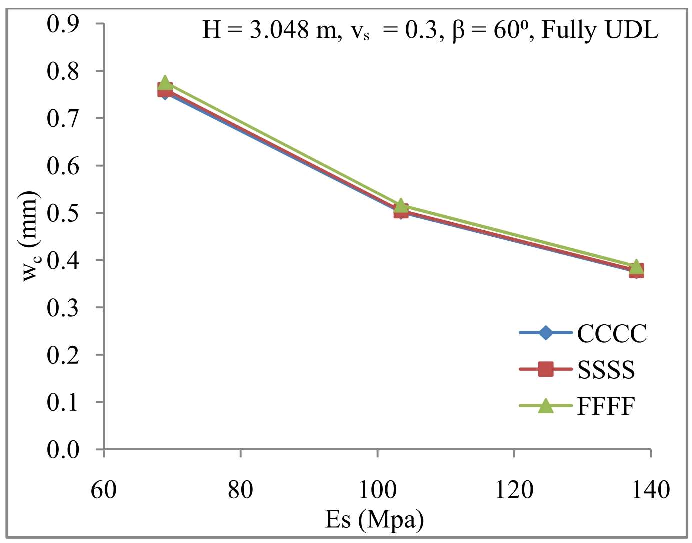

Fig. 5.28 Central deflection vs sub-soil elastic modulus

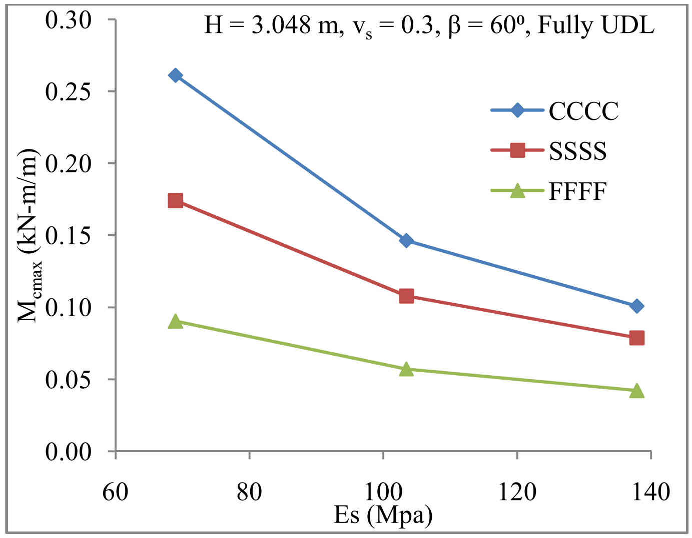

Fig. 5.29 Central maximum bending moment vs sub-soil elastic modulus

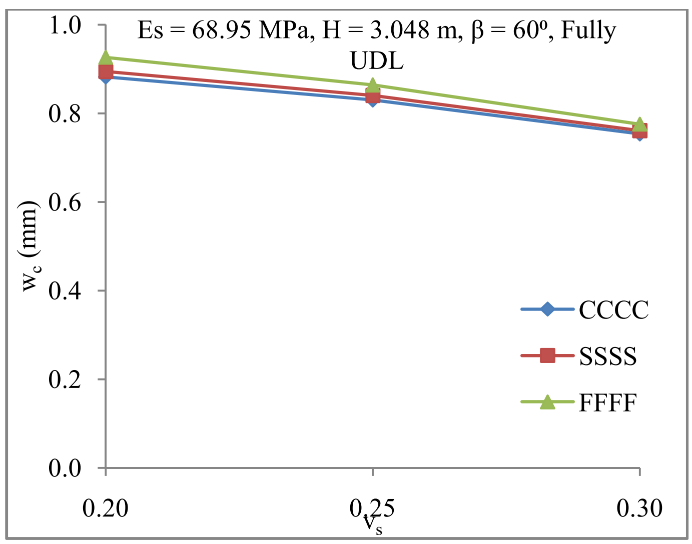

Fig. 5.30 Central deflection vs sub-soil Poisson's ratio

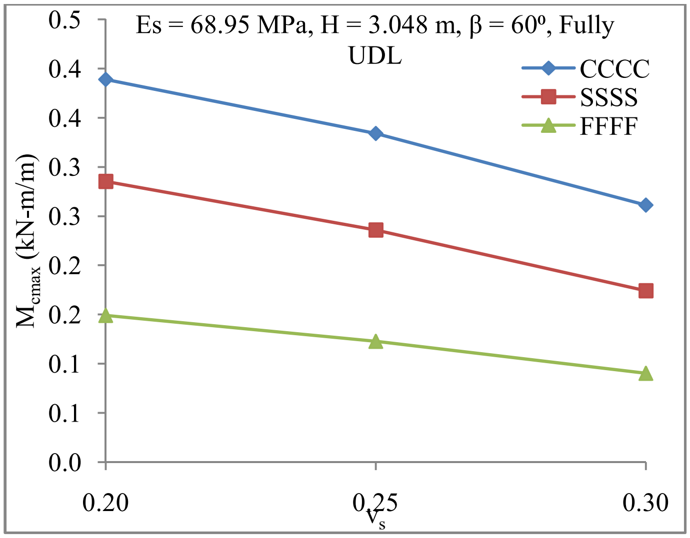

Fig. 5.31 Central maximum bending moment vs sub-soil Poisson's ratio

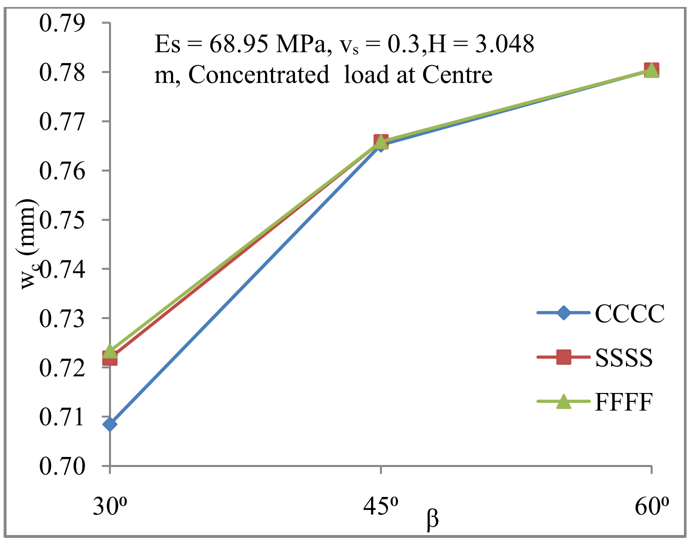

Fig. 5.32 Central deflection vs skew angle of the plate

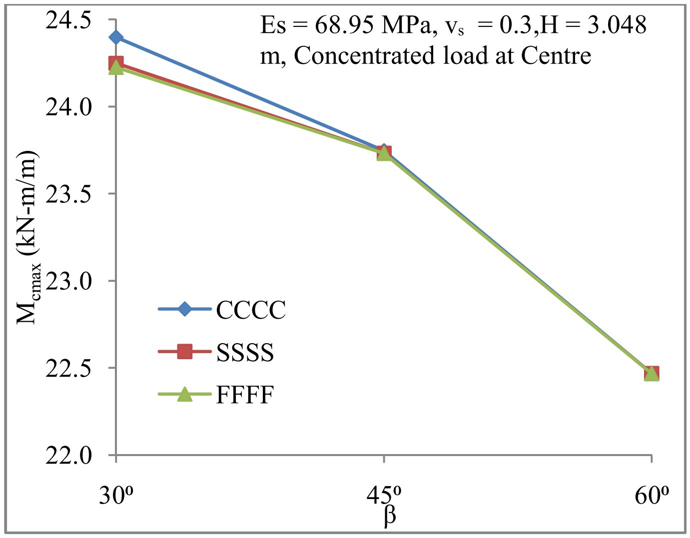

Fig. 5.33 Central maximum bending moment vs skew angle of the plate

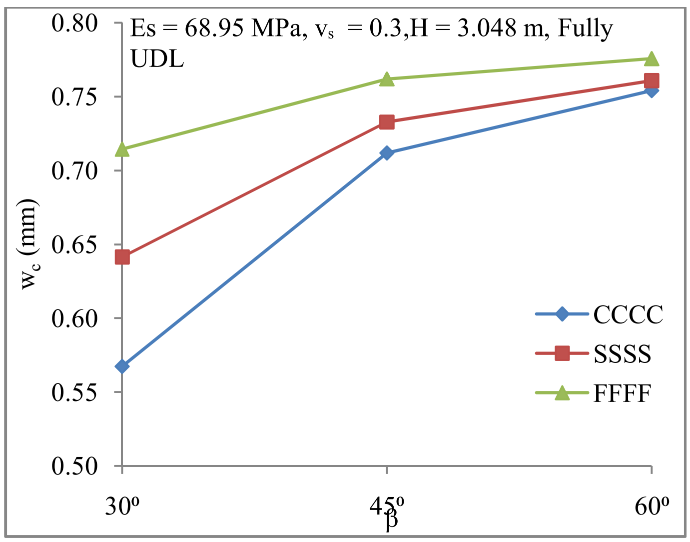

Fig. 5.34 Central deflection vs skew angle of the plate

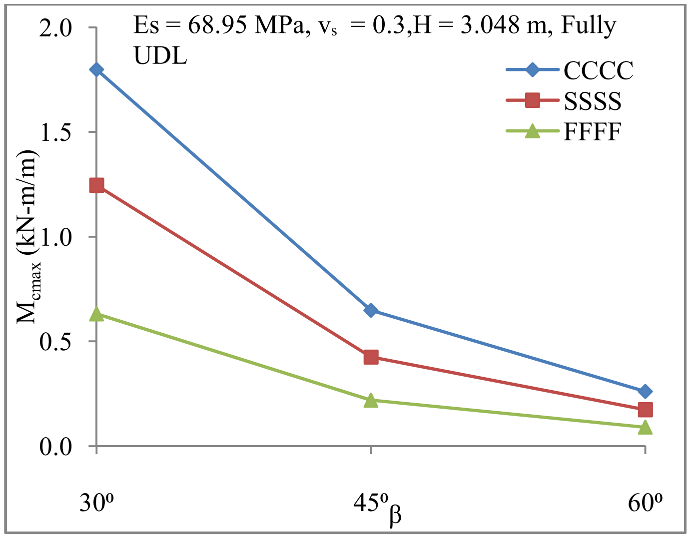

Fig. 5.35 Central maximum bending moment vs skew angle of the plate

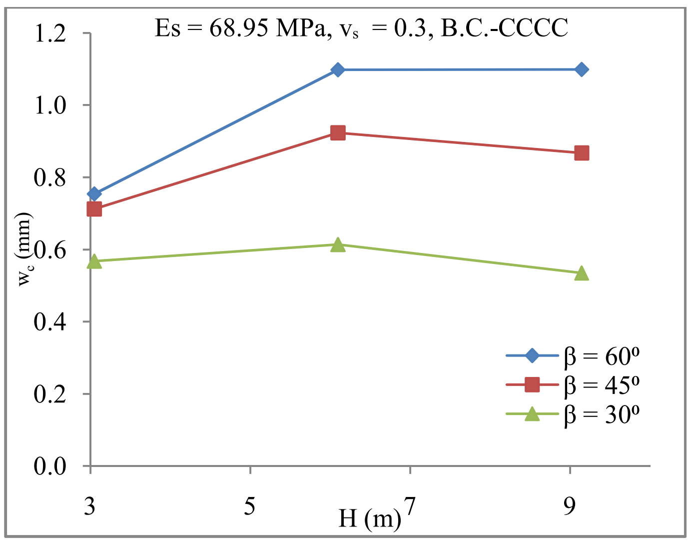

Fig. 5.36 Central deflection vs sub-soil depth

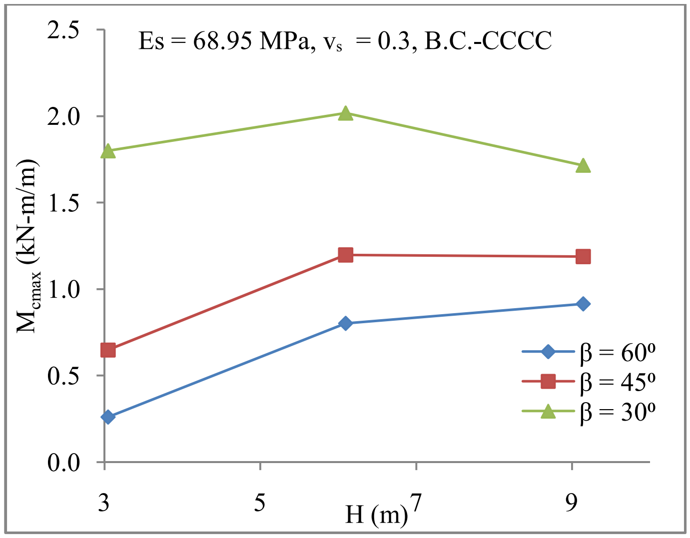

Fig. 5.37 Central maximum bending moment vs sub-soil depth

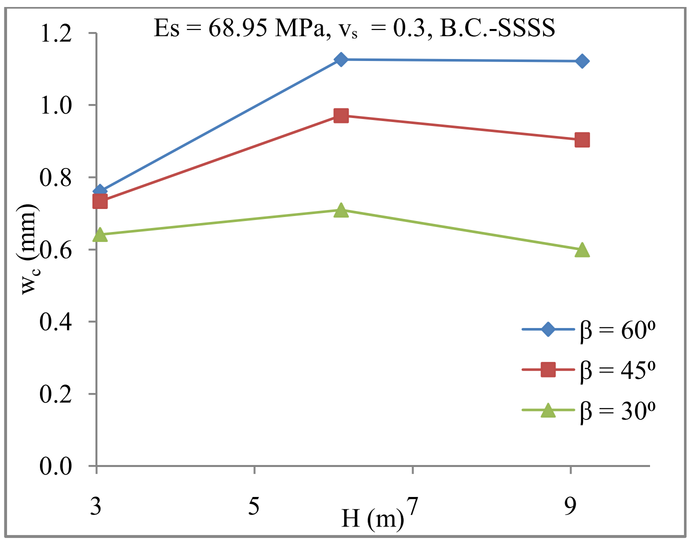

Fig. 5.38 Central deflection vs sub-soil depth

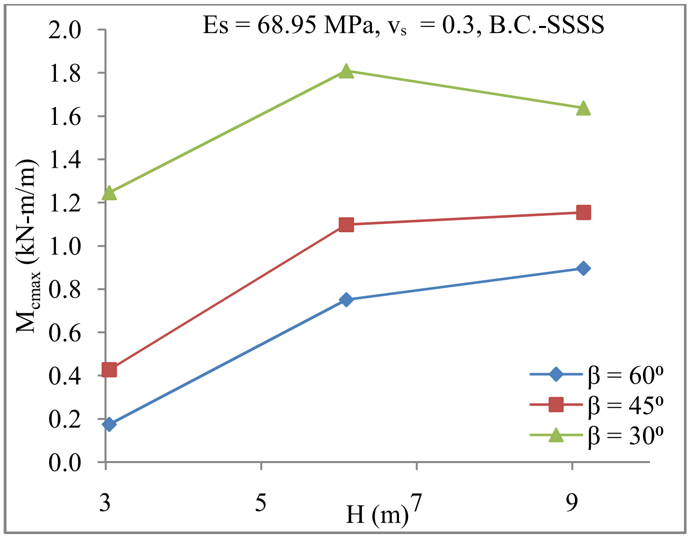

Fig. 5.39 Central maximum bending moment vs sub-soil depth

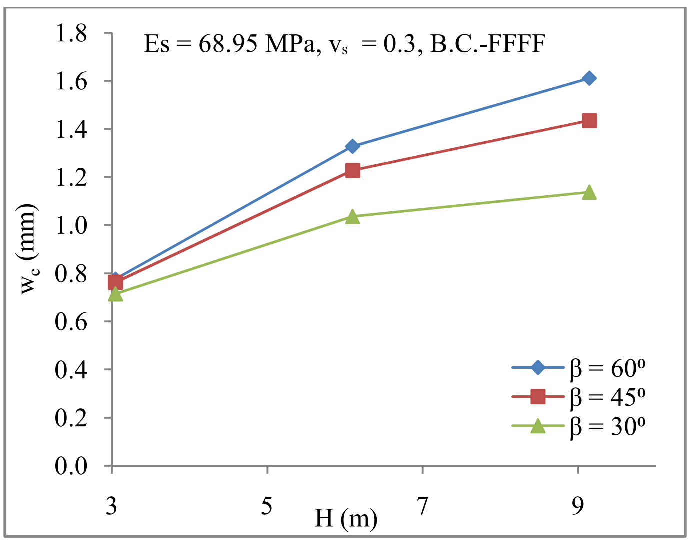

Fig. 5.40 Central deflection vs sub soil depth

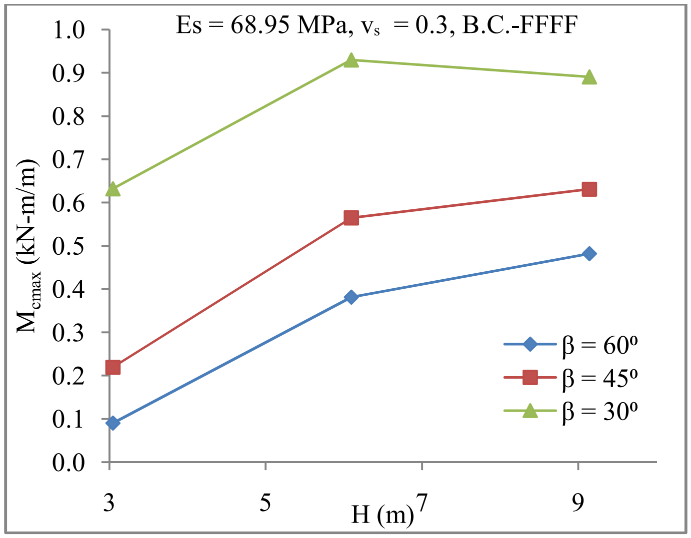

Fig. 5.41 Central maximum bending moment vs sub soil depth

As sub soil elastic modulus increases, for any loading situations, the central displacement and bending moment of the plate always decreases (Figures 5.28, 5.29 and tables 5.18 – 5.23). As subsoil depth (H) increases, for any loading condition, the central displacement and bending moment of the plate often increases (Figures 5.26, 5.27 and 5.37 - 5.41) but after certain depth, the central displacement and bending moment of the plate decreases or tends to stable. It is also observed that sub soil Poisson's ratio have negligible effect for any loading conditions (Figures 5.30, 5.31). As skew angle (β) of the plate increases, for any loading condition, the central displacement is increases (Figures 5.26, 5.27 and 5.37 - 5.41) and but central bending moment of the plate decreases (Figures 5.32 – 5.35) as the value of β increases, the curves get rather closer to each other. By decreasing the skew angle (β) edges of the plate become closer to each other so deflections and bending moment decrease with decreasing the skew angle (β). It is also observed that sub soil Poisson's ratio have negligible effect for any loading conditions (Figures 5.30, 5.31). It is also observed that the central displacement and bending moment decreases with increase of constrains on the edges this shows that higher constraints on the edges increase the flexural rigidity of the plate and hence lower displacement.

5.4 HSDT Rectangular Plate

Simply supported condition (denoted by S), $w = \theta_x = w^* = \theta_x^* = 0$ – at the boundary line parallel to the x-axis and $w = \theta_y = w^* = \theta_y^* = 0$ – at the boundary line parallel to the y-axis.

Clamped condition (denoted by C), $w = \theta_y = \theta_x = w^* = \theta_y^* = \theta_x^* = 0$. Free boundary condition (denoted by F), $w \neq 0$, $\theta_y \neq 0$, $\theta_x \neq 0$, $w^* \neq 0$, $\theta_y^* \neq 0$, $\theta_x^* \neq 0$.

(Meghre and Kadam, 2014; Meghre and Kadam, 2010) used selective integration techniques based on the Gauss-Legendre product rules of 3× 3 and 2× 2 to compute the flexure and shear contributions to the element stiffness matrix.

5.4.1 Convergence study and test the formulation

The present formulation was initially tested on a square plate without foundation. Then, for each boundary condition for the central deflections and the bending moments, a convergence study is carried out for the CCCC and SSSS plate under uniformly distributed load (UDL) and central concentrated load (PL). A mesh size of 12 × 12 is ultimately chosen for a good outcome.

5.4.2 Validation work

A square simply supported and clamped plate under a uniform distributed load without an elastic foundation is analyzed first to check whether the proposed formulation and programming are correct. The results based on the present formulation compared (Tables 5.24 and 5.25) with the results of (Kant, 1982; Kant et al., 1982) and, as seen from tables for displacements and moment values, are in excellent agreement with the results given in (Kant, 1982; Kant et al., 1982). The performance of the present formulation is impressive.

For this particular problem, the boundary condition considered as given in (Kant, 1982; Kant et al., 1982) simply supported edge, $w = \theta_x = w^* = \theta_x^* = 0$ – at the boundary line parallel to the x-axis and $w = \theta_y = w^* = \theta_y^* = 0$ – at boundary line parallel to the y-axis.

Table 5.24

Comparisons of central displacements (w_c) and maximum central moments (M_{cmax}) of plates with UDL

	CCCC						SSSS					
B/t	W_c (Kant et al., 1982)	W_c PS	Diff. (%)	M_{cmax} (Kant et al., 1982)	M_{cmax} PS	Diff. (%)	W_c (Kant et al., 1982)	W_c PS	Diff. (%)	M_{cmax} (Kant et al., 1982)	M_{cmax} PS	Diff. (%)
5	0.211	0.212	0.47	2.560	2.460	3.91	0.480	0.480	0.00	4.85	4.81	0.82
10	0.146	0.148	1.37	2.360	2.310	2.12	0.424	0.425	0.24	4.80	4.77	0.63
50	0.123	0.126	2.44	2.270	2.250	0.88	0.407	0.407	0.00	4.79	4.75	0.84
100	0.123	0.125	1.63	2.270	2.250	0.88	0.406	0.406	0.00	4.79	4.75	0.84

Table 5.25

Comparisons of central displacements (w_c) and maximum central moments (M_{cmax}) of plates with UDL

B/t	SFSF						CSCS					
	W_c			M_{cmax}			W_c			M_{cmax}		
	(Kant, 1982; Kant et al., 1982)	PS	Diff. (%)	(Kant, 1982; Kant et al., 1982)	PS	Diff. (%)	(Kant, 1982; Kant et al., 1982)	PS	Diff. (%)	(Kant, 1982; Kant et al., 1982)	PS	Diff. (%)
5	14.3	14.34	0.28	12.3	12.2	0.49	2.93	3.01	2.73	3.4	3.5	2.06
10	13.4	13.41	0.04	12.2	12.2	0.16	2.18	2.22	1.79	3.34	3.4	1.20
50	13.1	13.11	0.05	12.2	12.2	0.25	1.92	1.92	0.00	3.32	3.3	0.60
100	13.1	13.1	0.02	12.2	12.2	0.33	1.92	1.91	0.68	3.32	3.3	0.90

To validate the present formulation and demonstrate the effects of normal strain in a moderately thick plate limit scenario, an example from the. (Özgan and Daloğlu, 2008) The study has been used. The plate-soil system has the following characteristics. The plate's thickness is considered as h = 1.8288 m, i.e. L/h = 5 is the moderate thick plate limit. The modulus of elasticity of the subsoil is 68950 kN/m², the Poisson's ratio of the subsoil is 0.25, and the modulus of elasticity of the plate is 20685000 kN/m², the Poisson's ratio of the plate is equal to 0.20. The plate measures (L × B) 9.144 × 12.192 m. The PL on the plate is 133.34 kN, while the UDL is 23.94 kN/m². The calculations are done for all edges of the free plate for H = 3.048, 6.096, 9.144, and 15.240 m depths in the soil stratum. The convergence study discretizes the plate into 10×12 elements. Figures 5.42, 5.43, 5.45, and 5.46 demonstrate UDL and PL instances. Tables 5.26 and 5.27 provide results.

The displacement and moment values curves may be observed in the tables and be in excellent agreement with the findings in (Özgan and Daloğlu, 2008). As the depth of the subsoil increases, they move a little closer to one another for any loading situations; thus, the effect of normal strain is less noticeable in displacement situations. The impact of normal strain is less evident in the case of bending moments since they tend to get quite near one another and are in excellent agreement with the results provided in (Özgan and Daloğlu, 2008) for the uniformly distributed loading situation. Even Nevertheless, intense loading clearly shows the effects of normal strain.

For PL cases compared to distributed load cases, the influence of normal strain on displacement and bending moments is more significant, and the effect grows as h/L increases.

(Buczkowski and Torbacki, 2001) take into account the same example. However, the results from (Buczkowski and Torbacki, 2001; Dutta et al., 2021) are in excellent agreement with only the subsoil depth H = 15.24 m varied B/h ratio from 2 to 10^6, i.e. the thin to thick plate limit for the uniformly distributed loading case and from Table 5.27 and the displacements figure 5.44.

The effect of normal strain on the displacement and bending moments is more significant for the PL case than for the distributed load case, and the effect increases with increasing h/L.

Table 5.26

Maximum moments (Mx) and displacements (w) for a free plate under uniform load (h/L = 0.2)

H(m)	w_{max} (mm)			M_{xmax} (kN-m/m)		
	(Özgan and Daloğlu, 2008)	PS	Diff. (%)	(Özgan and Daloğlu, 2008)	PS	Diff. (%)
3.048	0.6679	0.6749	1.05	40.98	39.49	3.64
6.096	1.0308	1.0480	1.67	65.39	63.98	2.16
9.144	1.2432	1.2654	1.79	80.33	78.96	1.71
15.24	1.4566	1.4810	1.68	96.35	94.05	2.39

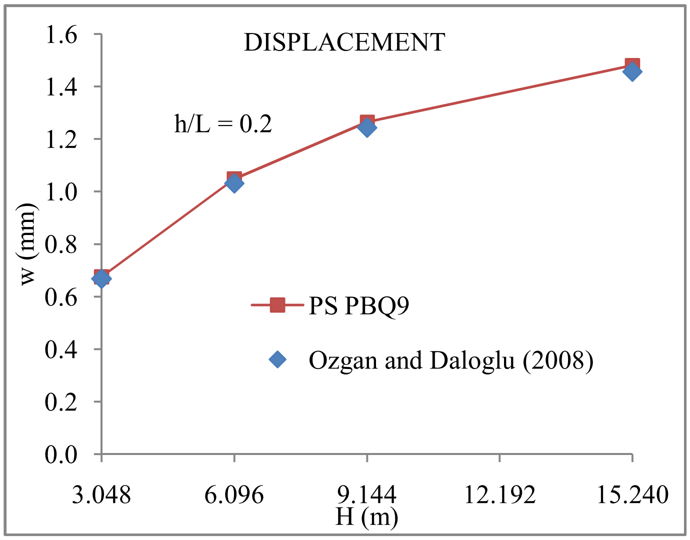

Fig. 5.42 Comparison of free plate deflection with UDL

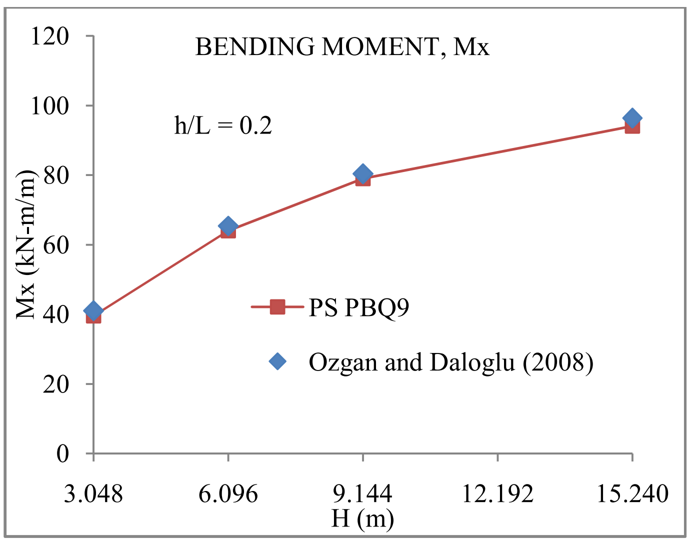

Fig. 5.43 Comparison of bending moment M_x with a UDL of a free plate

Table 5.27

Maximum displacements (w) with uniform load for the free plate

B/t	Maximum deflection (mm)		
	P.S.	(Buczkowski and Torbacki, 2001)	(Dutta et al., 2021)
2	1.3541	1.3584	1.3727
4	1.3862	1.3737	1.4013
10	1.6326	1.5342	1.7001
20	1.9168	1.9350	2.1230

80	2.1524	2.2055	2.2778
100	2.1614	2.2090	2.2811
500	2.2141	2.2104	2.2937
10^3	2.2341	2.2104	2.2940
10^6	2.2731	2.2104	2.2940

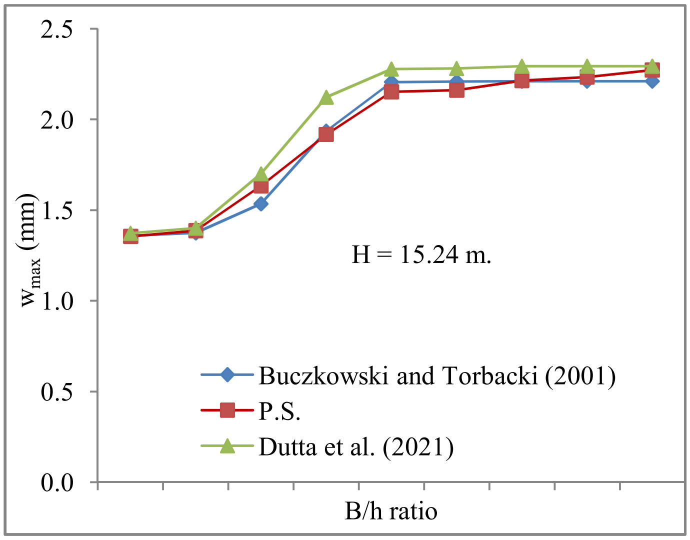

Fig. 5.44 Comparison of deflection w of a free plate with UDL

Table 5.28

Maximum moments (Mx) and displacements (w) with a PL for the free plate (h/L = 0.2)

H(m)	w_{max} (mm)			M_{xmax} (kN-m/m)		
	(Özgan and Daloğlu, 2008)	PS	Diff. (%)	(Özgan and Daloğlu, 2008)	PS	Diff. (%)
3.048	0.0506	0.047	6.52	44.77	43.8	2.21
6.096	0.0699	0.067	4.15	46.03	45	2.32
9.144	0.0811	0.078	3.33	46.68	45.5	2.53
15.24	0.0923	0.089	3.25	47.24	45.8	3.13

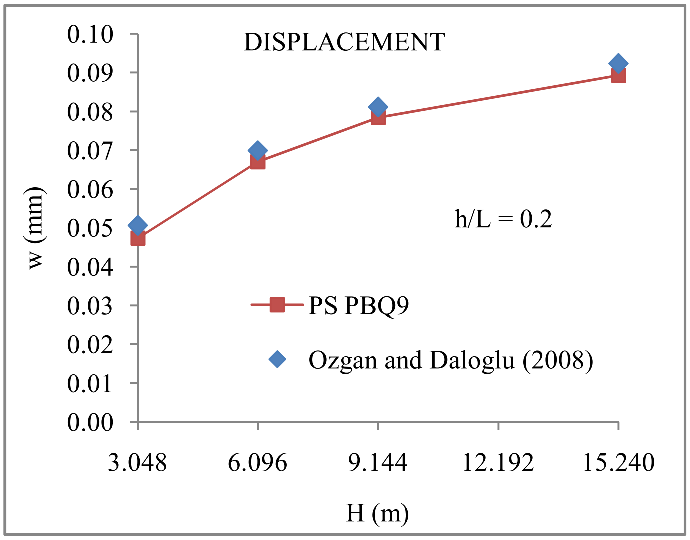

Fig. 5.45 Comparison of deflection w of a free plate with a PL

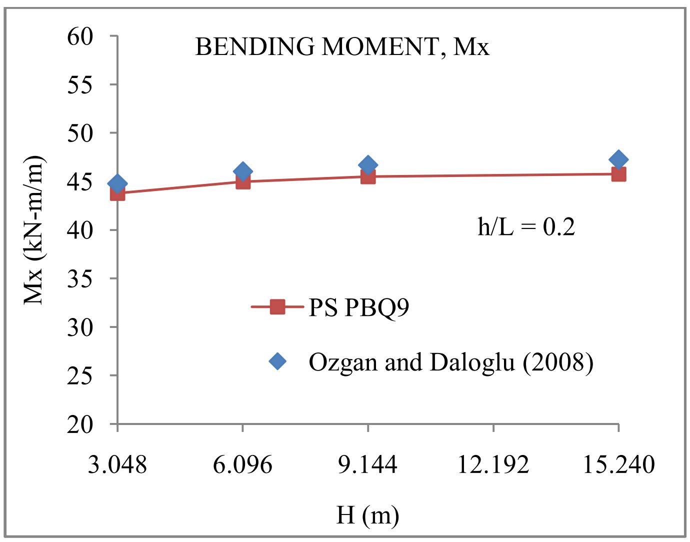

Fig. 5.46 Comparison of bending moment M_x of a free plate with a PL

5.4.3 The effectiveness of Lagrange elements.

The preceding illustration takes into consideration various boundary conditions. The plate-soil system's characteristics remain the same. The shorter side of the plate's thickness, h, to length, L, is assumed to be 0.30, 0.40, or 0.50. The issue is resolved with a 9-nodded element based on higher-order shear deformable plate theory to show the effect of the normal strain. In tabular and graphical formats, the displacements and bending moments of the plate for various subsoil depths, the Poisson's ratio, the subsoil's elasticity modulus, and the plate's thickness are shown in tables 5.29-5.38 and figures 5.47-5.54

Table 5.29

The plate's central displacement and maximum and minimum central bending moment (ν_s = 0.25; B.C. - FFFF) with the UDL.

h/L	E_s (kN/m²)	H (m)	w (mm)	M_{zc} (kN-m/m)	M_{cmax} (kN-m/m)	M_{cmin} (kN-m/m)
0.3	68950	3.048	0.6509	4.60	51.69	41.65
0.4			0.6440	8.53	53.71	42.07
0.5			0.6413	13.54	54.47	42.10
0.3		6.096	1.0022	7.47	88.57	67.38
0.4			0.9889	13.75	92.09	67.88
0.5			0.9837	21.76	93.51	67.76
0.3		9.144	1.2042	9.29	114.80	84.03
0.4			1.1856	17.10	120.21	84.74
0.5			1.1783	27.07	122.47	84.53
0.3	103425	3.048	0.4380	4.46	50.03	41.11
0.4			0.4313	8.41	52.88	41.81
0.5			0.4287	13.42	53.99	41.95
0.3		6.096	0.6759	7.28	85.78	66.50
0.4			0.6631	13.59	90.71	67.47
0.5			0.6581	21.61	92.71	67.53
0.3		9.144	0.8137	9.05	110.64	82.71
0.4			0.7959	16.90	118.14	84.14
0.5			0.7888	26.89	121.28	84.19
0.3	137900	3.048	0.3314	4.32	48.48	40.58
0.4			0.3250	8.28	52.07	41.56
0.5			0.3224	13.31	53.52	41.80
0.3		6.096	0.5125	7.11	83.16	65.64
0.4			0.5002	13.43	89.37	67.07
0.5			0.4952	21.47	91.93	67.31
0.3		9.144	0.6180	8.83	106.78	81.40
0.4			0.6009	16.70	116.13	83.53
0.5			0.5940	26.70	120.11	83.86

Table 5.30

The plate's central displacement and maximum and minimum central bending moment (h/L = 0.3; E_s = 68950 kN/m²; ν_s = 0.25) with UDL.

H (m)	B.C.	w (mm)	M_{zc} (kN-m/m)	M_{cmax} (kN-m/m)	M_{cmin} (kN-m/m)
3.048	SSSS	0.04280	17.00	155.76	101.28
6.096		0.04323	17.32	157.43	102.44
9.144		0.04328	17.38	157.62	102.58
3.048	CCCC	0.01808	17.53	69.26	47.74
6.096		0.01817	17.66	69.64	48.03
9.144		0.01818	17.68	69.71	48.08

Table 5.31

The plate's central displacement and maximum and minimum central bending moment (h/L = 0.3; ν_s = 0.25; H = 6.096 m) with UDL.

E_s (kN/m²)	B.C.	w (mm)	M_{zc} (kN-m/m)	M_{cmax} (kN-m/m)	M_{cmin} (kN-m/m)
68950	SSSS	0.04323	17.32	157.43	102.44
103425		0.04262	16.99	155.10	100.87
137900		0.04202	16.66	152.83	99.34
68950	CCCC	0.01817	17.66	69.64	48.03
103425		0.01806	17.50	69.18	47.69
137900		0.01795	17.35	68.73	47.35

Table 5.32

The plate's central displacement and maximum and minimum central bending moment (h/L = 0.3; E_s = 68950 kN/m²; H = 6.096 m) with UDL.

ν_s	B.C.	w (mm)	M_{zc} (kN-m/m)	M_{cmax} (kN-m/m)	M_{cmin} (kN-m/m)
0.20	FFFF	1.05117	7.74	92.34	69.82
0.25		1.00218	7.47	88.57	67.38
0.30		0.92695	7.11	83.67	64.19
0.20	SSSS	0.04327	17.34	157.56	102.53
0.25		0.04323	17.32	157.43	102.44
0.30		0.04316	17.27	157.16	102.26

0.20	CCCC	0.01817	17.67	69.68	48.05
0.25		0.01817	17.66	69.64	48.03
0.30		0.01815	17.64	69.59	47.98

Table 5.33

The plate's central displacement and maximum and minimum central bending moment (h/L = 0.3; E_s = 68950 kN/m²; H = 6.096 m) with UDL.

h/L	B.C	w (mm)	Mzc (kN-m/m)	M_{cmax} (kN-m/m)	M_{cmin} (kN-m/m)
0.3	SSSS	0.04323	17.32	157.43	102.44
0.4		0.02175	31.42	164.35	109.02
0.5		0.01313	49.47	168.08	114.47
0.3	CCCC	0.01817	17.66	69.64	48.03
0.4		0.01060	31.68	72.20	53.39
0.5		0.00726	49.72	75.34	58.94

Table 5.34

Central displacement and a plate's maximum and minimum central bending moment (ν_s = 0.25; B.C. - FFFF) with a central PL.

h/L	E_s (kN/m²)	H (m)	w (mm)	Mzc (kN-m/m)	M_{cmax} (kN-m/m)	M_{cmin} (kN-m/m)
0.3	68950	3.048	0.03714	129.68	57.47	51.39
0.4			0.03401	189.65	64.45	58.03
0.5			0.03274	244.11	70.37	63.87
0.3		6.096	0.05504	129.51	59.29	52.61
0.4			0.05141	189.51	66.32	59.25
0.5			0.04994	244.05	72.26	65.07
0.3		9.144	0.06535	129.27	60.41	53.32
0.4			0.06134	189.26	67.59	59.98
0.5			0.05973	243.85	73.59	65.81
0.3	103425	3.048	0.02641	129.39	56.86	51.18
0.4			0.02337	189.30	64.10	57.89
0.5			0.02212	243.71	70.13	63.75
0.3		6.096	0.03865	129.06	58.62	52.34
0.4			0.03511	188.95	65.92	59.05
0.5			0.03367	243.42	71.98	64.91
0.3		9.144	0.04573	128.66	59.57	52.97

0.4			0.04185	188.49	67.09	59.72
0.5			0.04026	242.97	73.23	65.59
0.3	137900	3.048	0.02100	129.10	56.29	50.96
0.4			0.01803	188.95	63.76	57.74
0.5			0.01680	243.30	69.90	63.63
0.3		6.096	0.03039	128.61	57.98	52.08
0.4			0.02695	188.39	65.53	58.86
0.5			0.02553	242.78	71.69	64.74
0.3		9.144	0.03584	128.05	58.79	52.61
0.4			0.03209	187.72	66.60	59.47
0.5			0.03052	242.10	72.87	65.36

Table 5.35

Central displacement and maximum and minimum central bending moment of the plate (h/L = 0.3; E_s = 68950 kN/m²; ν_s = 0.25) with central PL.

H (m)	B.C.	w (mm)	M_{zc} (kN-m/m)	M_{cmax} (kN-m/m)	M_{cmin} (kN-m/m)
3.048	SSSS	0.00649	130.33	58.70	53.83
6.096		0.00654	130.15	58.85	53.92
9.144		0.00655	130.05	58.85	53.91
3.048	CCCC	0.00379	130.39	49.24	47.65
6.096		0.00380	130.23	49.25	47.65
9.144		0.00380	130.16	49.24	47.64

Table 5.36

Central displacement and maximum and minimum central bending moment of the plate (h/L = 0.3; ν_s = 0.25; H = 6.096 m) with central PL.

E_s (kN/m²)	B.C.	w (mm)	M_{zc} (kN-m/m)	M_{cmax} (kN-m/m)	M_{cmin} (kN-m/m)
68950.0	SSSS	0.00654	130.15	58.85	53.92
103425.0		0.00647	129.77	58.47	53.62
137900.0		0.00639	129.39	58.10	53.33
68950.0	CCCC	0.00380	130.23	49.25	47.65
103425.0		0.00378	129.89	49.09	47.51
137900.0		0.00377	129.55	48.93	47.36

Table 5.37

Central displacement and maximum and minimum central bending moment of the plate (h/L = 0.3; E_s = 68950 kN/m²; H = 6.096 m) with central PL.

ν_s	B.C.	w (mm)	M_{zc} (kN-m/m)	M_{cmax} (kN-m/m)	M_{cmin} (kN-m/m)
0.20	FFFF	0.05752	129.50	59.48	52.73
0.25		0.05504	129.51	59.29	52.61
0.30		0.05123	129.50	59.03	52.45
0.20	SSSS	0.00655	130.15	58.87	53.93
0.25		0.00654	130.15	58.85	53.92
0.30		0.00653	130.14	58.82	53.90
0.20	CCCC	0.00380	130.23	49.25	47.66
0.25		0.00380	130.23	49.25	47.65
0.30		0.00380	130.22	49.24	47.64

Table 5.38

Central displacement and maximum and minimum central bending moment of the plate (h/L = 0.3; E_s = 68950 kN/m²; H = 6.096 m) with central PL.

h/L	B.C.	w (mm)	M_{zc} (kN-m/m)	M_{cmax} (kN-m/m)	M_{cmin} (kN-m/m)
0.3	SSSS	0.00654	130.15	58.85	53.92
0.4		0.00287	190.58	66.11	60.97
0.5		0.00136	245.67	72.32	67.18
0.3	CCCC	0.00380	130.23	49.25	47.65
0.4		0.00164	190.67	55.72	54.71
0.5		0.00071	245.76	61.58	61.00

For PL cases compared to distributed load cases, the influence of normal strain on displacement is more significant, and the effect increases as h/L increases. According to the findings, a 9-nodded Lagrange plate bending element is ideal when considering the impact of the type strain. For any loading situation, the plate's centre displacement and bending moment always decrease as subsoil elastic modulus increases (Figures 5.48, 5.52 and tables 5.29, 5.34). On the other hand, the plate's central displacement and bending moment frequently increase as subsoil depth (H) increases for any loading situation (Figures 5.47,5.51 and tables 5.30,5.35). Still, after a certain depth, they often decrease or begin to stabilize.

Additionally, it is found that any loading conditions are hardly impacted by the subsoil Poisson's ratio (Figures 5.49, 5.53). Additionally, it is seen that the centre displacement and bending moment drop when the edge limits are tightened, indicating that the plate becomes more rigid and has a lower displacement as a result. For any loading and boundary conditions, the plate displacement continually decreases with an increasing h/L ratio for a constant value of H. In contrast, the plate's bending moment rises, as shown in Tables 5.33- 5.38 and Figures 5.50 -5.54.

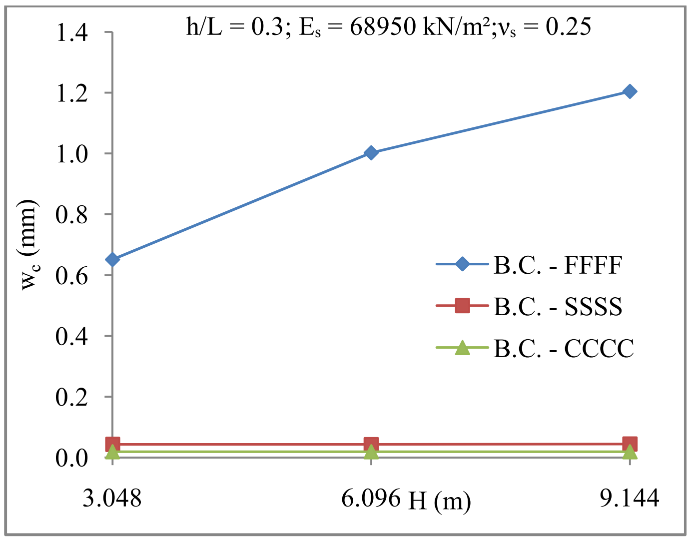

Fig.5.47 Central deflection vs sub-soil depth

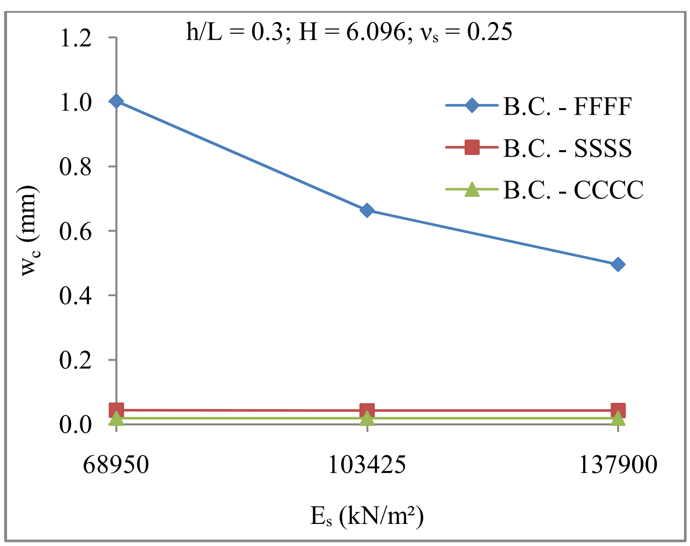

Fig. 5.48 Central deflection vs sub-soil elastic modulus

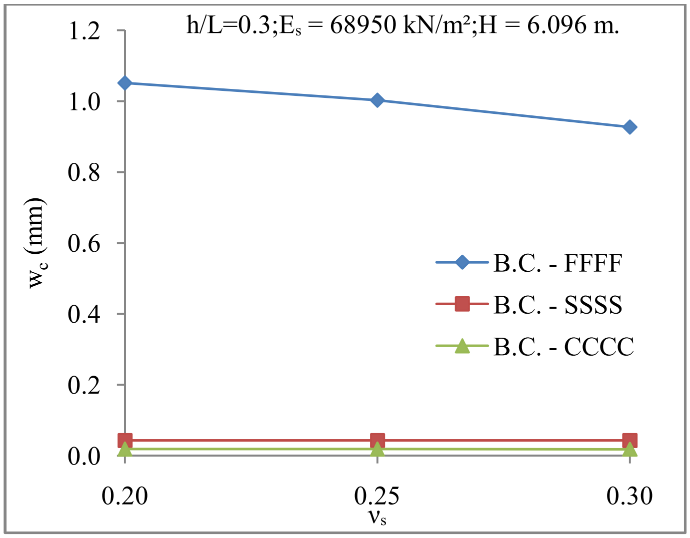

Fig. 5.49 Central deflection vs sub-soil Poisson's ratio

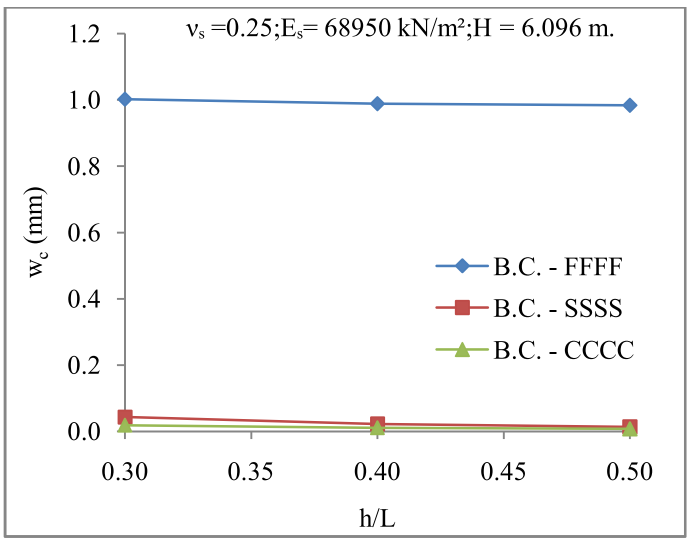

Fig. 5.50 Central deflection vs h/L ratio

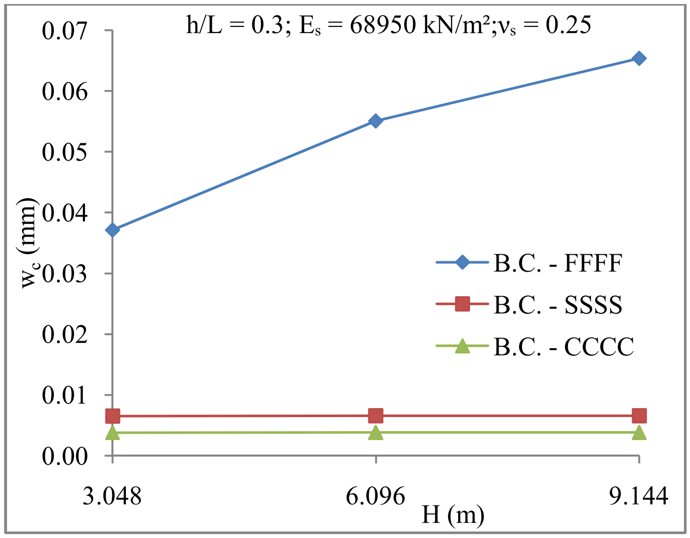

Fig. 5.51 Central deflection vs sub-soil depth

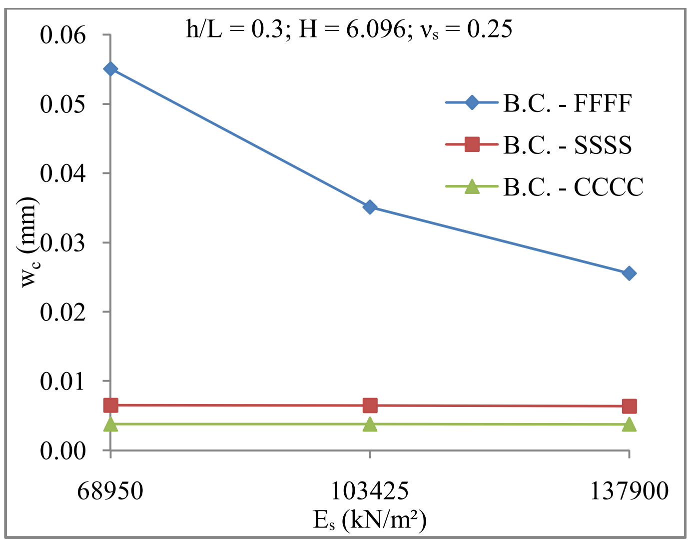

Fig. 5.52 Central deflection vs sub-soil elastic modulus

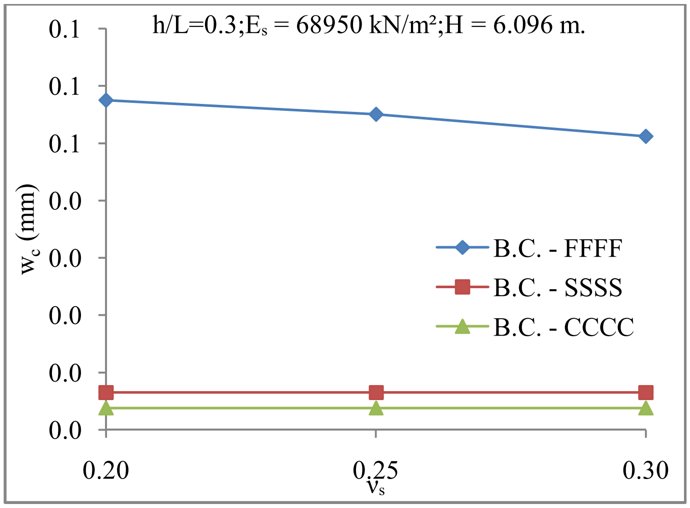

Fig. 5.53 Central deflection vs sub-soil Poisson's ratio

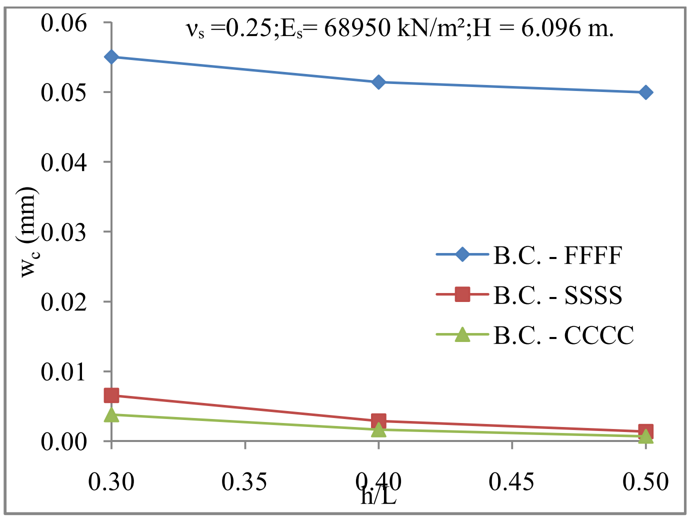

Fig. 5.54 Central deflection vs h/L ratio

5.5 HSDT Circular Plate

5.5.1 Convergence Study

For the study of convergence for a C and S.S. plate under a load that is evenly distributed (q) and a load that is concentrated in the middle (P), we start by looking at a circular plate (ν = 0.25) that doesn't have a base. We initially tested the present formulation on a square plate without a foundation. Then, a convergence study is carried out for the C and S.S. plates under uniformly distributed load (UDL) and central concentrated load (PL). We ultimately choose a mesh size of 10 ring elements for a good outcome.

5.5.2 Validation

(Yue et al., 2019) studies were used as examples to validate the current formulation for uniform loading circumstances. A solid circular plate with a radius of 0.4 m is the same thickness throughout 0.05 m and has a uniformly distributed loading of 1000 kN/m² intensity. The plate's material characteristics are $E = 2.8\times10^4$ MN/m² and a Poisson's ratio of 0.15, and foundation characteristics are $E_s = 6.9 \times 10^4$ kN/m², $\nu_s = 0.3$ and H = 1 m.

Table 5.399 compares the present study's (P.S.) results with those of (Yue et al., 2019). The reference's findings can be regarded as having full conformity.

Table 5.39

Comparison of the Deflections (in mm) at the centre of the plate with the Reference Value

Deflections (in mm)		Difference (%)
PS	(Yue et al., 2019)	
5.063	5.083	0.39

(Yue et al., 2019) Studies were used as an example to validate the current formulation for the concentrated loading condition. A concentrated load of 98.1 kN is applied to the centre of a solid circular plate with a radius of 5 m and an elastic foundation. This plate has a uniform thickness of 0.5 m. The plate's material characteristics are $E = 1.7658\times10^4$ MN/m² and a Poisson's ratio of 0.17, and foundation characteristics are $E_s = 8.6 \times 10^3$ kN/m², $\nu_s = 0.2$ and H = 1 m.

Table 5.40 compares the P.S. with (Yue et al., 2019) and provides the results. Again, the reference's findings can be regarded as a solid agreement.

Table 5. 40

Comparison of the Deflections (in mm) at the centre of the plate with the Reference Value

Deflections (in mm)		Difference (%)
PS	(Yue et al., 2019)	
0.335	0.320	4.74

(Yue et al., 2019) Studies were used as an example to validate the current formulation for the patch loading condition. As shown in Table 5.41, the parameter of the solid circular plate with a radius of 1.35 m is supported by an elastic foundation. The plate's centre is subjected to a patch load with an intensity of 1000 kN/m² and a radius of 0.18 m. The plate's material characteristics are $E = 2.45\times10^4$ MN/m², thickness of the plate h = 0.25 m and a Poisson's ratio of 1/6 and foundation characteristics are $E_s = 62.5 \times 10^3$ kN/m², $\nu_s = 0.25$ and H = 2 m.

Table 5.11 compares the P.S. solution to (Yue et al., 2019). Again, the results concerning the reference can be accepted as a fair agreement.

Table 5.41

Comparison of the Deflections (in mm) at the centre of the plate with the Reference Value

Deflections (in mm)		
PS	(Yue et al., 2019)	Difference (%)
0.351	0.345	1.74

5.5.3 The effectiveness of the formulation

We used a solid circular plate with a radius of 3 meters (B = 2R), an elasticity modulus (E_p) 2.5×10^4 MN/m², ν = 0.15 and 0.20, and t or h = 200, 300, 400, 600, and 1200 mm. The elasticity modulus of the foundation soil (E_s) was 20 to 50 MN/m², and the Poisson's ratio (v_s) of the foundation was 0.15, 0.20, 0.25, 0.30, and 0.35. The depth of the foundation soil (H) was 3 to 18 meters, and the plate's load was evenly distributed at 40 kN/m². To show the results of the parametric study better, a normalized plate modulus K_p is defined as follows in this study: $K_p = \frac{qB^2}{w_c E_p t_p}$ in this equation, q stands for the applied uniformly distributed load, w_c for the settlement at the plate center, E_p for the Young's modulus of the plate, B for the plate diameter, and tp for the plate thickness. The results are shown in figures 5.55–5.69.

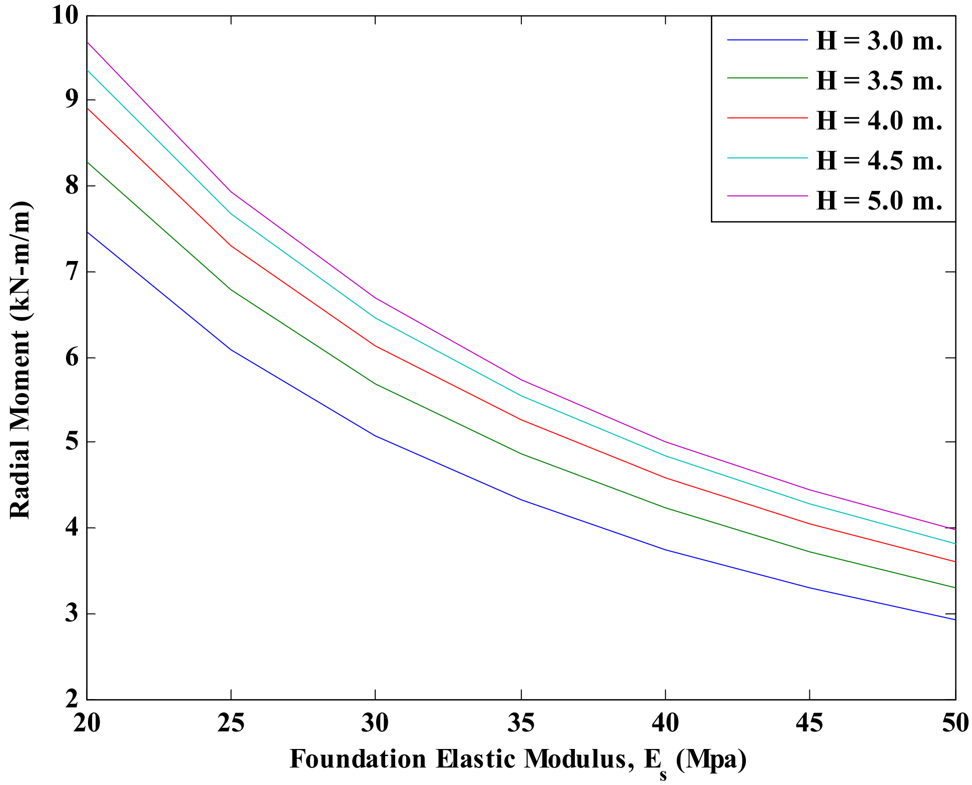

Fig. 5.55 Central Radial Moment vs sub-soil elastic modulus ($\nu_s = 0.35$)

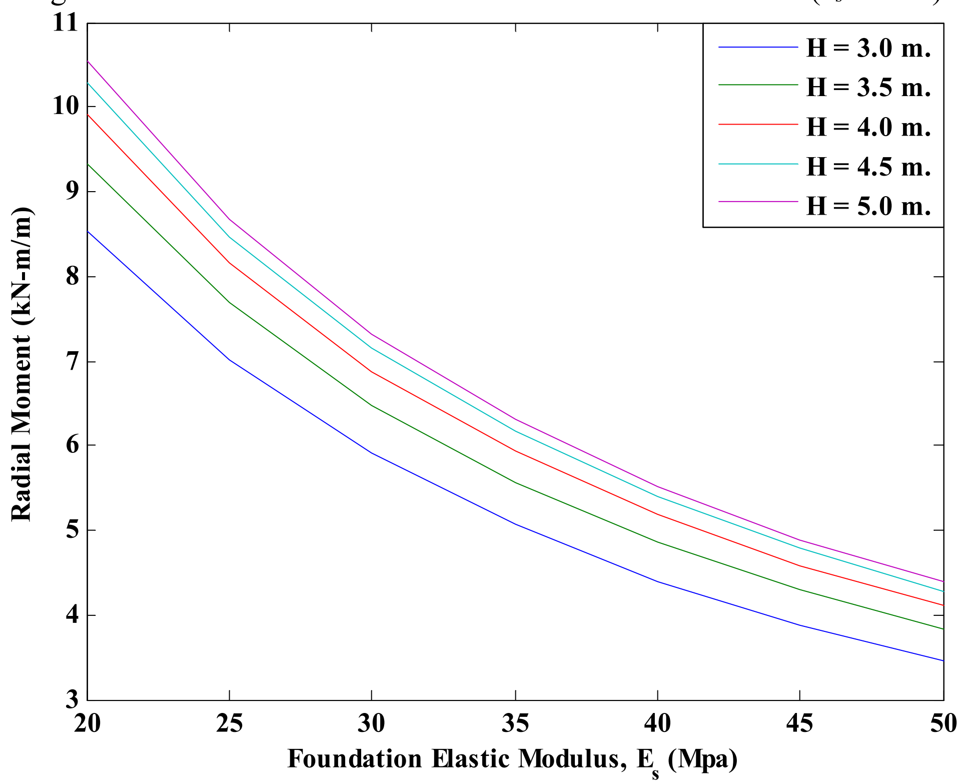

Fig. 5.56 Central Radial Moment vs sub-soil elastic modulus ($\nu_s = 0.30$)

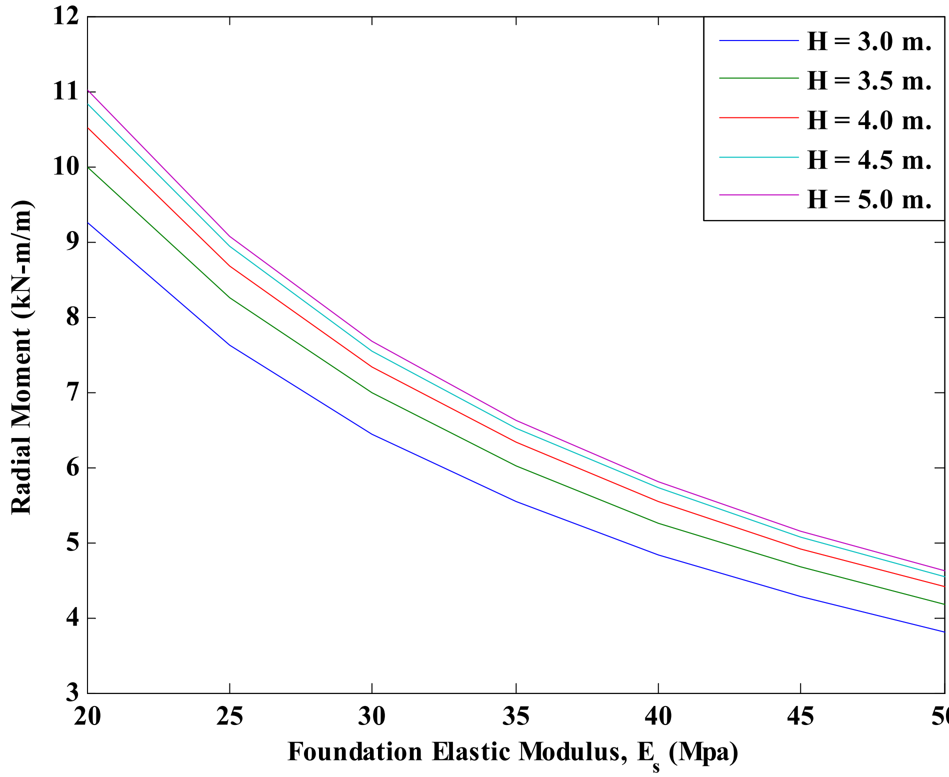

Fig. 5.57 Central Radial Moment vs sub-soil elastic modulus ($\nu_s = 0.25$)

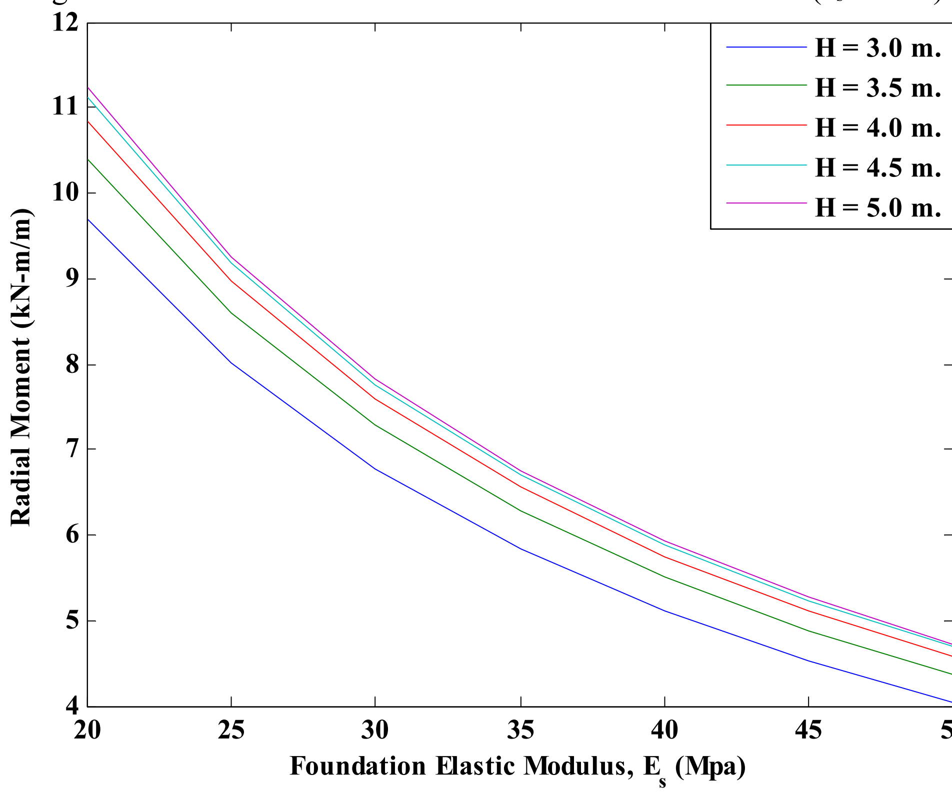

Fig. 5.58 Central Radial Moment vs sub-soil elastic modulus ($\nu_s = 0.20$)

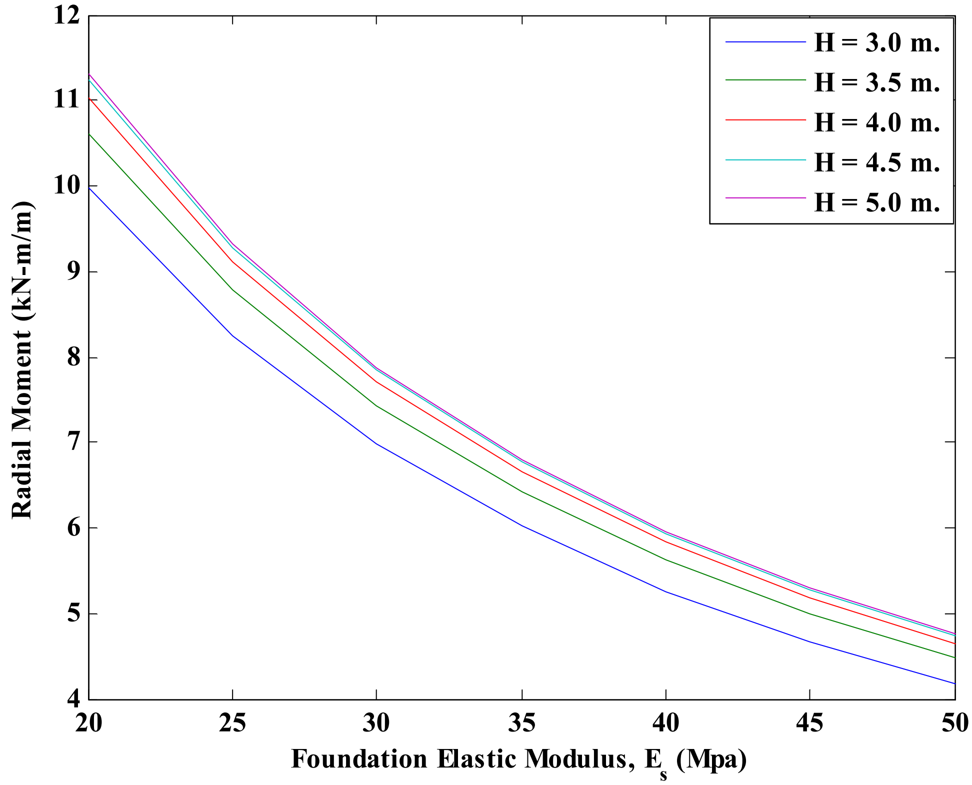

Fig. 5.59 Central Radial Moment vs sub-soil elastic modulus ($\nu_s = 0.15$)

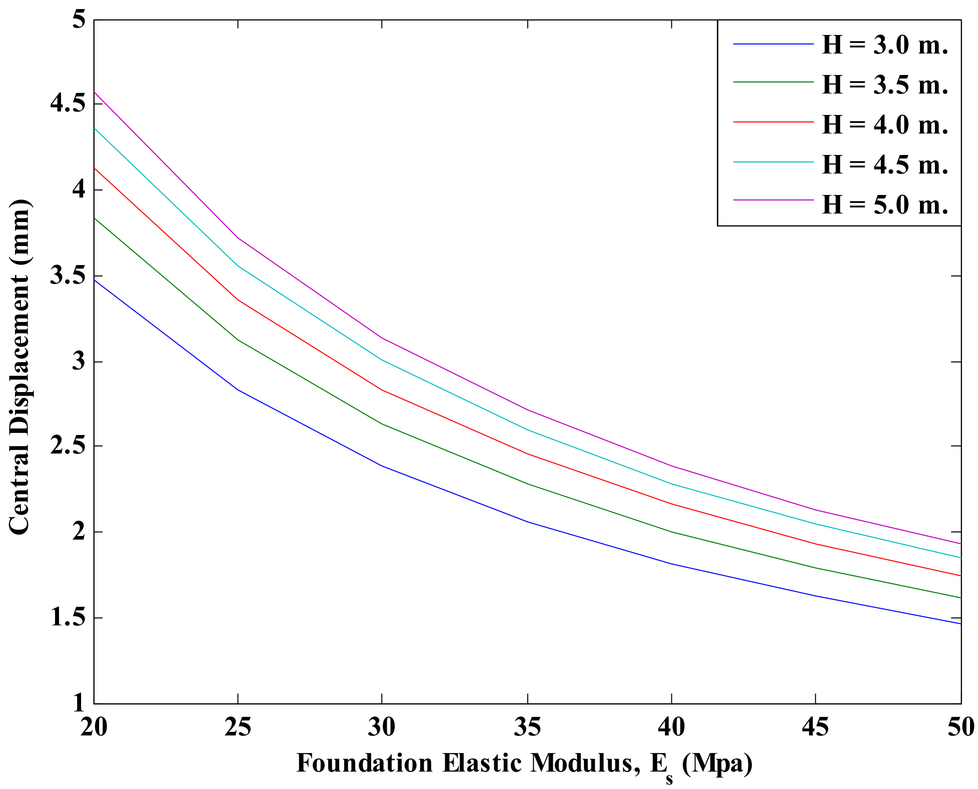

Fig. 5.60 Central Displacement vs sub-soil elastic modulus ($\nu_s = 0.35$)

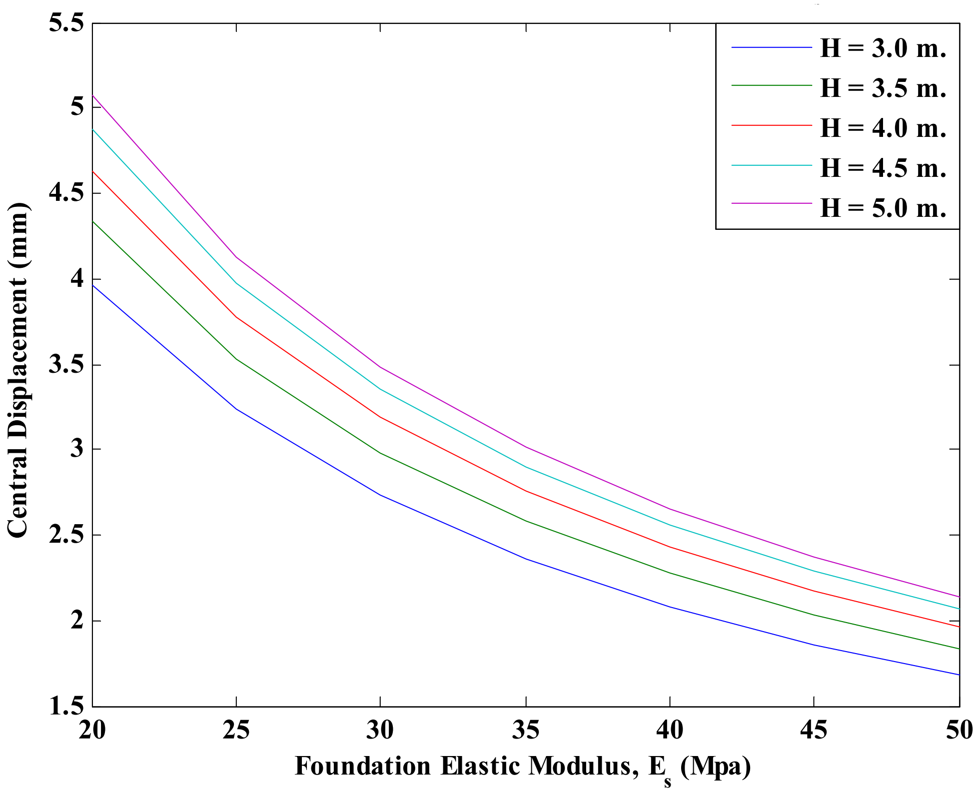

Fig. 5.61 Central Displacement vs sub-soil elastic modulus ($\nu_s = 0.30$)

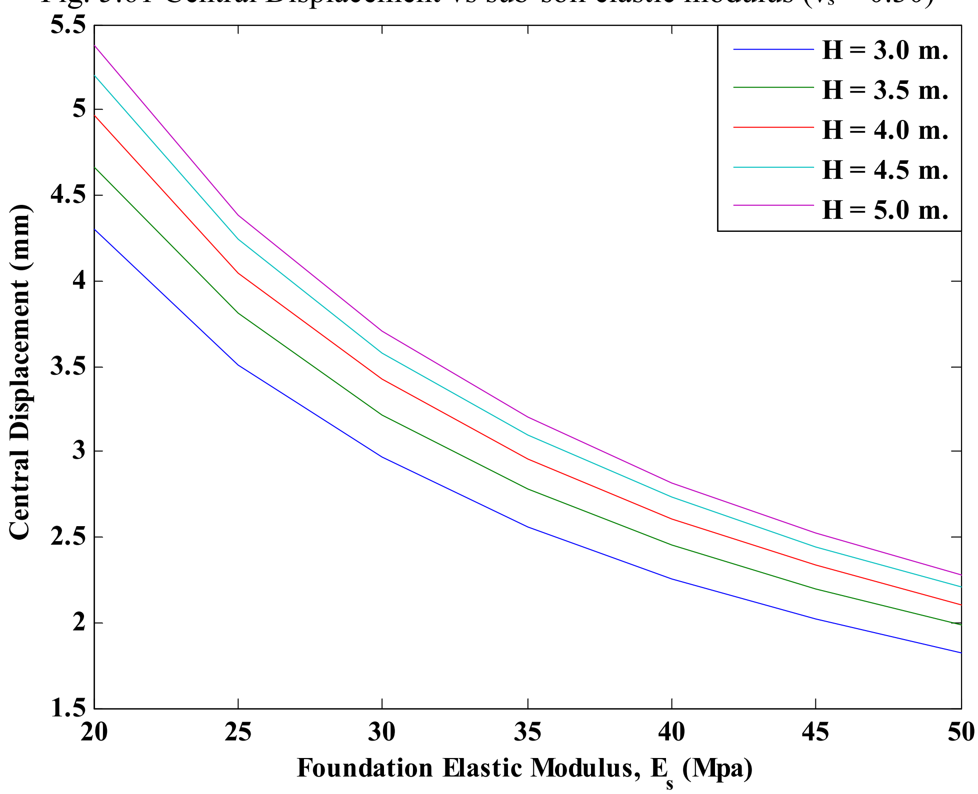

Fig. 5.62 Central Displacement vs sub-soil elastic modulus ($\nu_s = 0.25$)

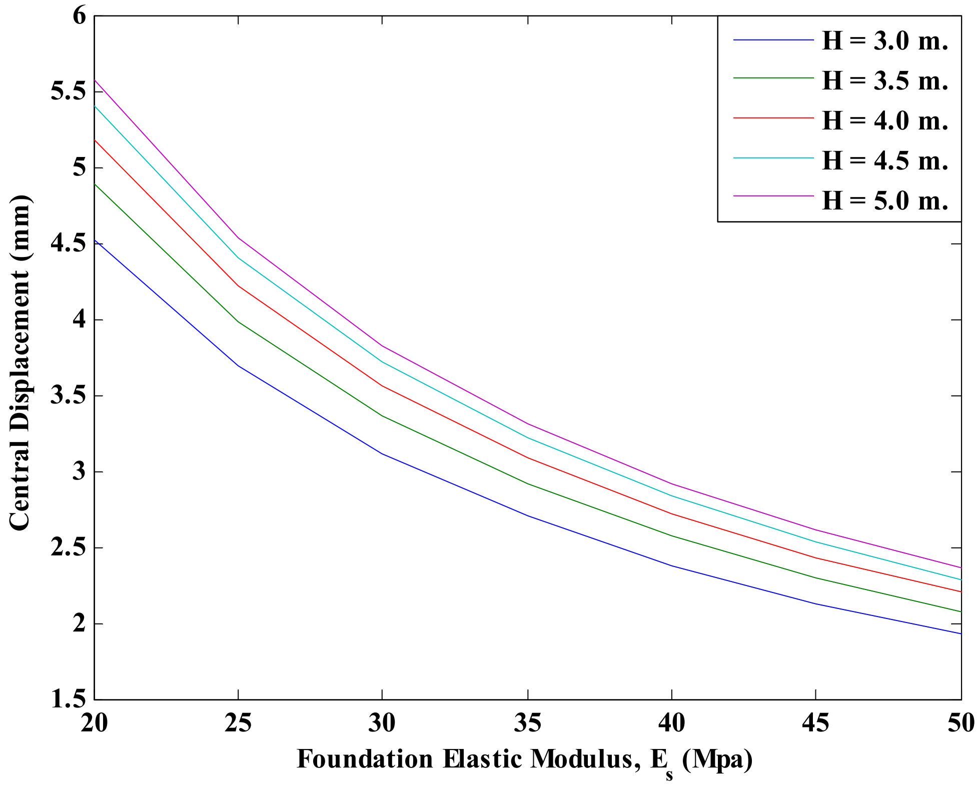

Fig. 5.63 Central Displacement vs sub-soil elastic modulus (ν_s = 0.20)

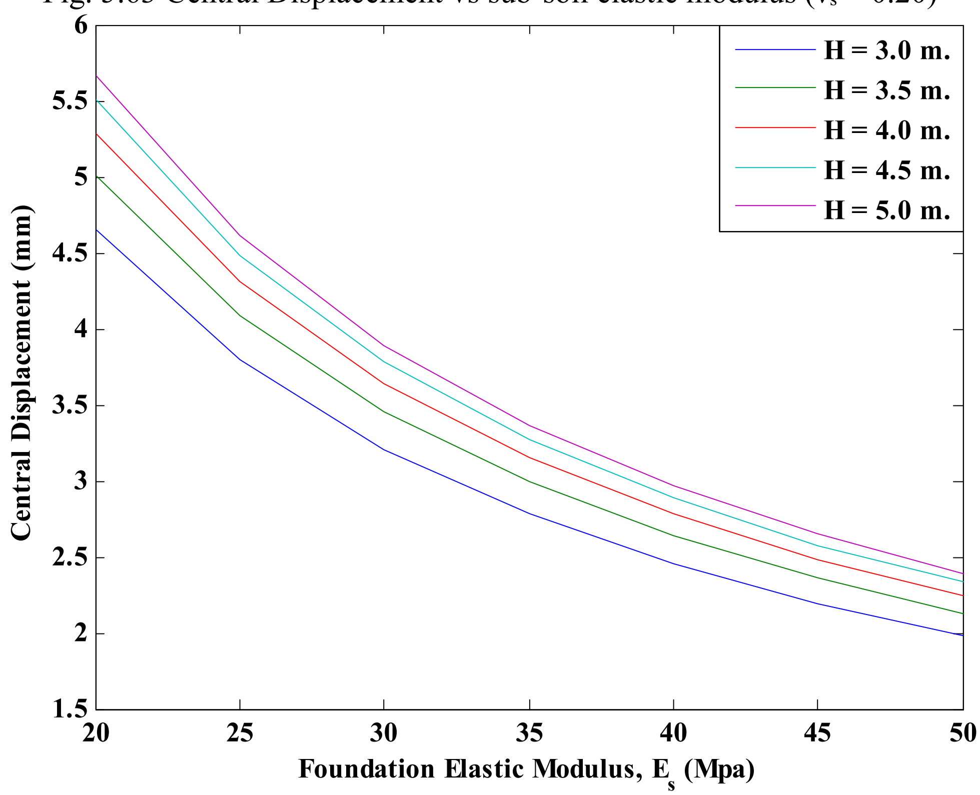

Fig. 5.64 Central Displacement vs sub-soil elastic modulus (ν_s = 0.15)

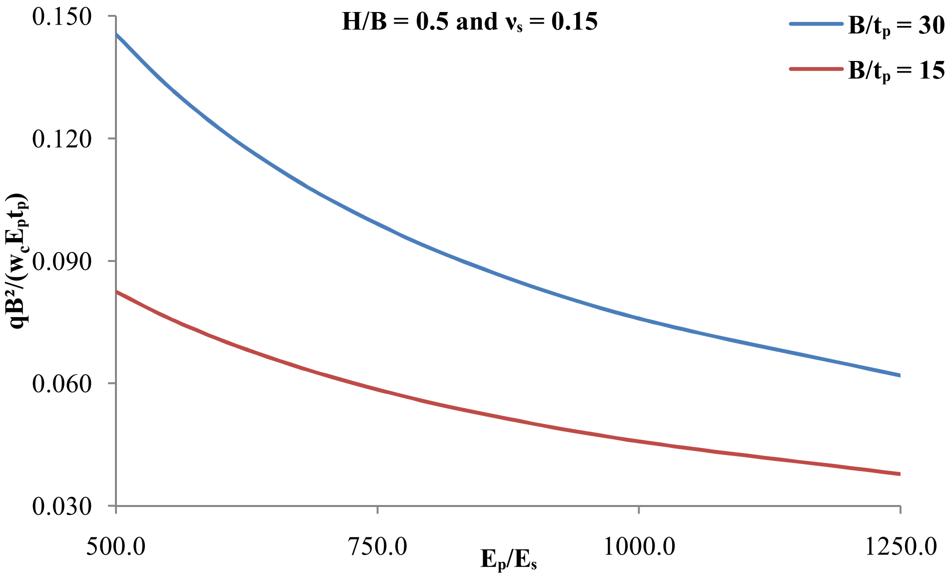

Fig. 5.65 Normalized plate modulus [$K_p = qB^2/(w_cE_pt_p)$] versus stiffness ratio of plate to soil (E_p/E_s) for various values of plate diameter-to-thickness ratio (B/t_p)

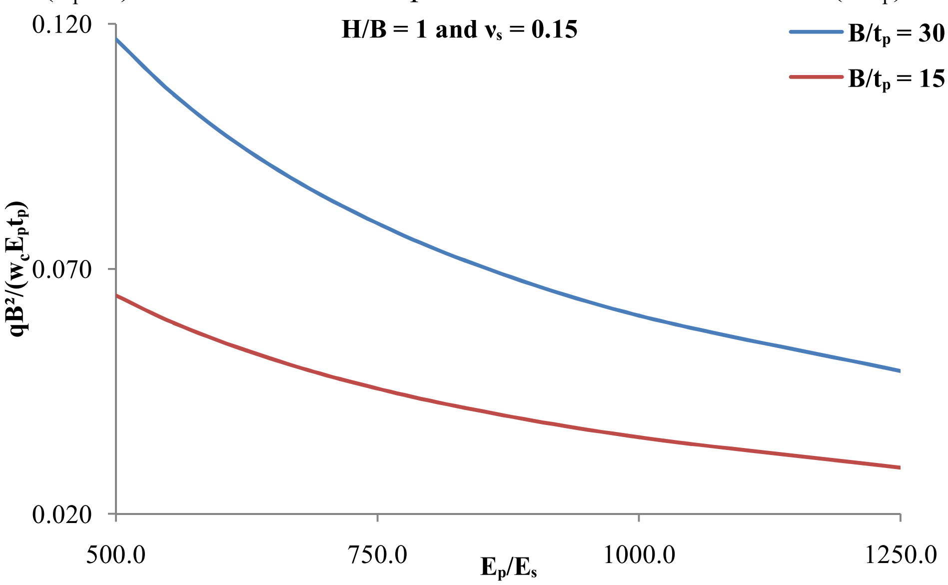

Fig. 5.66 Normalized plate modulus [$K_p = qB^2/(w_cE_pt_p)$] versus stiffness ratio of plate to soil (E_p/E_s) for various values of plate diameter-to-thickness ratio (B/t_p)

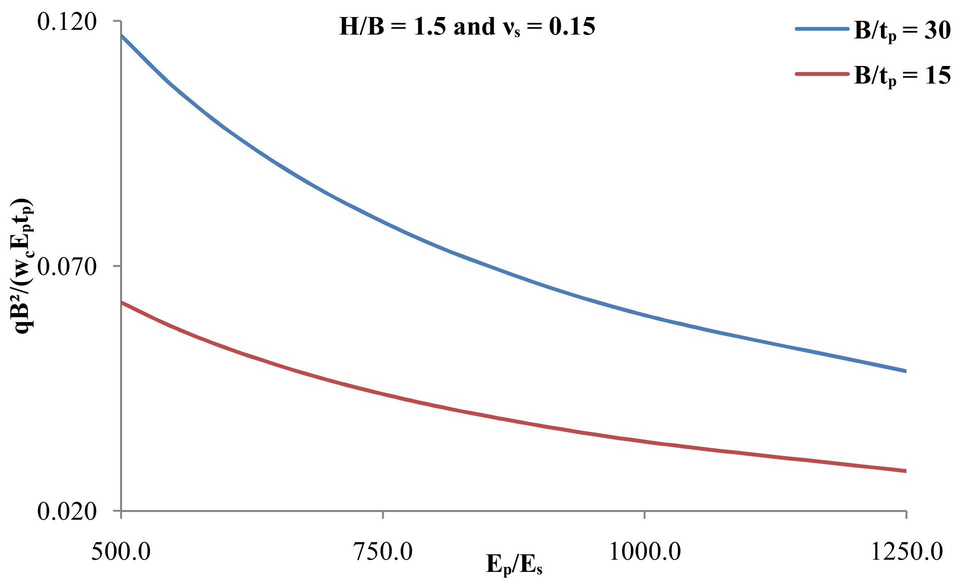

Fig. 5.67 Normalized plate modulus [K_p= $qB^2/(w_cE_pt_p)$] versus stiffness ratio of plate to soil (E_p/E_s) for various values of plate diameter-to-thickness ratio (B/t_p)

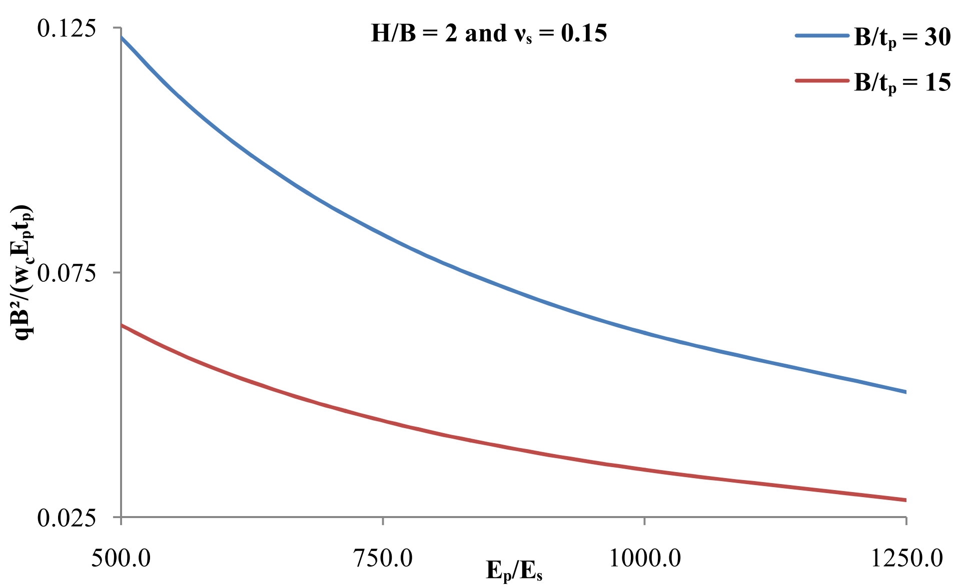

Fig. 5.68 Normalized plate modulus [K_p= $qB^2/(w_cE_pt_p)$] versus stiffness ratio of plate to soil (E_p/E_s) for various values of plate diameter-to-thickness ratio (B/t_p)

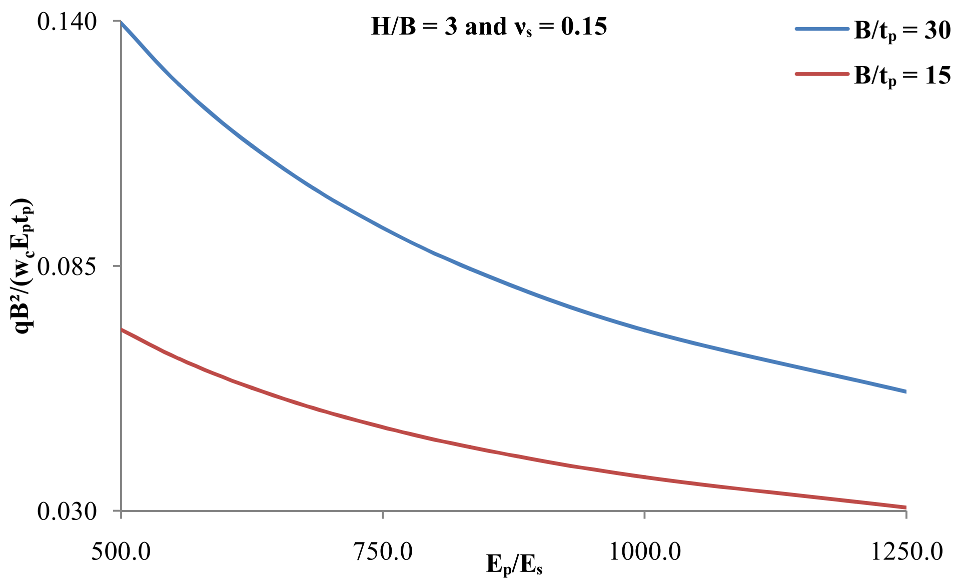

Fig. 5.69 Normalized plate modulus [$K_p = qB^2/(w_c E_p t_p)$] versus stiffness ratio of plate to soil (E_p/E_s) for various values of plate diameter-to-thickness ratio (B/t_p)

As the sub-soil elastic modulus increases, for any loading conditions, the plate's central displacement and bending moment always decrease. As subsoil depth (H) increases, for uniform loading conditions, the plate's central displacement and bending moment often increase, but the plate's central displacement and bending moment decrease as Poisson's ratio (ν_s) of subsoil increases. Additionally, it is noted that the central bending moment and displacement drop as the edge constraints increase, indicating that an increase in edge constraints increases the plate's flexural rigidity and reduces displacement.

We can see in Fig. 5.65 to 5.69 how the normalized plate modulus K_p changes with the stiffness ratio E_p/E_s of the plate to the soil for different plate diameter-to-thickness ratios B/t_p and subsoil depth-to-plate diameter ratios H/B, as long as the Poisson's ratio of the subsoil is kept at 0.15 for concrete tanks. When a loading condition, plate dimension, and soil properties are known, the normalized plate modulus K_p is obtained from Fig. 5.65 to 5.69 for the given properties of the plate and subsoil, and the center settlement is then computed from K_p= $qB^2/(wcE_p t_p)$ and use in the preliminary design of a circular storage tank.

5.6 Vibration Analysis Thin Rectangular Plate Using Higher-Order FEM

5.6.1 Convergence study

A square plate without foundation is considered first to test the present formulation. Simultaneously, a convergence study is performed for the clamped, simply supported and free plate for free vibration analysis. The mesh size of 12 × 12 is decided for the supported plate and 10 × 10 for a free plate for a reasonable result compared to 20 × 20 of a 12 DOF rectangular element, hence less uses of computer memory and time. The results are compared with those given in (Chakraverty, 2009), tabulated in Table 5.42 – 5.44. It shows the rapid convergence of the proposed formulation and is also observed for simply supported plates converging from opposite sides.

Table 5.42

Convergence study for natural frequency of CCCC plate for 1st mode

MESH SIZE	$\overline{\omega} = \omega a^2 \sqrt{\frac{\rho h}{D}}$
2 × 2	36.9846
4 × 4	36.0573
6 × 6	36.0015
8 × 8	35.9908
10 × 10	35.9876
12 × 12	35.9864
14 × 14	35.9859
(Chakraverty, 2009)	35.988

Table 5.43

Convergence study for natural frequency of SSSS plate for 1st mode

MESH SIZE	$\overline{\omega} = \omega a^2 \sqrt{\frac{\rho h}{D}}$
2 × 2	18.9162
4 × 4	19.7113
6 × 6	19.7356
8 × 8	19.7384
10 × 10	19.7389
12 × 12	19.7391
14 × 14	19.7392
(Chakraverty, 2009)	19.7390

Table 5.44

Convergence study for natural frequency of FFFF plate for 4th mode

MESH SIZE	$\overline{\omega} = \omega a^2 \sqrt{\frac{\rho h}{D}}$
2 × 2	13.5727
4 × 4	13.4773

6 × 6	13.4702
8 × 8	13.4689
10 × 10	13.4685
12 × 12	13.4683
14 × 14	13.4683
(Chakraverty, 2009)	13.714

5.6.2 Validation

This chapter starts with comparisons with similar studies done by other researchers. The present method can be applied to analyse the free vibration of a plate with various boundary conditions, including free-free.

One example from the study conducted by Gibigaye et al. (Gibigaye et al., 2018) has been selected. Following measurements were made of the plate for verification: Plate material properties: a = 5 m, b = 3.5 m, plate thickness, h = 0.25 m Young's modulus: E = 24000 MPa, Poisson's ratio (ν): 0.25, density (ρ): 2500 kg/ m³, and soil: E = 50 MPa, Poisson's ratio (ν_s): 0.35, density (ρ_s): 1800 kg/ m³, and H = 1.5 m, with a γ = 4.212. The frequency Parameter, $\lambda = \omega a^2\sqrt{(\rho h+m_\circ)/D}$ where a is the longer side of the plate (Gibigaye et al., 2018), has been compared with the frequency parameter that was obtained, which is presented in Figures 5.70-5.72. Precise findings exhibit strong agreement with (Gibigaye et al., 2018).

5.6.3 Parametric Study

For the parametric study of the parameter aspect ratio, β = a/b, depth of the rigid base, H, and vertical decay function, γ the dimensions of the plate were taken as follows: β = 1, 1.25, 1.5, 1.75, and 2, b/h = 100, and material properties of the plate: Young's modulus, E = 24500 MPa, Poisson's ratio, ν = 0.3, and density, ρ = 2550 kg/m³, and soil E_s = 51 to 60 MPa, Poisson's ratio, ν_s = 0.23, 0.28, and 0.33, density, ρ_s = 1850 kg/m³, and H = 1 to 10 m. γ = 1, 1.5, 2, and 3. Frequency Parameter, $\lambda = \omega a^2/\sqrt{(\rho h+m_\circ)/D}$; The results presented in Tables 5.45–5.53 show the nature of variation of the first ten frequency parameters with various parameters of soil and plate.

Table 5.45
Parametric study of frequency parameters for various parameters of FFFF plate

a/b (β) = 1, Es = 51 MPa, ν_s = 0.33, ρ_s = 1850 kg/m³, γ = 1										
H (m)	λ_1	λ_2	λ_3	λ_4	λ_5	λ_6	λ_7	λ_8	λ_9	λ_{10}
1	238.51	312.81	312.81	374.05	423.89	426.31	473.37	473.37	557.17	561.20

2	216.27	340.51	340.51	434.54	516.64	525.79	588.80	588.80	712.50	727.21	
3	213.08	376.90	376.90	495.18	602.06	617.04	690.89	690.89	844.63	867.63	
4	214.42	412.21	412.21	550.61	678.23	698.07	780.86	780.86	959.72	989.51	
5	217.41	445.45	445.45	601.41	747.17	771.20	861.85	861.85	1062.76	1098.36	
6	221.13	476.70	476.70	648.43	810.49	838.21	936.02	936.02	1156.80	1197.55	
7	225.21	506.18	506.18	692.36	869.33	900.38	1004.81	1004.81	1243.83	1289.22	
8	229.46	534.12	534.12	733.71	924.50	958.59	1069.22	1069.22	1325.19	1374.85	
9	233.79	560.74	560.74	772.87	976.61	1013.51	1129.99	1129.99	1401.85	1455.48	
10	238.15	586.18	586.18	810.16	1026.10	1065.63	1187.67	1187.67	1474.56	1531.90	
a/b (β) = 1, Es = 51 MPa, ν_s = 0.33, ρ_s = 1850 kg/m³, γ = 1.5											
1	238.92	306.56	306.56	363.00	408.48	410.32	454.53	454.53	532.46	535.36	
2	213.81	327.91	327.91	415.27	490.82	498.70	558.30	558.30	673.71	686.44	
3	209.25	360.18	360.18	470.37	569.11	582.43	652.29	652.29	795.86	816.39	
4	209.65	392.23	392.23	521.33	639.50	657.42	735.66	735.66	902.78	929.71	
5	211.89	422.68	422.68	568.26	703.45	725.33	810.93	810.93	998.70	1031.12	
6	214.96	451.44	451.44	611.83	762.31	787.69	879.96	879.96	1086.35	1123.63	
7	218.46	478.66	478.66	652.60	817.07	845.61	944.05	944.05	1167.52	1209.20	
8	222.17	504.52	504.52	691.02	868.47	899.88	1004.10	1004.10	1243.45	1289.16	
9	225.99	529.18	529.18	727.45	917.04	951.12	1060.79	1060.79	1315.02	1364.48	
10	229.87	552.78	552.78	762.16	963.20	999.76	1114.62	1114.62	1382.92	1435.87	
a/b (β) = 1, Es = 51 MPa, ν_s = 0.33, ρ_s = 1850 kg/m³, γ = 2											
1	243.18	303.34	303.34	354.40	395.01	396.23	437.23	437.23	508.63	510.25	
2	213.72	316.57	316.57	396.55	464.85	471.25	527.19	527.19	633.50	643.94	
3	207.21	343.92	343.92	445.22	534.99	546.37	612.00	612.00	744.49	762.17	

4	206.35	372.18	372.18	491.10	598.90	614.57	688.02	688.02	842.36	866.04
5	207.63	399.45	399.45	533.71	657.31	676.70	756.96	756.96	930.47	959.30
6	209.91	425.41	425.41	573.43	711.25	733.93	820.36	820.36	1011.13	1044.53
7	212.69	450.10	450.10	610.72	761.54	787.19	879.30	879.30	1085.92	1123.44
8	215.76	473.63	473.63	645.92	808.80	837.16	934.60	934.60	1155.94	1197.24
9	218.99	496.12	496.12	679.35	853.51	884.38	986.84	986.84	1221.98	1266.79
10	222.31	517.69	517.69	711.23	896.03	929.23	1036.47	1036.47	1284.66	1332.75
a/b (β) = 1, Es = 51 MPa, ν_s = 0.33, ρ_s = 1850 kg/m³, γ = 3										
1	261.42	307.84	307.84	348.77	380.48	380.77	415.48	415.48	474.13	474.13
2	220.40	302.64	302.64	368.92	423.87	427.57	476.68	476.68	566.31	572.45
3	208.91	319.65	319.65	404.58	477.88	485.54	543.58	543.58	655.86	668.12
4	205.03	340.32	340.32	440.58	529.39	540.69	605.65	605.65	736.80	754.28
5	204.13	361.36	361.36	474.95	577.37	591.91	662.78	662.78	810.44	832.46
6	204.66	381.94	381.94	507.45	622.14	639.58	715.74	715.74	878.26	904.31
7	205.96	401.81	401.81	538.23	664.14	684.22	765.23	765.23	941.37	971.06
8	207.72	420.96	420.96	567.46	703.79	726.28	811.80	811.80	1000.61	1033.64
9	209.76	439.40	439.40	595.34	741.41	766.13	855.91	855.91	1056.59	1092.71
10	211.98	457.17	457.17	622.01	777.27	804.07	897.90	897.90	1109.78	1148.80
a/b (β) = 1, Es = 51 MPa, ν_s = 0.28, ρ_s = 1850 kg/m³, γ = 1.5										
1	227.74	298.68	298.68	357.23	404.83	407.21	452.25	452.25	532.54	536.38
2	206.51	325.08	325.08	414.91	493.18	502.03	562.25	562.25	680.53	694.50
3	203.48	359.80	359.80	472.78	574.62	589.07	659.60	659.60	806.49	828.36
4	204.78	393.49	393.49	525.68	647.25	666.36	745.42	745.42	916.25	944.58
5	207.65	425.21	425.21	574.15	713.00	736.12	822.68	822.68	1014.52	1048.39

6	211.21	455.03	455.03	619.01	773.40	800.05	893.43	893.43	1104.21	1142.99
7	215.12	483.16	483.16	660.92	829.53	859.36	959.04	959.04	1187.21	1230.42
8	219.18	509.82	509.82	700.37	882.16	914.89	1020.49	1020.49	1264.82	1312.10
9	223.32	535.21	535.21	737.73	931.87	967.28	1078.46	1078.46	1337.95	1389.01
10	227.48	559.48	559.48	773.31	979.08	1017.00	1133.48	1133.48	1407.30	1461.90
a/b (β) = 1, Es = 51 MPa, ν_s = 0.23, ρ_s = 1850 kg/m³, γ = 1.5										
1	221.32	295.15	295.15	355.57	405.04	407.85	453.70	453.70	536.17	540.74
2	202.63	325.25	325.25	417.42	498.17	507.79	568.79	568.79	689.86	704.84
3	200.64	361.91	361.91	477.62	582.37	597.71	669.16	669.16	819.35	842.34
4	202.57	396.99	396.99	532.23	657.07	677.14	757.27	757.27	931.85	961.38
5	205.90	429.82	429.82	582.11	724.53	748.67	836.45	836.45	1032.44	1067.58
6	209.84	460.58	460.58	628.19	786.42	814.13	908.89	908.89	1124.18	1164.29
7	214.06	489.54	489.54	671.18	843.89	874.81	976.03	976.03	1209.04	1253.64
8	218.41	516.95	516.95	711.61	897.75	931.60	1038.86	1038.86	1288.34	1337.07
9	222.80	543.02	543.02	749.89	948.59	985.16	1098.13	1098.13	1363.06	1415.63
10	227.19	567.93	567.93	786.32	996.86	1035.97	1154.37	1154.37	1433.91	1490.06

Table 5.46

Parametric study of frequency parameters for various parameters of FFFF plate

a/b (β) = 1.25, Es = 51 MPa, ν_s = 0.33, ρ_s = 1850 kg/m³, γ = 1.5										
H (m)	λ_1	λ_2	λ_3	λ_4	λ_5	λ_6	λ_7	λ_8	λ_9	λ_{10}
1	363.51	439.99	471.07	533.72	557.47	633.54	635.68	682.73	703.69	767.38
2	320.33	452.74	502.09	599.99	649.20	762.10	765.98	834.40	880.21	960.74
3	310.85	487.83	551.18	674.76	744.82	882.27	892.28	973.56	1039.10	1131.10
4	309.65	525.09	600.22	744.94	832.63	990.27	1005.70	1097.38	1179.30	1280.98

5	311.59	561.42	646.92	810.02	913.11	1088.37	1108.59	1209.34	1305.41	1415.76
6	314.99	596.22	691.07	870.64	987.54	1178.67	1203.17	1312.10	1420.76	1539.07
7	319.14	629.45	732.87	927.51	1056.99	1262.68	1291.08	1407.55	1527.63	1653.37
8	323.71	661.22	772.59	981.20	1122.29	1341.54	1373.51	1497.02	1627.61	1760.34
9	328.51	691.64	810.47	1032.16	1184.09	1416.06	1451.35	1581.49	1721.87	1861.23
10	333.45	720.86	846.73	1080.76	1242.87	1486.88	1525.29	1661.70	1811.27	1956.96
a/b (β) = 1.5, Es = 51 MPa, ν_s = 0.33, ρ_s = 1850 kg/m³, γ = 1.5										
1	514.46	598.27	671.16	728.18	738.88	849.34	891.82	906.74	959.60	995.16
2	448.05	596.56	713.41	819.72	820.23	998.01	1084.16	1096.11	1171.61	1227.21
3	431.82	632.19	782.71	917.70	927.62	1146.22	1266.38	1277.13	1368.61	1437.66
4	428.12	673.39	852.30	1010.33	1029.46	1281.07	1429.34	1439.76	1544.43	1624.15
5	429.22	714.79	918.66	1096.67	1123.93	1404.27	1576.84	1587.30	1703.51	1792.38
6	432.58	755.06	981.45	1177.34	1211.87	1518.04	1712.25	1722.92	1849.56	1946.58
7	437.15	793.87	1040.93	1253.15	1294.26	1624.12	1838.00	1848.99	1985.19	2089.66
8	442.40	831.21	1097.45	1324.81	1371.96	1723.84	1955.85	1967.19	2112.30	2223.68
9	448.06	867.15	1151.37	1392.89	1445.64	1818.18	2067.10	2078.81	2232.29	2350.14
10	453.96	901.79	1202.98	1457.86	1515.84	1907.92	2172.73	2184.82	2346.21	2470.19
a/b (β) = 1.75, Es = 51 MPa, ν_s = 0.33, ρ_s = 1850 kg/m³, γ = 1.5										
1	691.92	781.89	906.93	922.42	978.89	1096.43	1101.55	1229.10	1253.05	1284.82
2	597.11	759.89	961.98	1006.92	1076.50	1267.44	1304.52	1485.51	1517.64	1565.00
3	572.28	793.78	1054.90	1124.27	1199.82	1445.95	1510.12	1731.08	1766.09	1826.76
4	565.13	837.65	1148.56	1238.54	1318.22	1610.22	1697.13	1951.76	1988.35	2060.59
5	564.81	883.28	1238.01	1345.93	1429.05	1761.08	1867.65	2152.00	2189.74	2272.24
6	567.76	928.42	1322.70	1446.63	1532.84	1900.80	2024.82	2336.08	2374.79	2466.58

7	572.47	972.37	1402.94	1541.41	1630.52	2031.33	2171.13	2507.17	2546.78	2647.09
8	578.20	1014.94	1479.22	1631.07	1722.94	2154.19	2308.48	2667.59	2708.06	2816.29
9	584.56	1056.12	1551.98	1716.28	1810.81	2270.54	2438.29	2819.08	2860.38	2976.02
10	591.31	1095.97	1621.64	1797.62	1894.71	2381.31	2561.64	2962.96	3005.07	3127.69
a/b (β) = 2, Es = 51 MPa, ν_s = 0.33, ρ_s = 1850 kg/m³, γ = 1.5										
1	896.01	991.20	1140.88	1178.48	1254.02	1333.60	1377.55	1543.33	1558.37	1600.77
2	767.65	943.14	1211.64	1247.90	1369.16	1539.48	1571.37	1839.59	1901.15	1935.65
3	732.33	973.02	1335.64	1367.85	1521.54	1765.04	1782.71	2127.62	2224.99	2258.58
4	720.75	1018.30	1460.74	1489.12	1669.10	1973.97	1979.22	2387.68	2513.43	2549.90
5	718.42	1067.32	1580.01	1605.07	1807.70	2160.49	2165.98	2624.31	2773.92	2814.64
6	720.56	1116.73	1692.71	1714.90	1937.74	2328.82	2343.73	2842.29	3012.81	3058.11
7	725.12	1165.36	1799.32	1819.00	2060.27	2486.35	2509.66	3045.20	3234.53	3284.40
8	731.12	1212.81	1900.50	1917.97	2176.28	2634.80	2665.70	3235.69	3442.27	3496.54
9	738.01	1258.94	1996.91	2012.40	2286.65	2775.51	2813.37	3415.74	3638.33	3696.83
10	745.47	1303.75	2089.09	2102.80	2392.08	2909.55	2953.83	3586.87	3824.46	3886.99

Table 5.47

Parametric study of frequency parameters for various parameters of FFFF plate

Es (Mpa)	λ_1	λ_2	λ_3	λ_4	λ_5	λ_6	λ_7	λ_8	λ_9	λ_{10}
a/b (β) = 1, H = 3 m, ν_s = 0.33, ρ_s = 1850 kg/m³, γ = 1.5										
51	209.25	360.18	360.18	470.37	569.11	582.43	652.29	652.29	795.86	816.39
52	211.27	363.67	363.67	474.90	574.63	588.05	658.57	658.57	803.49	824.23
53	213.28	367.12	367.12	479.39	580.10	593.61	664.79	664.79	811.05	832.01
54	215.27	370.54	370.54	483.84	585.51	599.12	670.95	670.95	818.54	839.71
55	217.24	373.93	373.93	488.25	590.88	604.57	677.06	677.06	825.97	847.34

56	219.19	377.29	377.29	492.61	596.20	609.98	683.11	683.11	833.32	854.90
57	221.12	380.61	380.61	496.94	601.47	615.34	689.10	689.10	840.61	862.39
58	223.04	383.91	383.91	501.23	606.69	620.66	695.05	695.05	847.84	869.82
59	224.94	387.18	387.18	505.48	611.87	625.93	700.94	700.94	855.00	877.19
60	226.82	390.43	390.43	509.69	617.01	631.15	706.78	706.78	862.10	884.50
a/b (β) = 1, H = 5 m, ν_s = 0.33, ρ_s = 1850 kg/m³, γ = 1.5										
51	211.89	422.68	422.68	568.26	703.45	725.33	810.93	810.93	998.70	1031.12
52	213.93	426.77	426.77	573.74	710.29	732.34	818.76	818.76	1008.33	1041.09
53	215.95	430.82	430.82	579.17	717.06	739.28	826.52	826.52	1017.86	1050.95
54	217.95	434.83	434.83	584.55	723.77	746.16	834.20	834.20	1027.31	1060.73
55	219.93	438.81	438.81	589.87	730.42	752.98	841.82	841.82	1036.67	1070.42
56	221.90	442.75	442.75	595.15	737.01	759.73	849.36	849.36	1045.95	1080.02
57	223.85	446.65	446.65	600.39	743.54	766.42	856.84	856.84	1055.14	1089.53
58	225.78	450.52	450.52	605.57	750.01	773.06	864.26	864.26	1064.26	1098.97
59	227.69	454.36	454.36	610.71	756.43	779.63	871.61	871.61	1073.30	1108.32
60	229.59	458.16	458.16	615.81	762.79	786.16	878.90	878.90	1082.26	1117.59
a/b (β) = 1, H = 7 m, ν_s = 0.33, ρ_s = 1850 kg/m³, γ = 1.5										
51	218.46	478.66	478.66	652.60	817.07	845.61	944.05	944.05	1167.52	1209.20
52	220.55	483.29	483.29	658.90	825.02	853.79	953.19	953.19	1178.80	1220.91
53	222.63	487.88	487.88	665.14	832.90	861.90	962.23	962.23	1189.98	1232.51
54	224.69	492.43	492.43	671.32	840.70	869.93	971.20	971.20	1201.05	1244.00
55	226.73	496.93	496.93	677.45	848.43	877.89	980.08	980.08	1212.03	1255.39
56	228.75	501.39	501.39	683.52	856.09	885.77	988.88	988.88	1222.90	1266.67
57	230.75	505.82	505.82	689.53	863.68	893.59	997.60	997.60	1233.68	1277.86

58	232.73	510.20	510.20	695.49	871.21	901.33	1006.25	1006.25	1244.36	1288.95
59	234.70	514.55	514.55	701.41	878.67	909.01	1014.82	1014.82	1254.95	1299.94
60	236.65	518.86	518.86	707.27	886.07	916.63	1023.33	1023.33	1265.45	1310.84

Table 5.48

Parametric study of frequency parameters for various parameters of SSSS plate

a/b = 1, Es = 51 MPa, ν_s = 0.33, ρ_s = 1850 kg/m³, γ = 1										
H (m)	λ_1	λ_2	λ_3	λ_4	λ_5	λ_6	λ_7	λ_8	λ_9	λ_{10}
1	290.40	400.97	400.97	488.50	540.44	540.45	610.13	610.13	695.78	695.78
2	341.72	517.19	517.19	647.22	722.87	722.93	821.67	821.67	942.31	942.31
3	400.78	620.92	620.92	781.16	874.19	874.31	994.32	994.32	1141.44	1141.44
4	455.32	711.61	711.61	896.76	1004.29	1004.48	1142.20	1142.20	1311.66	1311.66
5	505.12	792.68	792.68	999.57	1119.84	1120.09	1273.34	1273.34	1462.55	1462.55
6	550.94	866.51	866.51	1092.96	1224.73	1225.06	1392.31	1392.31	1599.42	1599.42
7	593.50	934.69	934.69	1179.09	1321.43	1321.83	1501.95	1501.95	1725.54	1725.54
8	633.37	998.32	998.32	1259.40	1411.58	1412.04	1604.14	1604.14	1843.09	1843.09
9	670.97	1058.18	1058.18	1334.92	1496.35	1496.87	1700.22	1700.22	1953.60	1953.60
10	706.64	1114.88	1114.88	1406.42	1576.58	1577.17	1791.15	1791.15	2058.21	2058.21
a/b = 1, Es = 51 MPa, ν_s = 0.33, ρ_s = 1850 kg/m³, γ = 1.5										
1	283.09	383.89	383.89	464.85	513.14	513.15	578.33	578.33	658.67	658.67
2	324.75	487.62	487.62	609.07	679.82	679.87	772.57	772.57	885.77	885.77
3	377.95	583.24	583.24	733.23	820.29	820.39	933.10	933.10	1071.04	1071.04
4	428.06	667.49	667.49	840.89	941.54	941.70	1071.02	1071.02	1229.84	1229.84
5	474.16	743.02	743.02	936.83	1049.40	1049.62	1193.49	1193.49	1370.75	1370.75
6	516.74	811.91	811.91	1024.06	1147.40	1147.68	1304.67	1304.67	1498.64	1498.64

7	556.37	875.59	875.59	1104.55	1237.78	1238.12	1407.16	1407.16	1616.53	1616.53
8	593.54	935.04	935.04	1179.63	1322.07	1322.46	1502.71	1502.71	1726.44	1726.44
9	628.63	991.00	991.00	1250.25	1401.33	1401.79	1592.56	1592.56	1829.79	1829.79
10	661.93	1044.01	1044.01	1317.11	1476.38	1476.89	1677.61	1677.61	1927.62	1927.62
a/b = 1, Es = 51 MPa, ν_s = 0.33, ρ_s = 1850 kg/m³, γ = 2										
1	278.85	368.42	368.42	441.87	486.05	486.06	546.18	546.18	620.63	620.63
2	308.24	456.98	456.98	568.97	634.35	634.39	720.49	720.49	825.64	825.64
3	354.39	543.33	543.33	682.12	762.72	762.80	867.57	867.57	995.63	995.63
4	399.38	620.38	620.38	781.03	874.25	874.37	994.60	994.60	1141.95	1141.95
5	441.30	689.82	689.82	869.45	973.72	973.89	1107.63	1107.63	1272.02	1272.02
6	480.26	753.30	753.30	949.97	1064.22	1064.44	1210.34	1210.34	1390.18	1390.18
7	516.64	812.06	812.06	1024.34	1147.75	1148.02	1305.09	1305.09	1499.17	1499.17
8	550.85	866.97	866.97	1093.74	1225.68	1226.01	1393.46	1393.46	1600.81	1600.81
9	583.18	918.69	918.69	1159.05	1299.00	1299.38	1476.58	1476.58	1696.41	1696.41
10	613.90	967.70	967.70	1220.91	1368.42	1368.85	1555.27	1555.27	1786.92	1786.92
a/b = 1, Es = 51 MPa, ν_s = 0.33, ρ_s = 1850 kg/m³, γ = 3										
1	282.97	350.99	350.99	409.82	446.05	446.06	496.39	496.39	559.68	559.68
2	285.15	406.77	406.77	500.96	556.42	556.44	630.34	630.34	720.85	720.85
3	316.18	474.46	474.46	592.64	661.48	661.52	751.86	751.86	862.12	862.12
4	350.68	537.66	537.66	675.06	754.84	754.91	858.67	858.67	985.46	985.46
5	384.33	595.62	595.62	749.55	838.86	838.97	954.41	954.41	1095.74	1095.74
6	416.32	649.08	649.08	817.77	915.65	915.80	1041.72	1041.72	1196.23	1196.23
7	446.56	698.80	698.80	880.97	986.72	986.90	1122.43	1122.43	1289.09	1289.09
8	475.21	745.42	745.42	940.07	1053.13	1053.35	1197.80	1197.80	1375.78	1375.78

9	502.43	789.41	789.41	995.76	1115.68	1115.93	1268.75	1268.75	1457.39	1457.39
10	528.39	831.15	831.15	1048.54	1174.95	1175.25	1335.97	1335.97	1534.71	1534.71
a/b = 1, Es = 51 MPa, ν_s = 0.28, ρ_s = 1850 kg/m³, γ = 1.5										
1	277.25	382.94	382.94	466.77	516.55	516.56	583.49	583.49	665.80	665.80
2	326.14	493.72	493.72	618.05	690.37	690.42	785.02	785.02	900.50	900.50
3	382.46	592.64	592.64	745.78	834.64	834.74	949.62	949.62	1090.25	1090.25
4	434.48	679.14	679.14	856.03	958.70	958.86	1090.63	1090.63	1252.52	1252.52
5	481.99	756.47	756.47	954.10	1068.90	1069.12	1215.69	1215.69	1396.38	1396.38
6	525.70	826.90	826.90	1043.18	1168.95	1169.23	1329.16	1329.16	1526.89	1526.89
7	566.31	891.94	891.94	1125.34	1261.18	1261.53	1433.73	1433.73	1647.15	1647.15
8	604.34	952.64	952.64	1201.95	1347.17	1347.58	1531.20	1531.20	1759.26	1759.26
9	640.21	1009.75	1009.75	1273.99	1428.02	1428.50	1622.84	1622.84	1864.66	1864.66
10	674.24	1063.84	1063.84	1342.20	1504.56	1505.09	1709.58	1709.58	1964.42	1964.42
a/b = 1, Es = 51 MPa, ν_s = 0.23, ρ_s = 1850 kg/m³, γ = 1.5										
1	275.29	385.11	385.11	471.46	522.56	522.58	591.12	591.12	675.25	675.25
2	329.51	501.46	501.46	628.59	702.47	702.53	799.04	799.04	916.84	916.84
3	388.34	603.31	603.31	759.66	850.35	850.47	967.59	967.59	1111.02	1111.02
4	442.02	691.96	691.96	872.46	977.22	977.40	1111.72	1111.72	1276.83	1276.83
5	490.81	771.07	771.07	972.68	1089.81	1090.05	1239.46	1239.46	1423.75	1423.75
6	535.60	843.04	843.04	1063.67	1191.97	1192.28	1355.31	1355.31	1556.98	1556.98
7	577.16	909.48	909.48	1147.55	1286.13	1286.50	1462.05	1462.05	1679.74	1679.74
8	616.05	971.46	971.46	1225.75	1373.91	1374.34	1561.53	1561.53	1794.15	1794.15
9	652.72	1029.77	1029.77	1299.29	1456.42	1456.92	1655.04	1655.04	1901.71	1901.71
10	687.49	1084.98	1084.98	1368.89	1534.53	1535.09	1743.56	1743.56	2003.52	2003.52

Table 5.49

Parametric study of frequency parameters for various parameters of SSSS plate

a/b (β) = 1.25, Es = 51 MPa, ν_s = 0.33, ρ_s = 1850 kg/m³, γ = 1.5										
H (m)	λ_1	λ_2	λ_3	λ_4	λ_5	λ_6	λ_7	λ_8	λ_9	λ_{10}
1	419.83	529.62	583.07	668.26	676.85	788.89	792.53	845.57	856.06	943.61
2	467.99	651.90	736.08	865.62	878.71	1043.72	1048.34	1125.33	1139.90	1263.65
3	539.68	773.85	879.24	1039.76	1056.13	1259.21	1264.31	1358.98	1376.38	1526.80
4	608.97	883.18	1005.78	1191.62	1210.74	1445.37	1450.75	1560.25	1579.96	1752.65
5	673.34	981.87	1119.39	1327.25	1348.78	1611.03	1616.61	1739.18	1760.86	1953.13
6	733.07	1072.19	1223.08	1450.71	1474.43	1761.57	1767.31	1901.69	1925.15	2135.10
7	788.81	1155.82	1318.95	1564.70	1590.42	1900.43	1906.29	2051.55	2076.64	2302.85
8	841.18	1233.99	1408.48	1671.06	1698.66	2029.94	2035.90	2191.29	2217.88	2459.23
9	890.67	1307.63	1492.77	1771.13	1800.49	2151.73	2157.79	2322.70	2350.70	2606.27
10	937.68	1377.43	1572.62	1865.90	1896.92	2267.04	2273.19	2447.11	2476.44	2745.47
a/b (β) = 1.5, Es = 51 MPa, ν_s = 0.33, ρ_s = 1850 kg/m³, γ = 1.5										
1	586.24	702.25	826.24	863.82	914.11	1046.11	1052.90	1125.80	1194.16	1210.25
2	640.99	840.74	1039.21	1097.29	1174.00	1370.90	1381.43	1488.24	1586.51	1609.08
3	734.31	990.74	1240.27	1312.54	1407.67	1650.54	1663.94	1795.32	1915.18	1942.29
4	826.34	1127.61	1418.38	1502.19	1612.35	1893.05	1908.92	2060.71	2198.47	2229.29
5	912.44	1251.99	1578.41	1672.23	1795.47	2109.16	2127.23	2296.93	2450.35	2484.39
6	992.63	1366.19	1724.51	1827.31	1962.30	2305.68	2325.76	2511.62	2679.14	2716.08
7	1067.63	1472.13	1859.64	1970.66	2116.39	2487.01	2508.95	2709.65	2890.13	2929.72
8	1138.17	1571.29	1985.85	2104.50	2260.23	2656.16	2679.83	2894.35	3086.87	3128.92
9	1204.88	1664.76	2104.68	2230.48	2395.58	2815.26	2840.57	3068.06	3271.90	3316.24

10	1268.29	1753.39	2217.26	2349.82	2523.77	2965.90	2992.76	3232.52	3447.05	3493.58
a/b (β) = 1.75, Es = 51 MPa, ν_s = 0.33, ρ_s = 1850 kg/m^3, γ = 1.5										
1	782.54	902.95	1075.85	1113.49	1203.14	1282.43	1340.72	1511.63	1515.14	1523.90
2	844.31	1056.05	1337.82	1397.18	1535.50	1656.00	1742.94	1995.27	1999.53	2013.48
3	962.63	1236.25	1592.17	1666.58	1838.64	1988.12	2095.18	2406.11	2410.60	2428.75
4	1081.10	1403.43	1818.88	1905.55	2105.05	2278.33	2401.87	2761.40	2765.93	2787.77
5	1192.57	1556.33	2023.06	2120.37	2343.70	2537.71	2675.59	3077.69	3082.19	3107.35
6	1296.65	1697.16	2209.70	2316.56	2561.25	2773.92	2924.68	3365.16	3369.61	3397.82
7	1394.14	1828.03	2382.41	2498.03	2762.28	2992.04	3154.61	3630.35	3634.72	3665.76
8	1485.92	1950.65	2543.81	2667.54	2949.95	3195.61	3369.15	3877.69	3881.97	3915.67
9	1572.78	2066.33	2695.80	2827.15	3126.58	3387.15	3570.98	4110.31	4114.51	4150.70
10	1655.37	2176.07	2839.83	2978.37	3293.89	3568.55	3762.10	4330.56	4334.67	4373.23
a/b (β) = 2, Es = 51 MPa, ν_s = 0.33, ρ_s = 1850 kg/m^3, γ = 1.5										
1	1008.84	1132.43	1314.29	1444.86	1535.73	1535.73	1677.43	1784.36	1859.92	1983.21
2	1078.24	1299.14	1602.16	1810.06	1950.87	1950.88	2166.21	2326.59	2437.59	2619.46
3	1225.08	1512.05	1897.19	2158.27	2333.61	2333.63	2600.45	2798.94	2934.98	3159.56
4	1373.80	1712.60	2163.27	2467.42	2670.82	2670.86	2979.81	3209.76	3366.35	3626.58
5	1514.32	1897.09	2404.01	2745.44	2973.17	2973.23	3318.83	3576.28	3750.78	4042.34
6	1645.80	2067.48	2624.55	2999.39	3248.94	3249.01	3627.53	3909.77	4100.37	4420.23
7	1769.08	2226.10	2828.91	3234.29	3503.82	3503.91	3912.60	4217.59	4422.94	4768.83
8	1885.22	2374.85	3020.02	3453.75	3741.82	3741.92	4178.63	4504.77	4723.84	5093.96
9	1995.19	2515.28	3200.08	3660.38	3965.84	3965.95	4428.94	4774.94	5006.87	5399.75
10	2099.79	2648.56	3370.77	3856.17	4178.04	4178.17	4665.99	5030.76	5274.85	5689.27

Table 5.50

Parametric study of frequency parameters for various parameters of SSSS plate

Es (Mpa)	λ_1	λ_2	λ_3	λ_4	λ_5	λ_6	λ_7	λ_8	λ_9	λ_{10}
$a/b = 1$, $H = 3$ m, $\nu_s = 0.33$, $\rho_s = 1850$ kg/m³, $\gamma = 1.5$										
51	377.95	583.24	583.24	733.23	820.29	820.39	933.10	933.10	1071.04	1071.04
52	381.62	588.88	588.88	740.28	828.17	828.27	942.00	942.00	1081.22	1081.22
53	385.26	594.47	594.47	747.26	835.97	836.08	950.81	950.81	1091.31	1091.31
54	388.87	600.01	600.01	754.18	843.70	843.81	959.54	959.54	1101.30	1101.30
55	392.44	605.50	605.50	761.03	851.36	851.47	968.19	968.19	1111.20	1111.20
56	395.98	610.93	610.93	767.83	858.95	859.07	976.77	976.77	1121.02	1121.02
57	399.49	616.32	616.32	774.56	866.48	866.59	985.27	985.27	1130.75	1130.75
58	402.97	621.66	621.66	781.24	873.93	874.06	993.70	993.70	1140.39	1140.39
59	406.41	626.96	626.96	787.85	881.33	881.46	1002.05	1002.05	1149.96	1149.96
60	409.83	632.21	632.21	794.42	888.66	888.79	1010.34	1010.34	1159.44	1159.44
$a/b = 1$, $H = 5$ m, $\nu_s = 0.33$, $\rho_s = 1850$ kg/m³, $\gamma = 1.5$										
51	474.16	743.02	743.02	936.83	1049.40	1049.62	1193.49	1193.49	1370.75	1370.75
52	478.78	750.23	750.23	945.87	1059.54	1059.76	1204.95	1204.95	1383.91	1383.91
53	483.35	757.37	757.37	954.84	1069.57	1069.80	1216.31	1216.31	1396.94	1396.94
54	487.87	764.44	764.44	963.71	1079.52	1079.75	1227.56	1227.56	1409.85	1409.85
55	492.36	771.45	771.45	972.51	1089.37	1089.61	1238.71	1238.71	1422.64	1422.64
56	496.80	778.39	778.39	981.23	1099.13	1099.38	1249.75	1249.75	1435.32	1435.32
57	501.21	785.28	785.28	989.87	1108.81	1109.06	1260.70	1260.70	1447.89	1447.89
58	505.58	792.10	792.10	998.43	1118.40	1118.66	1271.56	1271.56	1460.35	1460.35
59	509.91	798.86	798.86	1006.92	1127.91	1128.17	1282.32	1282.32	1472.71	1472.71

60	514.20	805.57	805.57	1015.34	1137.34	1137.61	1292.99	1292.99	1484.96	1484.96
a/b = 1, H = 7 m, ν_s = 0.33, ρ_s = 1850 kg/m³, γ = 1.5										
51	556.37	875.59	875.59	1104.55	1237.78	1238.12	1407.16	1407.16	1616.53	1616.53
52	561.79	884.09	884.09	1115.24	1249.77	1250.11	1420.72	1420.72	1632.12	1632.12
53	567.15	892.51	892.51	1125.83	1261.63	1261.99	1434.16	1434.16	1647.55	1647.55
54	572.47	900.86	900.86	1136.32	1273.39	1273.75	1447.47	1447.47	1662.84	1662.84
55	577.73	909.13	909.13	1146.71	1285.04	1285.41	1460.66	1460.66	1677.99	1677.99
56	582.95	917.32	917.32	1157.01	1296.59	1296.96	1473.73	1473.73	1693.01	1693.01
57	588.12	925.44	925.44	1167.22	1308.03	1308.41	1486.68	1486.68	1707.89	1707.89
58	593.25	933.49	933.49	1177.34	1319.37	1319.76	1499.52	1499.52	1722.65	1722.65
59	598.33	941.48	941.48	1187.37	1330.62	1331.02	1512.25	1512.25	1737.28	1737.28
60	603.37	949.39	949.39	1197.32	1341.77	1342.18	1524.88	1524.88	1751.79	1751.79

Table 5.51

Parametric study of frequency parameters for various parameters of CCCC plate

a/b = 1, Es = 51 MPa, ν_s = 0.33, ρ_s = 1850 kg/m³, γ = 1										
H (m)	λ_1	λ_2	λ_3	λ_4	λ_5	λ_6	λ_7	λ_8	λ_9	λ_{10}
1	298.25	415.37	415.37	507.99	562.25	562.25	636.29	636.29	725.42	725.42
2	351.91	534.26	534.26	670.03	747.63	747.63	851.85	851.85	975.10	975.10
3	412.29	639.80	639.80	806.61	901.35	901.35	1028.05	1028.05	1177.14	1177.14
4	467.89	732.09	732.09	924.61	1033.67	1033.67	1179.23	1179.23	1350.14	1350.14
5	518.61	814.63	814.63	1029.65	1151.30	1151.30	1313.47	1313.47	1503.65	1503.65
6	565.29	889.84	889.84	1125.15	1258.16	1258.16	1435.37	1435.37	1643.01	1643.01
7	608.66	959.32	959.32	1213.27	1356.73	1356.73	1547.78	1547.78	1771.51	1771.51
8	649.28	1024.19	1024.19	1295.48	1448.67	1448.67	1652.61	1652.61	1891.33	1891.33

9	687.60	1085.24	1085.24	1372.81	1535.14	1535.14	1751.20	1751.20	2004.02	2004.02
10	723.96	1143.08	1143.08	1446.04	1617.02	1617.02	1844.54	1844.54	2110.72	2110.72
a/b = 1, Es = 51 MPa, ν_s = 0.33, ρ_s = 1850 kg/m³, γ = 1.5										
1	290.58	397.88	397.88	483.86	534.54	534.55	603.97	603.97	687.93	687.93
2	334.58	504.21	504.21	631.22	703.98	703.98	801.86	801.86	917.85	917.85
3	389.05	601.52	601.52	757.75	846.61	846.61	965.56	965.56	1105.69	1105.69
4	440.15	687.22	687.22	867.59	969.85	969.85	1106.45	1106.45	1266.96	1266.96
5	487.11	764.09	764.09	965.55	1079.60	1079.60	1231.73	1231.73	1410.24	1410.24
6	530.47	834.24	834.24	1054.70	1179.38	1179.38	1345.57	1345.57	1540.39	1540.39
7	570.84	899.10	899.10	1137.01	1271.47	1271.47	1450.59	1450.59	1660.45	1660.45
8	608.71	959.69	959.69	1213.83	1357.39	1357.39	1548.56	1548.56	1772.43	1772.43
9	644.46	1016.74	1016.74	1286.11	1438.22	1438.22	1640.73	1640.73	1877.77	1877.77
10	678.40	1070.79	1070.79	1354.57	1514.78	1514.78	1728.00	1728.00	1977.53	1977.53
a/b = 1, Es = 51 MPa, ν_s = 0.33, ρ_s = 1850 kg/m³, γ = 2										
1	285.85	381.86	381.86	460.29	506.94	506.95	571.21	571.21	649.46	649.46
2	317.64	473.04	473.04	590.40	657.87	657.87	748.86	748.86	856.98	856.98
3	365.04	560.95	560.95	705.68	788.16	788.16	898.72	898.72	1029.20	1029.20
4	410.95	639.32	639.32	806.52	901.45	901.45	1028.37	1028.37	1177.69	1177.69
5	453.66	709.95	709.95	896.75	1002.59	1002.59	1143.89	1143.89	1309.85	1309.85
6	493.33	774.56	774.56	978.99	1094.68	1094.68	1248.99	1248.99	1430.02	1430.02
7	530.39	834.39	834.39	1054.99	1179.74	1179.74	1346.02	1346.02	1540.94	1540.94
8	565.23	890.33	890.33	1125.97	1259.14	1259.14	1436.57	1436.57	1644.44	1644.44
9	598.16	943.03	943.03	1192.78	1333.87	1333.87	1521.77	1521.77	1741.83	1741.83
10	629.46	992.99	992.99	1256.08	1404.66	1404.66	1602.48	1602.48	1834.08	1834.08

a/b = 1, Es = 51 MPa, ν_s = 0.33, ρ_s = 1850 kg/m³, γ = 3										
1	288.87	363.09	363.09	426.84	465.71	465.72	520.10	520.10	587.55	587.55
2	293.60	421.78	421.78	521.08	578.78	578.79	657.14	657.14	750.99	750.99
3	325.91	490.90	490.90	614.55	685.43	685.43	780.83	780.83	893.95	893.95
4	361.28	555.21	555.21	698.51	780.17	780.17	889.67	889.67	1018.91	1018.91
5	395.63	614.15	614.15	774.43	865.50	865.50	987.34	987.34	1130.79	1130.79
6	428.23	668.52	668.52	844.02	943.55	943.55	1076.52	1076.52	1232.84	1232.84
7	459.04	719.11	719.11	908.52	1015.82	1015.82	1159.04	1159.04	1327.20	1327.20
8	488.21	766.55	766.55	968.89	1083.40	1083.40	1236.16	1236.16	1415.38	1415.38
9	515.93	811.33	811.33	1025.79	1147.09	1147.09	1308.80	1308.80	1498.42	1498.42
10	542.36	853.85	853.85	1079.75	1207.46	1207.46	1377.65	1377.65	1577.12	1577.12
a/b = 1, Es = 51 MPa, ν_s = 0.28, ρ_s = 1850 kg/m³, γ = 1.5										
1	285.05	397.25	397.25	486.10	538.23	538.24	609.44	609.44	695.31	695.31
2	336.17	510.52	510.52	640.44	714.75	714.75	814.61	814.61	932.82	932.82
3	393.73	611.12	611.12	770.59	861.21	861.22	982.46	982.46	1125.22	1125.22
4	446.74	699.10	699.10	883.07	987.32	987.32	1126.52	1126.52	1290.03	1290.03
5	495.11	777.80	777.80	983.22	1099.45	1099.45	1254.48	1254.48	1436.33	1436.33
6	539.63	849.52	849.52	1074.27	1201.34	1201.34	1370.68	1370.68	1569.16	1569.16
7	580.98	915.77	915.77	1158.29	1295.33	1295.33	1477.85	1477.85	1691.65	1691.65
8	619.73	977.64	977.64	1236.68	1382.99	1382.99	1577.80	1577.80	1805.88	1805.88
9	656.28	1035.86	1035.86	1310.43	1465.45	1465.45	1671.80	1671.80	1913.33	1913.33
10	690.96	1091.02	1091.02	1380.27	1543.54	1543.54	1760.82	1760.82	2015.07	2015.07
a/b = 1, Es = 51 MPa, ν_s = 0.23, ρ_s = 1850 kg/m³, γ = 1.5										
1	283.32	399.65	399.65	491.03	544.46	544.47	617.29	617.29	704.94	704.94

2	339.70	518.44	518.44	651.21	727.06	727.06	828.92	828.92	949.39	949.39
3	399.76	621.99	621.99	784.76	877.20	877.20	1000.82	1000.82	1146.31	1146.31
4	454.44	712.16	712.16	899.85	1006.17	1006.18	1148.10	1148.10	1314.75	1314.75
5	504.11	792.67	792.67	1002.21	1120.75	1120.75	1278.81	1278.81	1464.18	1464.18
6	549.72	865.97	865.97	1095.22	1224.81	1224.81	1397.47	1397.47	1599.81	1599.81
7	592.05	933.66	933.66	1181.02	1320.77	1320.77	1506.88	1506.88	1724.85	1724.85
8	631.67	996.83	996.83	1261.05	1410.26	1410.26	1608.90	1608.90	1841.45	1841.45
9	669.03	1056.28	1056.28	1336.33	1494.43	1494.43	1704.85	1704.85	1951.12	1951.12
10	704.46	1112.59	1112.59	1407.61	1574.12	1574.12	1795.70	1795.70	2054.94	2054.94

Table 5.52

Parametric study of frequency parameters for various parameters of CCCC plate

a/b (β) = 1.25, Es = 51 MPa, ν_s = 0.33, ρ_s = 1850 kg/m³, γ = 1.5										
H (m)	λ_1	λ_2	λ_3	λ_4	λ_5	λ_6	λ_7	λ_8	λ_9	λ_{10}
1	429.09	544.52	603.23	692.30	698.59	821.00	822.07	874.68	891.30	979.70
2	480.50	670.21	760.06	893.85	903.97	1079.81	1082.54	1158.04	1179.92	1304.88
3	553.92	794.19	905.58	1070.96	1083.83	1298.33	1302.24	1394.59	1420.37	1572.55
4	624.52	905.22	1034.15	1225.49	1240.62	1487.27	1492.13	1598.55	1627.65	1802.65
5	690.01	1005.44	1149.62	1363.59	1380.68	1655.55	1661.23	1780.00	1812.05	2007.15
6	750.75	1097.18	1255.05	1489.39	1508.24	1808.58	1814.98	1944.92	1979.65	2192.94
7	807.44	1182.16	1352.56	1605.58	1626.05	1949.81	1956.87	2097.08	2134.28	2364.30
8	860.70	1261.62	1443.67	1714.06	1736.01	2081.59	2089.25	2239.01	2278.54	2524.14
9	911.04	1336.48	1529.46	1816.15	1839.50	2205.57	2213.79	2372.53	2414.24	2674.49
10	958.86	1407.45	1610.76	1912.85	1937.52	2322.98	2331.73	2498.96	2542.75	2816.85

a/b (β) = 1.5, Es = 51 MPa, ν_s = 0.33, ρ_s = 1850 kg/m³, γ = 1.5										
1	598.00	718.86	854.25	886.66	945.08	1081.55	1082.63	1171.23	1241.92	1251.27
2	657.17	861.75	1072.56	1124.54	1210.53	1412.24	1415.61	1539.23	1640.51	1656.42
3	752.84	1014.25	1276.88	1342.62	1447.96	1696.34	1701.37	1850.46	1974.19	1994.87
4	846.59	1153.12	1457.74	1534.71	1655.96	1942.91	1949.29	2119.67	2262.13	2286.73
5	934.17	1279.30	1620.28	1707.00	1842.14	2162.81	2170.35	2359.48	2518.40	2546.40
6	1015.69	1395.16	1768.75	1864.19	2011.85	2362.90	2371.47	2577.57	2751.36	2782.41
7	1091.91	1502.67	1906.10	2009.53	2168.68	2547.63	2557.12	2778.85	2966.32	3000.15
8	1163.61	1603.31	2034.45	2145.27	2315.12	2720.01	2730.35	2966.66	3166.85	3203.26
9	1231.42	1698.19	2155.31	2273.07	2452.97	2882.20	2893.34	3143.36	3355.51	3394.33
10	1295.88	1788.19	2269.86	2394.16	2583.56	3035.81	3047.70	3310.70	3534.16	3575.26
a/b (β) = 1.75, Es = 51 MPa, ν_s = 0.33, ρ_s = 1850 kg/m³, γ = 1.5										
1	797.48	922.02	1100.53	1150.95	1242.84	1313.51	1383.97	1549.59	1563.03	1585.24
2	865.11	1080.73	1367.95	1441.82	1582.46	1692.48	1793.62	2038.66	2055.16	2082.24
3	986.54	1264.03	1625.61	1715.54	1890.33	2028.28	2151.22	2453.60	2472.33	2503.03
4	1107.27	1433.64	1855.11	1958.15	2160.87	2321.73	2462.73	2812.62	2833.26	2867.09
5	1220.64	1588.68	2061.83	2176.29	2403.31	2584.11	2740.93	3132.39	3154.76	3191.42
6	1326.44	1731.47	2250.83	2375.58	2624.44	2823.14	2994.24	3423.17	3447.13	3486.39
7	1425.51	1864.19	2425.78	2559.99	2828.85	3043.94	3228.18	3691.51	3716.94	3758.64
8	1518.77	1988.56	2589.30	2732.31	3019.76	3250.06	3446.53	3941.84	3968.67	4012.67
9	1607.05	2105.91	2743.32	2894.60	3199.48	3444.04	3652.01	4177.34	4205.49	4251.67
10	1690.98	2217.25	2889.30	3048.41	3369.76	3627.79	3846.64	4400.35	4429.76	4478.01
a/b (β) = 2, Es = 51 MPa, ν_s = 0.33, ρ_s = 1850 kg/m³, γ = 1.5										
1	896.01	991.20	1140.88	1178.48	1254.02	1333.60	1377.55	1543.33	1558.37	1600.77

2	767.65	943.14	1211.64	1247.90	1369.16	1539.48	1571.37	1839.59	1901.15	1935.65
3	732.33	973.02	1335.64	1367.85	1521.54	1765.04	1782.71	2127.62	2224.99	2258.58
4	720.75	1018.30	1460.74	1489.12	1669.10	1973.97	1979.22	2387.68	2513.43	2549.90
5	718.42	1067.32	1580.01	1605.07	1807.70	2160.49	2165.98	2624.31	2773.92	2814.64
6	720.56	1116.73	1692.71	1714.90	1937.74	2328.82	2343.73	2842.29	3012.81	3058.11
7	725.12	1165.36	1799.32	1819.00	2060.27	2486.35	2509.66	3045.20	3234.53	3284.40
8	731.12	1212.81	1900.50	1917.97	2176.28	2634.80	2665.70	3235.69	3442.27	3496.54
9	738.01	1258.94	1996.91	2012.40	2286.65	2775.51	2813.37	3415.74	3638.33	3696.83
10	745.47	1303.75	2089.09	2102.80	2392.08	2909.55	2953.83	3586.87	3824.46	3886.99

Table 5.53

Parametric study of frequency parameters for various parameters of CCCC plate

E_s (Mpa)	λ_1	λ_2	λ_3	λ_4	λ_5	λ_6	λ_7	λ_8	λ_9	λ_{10}
a/b = 1, H = 3 m, ν_s = 0.33, ρ_s = 1850 kg/m³, γ = 1.5										
51	389.05	601.52	601.52	757.75	846.61	846.61	965.56	965.56	1105.69	1105.69
52	392.77	607.24	607.24	764.93	854.60	854.60	974.62	974.62	1116.01	1116.01
53	396.46	612.90	612.90	772.03	862.51	862.51	983.61	983.61	1126.24	1126.24
54	400.11	618.52	618.52	779.07	870.35	870.35	992.51	992.51	1136.38	1136.38
55	403.72	624.08	624.08	786.05	878.12	878.12	1001.34	1001.34	1146.42	1146.42
56	407.31	629.60	629.60	792.96	885.83	885.83	1010.08	1010.08	1156.38	1156.38
57	410.86	635.06	635.06	799.82	893.46	893.46	1018.75	1018.75	1166.25	1166.25
58	414.39	640.48	640.48	806.61	901.03	901.03	1027.35	1027.35	1176.03	1176.03
59	417.88	645.85	645.85	813.35	908.54	908.54	1035.87	1035.87	1185.74	1185.74
60	421.34	651.18	651.18	820.03	915.98	915.98	1044.33	1044.33	1195.37	1195.37

a/b = 1, H = 5 m, ν_s = 0.33, ρ_s = 1850 kg/m³, γ = 1.5										
51	487.11	764.09	764.09	965.55	1079.60	1079.60	1231.73	1231.73	1410.24	1410.24
52	491.80	771.42	771.42	974.79	1089.90	1089.90	1243.46	1243.46	1423.62	1423.62
53	496.44	778.68	778.68	983.94	1100.11	1100.12	1255.08	1255.08	1436.88	1436.88
54	501.04	785.87	785.87	993.00	1110.23	1110.23	1266.59	1266.59	1450.01	1450.01
55	505.59	793.00	793.00	1001.98	1120.26	1120.26	1278.00	1278.00	1463.02	1463.02
56	510.11	800.06	800.06	1010.89	1130.19	1130.19	1289.30	1289.30	1475.92	1475.92
57	514.59	807.06	807.06	1019.71	1140.04	1140.04	1300.51	1300.51	1488.71	1488.71
58	519.02	814.01	814.01	1028.46	1149.81	1149.81	1311.62	1311.62	1501.39	1501.39
59	523.42	820.89	820.89	1037.13	1159.49	1159.49	1322.64	1322.64	1513.96	1513.96
60	527.79	827.71	827.71	1045.73	1169.09	1169.09	1333.56	1333.56	1526.43	1526.43
a/b = 1, H = 7 m, ν_s = 0.33, ρ_s = 1850 kg/m³, γ = 1.5										
51	570.84	899.10	899.10	1137.01	1271.47	1271.47	1450.59	1450.59	1660.45	1660.45
52	576.35	907.76	907.76	1147.95	1283.68	1283.68	1464.50	1464.50	1676.32	1676.32
53	581.81	916.34	916.34	1158.77	1295.77	1295.77	1478.27	1478.27	1692.04	1692.04
54	587.22	924.84	924.84	1169.50	1307.75	1307.75	1491.91	1491.91	1707.62	1707.62
55	592.57	933.26	933.26	1180.13	1319.63	1319.63	1505.43	1505.43	1723.05	1723.05
56	597.88	941.61	941.61	1190.67	1331.39	1331.39	1518.82	1518.82	1738.35	1738.35
57	603.15	949.88	949.88	1201.11	1343.05	1343.05	1532.10	1532.10	1753.52	1753.52
58	608.36	958.08	958.08	1211.46	1354.62	1354.62	1545.27	1545.27	1768.55	1768.55
59	613.54	966.21	966.21	1221.72	1366.08	1366.08	1558.33	1558.33	1783.46	1783.46
60	618.67	974.28	974.28	1231.90	1377.45	1377.45	1571.27	1571.27	1798.24	1798.24

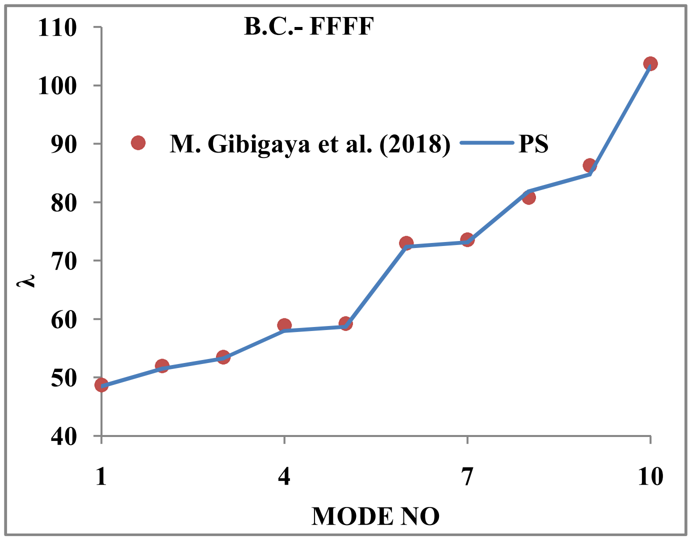

Fig. 5.70 Comparative studies of the frequency parameter of the FFFF plate

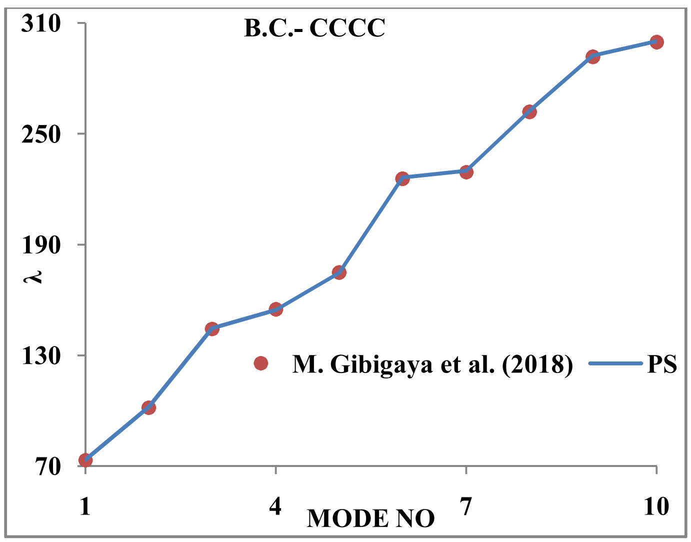

Fig. 5.71 Comparative studies of the frequency parameter of CCCC plate

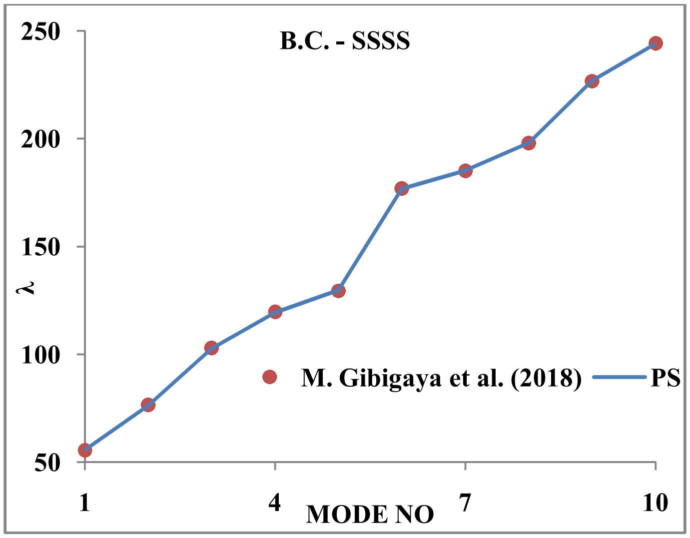

Fig. 5.72 Comparative studies of the frequency parameter of SSSS plate

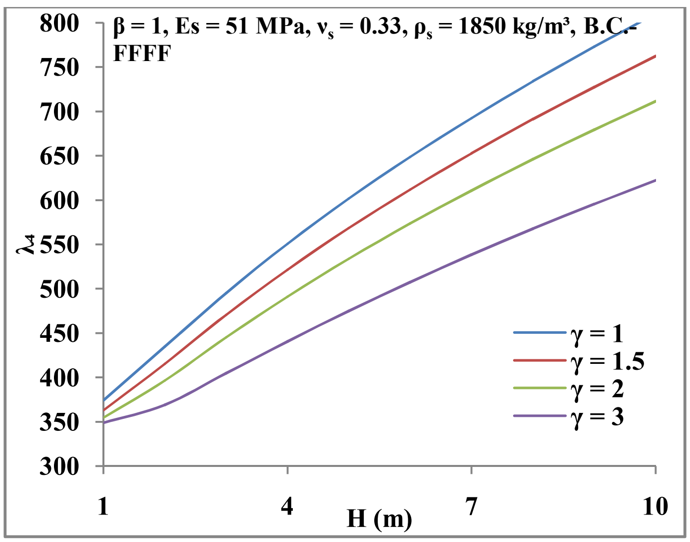

Fig. 5.73 Frequency parameter (λ_4) vs depth of the rigid base (H) of FFFF plate

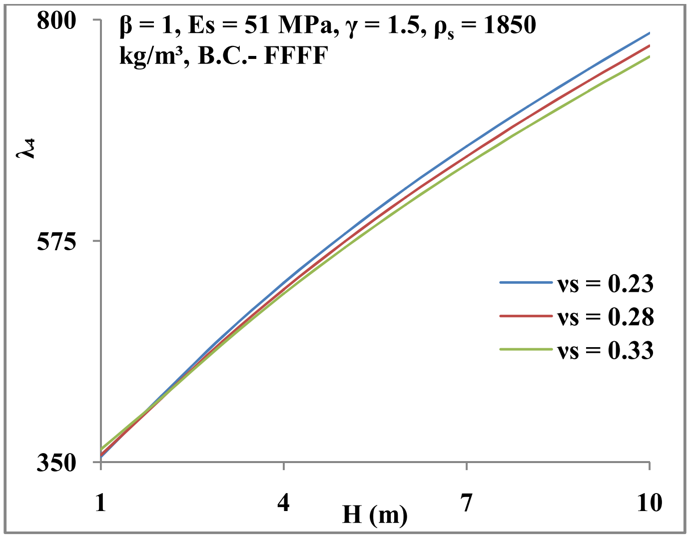

Fig. 5.74 Frequency parameter (λ_4) vs depth of the rigid base (H) of FFFF plate

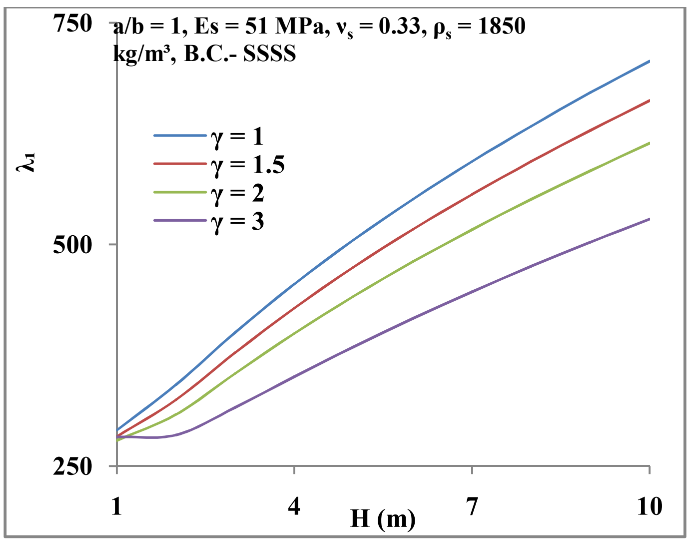

Fig. 5.75 Frequency parameter (λ_1) vs depth of the rigid base (H) of SSSS plate

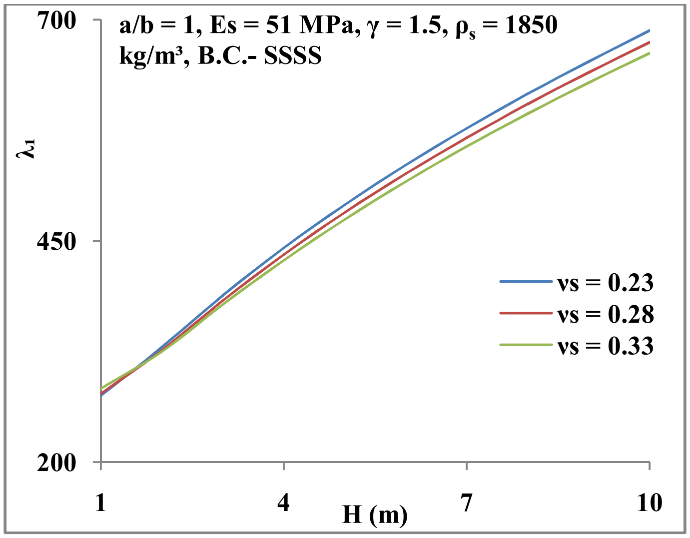

Fig.5.76 Frequency parameter (λ_1) vs depth of the rigid base (H) of SSSS plate

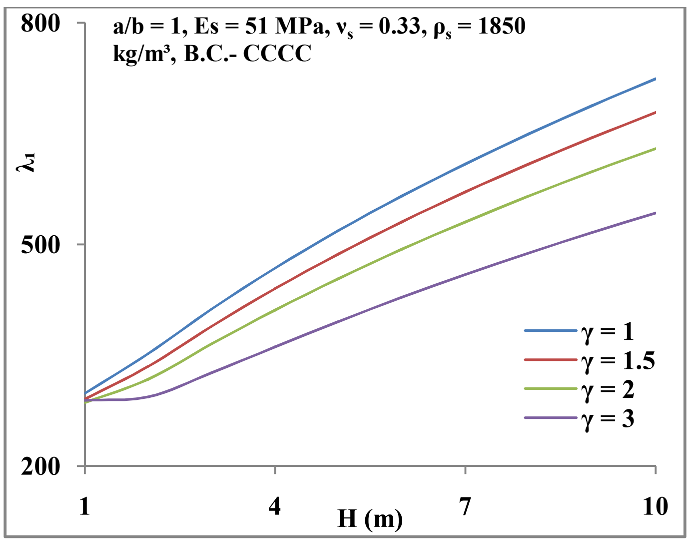

Fig. 5.77 Frequency parameter (λ_1) vs depth of the rigid base (H) of CCCC plate

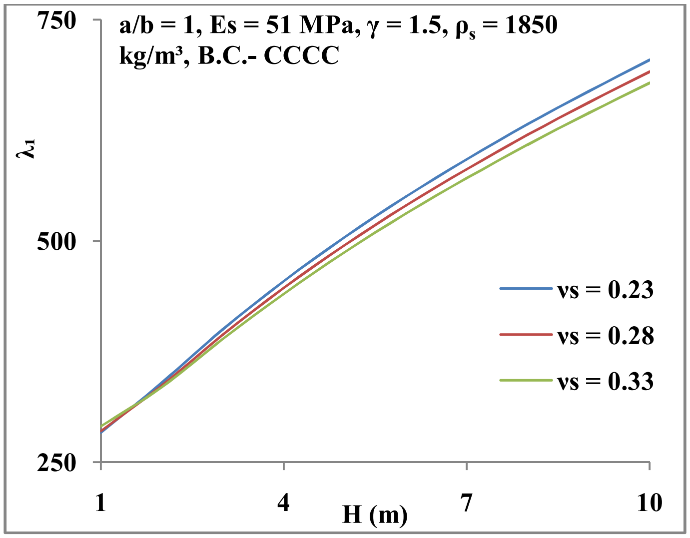

Fig. 5.78 Frequency parameter (λ_1) vs depth of the rigid base (H) of CCCC plate

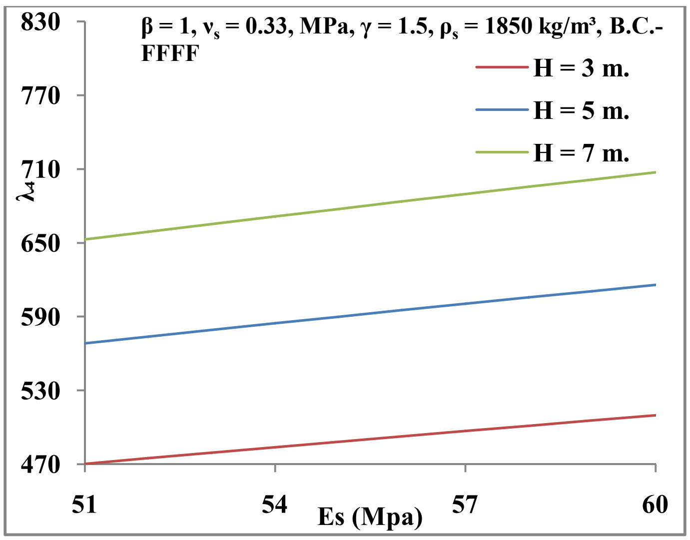

Fig. 5.79 Frequency parameter (λ_4) vs. elastic modulus of soil (Es) of FFFF plate

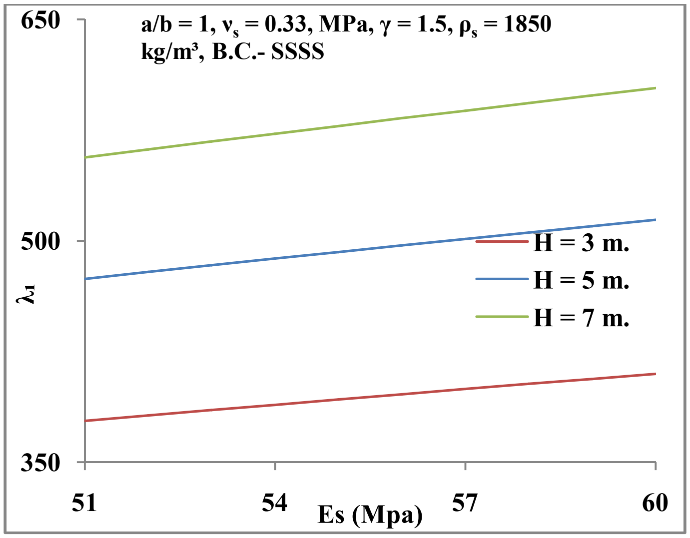

Fig. 5.80 Frequency parameter (λ_1) vs depth of the rigid base (H) of SSSS plate

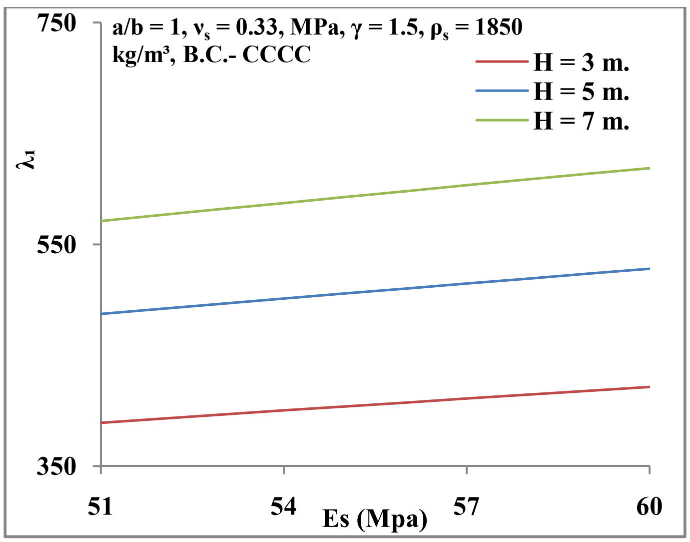

Fig. 5.81 Frequency parameter (λ_1) vs elastic modulus of soil (Es) of CCCC plate

The results presented in Figs. 5.73–5.87 shows the nature of the variation of the frequency parameters with various parameters of soil and plate.

It is observed from Figures 5.73–5.78 that the frequency parameter increases with the depth of the rigid base and the vertical decay function and decreases with the increase of the subgrade Poisson's ratio.

It is observed from Figures 5.79–5.81 that the frequency parameter increases with an increase in subgrade elastic modulus.

It is observed from Figures 5.82–5.84 that the frequency parameter increases with an increase in aspect ratio (β).

It is observed from Figures 5.85–5.87 that the frequency parameter increases with an increase in subsoil depth (H).

It is observed that the first foundation parameter, K, increases with an increase of **γ**, and the second foundation parameter, 2t, and activated mass, m_0, decreases with a rise in **γ.**

It is observed that the frequency parameter increases with the increase in constraints on the edges; the higher the constraints on the edges, the higher the flexural rigidity of the plate and, hence, the higher the frequency response.

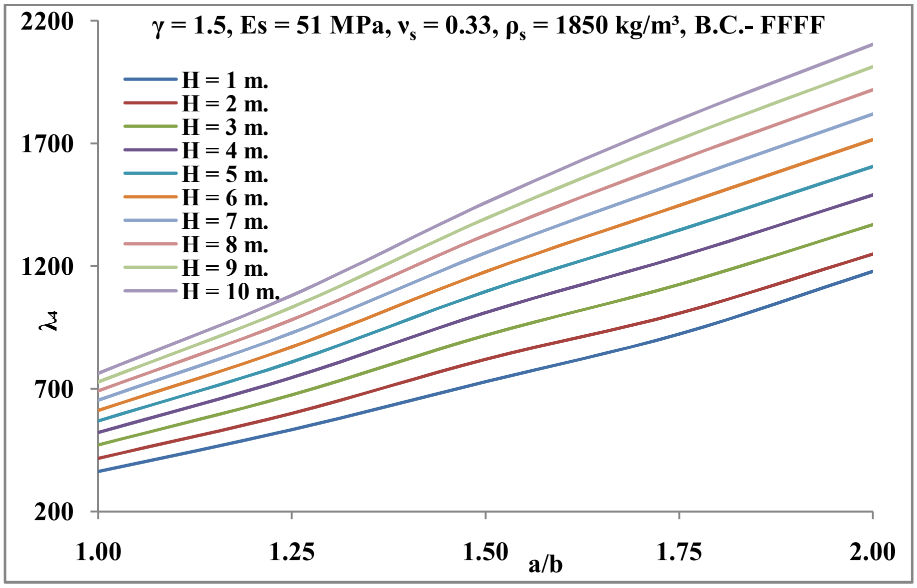

Fig. 5.82 Frequency parameter (λ_4) vs aspect ratio (β) of FFFF plate

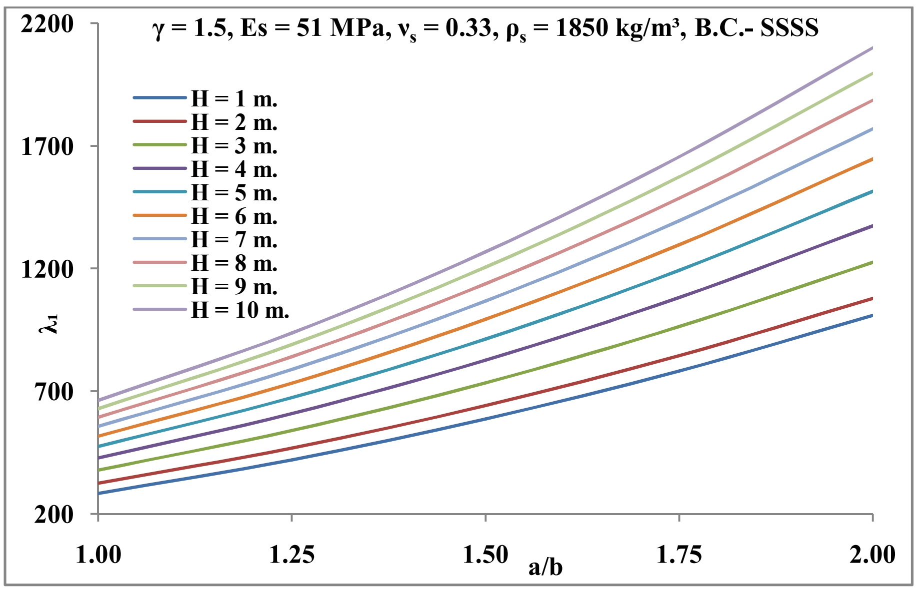

Fig. 5.83 Frequency parameter (λ_1) vs aspect ratio (β) of SSSS plate

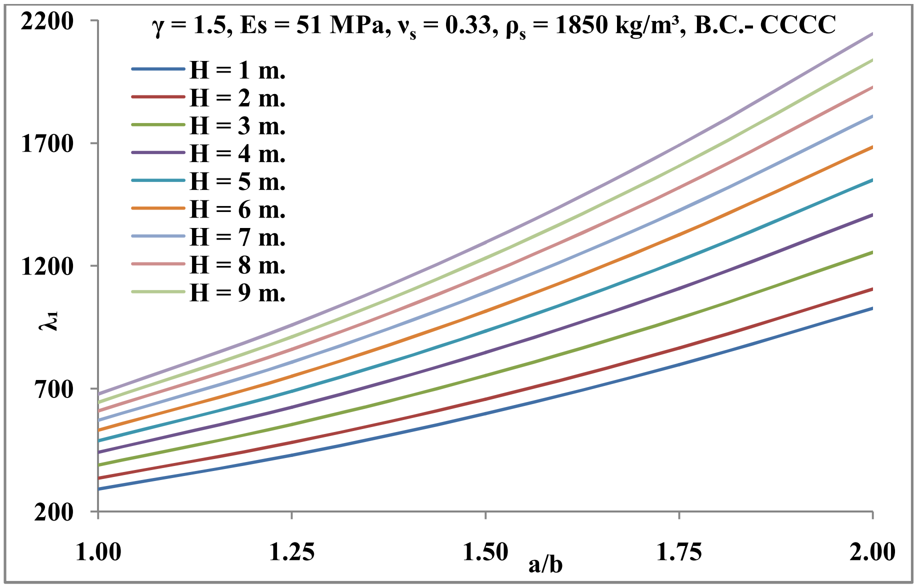

Fig. 5.84 Frequency parameter (λ_1) vs aspect ratio (β) of CCCC plate

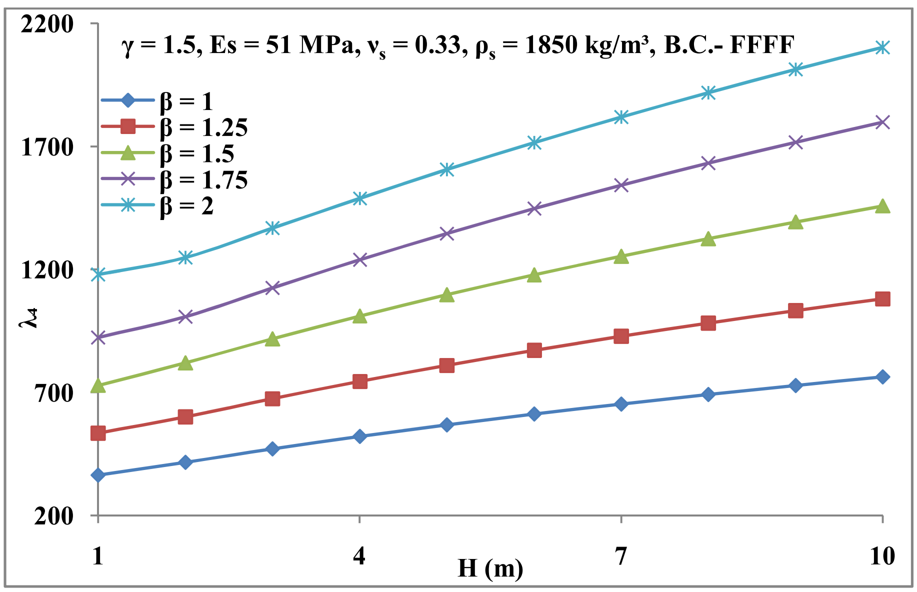

Fig. 5.85 Frequency parameter (λ_4) vs depth of the rigid base (H) of FFFF plate

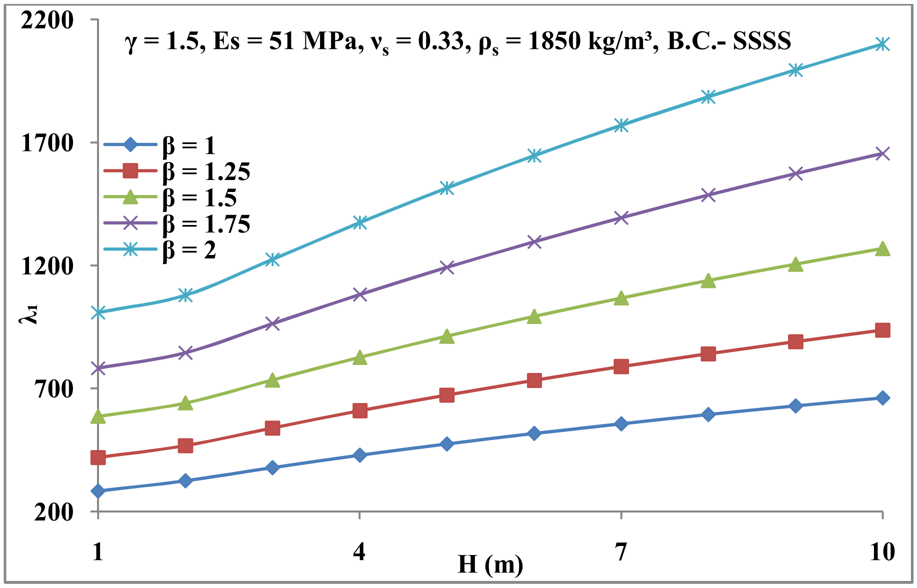

Fig. 5.86 Frequency parameter (λ_1) vs depth of the rigid base (H) of SSSS plate

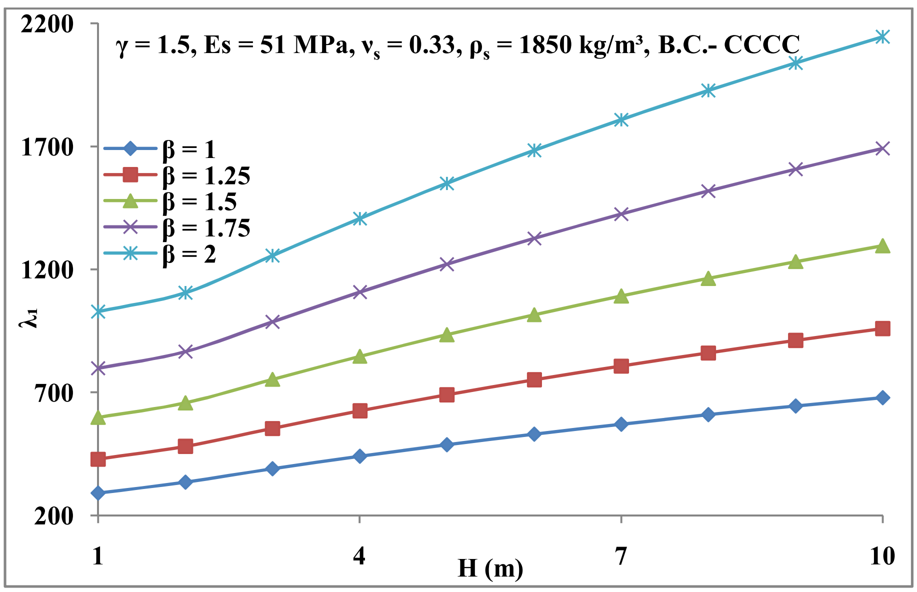

Fig. 5.87 Frequency parameter (λ_1) vs depth of the rigid base (H) of CCCC plate

5.7 Vibration Analysis HSDT Plate

5.7.1 Validation work

An example has been chosen from the study done by (Gibigaye et al., 2018). The dimensions of the plate for verification were taken as follows: a = 3.5 m, b = 5 m, plate thickness, h= 0.25 m material properties of plate: Young's modulus, E = 24000 MPa, Poisson's ratio, ν = 0.25 and density, ρ = 2500 kg/m³ and soil E = 50 MPa, Poisson's ratio, ν = 0.35, density, ρ = 1800 kg/m³ and H = 1.5 m, Gamma value 4.212. Frequency Parameter, $\lambda = \omega a^2\sqrt{(\rho h+m_{\circ})/D}$; The obtained frequency parameter listed in table 5.54 and has been compared with (Gibigaye et al., 2018) and the exact solution where possible shows excellent agreement.

Table 5.54

Comparisons of the first ten natural frequency parameters

THEORY	B.C	λ_1	λ_2	λ_3	λ_4	λ_5	λ_6	λ_7	λ_8	λ_9	λ_{10}
PS	FFFF	48.73	51.73	53.49	58.26	58.98	72.72	73.48	82.23	85.18	103.78
(Gibigaye et al., 2018)		48.65	52.00	53.47	58.97	59.20	72.97	73.57	80.81	86.29	103.71
PS	CCCC	73.82	102.58	145.32	155.35	175.44	227.44	231.07	263.71	293.80	301.60
(Gibigaye et al., 2018)		73.35	101.76	144.37	154.91	174.84	225.53	229.27	261.74	291.56	299.52
PS	SSSS	55.92	76.69	103.11	120.05	130.39	177.62	186.14	199.02	228.02	245.38
Exact		55.64	76.31	102.58	119.43	129.72	176.73	185.11	197.81	226.71	244.10
(Gibigaye et al., 2018)		55.46	76.48	102.95	119.67	129.55	176.89	185.08	197.93	226.81	244.19

5.7.2 Parametric study

For parametric study for the parameter aspect ratio, a/b, depth of rigid base, H and vertical decay function, γ the dimensions of the plate were taken as follows: a/b = 0.7, 1, 1.43,2 b/h = 100 and material properties of plate: Young's modulus, E = 24000 MPa, Poisson's ratio, ν = 0.25 and density, ρ = 2500 kg/m³ and soil E = 50 MPa, Poisson's ratio, ν = 0.35, density, ρ = 1800 kg/m³ and H = 1 m, 3.5 m, 6 m and 8.5 m. γ = 1,2,3,4. Frequency Parameter, $\lambda = \omega a^2/\pi^2\sqrt{(\rho h+m_{\circ})/D}$; Results are presented in Table 5.55-5.58 shows the variation of the first ten frequency parameter.

Table 5.55

Parametric study of frequency parameters for parameter subsoil depth (H = 1 m.)

B.C	a/b	γ	λ_1	λ_2	λ_3	λ_4	λ_5	λ_6	λ_7	λ_8	λ_9	λ_{10}
FFFF	0.7	1	22.424	23.176	23.894	24.510	24.658	25.999	26.509	26.586	27.346	27.987
	1		45.322	46.853	46.853	48.414	49.571	49.580	51.168	51.168	53.668	53.668
	1.43		78.081	80.523	82.757	84.630	85.111	89.082	90.434	90.686	92.911	94.715

	2		131.244	135.091	141.435	144.466	147.857	150.173	153.541	161.161	161.515	165.987
CCCC	0.7		22.875	24.003	25.418	25.992	26.634	28.742	28.956	30.014	31.324	31.824
	1		45.785	48.048	48.048	50.418	52.058	52.061	54.571	54.571	58.060	58.060
	1.43		79.214	82.533	86.303	88.042	89.594	95.060	95.716	97.988	101.242	102.683
	2		134.641	139.673	147.824	155.565	158.824	160.196	167.760	172.403	178.067	187.401
SSSS	0.7		22.632	23.581	24.624	25.274	25.670	27.501	27.835	28.343	29.507	30.213
	1		45.544	47.441	47.441	49.447	50.839	50.840	53.000	53.000	56.006	56.006
	1.43		78.753	81.745	84.861	86.733	87.851	92.836	93.720	95.049	98.036	99.818
	2		133.528	138.241	145.895	151.874	156.250	156.251	163.406	169.064	173.167	180.128
FFFF	0.7	2	23.998	24.571	25.147	25.625	25.761	26.861	27.268	27.366	28.008	28.533
	1		48.635	49.791	49.791	51.007	51.925	51.929	53.220	53.220	55.276	55.276
	1.43		83.561	85.377	87.103	88.494	88.918	92.025	93.022	93.320	95.115	96.519
	2		139.879	142.734	147.493	150.008	152.637	154.154	157.055	162.698	163.293	166.998
CCCC	0.7		24.331	25.197	26.342	26.792	27.337	29.114	29.288	30.241	31.385	31.805
	1		48.969	50.681	50.681	52.540	53.861	53.865	55.927	55.927	58.878	58.878
	1.43		84.339	86.780	89.652	90.953	92.182	96.485	96.986	98.888	101.532	102.670
	2		142.152	145.822	151.885	157.886	160.277	161.454	167.362	170.934	175.563	183.295
SSSS	0.7		24.125	24.831	25.636	26.150	26.468	27.973	28.253	28.682	29.677	30.289
	1		48.768	50.161	50.161	51.690	52.780	52.781	54.512	54.512	56.988	56.988
	1.43		83.961	86.123	88.425	89.833	90.682	94.534	95.227	96.276	98.660	100.098
	2		141.256	144.658	150.288	154.772	158.100	158.101	163.620	168.045	171.291	176.847
FFFF	0.7	3	27.184	27.597	28.038	28.391	28.509	29.379	29.689	29.800	30.326	30.740
	1		55.233	56.053	56.053	56.951	57.646	57.647	58.650	58.650	60.277	60.277

	1.43		94.665	95.925	97.178	98.145	98.494	100.793	101.484	101.795	103.174	104.210
	2		157.854	159.822	163.150	165.117	167.028	167.902	170.260	174.152	174.874	177.814
CCCC	0.7		27.418	28.046	28.926	29.261	29.702	31.135	31.270	32.092	33.054	33.392
	1		55.461	56.681	56.681	58.061	59.073	59.078	60.690	60.690	63.076	63.076
	1.43		95.165	96.839	98.892	99.799	100.717	103.907	104.265	105.778	107.812	108.658
	2		159.253	161.734	165.920	170.273	171.880	172.836	177.150	179.704	183.273	189.345
SSSS	0.7		27.253	27.746	28.332	28.717	28.959	30.135	30.359	30.705	31.519	32.026
	1		55.302	56.259	56.259	57.357	58.164	58.164	59.480	59.480	61.421	61.421
	1.43		94.873	96.323	97.907	98.894	99.496	102.286	102.798	103.577	105.369	106.465
	2		158.574	160.843	164.675	167.792	170.143	170.143	174.105	177.336	179.739	183.900
FFFF	0.7	4	30.798	31.106	31.453	31.724	31.827	32.534	32.780	32.892	33.333	33.670
	1		62.673	63.276	63.276	63.962	64.505	64.505	65.307	65.307	66.631	66.631
	1.43		107.263	108.165	109.099	109.798	110.082	111.834	112.335	112.628	113.714	114.505
	2		178.433	179.831	182.226	183.767	185.190	185.711	187.615	190.399	191.119	193.482
CCCC	0.7		30.974	31.447	32.146	32.403	32.766	33.945	34.053	34.767	35.584	35.862
	1		62.839	63.746	63.746	64.809	65.608	65.613	66.907	66.907	68.875	68.875
	1.43		107.608	108.804	110.326	110.980	111.686	114.120	114.383	115.609	117.210	117.853
	2		179.359	181.099	184.083	187.329	188.432	189.217	192.437	194.299	197.095	201.867
SSSS	0.7		30.838	31.197	31.640	31.938	32.128	33.071	33.254	33.538	34.214	34.640
	1		62.711	63.399	63.399	64.219	64.837	64.837	65.867	65.867	67.427	67.427
	1.43		107.376	108.390	109.522	110.239	110.681	112.763	113.151	113.745	115.126	115.980
	2		178.829	180.399	183.094	185.324	187.028	187.028	189.939	192.346	194.157	197.326

Table 5.56

Parametric study of frequency parameters for parameter subsoil depth (H = 3.5 m.)

H = 3.5 m.												
B.C	a/b	γ	λ_1	λ_2	λ_3	λ_4	λ_5	λ_6	λ_7	λ_8	λ_9	λ_{10}
FFFF	0.7	1	14.161	16.784	18.723	20.830	20.897	24.350	25.725	26.140	27.379	29.083
	1		27.646	33.189	33.189	37.997	41.753	41.808	45.797	45.797	52.627	52.639
	1.43		49.293	58.289	64.907	71.999	72.249	83.771	88.392	89.729	93.800	99.356
	2		86.406	100.414	122.505	126.973	136.748	150.360	153.644	176.695	181.945	186.350
CCCC	0.7		16.989	20.989	24.868	26.541	27.935	32.572	33.113	34.859	37.333	38.422
	1		31.108	39.914	39.914	47.314	51.770	51.771	57.956	57.956	65.545	65.545
	1.43		58.330	71.601	83.976	89.687	93.901	108.639	110.541	115.433	123.119	126.781
	2		111.709	130.765	157.614	179.064	189.139	191.744	211.291	223.589	236.146	256.005
SSSS	0.7		16.416	20.164	23.536	25.391	26.453	30.860	31.596	32.683	35.050	36.417
	1		30.471	38.644	38.644	45.564	49.746	49.749	55.564	55.564	62.716	62.716
	1.43		57.048	69.761	81.022	87.141	90.614	104.853	107.217	110.677	118.120	122.371
	2		108.490	127.096	153.292	171.563	184.027	184.033	203.218	217.580	227.552	244.000
FFFF	0.7	2	14.582	16.673	18.285	20.009	20.032	22.958	24.102	24.377	25.529	26.957
	1		28.702	33.103	33.103	37.037	40.055	40.061	43.461	43.461	49.097	49.097
	1.43		50.762	57.901	63.343	69.102	69.181	78.833	82.570	83.424	87.186	91.747
	2		88.209	99.335	116.987	121.287	129.371	139.638	143.224	162.233	165.794	170.435
CCCC	0.7		16.609	19.837	23.110	24.504	25.727	29.758	30.215	31.816	34.010	34.949
	1		31.090	38.069	38.069	44.182	47.946	47.947	53.247	53.247	59.862	59.862
	1.43		57.038	67.571	77.748	82.443	86.013	98.477	100.061	104.346	110.950	114.056
	2		106.265	121.602	143.713	161.817	170.169	172.513	189.111	199.492	210.374	227.645

SSSS	0.7		16.101	19.076	21.851	23.408	24.308	28.098	28.738	29.688	31.770	32.981
	1		30.539	36.910	36.910	42.544	46.028	46.030	50.952	50.952	57.112	57.112
	1.43		55.946	65.942	75.075	80.119	83.004	94.965	96.966	99.906	106.267	109.920
	2		103.550	118.435	139.906	155.124	165.600	165.605	181.841	194.066	202.598	216.697
FFFF	0.7	3	15.862	17.442	18.733	20.027	20.123	22.470	23.402	23.535	24.599	25.747
	1		31.524	34.825	34.825	37.891	40.184	40.203	42.970	42.970	47.440	47.440
	1.43		55.221	60.567	64.852	69.096	69.437	77.011	79.926	80.304	83.732	87.292
	2		94.898	103.253	116.627	120.691	127.097	134.158	137.963	152.979	154.900	159.840
CCCC	0.7		17.185	19.629	22.266	23.373	24.412	27.819	28.191	29.636	31.549	32.340
	1		33.012	38.172	38.172	42.952	45.991	45.993	50.367	50.367	55.972	55.972
	1.43		59.124	66.906	74.803	78.454	81.349	91.460	92.725	96.374	101.876	104.421
	2		106.456	117.991	135.201	149.833	156.433	158.495	172.087	180.538	189.727	204.411
SSSS	0.7		16.759	18.960	21.116	22.362	23.092	26.239	26.780	27.588	29.378	30.430
	1		32.564	37.170	37.170	41.481	44.236	44.237	48.227	48.227	53.354	53.354
	1.43		58.247	65.534	72.478	76.407	78.680	88.278	89.905	92.311	97.559	100.600
	2		104.292	115.385	131.966	144.026	152.451	152.454	165.669	175.721	182.795	194.537
FFFF	0.7	4	17.479	18.691	19.738	20.729	20.861	22.776	23.558	23.592	24.574	25.506
	1		34.994	37.505	37.505	39.920	41.706	41.726	43.999	43.999	47.619	47.619
	1.43		60.851	64.904	68.312	71.487	71.943	77.964	80.300	80.365	83.455	86.258
	2		103.615	109.970	120.242	123.979	129.103	133.956	137.734	149.729	150.550	155.585
CCCC	0.7		18.372	20.237	22.368	23.252	24.138	27.034	27.341	28.650	30.332	31.006
	1		35.961	39.818	39.818	43.570	46.032	46.035	49.659	49.659	54.437	54.437
	1.43		63.349	69.127	75.257	78.093	80.439	88.654	89.665	92.784	97.390	99.486

	2		111.125	119.794	133.153	144.970	150.173	151.986	163.142	170.039	177.844	190.426
SSSS	0.7		18.018	19.656	21.335	22.334	22.928	25.549	26.009	26.701	28.250	29.170
	1		35.597	38.961	38.961	42.269	44.451	44.452	47.693	47.693	51.976	51.976
	1.43		62.645	67.980	73.253	76.308	78.096	85.792	87.117	89.087	93.430	95.970
	2		109.398	117.656	130.414	139.942	146.706	146.709	157.467	165.751	171.639	181.470

Table 5.57

Parametric study of frequency parameters for parameter subsoil depth (H = 6 m.)

H = 6 m.												
B.C	a/b	γ	λ_1	λ_2	λ_3	λ_4	λ_5	λ_6	λ_7	λ_8	λ_9	λ_{10}
FFFF	0.7	1	12.700	16.767	19.533	22.530	22.948	27.567	29.596	30.383	31.783	34.136
	1		24.280	32.908	32.908	39.895	45.665	46.015	51.238	51.238	60.690	61.291
	1.43		44.170	58.198	67.768	77.935	79.471	95.099	102.158	104.828	109.384	117.313
	2		78.975	100.905	134.854	138.939	152.898	175.784	177.452	210.454	220.371	223.856
CCCC	0.7		18.260	24.153	29.457	31.787	33.579	39.637	40.380	42.477	45.614	47.056
	1		31.718	45.165	45.165	55.619	61.697	61.698	69.951	69.951	79.829	79.829
	1.43		62.727	82.709	100.229	108.289	113.985	133.963	136.594	142.898	153.084	158.027
	2		127.194	155.030	192.791	221.902	235.898	239.119	265.419	282.094	298.523	324.390
SSSS	0.7		17.545	23.198	27.975	30.523	31.961	37.806	38.767	40.176	43.212	44.949
	1		30.876	43.666	43.666	53.644	59.458	59.464	67.350	67.350	76.815	76.815
	1.43		60.989	80.397	96.647	105.246	110.072	129.541	132.738	137.394	147.325	152.955
	2		122.781	150.202	187.284	212.523	229.521	229.531	255.447	274.700	287.973	309.821
FFFF	0.7	2	12.759	16.072	18.399	20.929	21.173	25.169	26.849	27.461	28.749	30.768
	1		24.601	31.623	31.623	37.475	42.193	42.389	46.960	46.960	55.025	55.335
	1.43		44.395	55.798	63.804	72.361	73.254	86.693	92.459	94.495	98.707	105.414

	2		78.770	96.551	124.306	128.472	140.230	158.398	160.760	188.514	196.136	199.819
CCCC	0.7		16.926	21.864	26.438	28.423	30.008	35.312	35.946	37.856	40.635	41.884
	1		29.979	41.102	41.102	49.998	55.237	55.238	62.408	62.408	71.071	71.071
	1.43		58.059	74.650	89.526	96.358	101.279	118.481	120.720	126.271	135.111	139.361
	2		115.307	138.646	170.711	195.763	207.656	210.550	233.208	247.508	261.829	284.408
SSSS	0.7		16.268	20.961	25.018	27.207	28.448	33.535	34.376	35.613	38.289	39.827
	1		29.221	39.693	39.693	48.115	53.087	53.091	59.896	59.896	68.138	68.138
	1.43		56.529	72.557	86.247	93.557	97.676	114.383	117.136	121.154	129.751	134.638
	2		111.477	134.398	165.816	187.370	201.950	201.958	224.257	240.864	252.344	271.246
FFFF	0.7	3	13.456	16.040	17.942	20.011	20.091	23.473	24.827	25.247	26.449	28.126
	1		26.237	31.699	31.699	36.423	40.126	40.193	44.095	44.095	50.803	50.840
	1.43		46.835	55.696	62.183	69.143	69.431	80.704	85.244	86.598	90.537	95.998
	2		82.199	95.997	117.731	121.999	131.591	145.073	148.172	170.770	176.014	180.173
CCCC	0.7		16.309	20.260	24.088	25.729	27.107	31.670	32.199	33.930	36.365	37.431
	1		29.743	38.460	38.460	45.757	50.146	50.147	56.236	56.236	63.708	63.708
	1.43		55.934	69.019	81.191	86.785	90.928	105.376	107.232	112.046	119.576	123.153
	2		107.511	126.233	152.545	173.565	183.386	185.963	205.068	217.061	229.354	248.792
SSSS	0.7		15.728	19.428	22.747	24.572	25.616	29.951	30.675	31.745	34.074	35.420
	1		29.096	37.176	37.176	43.994	48.109	48.112	53.831	53.831	60.866	60.866
	1.43		54.644	67.175	78.240	84.243	87.649	101.605	103.920	107.309	114.600	118.765
	2		104.307	122.592	148.268	166.147	178.336	178.343	197.096	211.130	220.875	236.941
FFFF	0.7	4	14.453	16.497	18.077	19.763	19.789	22.660	23.783	24.050	25.186	26.589
	1		28.459	32.760	32.760	36.612	39.566	39.571	42.908	42.908	48.437	48.437

	1.43		50.311	57.285	62.613	68.237	68.330	77.782	81.438	82.261	85.970	90.438
	2		87.384	98.254	115.507	119.748	127.668	137.666	141.230	159.846	163.285	167.886
CCCC	0.7		16.428	19.590	22.809	24.175	25.382	29.355	29.802	31.390	33.557	34.480
	1		30.781	37.608	37.608	43.606	47.305	47.307	52.522	52.522	59.042	59.042
	1.43		56.405	66.699	76.671	81.267	84.775	97.009	98.561	102.784	109.276	112.323
	2		104.929	119.920	141.566	159.332	167.501	169.820	186.104	196.277	206.979	223.970
SSSS	0.7		15.923	18.832	21.552	23.082	23.966	27.695	28.326	29.263	31.316	32.512
	1		30.234	36.455	36.455	41.974	45.392	45.394	50.231	50.231	56.294	56.294
	1.43		55.325	65.085	74.020	78.960	81.787	93.519	95.483	98.370	104.619	108.209
	2		102.253	116.796	137.807	152.714	162.984	162.988	178.913	190.909	199.286	213.129

Table 5.58

Parametric study of frequency parameters for parameter subsoil depth (H = 8.5 m.)

H = 8.5 m.												
B.C	a/b	γ	λ_1	λ_2	λ_3	λ_4	λ_5	λ_6	λ_7	λ_8	λ_9	λ_{10}
FFFF	0.7	1	12.215	17.493	20.925	24.613	25.358	30.858	33.45	34.491	36.058	38.876
	1		23.059	34.245	34.245	42.924	50.353	51.045	57.097	57.097	68.607	69.757
	1.43		42.441	60.685	72.621	85.173	87.898	106.617	115.725	119.327	124.38	134.019
	2		76.702	105.393	149.022	152.604	169.843	200.161	200.43	241.191	254.562	257.94
CCCC	0.7		20.268	27.538	33.891	36.716	38.808	45.958	46.858	49.235	52.895	54.614
	1		34.365	51.2	51.2	63.888	71.173	71.173	80.985	80.985	92.625	92.625
	1.43		69.761	94.619	115.91	125.718	132.522	156.467	159.653	167.05	179.165	185.097
	2		144.832	179.071	224.923	259.825	276.796	280.5	311.992	332.044	351.503	382.1
SSSS	0.7		19.473	26.51	32.315	35.379	37.098	44.036	45.171	46.83	50.388	52.417
	1		33.406	49.575	49.575	61.781	68.800	68.808	78.245	78.245	89.472	89.473

	1.43		67.723	91.989	111.884	122.317	128.149	151.554	155.386	160.954	172.795	179.489
	2		139.578	173.405	218.526	248.998	269.435	269.448	300.515	323.542	339.376	365.436
FFFF	0.7	2	12.085	16.428	19.331	22.472	22.984	27.765	29.917	30.771	32.185	34.63
	1		22.994	32.204	32.204	39.55	45.692	46.146	51.499	51.499	61.365	62.127
	1.43		42.02	57.007	67.067	77.73	79.603	95.802	103.314	106.228	110.805	119.081
	2		75.442	98.918	135.035	138.821	153.461	178.123	179.282	213.868	224.65	227.924
CCCC	0.7		18.309	24.502	30.019	32.445	34.295	40.558	41.329	43.479	46.71	48.202
	1		31.474	45.691	45.691	56.607	62.925	62.925	71.479	71.479	81.688	81.688
	1.43		62.89	83.931	102.215	110.614	116.524	137.247	139.98	146.486	157.022	162.144
	2		128.772	157.924	197.258	227.455	241.996	245.306	272.545	289.824	306.792	333.493
SSSS	0.7		17.569	23.526	28.513	31.163	32.655	38.707	39.7	41.155	44.286	46.076
	1		30.593	44.154	44.154	54.597	60.652	60.658	68.845	68.845	78.642	78.642
	1.43		61.073	81.545	98.537	107.496	112.517	132.729	136.044	140.868	151.149	156.972
	2		124.17	152.921	191.578	217.803	235.436	235.447	262.301	282.231	295.961	318.555
FFFF	0.7	3	12.483	15.925	18.321	20.925	21.208	25.294	27.03	27.678	28.973	31.045
	1		24.012	31.309	31.309	37.344	42.241	42.472	47.132	47.132	55.411	55.787
	1.43		43.431	55.283	63.534	72.347	73.379	87.136	93.116	95.279	99.504	106.406
	2		77.229	95.72	124.519	128.587	140.693	159.712	161.866	190.441	198.499	202.048
CCCC	0.7		16.929	22.028	26.719	28.757	30.373	35.788	36.438	38.376	41.205	42.482
	1		29.806	41.336	41.336	50.485	55.855	55.856	63.19	63.19	72.033	72.033
	1.43		58.062	75.225	90.521	97.539	102.578	120.189	122.485	128.145	137.177	141.525
	2		116.014	140.075	173.009	198.658	210.853	213.794	236.969	251.601	266.216	289.249
SSSS	0.7		16.256	21.114	25.286	27.53	28.801	34.001	34.859	36.121	38.849	40.415

	1	4	29.027	39.96	39.96	48.581	53.685	53.689	60.659	60.659	69.083	69.083
	1.43		56.489	73.09	87.188	94.697	98.923	116.041	118.858	122.968	131.757	136.75
	2		112.081	135.731	168.019	190.118	205.048	205.057	227.872	244.851	256.581	275.892
FFFF	0.7	4	13.155	15.927	17.938	20.127	20.249	23.789	25.226	25.698	26.919	28.687
	1		25.566	31.431	31.431	36.449	40.414	40.511	44.589	44.589	51.647	51.755
	1.43		45.786	55.302	62.18	69.554	69.998	81.831	86.683	88.221	92.221	98.01
	2		80.624	95.444	118.73	122.963	133.115	147.821	150.716	174.646	180.524	184.518
CCCC	0.7		16.344	20.558	24.584	26.315	27.747	32.503	33.059	34.836	37.359	38.471
	1		29.544	38.9	38.9	46.621	51.235	51.236	57.608	57.608	65.389	65.389
	1.43		56.044	70.06	82.948	88.866	93.214	108.377	110.332	115.337	123.204	126.953
	2		108.826	128.769	156.591	178.659	189.015	191.674	211.692	224.274	237.085	257.32
SSSS	0.7		15.74	19.704	23.219	25.14	26.236	30.767	31.521	32.634	35.052	36.447
	1		28.863	37.578	37.578	44.821	49.163	49.166	55.17	55.17	62.519	62.519
	1.43		54.686	68.146	79.906	86.252	89.845	104.518	106.947	110.499	118.126	122.477
	2		105.451	124.964	152.15	170.985	183.794	183.801	203.468	218.161	228.349	245.138

Figure 5.88 – 5.91 shows the variation of frequency parameters with aspect ratio. The figure shows that the frequency parameter decreases with an increase in aspect ratio.

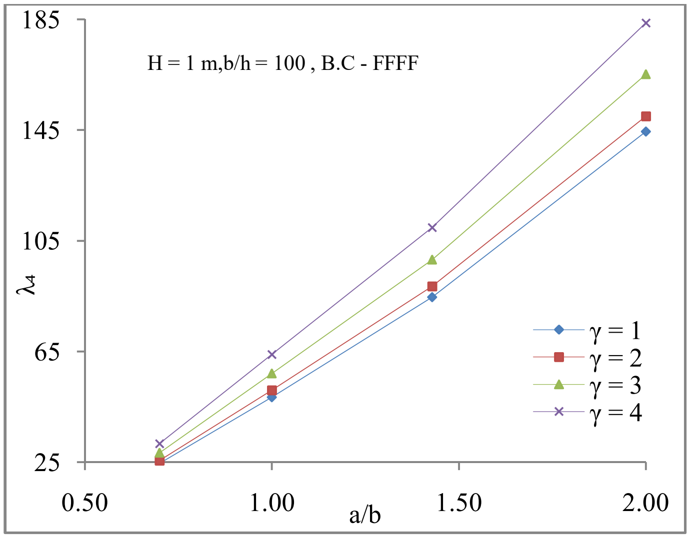

Fig. 5.88 Frequency parameter vs aspect ratio

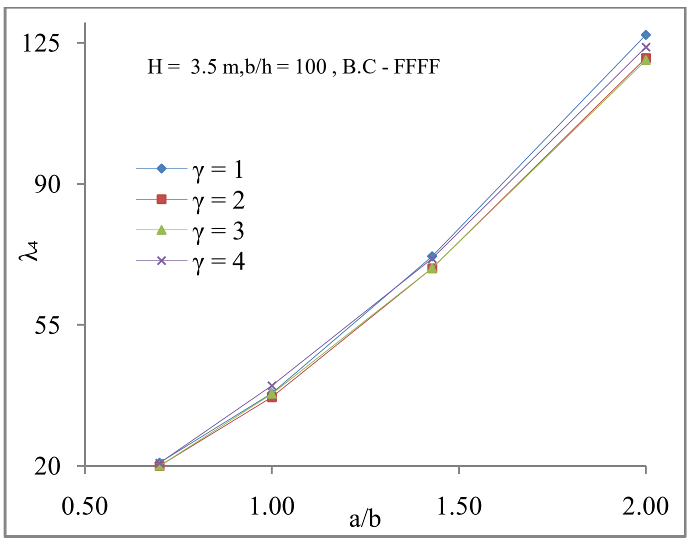

Fig. 5.89 Frequency parameter vs aspect ratio

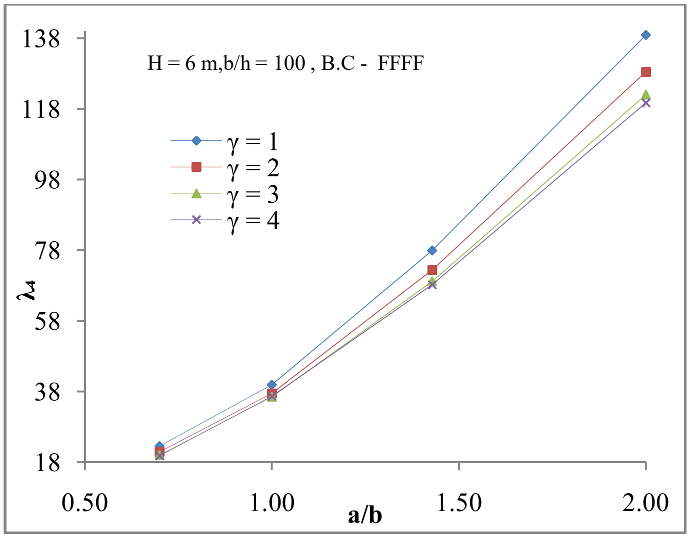

Fig. 5.90 Frequency parameter vs aspect ratio

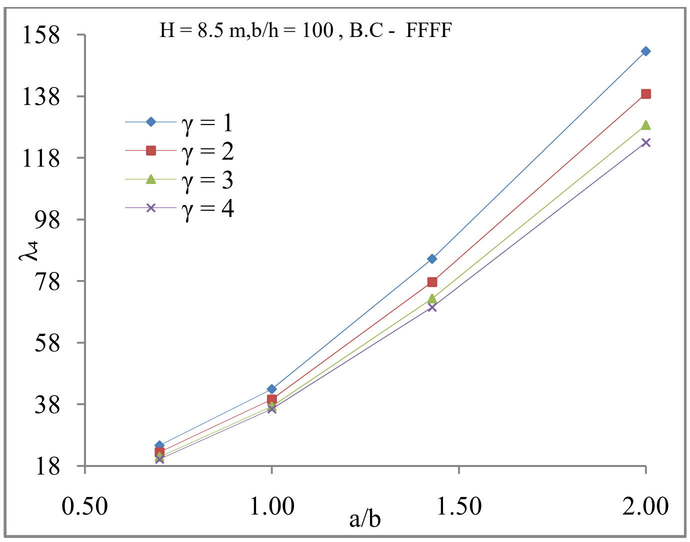

Fig. 5.91 Frequency parameter vs aspect ratio

Figure 5.92-5.95 shows the variation of frequency parameters with vertical decay function.

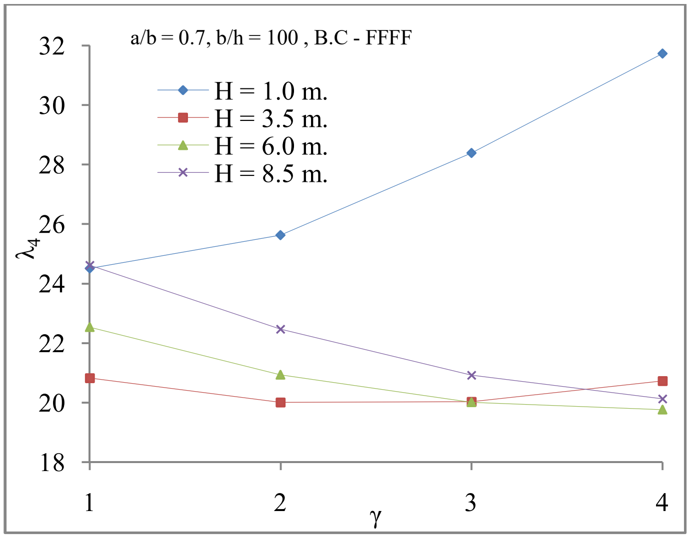

Fig. 5.92 Frequency parameter vs γ

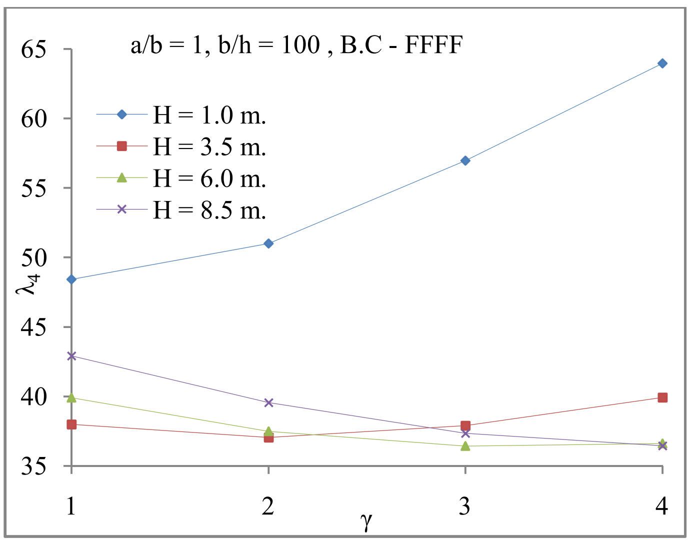

Fig. 5.93 Frequency parameter vs γ

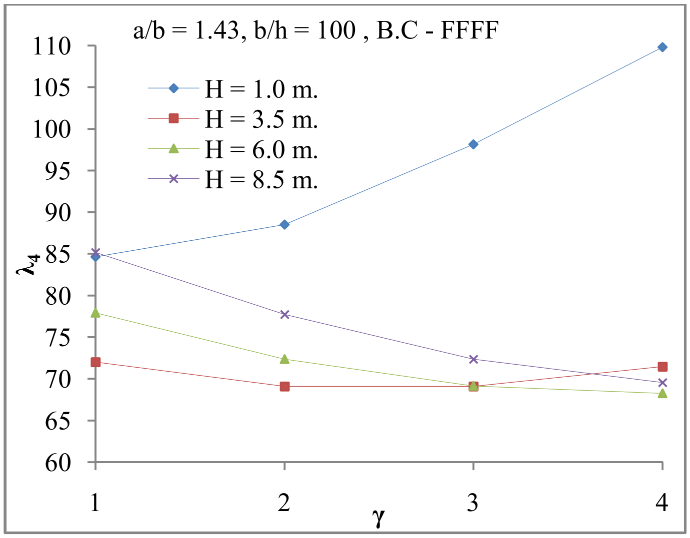

Fig. 5.94 Frequency parameter vs γ

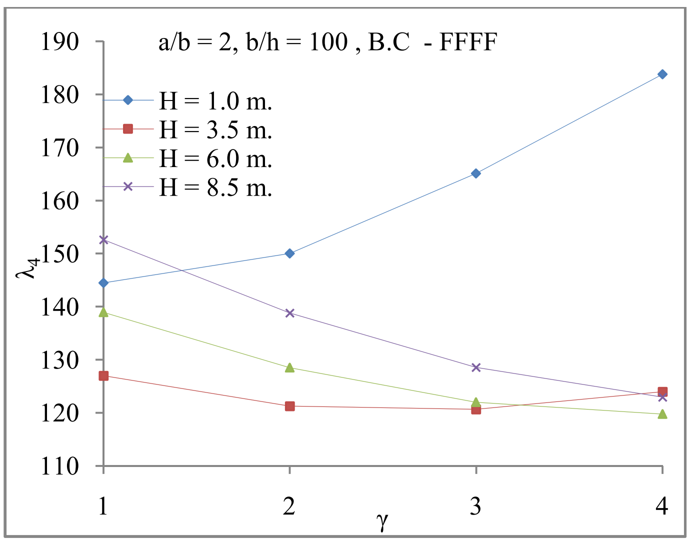

Fig. 5.95 Frequency parameter vs γ

It is observed that the frequency parameter increases with an increase of vertical decay function up to b/H ratio 2.5 and decreases after that.

Figure 5.96 – 5.98 shows the variation of the foundation parameter and activated mass with the vertical decay parameter,γ.

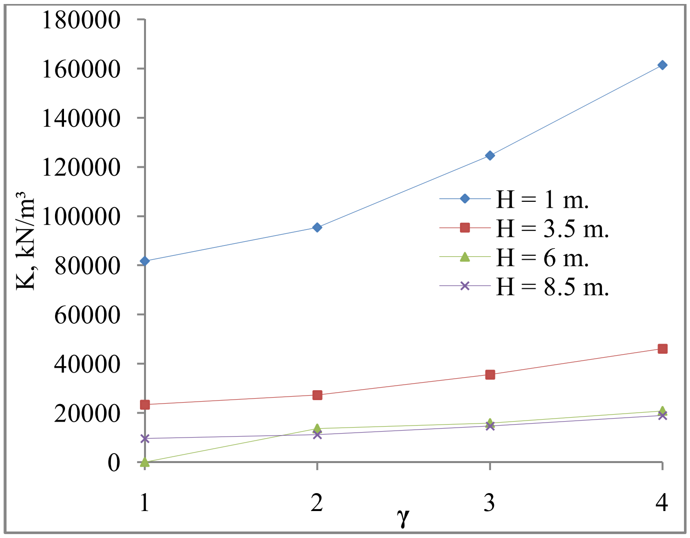

Fig.5.96 Foundation parameter,K vs γ

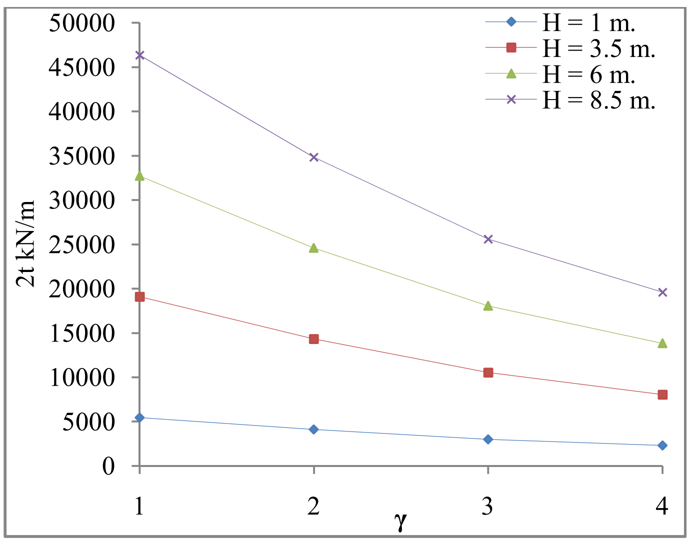

Fig.5.97 Foundation parameter,2t vs γ

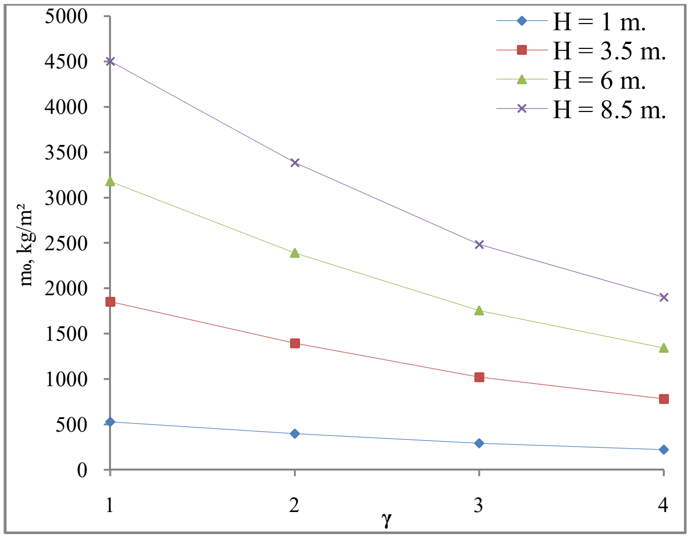

Fig.5.98 Activated mass,m_o vs γ

It is observed that the first foundation parameter, K, increases with the increase of **γ** and the second foundation parameter, 2t and activated mass, m_0, decreases with a rise in **γ.**

Tables 5.59 and 5.60 show the variation of frequency parameters with boundary conditions.

Table 5.59

Show the variation of frequency parameters with boundary conditions

a/b = 0.7, b/h = 20, H = 1.5 m., γ = 4.212										
B.C	λ_1	λ_2	λ_3	λ_4	λ_5	λ_6	λ_7	λ_8	λ_9	λ_{10}
FFFF	48.487	51.473	53.219	57.974	58.69	72.362	73.109	81.821	84.762	103.258
CFFF	48.753	53.874	54.168	63.738	72.267	75.924	89.247	96.249	116.954	134.657
SFSF	49.265	56.857	63.011	76.192	83.588	101.766	114.75	118.108	152.434	165.086
SSSF	50.688	66.184	68.69	94.16	106	126.568	140.103	158.693	170.246	207.009
SCSF	52.329	67.59	77.235	102.635	107.059	147.436	147.607	171.033	177.687	213.361
CFCF	53.263	60.966	78.87	87.563	90.967	127.555	130.716	145.016	155.452	188.246
SSSS	55.641	76.308	102.599	119.447	129.735	176.741	185.209	198.026	226.893	244.159
SCSC	59.932	91.288	105.905	141.306	146.386	198.758	200.337	223.508	235.461	277.237
SSSC	61.239	81.439	120.789	123.611	145.88	188.519	190.454	227.86	254.532	255.685
CCCC	73.446	102.075	144.598	154.583	174.568	226.311	229.916	262.399	292.345	300.096

Table 5.60

Show the variation of frequency parameters with boundary conditions

a/b = 1, b/h = 20, H = 1.5 m., γ = 4.212										
B.C	λ_1	λ_2	λ_3	λ_4	λ_5	λ_6	λ_7	λ_8	λ_9	λ_{10}
FFFF	47.704	50.979	50.979	54.690	57.985	58.976	65.580	65.580	82.824	82.824
CFFF	48.003	51.551	53.423	58.736	60.084	72.201	74.119	80.967	85.631	104.977
SFSF	48.537	53.019	62.524	64.741	69.685	89.033	93.465	101.588	110.078	124.743
SSSF	49.156	57.215	64.092	77.740	80.545	103.700	108.085	120.722	127.344	155.384
SCSF	49.852	60.316	64.621	81.012	89.025	104.072	115.920	123.543	141.899	162.226
CFCF	52.609	57.081	68.892	78.511	84.958	97.201	103.069	130.612	136.966	137.927
SSSS	50.592	68.398	68.398	92.468	110.042	110.043	137.489	137.490	175.288	175.289
SCSC	54.895	72.417	84.056	106.195	113.229	138.090	148.711	162.581	177.760	206.235
SSSC	52.271	70.109	75.435	98.696	111.460	123.305	142.629	149.295	176.413	194.284
CCCC	58.953	87.465	87.465	118.562	140.437	141.012	172.395	172.395	216.791	216.791

It is observed that the frequency parameter increases with an increase of constraints on the edges, that the higher constraints on the edges increase the flexural rigidity of the plate, and hence, the higher frequency response.

5.8 Vibration Analysis Skew Plate Using Higher-order FEM

In the case of FFFF boundary conditions for the first three rigid body modes in a normal modes analysis with no loads or constraints, one translational mode and two rotational modes are used. The modal frequency of the first three modes will be zero or close to zero. It refers to a rigid body motion rather than a vibrating system. That is why we always take the fourth mode in case of free plate.

5.8.1 Convergence study

A skewed plate (a/b = 1) on elastic foundation (Kw = 100, Ks = 100 where Kw = Ka²b²/D and Ks = 2tab/D) is considered first for a convergence study for the clamped, simply supported and free plate for free vibration analysis, and the mesh size of 20 × 20 is decided for a reasonable result compared to 30 × 30 of a three DOF per node skewed plate element, hence less uses of computer memory, resources and time. The frequency parameter ($\lambda = 4\omega a^2\sqrt{(\rho h/D)}$) is compared with the results given in Ketabdari et al.(Ketabdari et al., 2016) and tabulated in Table 5.61. It shows the proposed formulation's rapid convergence, observed for simply supported plate, and free plate converges from the reverse direction.

Table 5.61

Convergence study for natural frequency of CCCC, SSSS plate for 1st mode and FFFF plate for 4th mode

Mesh Size	CCCC	SSSS	FFFF
	λ_1	λ_1	λ_4
4 × 4	70.5631	52.2650	62.7920
8 × 8	69.2022	52.4650	64.3773
12 × 12	68.9118	52.4899	64.7932
16 × 16	68.8018	52.4986	64.9720
18 × 18	68.7707	52.5011	65.0270
20 × 20	68.7478	52.5031	65.0693
24 × 24	68.7169	52.5059	65.1301
(Ketabdari et al., 2016)	69.1550	53.6150	-
Difference (%)	0.634	2.069	-

To the authors' knowledge, the works regarding using the modified Vlasov model for the vibration analysis of skew plates resting on elastic foundations are still unavailable in the literature. Due to a lack of valid data for vibration analysis of skew plates on elastic foundations using the modified Vlasov model, the results of vibration analysis of the plate on the Vlasov foundation have been compared with rectangular results in the literature by setting skew angle, $\beta = 90°$.

5.8.2 Validation

An example has been chosen from the study done by Gibigaye et al. (Gibigaye et al., 2018) to validate the present formulation in the case of a thin plate. The dimensions of the plate for verification were taken as follows: plate dimension (5 m × 3.5 m × 0.25) and material properties of plate: Young's modulus, E = 24000 MPa, Poisson's ratio, $\nu = 0.25$ and density, $\rho = 2500$ kg/m³ and soil $E_s = 50$ MPa, Poisson's ratio, $\nu_s = 0.35$, density, $\rho_s = 1800$ kg/m³ and H = 1.5 m, Gamma value 4.212. Frequency Parameter, $\lambda = 4\omega a^2\sqrt{(\rho h+m_\circ)/D}$; The obtained frequency parameter listed in Table 5.62 and has been compared with Gibigaye et al. (Gibigaye et al., 2018) and the exact solution, where possible, shows excellent agreement.

Table 5.62

Comparisons of the natural frequency parameters

Reference	B.C	λ_1	λ_2	λ_3	λ_4	λ_5	λ_6	λ_7	λ_8	λ_9	λ_{10}
PS	FFFF	48.49	51.47	53.22	57.97	58.69	72.36	73.11	81.82	84.76	103.26
(Gibigaye et al., 2018)		48.69	52.00	53.47	58.97	59.20	72.97	73.57	80.81	86.29	103.71
PS	CCCC	73.45	102.07	144.60	154.58	174.57	226.31	229.92	262.40	292.34	300.10
(Gibigaye et al., 2018)		73.35	101.76	144.37	154.91	174.84	225.53	229.27	261.74	291.56	299.52
PS	SSSS	55.64	76.31	102.60	119.45	129.74	176.74	185.21	198.03	226.89	244.16
Exact		55.64	76.31	102.58	119.43	129.72	176.73	185.11	197.81	226.71	244.10
(Gibigaye et al., 2018)		55.46	76.48	102.95	119.67	129.55	176.89	185.08	197.93	226.81	244.19

5.8.3 Parametric study

For parametric study for the parameter aspect ratio, a/b, depth of rigid base, H, skew angle β and vertical decay function, γ the dimensions of the plate were taken as follows: a/b = 0.5,1.0,2.0 and material properties of plate: Young's modulus, E = 200 GPa, Poisson's ratio, ν = 0.3 and density, ρ = 7850 kg/m³ and soil E_s = 50 MPa, 60 MPa, 75 MPa, 90 MPa, Poisson's ratio, ν_s =0.20, 0.25, 0.30, density, ρ_s = 1700 kg/m³ and H = 1 m, 3 m, 5 m and 6 m. γ = 1,2,3. Frequency Parameter, $\lambda = 4\omega a^2/\pi^2\sqrt{(\rho h+m_o)/D}$; Results are presented in Table 5.63 – 5.71, which shows the variation of the first ten frequency parameters.

Table 5.63

Natural frequency parameter of skew plate, B.C.- CCCC, β = 30º, ν_s = 0.20, ρ_s = 1700 kg/m³ and γ =1.

a/b	E_s MN/m²)	H (m)	λ_1	λ_2	λ_3	λ_4	λ_5	λ_6	λ_7	λ_8	λ_9	λ_{10}
0.5	50	1.0	95.11	112.82	139.03	171.70	209.70	241.52	255.15	269.05	305.25	311.43
		3.0	109.24	133.84	168.22	208.23	250.99	262.43	293.04	297.62	341.26	350.00

		5.0	121.42	150.67	191.07	237.14	280.88	283.60	315.36	331.70	369.77	386.42
		6.0	126.91	158.06	201.00	249.75	289.51	297.56	326.14	346.21	383.68	402.28
	60	1.0	96.94	115.46	142.59	176.02	214.49	243.99	259.86	271.67	310.27	314.60
		3.0	113.19	139.33	175.65	217.58	261.57	268.19	299.91	308.69	349.95	361.72
		5.0	126.97	158.10	201.03	249.77	289.54	297.59	326.17	346.23	383.70	402.30
		6.0	133.14	166.29	211.98	263.69	299.47	312.67	338.90	361.93	400.05	419.75
	75	1.0	99.60	119.25	147.67	182.23	221.42	247.49	266.82	275.53	317.60	319.29
		3.0	118.76	146.94	185.92	230.54	276.18	276.52	309.98	323.95	362.81	378.02
		5.0	134.70	168.30	214.62	267.04	301.93	316.22	342.08	365.63	404.10	423.90
		6.0	141.78	177.55	226.91	282.67	313.64	332.53	357.69	382.82	423.80	443.41
	90	1.0	102.16	122.84	152.50	188.15	228.04	250.85	273.59	279.32	323.93	324.68
		3.0	123.98	153.95	195.34	242.47	284.51	289.49	319.82	337.80	375.47	393.02
		5.0	141.86	177.61	226.95	282.70	313.68	332.56	357.72	382.85	423.83	443.44
		6.0	149.75	187.80	240.41	299.82	327.02	349.82	376.00	401.39	446.44	464.76
1.0	50	1.0	163.71	244.58	319.71	329.78	399.81	455.40	483.22	570.50	574.17	577.10
		3.0	205.94	322.75	389.43	426.84	534.39	550.72	625.87	659.17	688.48	753.89
		5.0	240.86	381.13	438.73	505.01	625.64	633.31	695.12	767.74	780.96	884.09
		6.0	256.14	406.14	460.69	538.20	658.44	675.45	723.15	817.53	821.16	937.24
	60	1.0	171.27	255.91	334.23	337.88	417.24	467.43	502.68	582.92	584.84	598.77
		3.0	218.02	342.28	405.58	452.79	566.98	575.13	650.64	692.13	718.53	796.97
		5.0	256.58	406.42	460.93	538.41	658.61	675.62	723.31	817.66	821.30	937.36
		6.0	273.41	433.83	485.47	574.64	694.98	721.71	754.62	865.64	872.68	992.49
	75	1.0	181.79	271.60	349.44	354.38	441.60	484.54	529.87	595.82	605.36	629.50

		3.0	234.58	368.89	428.15	488.04	608.93	611.38	680.79	741.96	760.10	855.24
		5.0	278.02	440.70	491.69	583.48	703.89	732.83	762.35	876.36	885.92	1005.21
		6.0	296.93	471.31	519.70	623.71	745.03	784.13	798.39	926.09	947.57	1062.36
	90	1.0	191.51	286.02	360.41	372.95	464.19	500.70	554.87	608.63	624.83	658.34
		3.0	249.70	393.03	449.12	519.89	640.07	651.61	707.50	788.93	798.24	906.91
		5.0	297.50	471.67	520.03	623.99	745.26	784.34	798.60	926.28	947.75	1062.52
		6.0	318.25	505.11	551.15	667.74	790.67	839.03	840.22	980.72	1015.13	1122.67
2.0	50	1.0	382.34	453.24	556.99	685.37	835.08	975.75	1019.38	1086.89	1218.17	1249.32
		3.0	437.99	536.41	673.12	831.56	1001.49	1059.94	1180.52	1188.39	1366.06	1397.43
		5.0	486.05	603.22	764.30	947.30	1131.96	1133.32	1267.18	1326.51	1477.68	1543.44
		6.0	507.76	632.57	803.96	997.82	1165.66	1189.92	1308.97	1385.33	1532.30	1606.95
	60	1.0	389.56	463.68	571.13	702.68	854.40	986.37	1037.41	1097.17	1238.26	1261.73
		3.0	453.57	558.16	702.75	868.98	1044.20	1082.47	1207.24	1233.20	1400.08	1444.41
		5.0	507.98	632.75	804.10	997.94	1165.76	1190.02	1309.06	1385.41	1532.38	1607.02
		6.0	532.37	665.30	847.87	1053.76	1204.50	1251.27	1358.43	1448.86	1596.91	1676.81
	75	1.0	400.03	478.64	591.36	727.55	882.28	1000.84	1064.72	1112.29	1267.56	1280.12
		3.0	475.57	588.38	743.74	920.89	1103.27	1114.97	1246.32	1295.07	1450.39	1509.81
		5.0	538.54	673.31	858.46	1067.18	1214.07	1265.70	1370.81	1463.81	1612.95	1693.42
		6.0	566.53	710.12	907.63	1129.93	1259.78	1331.81	1431.67	1532.92	1691.20	1771.32
	90	1.0	410.12	492.87	610.56	751.23	908.95	1014.33	1091.65	1127.11	1295.90	1298.28
		3.0	496.19	616.27	781.37	968.66	1146.17	1157.17	1284.48	1351.23	1500.04	1569.90
		5.0	566.83	710.36	907.82	1130.08	1259.92	1331.93	1431.79	1533.03	1691.30	1771.41
		6.0	598.01	750.95	961.74	1198.85	1311.99	1401.47	1503.70	1607.21	1781.60	1856.49

Table 5.64

Natural frequency parameter of skew plate, B.C.- SSSS, β = 30º, v_s = 0.20, ρ_s = 1700 kg/m³ and γ =1.

a/b	E_s MN/m²)	H (m)	λ_1	λ_2	λ_3	λ_4	λ_5	λ_6	λ_7	λ_8	λ_9	λ_{10}
0.5	50	1.0	54.08	70.54	93.34	119.65	147.44	158.76	178.61	180.16	213.08	215.39
		3.0	70.95	94.23	125.36	159.25	182.42	190.20	211.27	224.29	252.07	265.84
		5.0	84.53	112.13	149.08	188.43	203.45	219.08	241.30	256.30	288.38	302.97
		6.0	90.46	119.82	159.20	200.66	213.30	230.78	255.51	269.63	305.19	318.65
	60	1.0	56.51	73.76	97.49	124.62	152.85	161.48	183.52	184.28	217.24	221.46
		3.0	75.47	100.16	133.18	168.87	189.01	199.97	220.48	234.94	263.35	278.05
		5.0	90.54	119.87	159.25	200.70	213.34	230.81	255.54	269.65	305.22	318.67
		6.0	97.09	128.30	170.31	213.80	224.78	243.46	271.66	284.17	324.21	335.82
	75	1.0	59.95	78.26	103.30	131.61	160.46	165.45	188.48	192.31	223.39	230.10
		3.0	81.71	108.26	143.84	181.94	198.51	212.81	234.07	249.20	279.72	294.61
		5.0	98.75	130.38	172.99	216.90	227.63	246.49	275.57	287.64	328.79	339.90
		6.0	106.12	139.80	185.31	230.97	241.36	260.57	294.05	303.83	350.54	359.03
	90	1.0	63.18	82.45	108.71	138.14	167.54	169.30	193.37	199.80	229.46	238.25
		3.0	87.42	115.63	153.50	193.69	207.62	224.09	247.23	261.94	295.35	309.55
		5.0	106.22	139.88	185.36	231.02	241.40	260.61	294.08	303.87	350.57	359.06
		6.0	114.31	150.17	198.78	245.95	257.16	276.07	314.52	321.59	374.66	379.97
1.0	50	1.0	119.37	182.14	242.82	243.56	308.39	348.86	375.63	442.21	442.62	451.21
		3.0	161.57	259.09	307.72	347.78	441.08	447.34	508.14	543.88	564.22	629.43
		5.0	197.34	317.18	359.72	424.40	523.40	537.71	575.83	655.56	657.19	755.48

		6.0	212.89	342.03	382.58	456.91	556.46	578.80	604.94	697.22	704.44	805.50
	60	1.0	127.73	193.83	252.72	257.53	326.11	361.73	395.51	452.63	457.59	473.87
		3.0	174.17	278.66	324.96	373.32	472.27	473.03	530.93	579.64	594.65	671.69
		5.0	213.42	342.36	382.88	457.16	556.66	578.99	605.13	697.39	704.60	805.64
		6.0	230.44	369.55	408.24	492.62	593.18	623.89	637.64	741.36	758.31	857.23
	75	1.0	139.21	209.91	265.68	277.81	350.66	379.87	422.79	467.42	479.35	505.56
		3.0	191.30	305.26	348.83	407.96	506.64	516.46	561.18	630.14	636.44	728.08
		5.0	235.20	376.43	414.69	501.33	602.14	634.76	645.69	752.00	771.24	869.24
		6.0	254.19	406.71	443.38	540.68	643.27	682.92	684.68	801.12	831.20	923.79
	90	1.0	149.72	224.62	277.85	296.39	373.25	396.85	447.20	482.35	499.76	534.97
		3.0	206.83	329.34	370.80	439.23	538.13	555.75	588.81	674.57	676.56	777.21
		5.0	254.86	407.13	443.76	540.99	643.54	683.17	684.93	801.33	831.41	923.97
		6.0	275.59	440.14	475.40	583.76	688.76	724.67	739.28	854.95	896.81	982.49
2.0	50	1.0	216.50	282.56	373.54	478.24	589.20	640.57	713.95	726.20	855.50	860.30
		3.0	283.79	377.10	501.44	636.63	734.00	761.52	848.00	897.65	1009.27	1061.91
		5.0	337.99	448.61	596.35	753.65	816.84	878.36	965.66	1026.46	1152.85	1210.35
		6.0	361.66	479.32	636.85	802.83	855.60	925.35	1021.83	1079.88	1219.63	1273.07
	60	1.0	226.23	295.39	390.11	498.10	610.93	651.34	736.68	739.41	871.92	884.53
		3.0	301.84	400.79	532.71	675.17	760.02	801.11	883.97	940.58	1053.79	1110.72
		5.0	361.97	479.56	637.03	802.98	855.73	925.47	1021.94	1079.98	1219.72	1273.16
		6.0	388.10	513.25	681.35	855.75	900.70	976.05	1085.96	1138.06	1295.28	1341.71
	75	1.0	239.95	313.36	413.33	526.08	641.52	667.04	758.91	768.88	896.21	919.07
		3.0	326.72	433.16	575.35	727.59	797.43	853.08	937.21	997.94	1118.53	1176.93

		5.0	394.74	521.56	692.06	868.21	911.92	988.12	1101.53	1151.91	1313.57	1358.03
		6.0	424.13	559.21	741.42	924.79	966.11	1044.17	1175.21	1216.53	1400.30	1434.51
	90	1.0	252.80	330.06	434.91	552.20	669.99	682.27	778.08	798.98	920.16	951.65
		3.0	349.52	462.61	614.03	774.78	833.28	898.52	989.06	1049.09	1180.53	1236.67
		5.0	424.53	559.51	741.65	924.98	966.28	1044.33	1175.35	1216.67	1400.42	1434.63
		6.0	456.80	600.67	795.44	984.64	1028.89	1105.69	1257.05	1287.32	1496.66	1518.26

Table 5.65

Natural frequency parameter of skew plate, B.C.- FFFF, $\beta = 30^o$, $v_s = 0.20$, $\rho_s = 1700$ kg/m³ and $\gamma = 1$.

a/b	E_s MN/m²)	H (m)	λ_1	λ_2	λ_3	λ_4	λ_5	λ_6	λ_7	λ_8	λ_9	λ_{10}
0.5	50	1.0	28.19	37.38	49.39	53.29	62.77	63.23	77.37	78.18	93.28	94.68
		3.0	29.07	45.49	66.84	69.31	85.17	89.90	107.98	113.85	130.69	138.24
		5.0	30.89	52.28	80.08	81.98	101.03	109.70	129.39	139.93	156.82	169.86
		6.0	31.76	55.27	85.76	87.50	107.76	118.10	138.38	150.93	167.95	183.00
	60	1.0	30.65	40.59	53.70	57.97	68.16	68.44	83.76	84.16	100.59	101.31
		3.0	31.63	49.35	72.62	75.25	91.97	97.67	116.47	123.54	140.66	149.71
		5.0	33.61	56.70	86.95	88.98	109.04	119.13	139.53	151.84	169.08	183.87
		6.0	34.55	59.94	93.10	94.96	116.30	128.23	149.22	163.75	181.18	197.88
	75	1.0	33.94	44.89	59.47	64.23	75.40	75.43	92.24	92.42	110.36	110.55
		3.0	35.10	54.54	80.36	83.21	101.03	108.10	127.80	136.57	154.08	165.12
		5.0	37.29	62.66	96.16	98.37	119.74	131.78	153.04	167.79	185.56	202.07
		6.0	38.32	66.23	102.94	104.99	127.72	141.80	163.66	180.90	198.97	215.91
	90	1.0	36.90	48.74	64.64	69.81	81.60	81.98	99.50	100.24	118.58	119.57

		3.0	38.22	59.20	87.29	90.32	109.09	117.45	137.86	148.25	166.13	178.88
		5.0	40.60	68.00	104.40	106.78	129.29	143.09	165.05	182.05	200.35	217.05
		6.0	41.72	71.87	111.74	113.97	137.93	153.93	176.50	196.21	214.93	232.13
1.0	50	1.0	89.07	124.93	143.87	158.65	192.87	196.24	226.15	235.75	241.48	275.92
		3.0	89.35	151.20	168.47	209.36	251.71	276.54	290.68	320.66	349.14	392.41
		5.0	94.26	174.55	192.51	248.29	299.63	336.06	339.64	383.85	428.86	469.19
		6.0	96.61	184.86	203.50	264.93	320.62	361.14	361.34	410.70	462.53	501.86
	60	1.0	96.85	135.91	155.19	172.59	208.88	213.50	242.35	254.86	260.95	298.61
		3.0	97.38	164.76	182.05	227.57	273.08	300.88	311.00	346.87	379.41	422.24
		5.0	102.74	190.14	208.46	269.59	325.33	364.58	365.35	415.10	465.87	505.43
		6.0	105.30	201.31	220.52	287.55	348.21	388.17	392.70	444.09	502.30	541.02
	75	1.0	107.38	150.69	170.20	191.32	230.26	236.76	263.45	280.49	287.85	329.01
		3.0	108.27	183.03	200.37	251.99	301.78	333.56	338.39	381.87	420.12	462.07
		5.0	114.23	211.10	230.04	298.12	359.89	398.37	404.59	456.79	515.43	554.21
		6.0	117.04	223.40	243.57	317.85	385.30	424.81	434.69	488.65	555.48	593.75
	90	1.0	116.90	163.97	183.53	208.12	249.32	257.67	281.97	303.40	312.38	356.03
		3.0	118.10	199.47	216.90	273.85	327.51	362.85	363.09	413.04	456.61	497.70
		5.0	124.59	229.90	249.55	323.65	390.90	428.93	439.67	493.94	559.67	598.02
		6.0	127.63	243.19	264.40	344.95	418.57	457.94	472.19	528.38	602.92	641.13
2.0	50	1.0	451.17	598.15	790.25	852.93	1004.24	1012.10	1237.81	1250.72	1492.34	1513.69
		3.0	465.12	727.92	1069.65	1109.48	1363.53	1438.93	1727.74	1822.39	2090.53	2212.96
		5.0	494.25	836.68	1281.62	1312.19	1617.58	1756.39	2070.39	2240.85	2509.12	2720.49
		6.0	508.22	884.52	1372.61	1400.41	1725.23	1891.19	2214.45	2417.44	2687.15	2931.27

	60	1.0	490.43	649.59	859.11	928.03	1090.52	1095.51	1340.11	1346.40	1609.43	1619.82
		3.0	506.16	789.71	1162.09	1204.61	1472.44	1563.42	1863.67	1977.77	2250.22	2397.06
		5.0	537.80	907.47	1391.73	1424.15	1745.76	1907.77	2232.81	2431.98	2705.25	2945.19
		6.0	552.89	959.30	1490.30	1519.82	1861.89	2053.84	2387.96	2623.31	2898.79	3164.87
	75	1.0	543.16	718.45	951.54	1028.31	1206.96	1207.00	1475.73	1478.79	1764.79	1768.84
		3.0	561.62	872.79	1286.09	1331.91	1617.51	1730.69	2044.94	2186.77	2465.16	2644.23
		5.0	596.64	1002.72	1539.36	1574.24	1916.93	2110.75	2449.04	2688.20	2968.89	3231.92
		6.0	613.24	1059.91	1648.02	1679.97	2044.63	2271.74	2619.05	2898.96	3183.26	3452.90
	90	1.0	590.49	780.04	1034.29	1117.60	1306.29	1311.71	1591.96	1604.05	1896.40	1913.38
		3.0	611.65	947.41	1397.09	1445.68	1746.61	1880.58	2206.10	2374.18	2658.03	2864.97
		5.0	649.71	1088.28	1671.43	1708.60	2069.74	2292.26	2641.28	2917.19	3205.36	3471.22
		6.0	667.64	1150.24	1789.09	1823.38	2207.94	2466.45	2824.67	3145.04	3438.41	3712.10

Table 5.66

Natural frequency parameter of skew plate, B.C.- CCCC, $\beta = 45^o$, $v_s = 0.20$, $\rho_s = 1700$ kg/m³ and $\gamma = 1$.

a/b	E_s MN/m²)	H (m)	λ_1	λ_2	λ_3	λ_4	λ_5	λ_6	λ_7	λ_8	λ_9	λ_{10}
0.5	50	1.0	61.11	74.85	95.36	120.57	142.45	146.00	158.81	169.34	188.25	197.71
		3.0	78.61	98.48	126.56	159.31	169.96	182.88	198.76	207.87	237.50	241.16
		5.0	92.77	116.61	149.88	187.87	193.59	209.21	232.83	237.28	274.62	277.40
		6.0	98.98	124.47	159.92	199.86	204.51	220.76	247.73	250.20	289.27	294.86
	60	1.0	63.56	78.02	99.41	125.45	145.65	150.98	163.06	174.17	193.79	203.00
		3.0	83.29	104.45	134.22	168.71	177.44	191.43	209.73	217.37	250.35	251.96
		5.0	99.05	124.53	159.97	199.90	204.54	220.79	247.76	250.23	289.29	294.89

		6.0	105.93	133.21	171.02	212.77	217.14	233.66	264.24	264.61	305.56	314.22
	75	1.0	67.02	82.47	105.07	132.32	150.30	157.79	169.43	180.91	201.91	210.46
		3.0	89.77	112.66	144.70	181.51	188.09	203.23	225.02	230.55	266.94	268.22
		5.0	107.66	135.35	173.71	215.82	220.25	236.78	268.08	268.19	309.47	318.85
		6.0	115.44	145.12	186.13	229.87	235.07	251.46	284.42	286.73	327.90	340.64
	90	1.0	70.29	86.62	110.34	138.72	154.80	163.92	175.78	187.18	209.77	217.47
		3.0	95.73	120.16	154.26	193.03	198.22	214.11	239.10	242.73	280.76	284.69
		5.0	115.53	145.20	186.18	229.92	235.11	251.50	284.46	286.77	327.94	340.68
		6.0	124.10	155.95	199.82	245.24	251.70	267.78	302.56	307.14	348.31	364.64
1.0	50	1.0	126.16	190.74	217.75	250.80	312.75	316.82	343.01	388.10	391.51	451.57
		3.0	170.70	270.47	288.91	356.78	417.48	434.70	451.37	515.31	547.12	591.25
		5.0	208.02	330.72	345.67	433.89	498.01	509.46	549.51	607.46	664.12	690.12
		6.0	224.27	356.61	370.49	466.70	533.01	542.72	591.39	646.99	714.09	733.45
	60	1.0	134.64	202.68	228.00	265.64	326.58	334.75	354.81	407.53	408.48	471.85
		3.0	183.74	290.68	307.77	382.46	443.90	458.92	483.77	545.61	585.56	623.38
		5.0	224.77	356.93	370.80	466.94	533.22	542.93	591.58	647.16	714.25	733.61
		6.0	242.60	385.32	398.25	502.84	571.90	580.07	637.46	690.63	769.02	781.80
	75	1.0	146.31	219.10	242.40	286.08	345.98	359.58	371.54	429.99	437.00	498.49
		3.0	201.50	318.22	333.77	417.30	480.27	492.79	527.86	587.03	637.99	667.80
		5.0	247.52	392.49	405.20	511.66	581.38	589.24	648.58	701.19	782.20	793.51
		6.0	267.47	424.25	436.16	551.71	624.98	631.58	699.84	749.98	843.35	848.24
	90	1.0	157.00	234.14	255.84	304.78	364.07	382.43	387.35	450.89	463.46	521.72
		3.0	217.64	343.22	357.63	448.80	513.60	524.26	567.84	624.71	685.58	708.75

		5.0	268.10	424.65	436.55	552.02	625.25	631.85	700.08	750.21	843.55	848.44
		6.0	289.93	459.41	470.64	595.80	673.22	678.81	756.13	803.82	908.98	910.37
2.0	50	1.0	244.18	299.35	381.63	482.47	569.61	583.96	635.36	677.48	752.81	791.04
		3.0	314.12	393.79	506.41	637.50	679.16	731.02	795.19	831.19	949.89	964.64
		5.0	370.62	466.24	599.74	751.60	773.48	835.70	931.92	948.31	1098.20	1110.03
		6.0	395.40	497.67	639.94	799.21	817.36	881.59	991.81	999.74	1156.66	1180.21
	60	1.0	253.96	312.02	397.81	502.02	582.35	603.88	652.29	696.81	774.93	812.20
		3.0	332.81	417.65	537.04	675.12	708.96	765.01	839.20	869.04	1001.42	1007.78
		5.0	395.68	497.89	640.12	799.35	817.50	881.72	991.93	999.85	1156.76	1180.31
		6.0	423.12	532.58	684.39	850.10	868.40	932.86	1057.07	1058.17	1221.68	1258.08
	75	1.0	267.82	329.81	420.46	529.49	600.89	631.07	677.73	723.75	807.37	842.06
		3.0	358.66	450.45	579.00	726.25	751.47	811.92	900.55	921.53	1067.56	1073.15
		5.0	430.04	541.14	695.14	862.11	881.01	945.26	1070.89	1074.08	1237.30	1276.71
		6.0	461.01	580.19	744.88	917.46	940.88	1003.48	1135.89	1148.72	1310.88	1364.51
	90	1.0	280.86	346.38	441.52	555.09	618.79	655.53	703.13	748.76	838.81	870.06
		3.0	382.44	480.46	617.27	772.13	792.02	855.21	957.12	970.00	1122.69	1139.32
		5.0	461.38	580.48	745.11	917.64	941.06	1003.65	1136.04	1148.86	1311.01	1364.63
		6.0	495.48	623.44	799.77	978.08	1007.93	1068.22	1208.02	1230.94	1392.33	1461.30

Table 5.67

Natural frequency parameter of skew plate, B.C.- SSSS, $\beta = 45^o$, $v_s = 0.20$, $\rho_s = 1700$ kg/m³ and $\gamma = 1$.

a/b	E_s MN/m²)	H (m)	λ_1	λ_2	λ_3	λ_4	λ_5	λ_6	λ_7	λ_8	λ_9	λ_{10}
0.5	50	1.0	42.07	55.18	74.03	95.43	102.16	110.93	124.04	130.95	151.23	157.99

		3.0	61.17	80.17	106.38	130.59	137.71	145.88	170.05	170.37	202.45	204.31
		5.0	75.98	98.83	130.12	155.61	166.78	172.88	200.14	205.55	236.45	245.06
		6.0	82.36	106.85	140.27	166.55	179.31	184.72	213.28	220.70	251.26	262.69
	60	1.0	44.97	58.71	78.36	100.35	106.17	115.36	129.66	135.80	157.58	163.44
		3.0	66.14	86.37	114.21	138.73	147.19	154.64	179.80	181.85	213.47	217.54
		5.0	82.45	106.91	140.32	166.60	179.34	184.75	213.31	220.73	251.29	262.72
		6.0	89.46	115.71	151.47	178.76	193.12	197.89	227.88	237.38	267.68	282.17
	75	1.0	48.97	63.58	84.37	107.02	112.06	121.55	137.69	142.63	166.65	171.13
		3.0	72.93	94.83	124.89	149.98	160.24	166.77	193.29	197.59	228.69	235.76
		5.0	91.24	117.89	154.18	181.71	196.44	201.07	231.40	241.38	271.62	286.82
		6.0	99.10	127.75	166.67	195.51	211.87	215.95	247.89	260.04	290.13	308.67
	90	1.0	52.66	68.05	89.89	112.97	117.87	127.33	145.25	149.03	175.21	178.33
		3.0	79.10	102.51	134.58	160.34	172.15	177.95	205.71	211.96	242.68	252.45
		5.0	99.21	127.83	166.73	195.56	211.92	216.00	247.94	260.09	290.16	308.70
		6.0	107.81	138.63	180.41	210.81	228.83	232.44	266.14	280.54	310.57	332.68
1.0	50	1.0	105.89	158.43	178.02	209.22	259.19	266.44	282.63	327.28	328.47	382.34
		3.0	149.82	237.91	252.07	314.60	366.65	379.66	400.25	453.31	487.10	520.73
		5.0	187.30	298.26	310.11	391.48	448.27	456.95	497.74	546.28	603.06	621.35
		6.0	203.58	324.12	335.27	424.19	483.55	490.95	539.32	586.08	652.55	665.27
	60	1.0	114.80	170.71	189.14	224.30	273.73	284.58	295.43	343.94	349.20	402.08
		3.0	163.05	258.26	271.51	340.27	393.55	404.90	432.49	483.97	525.27	553.51
		5.0	204.13	324.47	335.61	424.45	483.79	491.18	539.53	586.28	652.72	665.44
		6.0	221.95	352.81	363.32	460.22	522.68	528.94	585.08	629.99	706.94	714.13

	75	1.0	126.96	187.51	204.58	244.96	294.00	309.58	313.49	367.13	378.00	427.98
		3.0	181.00	285.90	298.13	375.06	430.44	439.91	476.33	525.78	577.26	598.74
		5.0	226.92	359.99	370.36	469.04	532.23	538.26	596.14	640.62	720.01	725.97
		6.0	246.81	391.63	401.48	508.93	575.93	581.04	647.01	689.63	780.54	781.08
	90	1.0	138.01	202.85	218.85	263.82	312.79	330.43	332.50	388.59	404.56	450.96
		3.0	197.25	310.94	322.42	406.50	464.12	472.21	516.06	563.76	624.42	640.33
		5.0	247.50	392.06	401.91	509.27	576.23	581.33	647.27	689.88	780.76	781.30
		6.0	269.23	426.65	436.07	552.85	624.23	628.57	702.89	743.67	842.14	846.90
2.0	50	1.0	168.14	220.78	296.38	381.84	408.15	443.42	496.46	523.96	605.29	632.32
		3.0	244.55	320.70	425.83	521.65	551.21	582.98	680.13	681.98	810.20	817.68
		5.0	303.76	395.36	520.83	621.51	667.75	690.79	800.26	823.01	946.19	981.01
		6.0	329.28	427.41	561.48	665.18	717.98	738.00	852.72	883.76	1005.39	1051.75
	60	1.0	179.73	234.87	313.72	401.41	424.26	461.12	518.96	543.36	630.67	654.16
		3.0	264.44	345.51	457.18	554.16	589.25	617.93	719.06	727.96	854.27	870.67
		5.0	329.63	427.68	561.69	665.35	718.14	738.15	852.85	883.89	1005.50	1051.86
		6.0	357.66	462.88	606.33	713.85	773.38	790.55	911.03	950.76	1071.05	1129.91
	75	1.0	195.75	254.35	337.75	427.93	448.03	485.84	551.07	570.65	666.91	684.93
		3.0	291.59	379.34	499.90	599.05	641.56	666.37	772.93	791.08	915.16	943.72
		5.0	364.78	471.58	617.19	725.64	786.70	803.25	925.07	966.79	1086.80	1148.60
		6.0	396.16	511.02	667.19	780.60	848.63	862.58	990.88	1041.80	1160.83	1236.39
	90	1.0	210.49	272.25	359.86	451.58	471.45	508.89	581.36	596.19	701.17	713.76
		3.0	316.26	410.08	538.71	640.38	689.30	711.01	822.51	848.69	971.10	1010.64
		5.0	396.59	511.35	667.45	780.81	848.83	862.78	991.05	1041.96	1160.98	1236.52

		6.0	430.96	554.57	722.26	841.52	916.73	928.28	1063.69	1124.23	1242.60	1332.96

Table 5.68

Natural frequency parameter of skew plate, B.C.- FFFF, β = 45º, v_s = 0.20, ρ_s = 1700 kg/m³ and γ =1.

a/b	E_s MN/m²)	H (m)	λ_1	λ_2	λ_3	λ_4	λ_5	λ_6	λ_7	λ_8	λ_9	λ_{10}
0.5	50	1.0	24.68	32.83	44.94	46.99	54.62	58.75	68.20	73.48	83.57	89.06
		3.0	25.25	40.55	62.11	62.97	74.63	85.58	95.30	109.00	118.83	126.42
		5.0	26.93	47.40	75.46	75.91	89.86	105.37	115.00	134.45	144.84	152.94
		6.0	27.73	50.43	81.23	81.57	96.46	113.82	123.45	145.24	156.02	164.28
	60	1.0	26.91	35.69	48.77	51.02	59.04	63.67	73.35	79.38	89.69	95.74
		3.0	27.55	44.12	67.51	68.47	80.77	92.98	102.73	118.19	128.28	135.89
		5.0	29.35	51.58	82.08	82.62	97.41	114.56	124.22	145.91	156.77	164.88
		6.0	30.21	54.88	88.38	88.81	104.62	123.77	133.46	157.64	169.01	177.30
	75	1.0	29.93	39.55	53.93	56.42	64.96	70.31	80.24	87.38	97.96	104.24
		3.0	30.65	48.95	74.81	75.89	89.06	102.97	112.74	130.58	141.07	148.68
		5.0	32.62	57.22	91.02	91.68	107.61	126.96	136.68	161.33	172.89	181.04
		6.0	33.56	60.88	98.03	98.59	115.65	137.19	146.99	174.33	186.56	194.90
	90	1.0	32.66	43.04	58.56	61.25	70.25	76.30	86.41	94.60	105.42	111.61
		3.0	33.46	53.30	81.38	82.58	96.53	111.96	121.74	141.72	152.60	160.21
		5.0	35.56	62.30	99.07	99.86	116.81	138.11	147.92	175.17	187.44	195.62
		6.0	36.57	66.28	106.71	107.41	125.60	149.25	159.21	189.32	202.40	210.81
1.0	50	1.0	81.36	113.86	120.83	144.84	169.99	182.16	183.59	207.65	225.62	248.13
		3.0	79.43	140.59	146.84	192.72	231.57	246.27	263.17	286.57	333.78	349.89

		5.0	83.33	165.05	172.39	230.94	281.79	299.01	323.06	346.38	412.16	427.61
		6.0	85.34	175.89	183.93	247.57	303.77	322.11	348.75	372.25	445.42	461.27
	60	1.0	88.87	124.13	130.91	157.51	184.12	195.71	199.54	224.11	244.63	266.40
		3.0	86.79	153.46	159.78	209.64	251.90	266.46	286.47	309.94	362.68	378.12
		5.0	90.97	180.09	187.86	251.29	306.99	324.49	351.76	375.31	447.98	463.50
		6.0	93.11	191.87	200.50	269.42	331.06	349.84	379.75	403.62	484.17	500.42
	75	1.0	99.06	138.04	144.55	174.60	203.16	213.99	221.10	246.14	270.37	291.01
		3.0	96.75	170.84	177.34	232.48	279.42	293.92	317.90	341.46	401.62	416.41
		5.0	101.28	200.35	208.81	278.76	341.08	359.06	390.46	414.43	496.20	512.15
		6.0	103.60	213.38	222.95	298.91	367.96	387.44	421.55	446.08	536.35	553.46
	90	1.0	108.28	150.61	156.89	190.00	220.29	230.51	240.56	265.84	293.61	313.17
		3.0	105.74	186.51	193.24	253.08	304.29	318.82	346.22	369.86	436.63	451.08
		5.0	110.58	218.58	227.75	303.52	371.84	390.34	425.28	449.77	539.53	556.12
		6.0	113.06	232.73	243.22	325.47	401.24	421.41	459.14	484.42	583.23	601.37
2.0	50	1.0	98.70	131.37	179.81	187.93	218.54	235.05	273.01	293.96	334.26	356.31
		3.0	100.99	162.23	248.53	251.82	298.53	342.42	381.41	436.14	475.24	505.69
		5.0	107.70	189.62	301.92	303.54	359.45	421.61	460.24	538.02	579.25	611.77
		6.0	110.94	201.76	325.03	326.18	385.82	455.44	494.05	581.18	623.95	657.14
	60	1.0	107.62	142.80	195.14	204.05	236.22	254.74	293.60	317.58	358.71	383.04
		3.0	110.18	176.51	270.14	273.80	323.09	372.03	411.14	472.92	513.05	543.59
		5.0	117.39	206.35	328.43	330.35	389.61	458.42	497.13	583.87	626.91	659.56
		6.0	120.86	219.56	353.66	355.10	418.43	495.31	534.10	630.85	675.84	709.20
	75	1.0	119.70	158.25	215.78	225.63	259.88	281.32	321.18	349.58	391.80	416.90

		3.0	122.62	195.82	299.32	303.46	356.24	412.00	451.17	522.50	564.16	594.75
		5.0	130.47	228.93	364.22	366.57	430.39	508.06	546.97	645.61	691.36	724.17
		6.0	134.25	243.57	392.30	394.14	462.53	549.04	588.27	697.69	746.01	779.64
	90	1.0	130.63	172.18	234.34	244.94	281.04	305.27	345.83	378.47	421.63	446.41
		3.0	133.84	213.24	325.62	330.20	386.12	447.99	487.17	567.10	610.26	640.85
		5.0	142.26	249.28	396.47	399.21	467.18	552.73	591.97	701.06	749.52	782.50
		6.0	146.30	265.20	427.10	429.32	502.30	597.37	637.21	757.72	809.31	843.24

Table 5.69

Natural frequency parameter of skew plate, B.C.- CCCC, $\beta = 60^o$, $v_s = 0.20$, $\rho_s = 1700$ kg/m³ and $\gamma = 1$.

a/b	E_s MN/m²)	H (m)	λ_1	λ_2	λ_3	λ_4	λ_5	λ_6	λ_7	λ_8	λ_9	λ_{10}
0.5	50	1.0	50.17	62.20	80.34	102.94	108.40	117.28	130.79	133.90	157.23	160.08
		3.0	69.26	86.95	111.96	139.53	142.54	152.57	172.92	175.94	200.44	211.65
		5.0	84.23	105.84	135.79	165.60	171.37	180.46	203.76	210.52	234.69	251.68
		6.0	90.74	114.01	146.10	177.00	183.95	192.73	217.34	225.54	249.78	269.15
	60	1.0	52.94	65.59	84.49	107.78	112.36	121.60	136.31	138.60	162.37	166.25
		3.0	74.25	93.18	119.77	148.02	151.87	161.58	182.87	187.17	211.47	224.59
		5.0	90.81	114.07	146.15	177.04	183.99	192.77	217.37	225.57	249.81	269.17
		6.0	97.99	123.09	157.53	189.72	197.91	206.42	232.47	242.19	266.62	288.54
	75	1.0	56.82	70.32	90.27	114.53	118.07	127.74	144.13	145.32	169.73	175.04
		3.0	81.10	101.74	130.50	159.72	164.83	174.11	196.71	202.65	226.81	242.50
		5.0	99.80	125.32	160.30	192.79	201.27	209.73	236.12	246.18	270.68	293.18
		6.0	107.86	135.47	173.13	207.18	216.99	225.23	253.29	264.95	289.81	315.09

	90	1.0	60.42	74.71	95.64	120.74	123.57	133.54	151.48	151.67	176.70	183.34
		3.0	87.36	109.55	140.30	170.50	176.75	185.69	209.51	216.85	241.02	258.98
		5.0	107.96	135.55	173.19	207.24	217.04	225.28	253.33	264.99	289.84	315.12
		6.0	116.83	146.72	187.31	223.16	234.37	242.44	272.34	285.69	311.05	339.30
1.0	50	1.0	114.61	172.16	182.42	224.99	263.33	271.92	287.17	325.05	352.78	375.98
		3.0	160.16	253.26	259.66	329.50	374.38	377.69	420.81	449.13	510.36	512.00
		5.0	198.47	314.88	319.85	406.73	458.83	460.67	519.33	542.69	617.67	619.90
		6.0	215.13	341.37	345.92	439.88	495.37	496.86	561.62	583.27	663.85	665.80
	60	1.0	123.49	184.44	193.89	239.76	278.26	285.81	305.04	341.37	373.21	393.11
		3.0	173.59	273.95	279.79	355.15	402.17	404.87	453.27	479.78	546.35	548.48
		5.0	215.66	341.70	346.25	440.13	495.60	497.08	561.82	583.46	664.02	665.97
		6.0	233.93	370.80	374.97	476.57	535.91	537.12	608.32	628.34	715.21	716.98
	75	1.0	135.63	201.30	209.81	260.08	299.08	305.41	329.79	364.13	401.65	417.30
		3.0	191.84	302.13	307.35	390.10	440.31	442.39	497.57	521.90	593.86	596.30
		5.0	238.97	378.15	382.23	485.56	545.79	546.96	619.63	639.28	727.64	729.38
		6.0	259.42	410.74	414.50	526.45	591.14	592.15	671.82	689.96	785.55	787.22
	90	1.0	146.71	216.72	224.51	278.68	318.39	323.79	352.57	385.23	427.94	439.98
		3.0	208.40	327.71	332.47	421.85	475.16	476.83	537.88	560.46	637.58	639.68
		5.0	260.08	411.15	414.91	526.77	591.43	592.44	672.07	690.20	785.77	787.44
		6.0	282.48	446.89	450.36	571.65	641.30	642.25	729.37	746.09	849.68	851.40
2.0	50	1.0	200.50	248.74	321.53	412.01	432.90	468.59	523.60	535.35	629.12	640.80
		3.0	276.85	347.74	447.98	557.46	570.39	609.60	691.25	704.40	801.79	847.37
		5.0	336.71	423.26	543.32	661.42	685.91	720.96	814.44	842.92	938.61	1007.80

		6.0	362.68	455.94	584.56	706.88	736.30	769.92	868.62	903.13	998.90	1077.87
	60	1.0	211.59	262.32	338.10	431.34	448.79	485.86	545.68	554.15	649.68	665.50
		3.0	296.81	372.67	479.24	591.31	607.83	645.60	731.00	749.37	845.83	899.22
		5.0	363.00	456.19	584.76	707.04	736.46	770.07	868.75	903.25	999.02	1077.97
		6.0	391.63	492.24	630.30	757.55	792.23	824.51	929.03	969.89	1066.18	1155.68
	75	1.0	227.10	281.24	361.24	458.25	471.73	510.40	576.99	580.97	679.07	700.69
		3.0	324.19	406.88	522.14	637.97	659.74	695.63	786.27	811.39	907.16	971.01
		5.0	398.85	501.14	641.39	769.82	805.71	837.70	943.60	985.93	1082.39	1174.33
		6.0	431.04	541.71	692.70	827.10	868.68	899.48	1012.07	1061.22	1158.80	1262.30
	90	1.0	241.50	298.78	382.72	482.96	493.88	533.58	606.37	606.44	706.94	733.94
		3.0	349.20	438.12	561.36	680.96	707.46	741.85	837.36	868.32	963.92	1037.10
		5.0	431.44	542.03	692.95	827.31	868.88	899.67	1012.24	1061.38	1158.95	1262.43
		6.0	466.81	586.65	749.46	890.65	938.33	968.02	1088.04	1144.46	1243.67	1359.60

Table 5.70

Natural frequency parameter of skew plate, B.C.- SSSS, $\beta = 60^o$, $v_s = 0.20$, $\rho_s = 1700$ kg/m³ and $\gamma = 1$.

a/b	E_s MN/m²)	H (m)	λ_1	λ_2	λ_3	λ_4	λ_5	λ_6	λ_7	λ_8	λ_9	λ_{10}
0.5	50	1.0	38.69	50.04	66.79	82.33	87.97	92.27	108.61	111.71	131.55	137.40
		3.0	58.67	75.74	99.43	117.24	127.68	129.75	149.62	158.72	176.51	190.90
		5.0	74.00	94.99	123.66	144.05	157.27	158.58	181.31	193.98	211.46	231.21
		6.0	80.59	103.27	134.08	155.72	170.02	171.13	195.14	209.21	226.77	247.20
	60	1.0	41.76	53.69	71.18	86.79	93.08	96.98	113.68	117.59	137.01	143.93
		3.0	63.82	82.13	107.41	125.98	137.36	139.13	159.90	170.21	187.81	204.12

		5.0	80.68	103.34	134.14	155.76	170.06	171.17	195.18	209.25	226.80	247.23
		6.0	87.93	112.45	145.62	168.67	184.13	185.07	210.51	226.06	243.80	265.11
	75	1.0	45.98	58.73	77.25	93.06	100.22	103.63	120.84	125.85	144.76	153.15
		3.0	70.85	90.86	118.31	138.04	150.63	152.08	174.11	186.00	203.47	222.35
		5.0	89.77	114.70	148.41	171.81	187.53	188.43	214.21	230.10	247.90	269.44
		6.0	97.89	124.91	161.32	186.38	203.37	204.13	231.57	249.03	267.20	289.87
	90	1.0	49.83	63.34	82.84	98.92	106.83	109.86	127.57	133.55	152.06	161.81
		3.0	77.22	98.80	128.25	149.10	162.74	163.96	187.19	200.43	217.90	237.91
		5.0	97.99	125.00	161.38	186.44	203.42	204.18	231.61	249.07	267.24	289.91
		6.0	106.90	136.21	175.57	202.52	220.84	221.51	250.78	269.92	288.59	312.62
1.0	50	1.0	102.16	151.00	158.67	196.85	229.27	235.71	252.11	283.50	310.82	328.35
		3.0	146.98	232.18	237.36	301.89	342.60	345.11	386.51	410.45	468.52	469.45
		5.0	185.33	293.98	298.15	379.49	427.90	429.32	485.27	505.33	575.82	577.65
		6.0	202.00	320.52	324.38	412.75	464.68	465.82	527.61	546.32	622.47	624.07
	60	1.0	111.28	163.57	170.70	211.95	244.82	250.46	270.34	300.47	331.66	346.32
		3.0	160.50	253.00	257.78	327.72	370.77	372.82	419.10	441.62	503.52	505.95
		5.0	202.56	320.87	324.73	413.02	464.92	466.07	527.82	546.53	622.65	624.25
		6.0	220.84	349.99	353.57	449.55	505.42	506.35	574.35	591.78	674.26	675.68
	75	1.0	123.69	180.77	187.27	232.63	266.37	271.09	295.47	324.01	360.54	371.54
		3.0	178.86	281.30	285.64	362.87	409.30	410.90	463.54	484.34	551.76	553.76
		5.0	225.92	357.37	360.88	458.58	515.36	516.25	585.68	602.81	686.79	688.17
		6.0	246.35	389.96	393.23	499.52	560.87	561.61	637.87	653.80	745.05	746.33
	90	1.0	134.95	196.43	202.45	251.49	286.24	290.26	318.52	345.73	387.13	395.06

		3.0	195.47	306.97	310.98	394.77	444.43	445.72	503.92	523.36	596.00	597.73
		5.0	247.04	390.39	393.66	499.86	561.17	561.91	638.13	654.06	745.28	746.55
		6.0	269.41	426.11	429.15	544.78	611.18	611.81	695.41	710.21	809.50	810.72
2.0	50	1.0	154.69	200.17	267.38	328.73	352.22	368.64	434.37	447.29	526.64	550.12
		3.0	234.61	302.96	397.90	468.44	511.12	518.61	598.32	635.47	706.34	764.24
		5.0	295.94	379.99	494.81	575.70	629.50	633.91	725.04	776.65	846.08	923.18
		6.0	322.33	413.11	536.52	622.36	680.56	684.10	780.35	837.65	907.29	987.05
	60	1.0	166.98	214.79	284.92	346.59	372.67	387.51	454.62	470.85	548.47	576.24
		3.0	255.24	328.55	429.81	503.42	549.86	556.14	639.43	681.48	751.51	817.17
		5.0	322.68	413.39	536.73	622.54	680.72	684.27	780.49	837.78	907.41	987.17
		6.0	351.66	449.81	582.67	674.15	737.03	739.82	841.81	905.12	975.42	1058.59
	75	1.0	183.85	234.93	309.21	371.68	401.23	414.12	483.27	503.90	579.45	613.16
		3.0	283.34	363.46	473.42	551.65	602.95	607.91	696.26	744.67	814.12	889.96
		5.0	359.01	458.82	593.86	686.67	750.64	753.27	856.61	921.31	991.82	1075.85
		6.0	391.48	499.68	645.50	744.93	814.04	816.03	926.00	997.18	1068.98	1157.40
	90	1.0	199.28	253.40	331.56	395.12	427.70	439.03	510.19	534.70	608.63	647.79
		3.0	308.85	395.20	513.16	595.89	651.42	655.45	748.54	802.45	871.85	949.93
		5.0	391.91	500.02	645.76	745.16	814.25	816.24	926.18	997.35	1069.14	1157.54
		6.0	427.52	544.89	702.53	809.38	884.03	885.46	1002.81	1080.90	1154.54	1248.15

Table 5.71

Natural frequency parameter of skew plate, B.C.- FFFF, β = 60º, v_s = 0.20, ρ_s = 1700 kg/m³ and γ =1.

a/b	E_s MN/m^2)	H (m)	λ_1	λ_2	λ_3	λ_4	λ_5	λ_6	λ_7	λ_8	λ_9	λ_{10}
0.5	50	1.0	23.20	30.74	42.55	43.75	50.06	56.68	61.89	71.42	77.12	81.07
		3.0	23.53	38.54	59.92	60.25	70.09	83.59	88.14	106.04	112.72	117.17
		5.0	25.15	45.57	73.61	73.62	85.71	103.68	108.03	131.19	139.23	144.02
		6.0	25.95	48.70	79.47	79.56	92.49	112.30	116.67	141.94	150.67	155.63
	60	1.0	25.35	33.49	46.19	47.53	54.19	61.37	66.61	77.03	82.97	86.77
		3.0	25.70	42.03	65.25	65.66	76.17	90.92	95.40	114.99	122.09	126.50
		5.0	27.43	49.70	80.26	80.33	93.29	112.93	117.28	142.52	151.23	156.08
		6.0	28.29	53.11	86.74	86.77	100.73	122.36	126.79	154.29	163.80	168.86
	75	1.0	28.27	37.21	51.11	52.64	59.77	67.74	72.97	84.64	90.89	94.50
		3.0	28.64	46.75	72.49	73.00	84.41	100.87	105.26	127.11	134.80	139.20
		5.0	30.52	55.28	89.26	89.42	103.57	125.45	129.85	157.87	167.53	172.49
		6.0	31.45	59.07	96.53	96.59	111.89	135.97	140.54	171.02	181.64	186.86
	90	1.0	30.90	40.58	55.57	57.25	64.81	73.50	78.71	91.53	98.03	101.49
		3.0	31.29	51.01	79.03	79.64	91.86	109.86	114.20	138.06	146.32	150.74
		5.0	33.30	60.31	97.39	97.64	112.87	136.75	141.27	171.74	182.30	187.40
		6.0	34.29	64.44	105.35	105.49	121.98	148.26	153.01	186.14	197.80	203.19
1.0	50	1.0	78.29	109.12	111.85	137.38	159.22	164.61	177.34	190.33	218.97	227.77
		3.0	74.77	136.31	139.07	184.72	223.52	233.37	257.27	268.04	324.55	333.21
		5.0	78.16	161.71	165.32	223.79	275.58	288.61	318.47	328.94	402.52	413.91

		6.0	80.04	173.02	177.12	240.89	298.31	312.63	344.88	355.47	435.99	448.81
	60	1.0	85.65	119.13	121.74	149.50	172.85	178.01	192.72	205.54	237.15	245.34
		3.0	81.76	148.95	151.81	201.38	243.79	253.93	280.41	291.02	352.81	361.74
		5.0	85.37	176.66	180.61	244.12	300.96	314.61	347.42	357.99	438.19	450.53
		6.0	87.38	188.99	193.53	262.82	325.90	340.95	376.32	387.13	474.85	488.87
	75	1.0	95.63	132.71	135.18	165.91	191.34	196.25	213.58	226.10	261.81	269.22
		3.0	91.21	166.05	169.10	223.95	271.29	281.88	311.76	322.25	391.08	400.55
		5.0	95.10	196.86	201.32	271.64	335.37	349.88	386.60	397.44	486.51	500.27
		6.0	97.28	210.56	215.76	292.49	363.29	379.35	418.86	430.12	527.50	543.25
	90	1.0	104.65	145.01	147.37	180.75	208.08	212.82	232.46	244.68	284.13	290.88
		3.0	99.75	181.48	184.75	244.35	296.19	307.21	340.10	350.57	425.67	435.77
		5.0	103.88	215.07	220.05	296.49	366.50	381.79	421.99	433.19	530.20	545.32
		6.0	106.21	230.00	235.86	319.28	397.10	414.07	457.26	469.06	575.09	592.48
2.0	50	1.0	92.81	122.99	170.25	174.93	200.22	226.74	247.74	285.71	308.37	324.40
		3.0	94.14	154.16	239.71	240.94	280.36	334.39	352.70	424.20	450.82	468.73
		5.0	100.59	182.31	294.43	294.48	342.82	414.76	432.25	524.80	556.86	576.10
		6.0	103.79	194.80	317.82	318.27	369.96	449.24	466.81	567.81	602.63	622.53
	60	1.0	101.40	133.97	184.80	190.08	216.75	245.53	266.58	308.13	331.80	347.18
		3.0	102.82	168.12	261.05	262.60	304.65	363.73	381.71	459.98	488.29	506.04
		5.0	109.73	198.82	321.07	321.26	373.15	451.75	469.24	570.12	604.86	624.32
		6.0	113.16	212.44	346.90	347.12	402.90	489.47	507.28	617.21	655.16	675.43
	75	1.0	113.06	148.86	204.50	210.51	239.07	271.00	292.01	338.57	363.47	378.09
		3.0	114.56	187.00	289.98	291.96	337.61	403.50	421.14	508.46	539.15	556.82

		5.0	122.07	221.14	357.09	357.61	414.28	501.82	519.56	631.51	670.06	689.95
		6.0	125.80	236.28	386.19	386.27	447.54	543.92	562.31	684.13	726.51	747.40
	90	1.0	123.60	162.34	222.32	228.94	259.23	294.04	314.96	366.16	392.04	406.05
		3.0	125.15	204.06	316.14	318.51	367.43	439.46	456.91	552.28	585.24	602.96
		5.0	133.19	241.27	389.64	390.46	451.47	547.05	565.22	687.00	729.16	749.54
		6.0	137.19	257.78	421.49	421.84	487.90	593.07	612.24	744.63	791.17	812.71

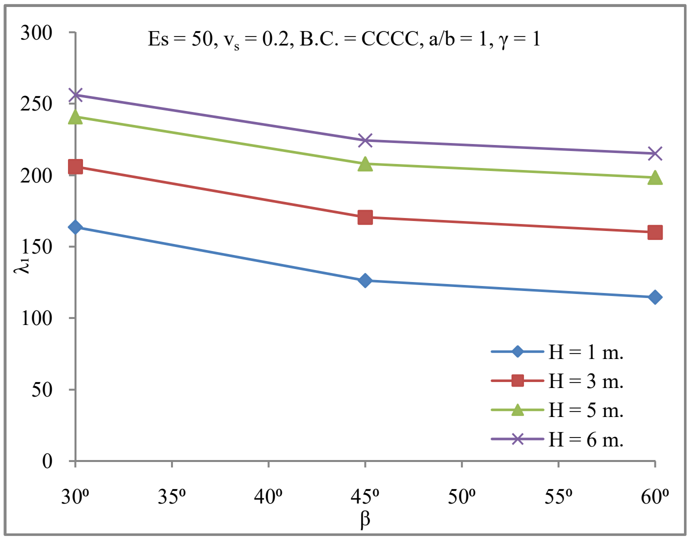

Fig. 5.99 Frequency parameter vs skew angle of the plate

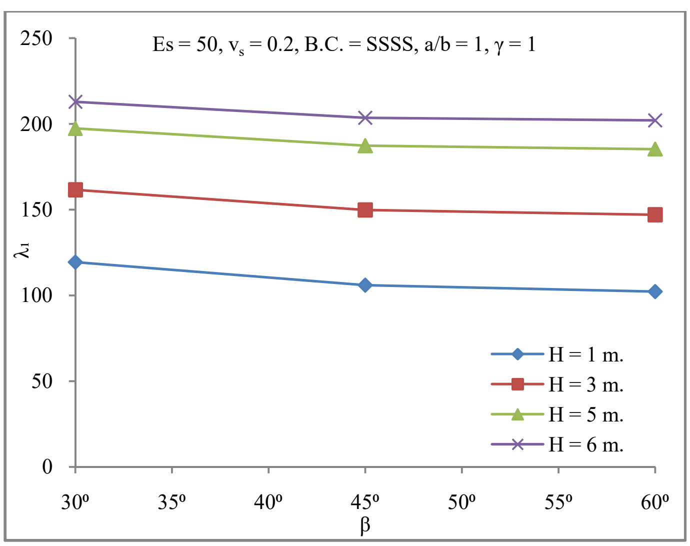

Fig. 5.100 Frequency parameter vs skew angle of the plate

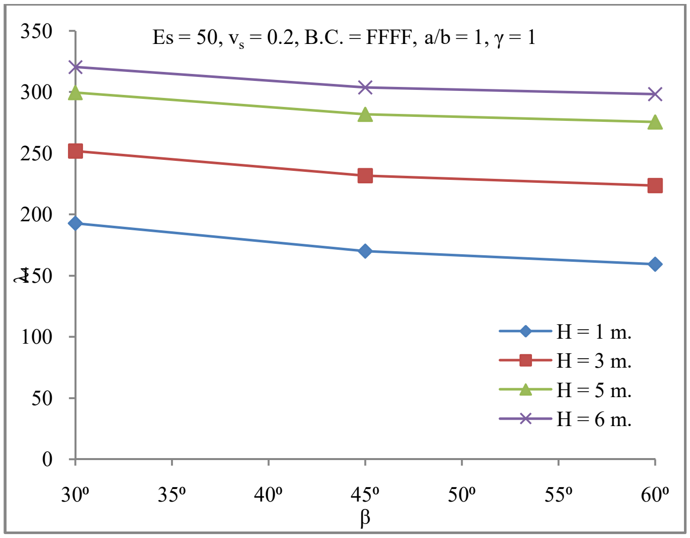

Fig. 5.101 Frequency parameter vs skew angle of the plate

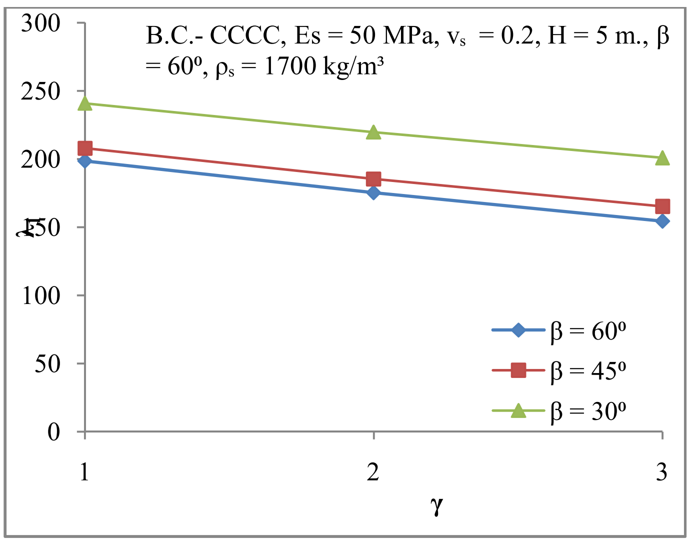

Fig. 5.102 Frequency parameter vs vertical decay parameter, γ

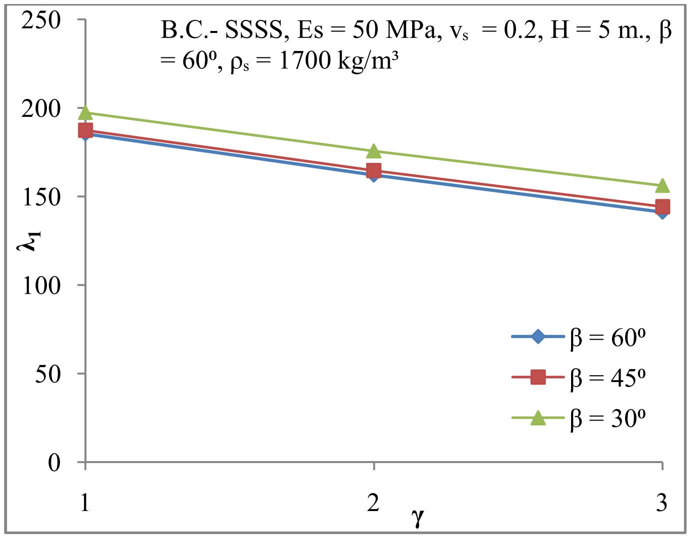

Fig. 5.103 Frequency parameter vs vertical decay parameter, γ

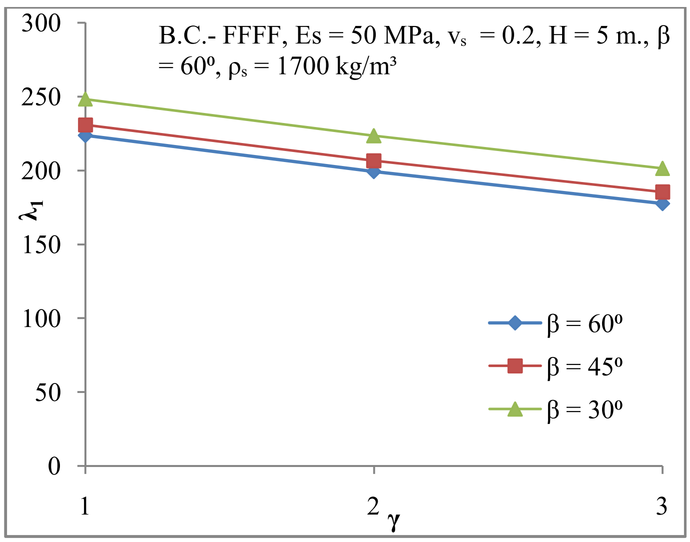

Fig. 5.104 Frequency parameter vs vertical decay parameter, γ

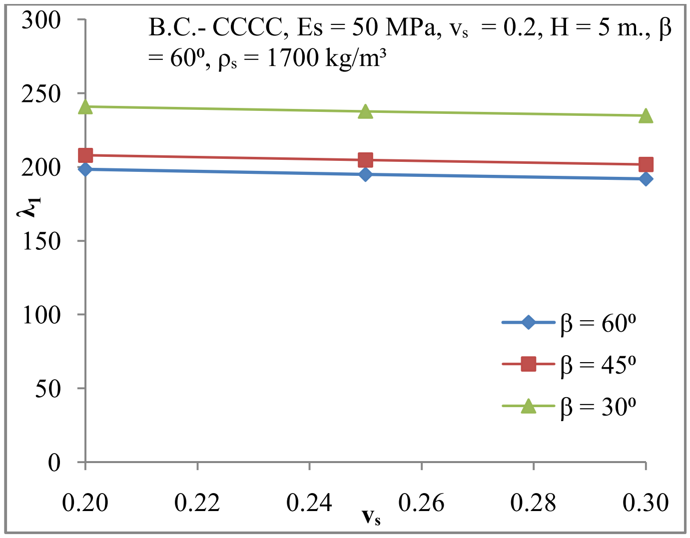

Fig. 5.105 Frequency parameter vs sub-soil Poisson's ratio, **v_s**

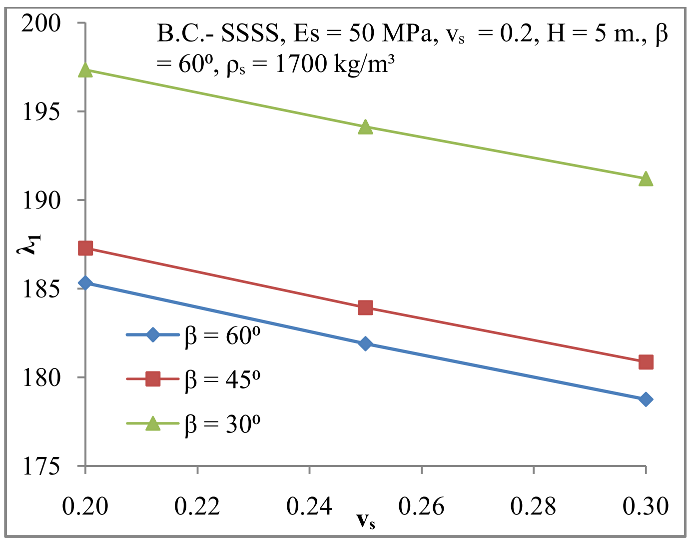

Fig. 5.106 Frequency parameter vs sub-soil Poisson's ratio, **v_s**

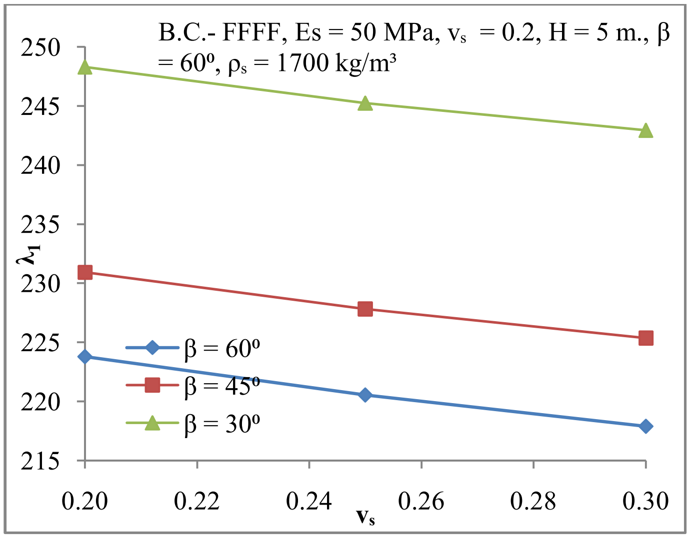

Fig. 5.107 Frequency parameter vs sub-soil Poisson's ratio, $\mathbf{v_s}$

Figures 5.99- 5.101 show the variation of the frequency parameter with a skew angle of the plate. It is observed from Figures 5.99- 5.101 that the frequency parameter decreases with an increase in skew angle for CCCC plate, but in the case of FFFF and SSSS plate, the skew angle has a negligible effect on the frequency parameter.

Figures 5.102- 5.104 show the variation of the frequency parameter with the vertical decay parameter, γ. It is observed that the frequency parameter decreases linearly with increases in the vertical decay parameter, γ

It is observed from figures 5.105- 5.107 that the frequency parameter has a negligible effect on sub-soil Poisson's ratio, $\mathbf{v_s}$.

It is also observed that the frequency parameter increases with increased constraints on the edges; this shows that higher constraints on the edges improve the flexural rigidity of the plate and, hence, higher frequency response. It is also observed that the first foundation parameter/Winkler parameter, K, increases with an increase of **γ** and the second foundation parameter, 2t and activated mass, m_0, decreases with a rise in **γ.**

It is observed that the frequency parameter of the plate increases as the aspect ratio increases, irrespective of boundary conditions and other parameters.

It is observed that the frequency parameter of the plate increases linearly as the sub-soil elastic modulus**,** E_s, increases irrespective of boundary conditions and other parameters.

It is observed that the frequency parameter of the plate increases as the sub-soil depth**,** H, increases, irrespective of boundary conditions and other parameters.

Chapter 6
Summary and Conclusions

6.1 Conclusions on static analysis of plate

This study deals with the effect of normal and shear strain, considering the higher-order shear deformable plate theory incorporating normal strain, resting on the two-parameter elastic foundation using a nine-nodded Lagrange element (PBQ9). In addition, the elements' accuracy and efficiency are tested, and a parametric study is performed. This study demonstrates that the PBQ9 element provides accurate findings for larger plate thicknesses and is the best alternative in light of the impact of normal strain. The thick plates on elastic foundations can be analyzed successfully using the PBQ9 element, regardless of the load case or boundary conditions. As the h/L ratio rises, the influence of normal strain on displacement is more significant for concentrated load cases than distributed load cases. The observations show that for free plates on an elastic foundation, the impact of normal strain and shear strain on the behaviour of the plate always plays a crucial role.

The examples highlight a few benefits of the suggested strategy for a finite element solution of a plate on an elastic foundation.

The following opportunities are provided by it:

- Application of various loads at any point or region on the plate;
- Application of force or displacement boundary conditions at the plate's ends;
- Application of the approach on thin to thick plates;
- Smooth variation of the stiffness of the plate and the soil medium along the plate's length;
- This method considers the influence of normal strain, and the shear strain adequately illustrates the impact on the case of thin to thick plates.

Circular plate bending elements resting on elastic foundations are analyzed using polar coordinates and the modified Vlasov model. Other researchers' data validate the proposed formulation's accuracy and efficacy for diverse foundation parameters, loading situations, and boundary conditions. A parametric study explains the effect of varying foundation parameters. Higher-order finite elements work effectively for uniform and concentrated load instances on a thin, solid circular plate resting on a two-parameter elastic foundation, producing an accurate deflection and stress approximation solution.

- The approach has a very rapid convergence and produces exceptionally accurate predictions.
- Stresses at an element's centre reduce the problem of evaluating moments under a point load.
- The numerical findings for uniform and concentrated loading conditions of the solid circular plate and support conditions will demonstrate the usefulness of the present elements. Still, they will also be a handy reference for future researchers in this field.
- The element's attractiveness and usefulness to practitioners and design engineers may be attributed to its straightforward formulation, capacity to produce accurate moment values, cost-effectiveness, and requirement for less computational effort, resources, and time.
- The outcomes of this study agree with the precise and quantitative findings reported in the literature.

6.2 Conclusions on vibration analysis of plate

In the present study, the modified Vlasov model uses higher-order finite elements for free vibration analysis of thin plates resting on a two-parameter elastic foundation. The effects of aspect ratio and skew angle of the plate, subsoil depth, Poisson's ratio of the subsoil, and vertical deformation parameter within the subsoil on frequency parameters are observed. Higher-order finite element results have a remarkable agreement with the exact solution and reference result and rapid convergence regardless of boundary conditions, aspect ratio, and foundation parameters. Higher-order finite element tabulates the first ten eigenvalues of a plate resting on a two-parameter elastic foundation for varying boundary conditions, rigid base depth, skew angle, vertical decay function, and aspect ratio. The Winkler parameter of the foundation affects the plate's natural frequency more than the shear parameter. Therefore, higher-order finite elements can be employed successfully and efficiently for free vibration analysis of thin plates on elastic foundations. According to numerical studies encompassing varying support conditions, higher-order finite elements for vibration analysis operate well for skew and thin rectangular plates on an elastic foundation and give an accurate approximation solution.

The numerical results in the previous section are used to make the conclusions below.

- ➢ The method converges rapidly and makes accurate predictions.
- ➢ Numerical results for the skew plate and various support conditions will demonstrate the present elements' effectiveness. Still, they will be a convenient reference for future academics,

practitioners, and design engineers due to their ease of formulation, capacity to produce an approximate solution, and cost-effectiveness.

In the present study, the free vibration of a thin plate resting on a two-parameter elastic foundation using a modified Vlasov model is investigated the effects of the aspect ratio of the plate, the subsoil depth, the ratio of the subsoil depth to the span of the plate and the vertical deformation parameter within the subsoil on the frequency parameters. C^2 compatible type plate element is used for free vibration analysis using finite element formulation. It is shown that the result obtained using C^2 compatible type plate element has excellent agreement with the exact solution and referred result and rapid convergence regardless of boundary conditions, aspect ratio, modulus of sub-grade reaction and shear modulus. Using C^2 compatible type plate element, the first ten eigenvalues of the plate on a two-parameter elastic foundation are tabulated for different boundary conditions, depth of rigid base, vertical decay function and aspect ratio.

- ✓ It is observed that the frequency parameter of the plate increases as the aspect ratio increases. However, as this ratio increases, the results of a thin plate deviate depending on boundary conditions, foundation parameters and the mode number.
- ✓ For a higher mode number, the effect of the aspect ratio is more prominent.
- ✓ The impact of elastic foundation parameters has been studied, and it is found that the Winkler parameter of the foundation has a more significant effect on the plate's natural frequency than the foundation's shear parameter.
- ✓ It is seen that the C^2 compatible type plate element can be used effectively and quickly for free vibration analysis of thin plates on elastic foundations under any boundary conditions.

6.3 Future scope of the work

- The present research work can be extended to consider the effect of layered soil and/or Gibson soil.
- The analysis can be further extended to account for the time-varying elastic properties of the soil.
- The model can be extended to consider a plate's dynamic and stability analysis on an elastic foundation.
- The model can be extended to consider the analysis of anisotropic, laminated and functionally graded plates on an elastic foundation.

References

Akhavan, H., Hosseini, S., Damavandi, H.R., Alibeigloo, A., and Vahabi, S. (2009). Exact solutions for rectangular Mindlin plates under in-plane loads resting on Pasternak elastic foundation . Part II : Frequency analysis: Vol. 44, pp. 951–961, DOI: 10.1016/j.commatsci.2008.07.001.

Ascione, L., and Grimaldi, A. (1984). Unilateral contact between a plate and an elastic foundation: *Mechanica*, Vol. 19, pp. 223–33.

Auersch, L. (1996). Dynamic plate - soil interaction - finite and infinite, flexible and rigid plates on homogeneous, layered or Winkler soil: *Soil Dynamics and Earthquake Engineering*, Vol. 15, pp. 51–59.

Bahmyari, E., and Rahbar-Ranji, A. (2012). Free vibration analysis of orthotropic plates with variable thickness resting on non-uniform elastic foundation by element free Galerkin method: *Journal of Mechanical Science and Technology*, Vol. 26, No. 9, pp. 2685–2694, DOI: 10.1007/s12206-012-0713-z.

Benyoucef, S., Mechab, I., Tounsi, A., Fekrar, A., Atmane, H.A., and Bedia, E.A.A. (2010). Bending of thick functionally graded plates resting on Winkler-Pasternak elastic foundations: *Mechanics of Composite Materials*, Vol. 46, No. 4, pp. 425–434, DOI: 10.1007/s11029-010-9159-5.

Bhattacharya, R., and Banerjee, B. (1991). Non-linear dynamic response of thick plate placed on elastic foundation: *Journal of Sound and Vibration*, Vol. 45, No. 3, pp. 499–502.

Biot, M.A. (1937). Bending of an infinite beam on an elastic foundation: *Journal of Applied Physics*, Vol. 12, No. 2, pp. 155–164, DOI: 10.1063/1.1712886.

Bogner, F.K., Fox, R.L., and Schmit, L.A. (1966). “The generation of inter-element-compatible stiffness and mass matrices by the use of interpolation formulas.” *Proceedings of the Conference on Matrix Methods in Structural Mechanics*,, p. 397–444.

Borowicka, H. (1936). “Influence of Rigidity of a Circular Foundation Slab on Distribution of Pressure Over the Contact Surface.” *Proc. 1St Int. Conf. Soil Mech. Found. Engng.*,, p. 144–49.

Bowles, J.E. (1996). *Foundation Analysis and design*, McGraw-Hill, New York.

Brown, P.T. (1974). Influence of soil inhomogeneity on raft behaviour: *Soil Foundation*, Vol. 14, pp. 61–70.

Brown, P.T. (1969a). Numerical analysis of uniformly loaded circular rafts on deep elastic foundation: *Geotechnique*, Vol. 19, No. 3, pp. 399–404.

Brown, P.T. (1969b). Numerical analysis of uniformly loaded circular rafts on elastic layers of finite depth: *Geotechnique*, Vol. 19, No. 2, pp. 301–306.

Buczkowski, R., Taczała, M., and Kleiber, M. (2015). A 16-node locking-free Mindlin plate resting on two-parameter elastic foundation – Static and eigenvalue analysis: *Computer Assisted Methods in Engineering and Science*, Vol. 22, No. 2, pp. 99–114.

Buczkowski, R., and Torbacki, W. (2010). Finite element analysis of plate on layered tensionless foundation: *Archives of Civil Engineering*, Vol. 56, No. 3, pp. 255–274, DOI: 10.2478/v.10169-010-0014-9.

Buczkowski, R., and Torbacki, W. (2001). Finite element modelling of thick plates on two-parameter elastic foundation: *International Journal for Numerical and Analytical Methods in Geomechanics*, Vol. 25, No. 14, pp. 1409–1427, DOI: 10.1002/nag.187.

Butalia, T.S., Kant, T., and Dixit, V.D.T. (1990). Performance of Heterosis Element For Bending of Skew Rhombic Plates: Vol. 34, No. I, pp. 23–49.

Caifeng, H., and Hartley, G.A. (1994). Analysis of thin plate on an elastic half-space: *Compurers & Structures*, Vol. 52, No. 2, pp. 227–235.

Celep, Z. (1988). Circular plates on tensionless Winkler foundation: *J. Eng. Mech*, Vol. 114, No. 10, pp. 1723–1739.

Celep, Z., and Turhan, D. (1990). Axisymmetric vibrations of circular plates on tensionless elastic foundations: *J Appl Mech*, Vol. 57, pp. 677–681, DOI: 10.1115/1.2897076.

Celik, M., and Omurtag, M.H. (2005). Determination of the Vlasov foundation parameters – quadratic variation of elasticity modulus - using FE analysis: *Structural Engineering and Mechanics*, Vol. 19, No. 6, pp. 619–637.

Celik, M., and Saygun, A. (1999a). Method for the analysis of plates on a two-parameter foundation: *International Journal of Solids and Structures*, Vol. 36, pp. 2891–15.

Celik, M., and Saygun, A. (1999b). Method for the analysis of plates on a two-parameter foundation: *Int J Solids Struct*, Vol. 36, pp. 2891–15.

Chakraverty, S. (2009). *Vibration of Plates*, CRC Press is an imprint of the Taylor & Francis Group.

Chandrasekharappa, G. (1992). Nonlinear Static & Dynamic damped response of a composite

Rectangular plate resting a two parameter elastic foundation: *Compurers & Structures*, Vol. 44, No. 3, pp. 609–618.

Chandrashekhara, K., and Antony, J. (1997). Elastic analysis of an annular slab-soil interaction problem using a hybrid method: *Computers and Geotechnics*, Vol. 20, pp. 161–76.

Cheung, Y.K., and Nag, D.K. (1968). Plates & beams on elastic foundations linear and non-linear behaviour: *Geotechnique*, Vol. 18, pp. 450–460.

Cheung, Y.K., and Zienkiewicz, O.C. (1965). Plates and Tanks on Elastic Foundations- an Application of Finite Element Method: *Int J Solids Struct*, Vol. 1, pp. 451–461.

Chun, P., and Lim, Y.M. (2011). Analytical Behavior Prediction for Skewed Thick Plates on Elastic Foundation: Vol. 2011, DOI: 10.1155/2011/509724.

Chun, P., and Ohga, M. (2012). Analytical method to predict the bending behavior of skewed thick plates on Winkler foundation: *Journal of Japan Society of Civil Engineers Ser A2 (Applied Mechanics (AM))*, Vol. 68, No. 2, pp. 33–43, DOI: 10.2208/iscejam.68.I.

CİVALEK, Ö. (2008). Static analysis of shear deformable rectangular plates on Winkler-Pasternak foundation: *Journal of Engineering and Natural Sciences*, Vol. 25, No. 4, pp. 380–386.

Daloglu, A.T., and Ozgan, K. (2004). The effective depth of soil stratum for plates resting on elastic foundation: *Structural Engineering and Mechanics*, Vol. 18, No. 2, pp. 263–276, DOI: 10.12989/sem.2004.18.2.263.

Davies, B.T.G., Asce, A.M., Sen, R., Banerjee, P.K., and Asce, M. (1986). Dynamic behavior of pile g r o u p s in inhomogeneous soil: Vol. I, No. 12, pp. 1365–1379.

Dutta, A.K., Bandyopadhyay, D., and Mandal, J.J. (2021). Response Analysis of Second - Order Continuity Rectangular Plate Bending Element Resting on Elastic Foundation Using Modified Vlasov Model: *International Journal of Pavement Research and Technology*, DOI: 10.1007/s42947-021-00096-0.

El-Zafrany, A., and Fadhil, S. (1996). A Modified Kirchhoff Theory for Boundary Element Analysis of Thin Plates Resting on Two-Parameter Foundation: *Engineering Structures*, Vol. 18, No. 2, pp. 102–114.

Elhuni, H., Bipin, K.G., and Basu, D. (2019). "A New Analysis of Circular Raft on Layered Elastic Soil." *Geo-Congress 2019 GSP 307*,, p. 509–520.

Feng, Y.T., and Owen, D.R. (1996). Iterative solution of coupled FE / BE discretisations for plate-foundation interaction problems: *International Journal for Numerical Methods in Engineering*, Vol. 39, pp. 1889–1901.

Ferreira, A.J.M., Roque, C.M.C., Neves, A.M.A., R.M.N., J., and Soares, C.M.. (2010). Analysis of plates on Pasternak foundations by radial basis functions: *Comput Mech*, pp. 791–803, DOI: 10.1007/s00466-010-0518-9.

Filonenko-Borodich, M.M. (1940). Some approximate theories of elastic foundation: *Uch. Zapi. Mosk. Gos, Univ. Mekh.*, Vol. 46, pp. 3–18.

Fraser, R.A., and Wardle, L.J. (1976). Numerical analysis of rectangular rafts on layered foundations: *Geotechnique*, Vol. 26, No. 4, pp. 613–630.

Galin, L.A. (1943). On the Winkler-Zimmermann hypothesis for beams: *Prikl. Mat. Mekh*, Vol. 7, No. 4, pp. 293–300.

Galletly, G.D. (1959). Circular plates on a generalized elastic foundation: *J Appl Mech*, Vol. 26, No. 297.

Ghosh, A.K. (1997a). Axisymmetric dynamic response of a circular plate on an elastic foundation: *Journal of Sound and Vibration*, Vol. 205, No. 1, pp. 112–120.

Ghosh, A.K. (1997b). Axisymmetric dynamic response of a circular plate on an elastic foundation: *Journal of Sound and Vibration*, Vol. 205, No. 1, pp. 112–120.

Gibigaye, M., Yabi, C.P., and Degan, G. (2018). Free vibration analysis of dowelled rectangular isotropic thin plate on a Modified Vlasov soil type by using discrete singular convolution method: *Applied Mathematical Modelling*, Vol. 61, pp. 618–633, DOI: 10.1016/j.apm.2018.05.019.

Gucunski, N., and Peek, R. (1993). Parametric study of vertical vibration of circular flexible foundation on layered media: *Earthquake Engineering and Structural Dynamics*, Vol. 22, pp. 685–694.

Guler, K., and Celep, Z. (1995a). Static and dynamic responses of a circular plate on a tensionless elastic foundation: *Journal of Sound and Vibration*, Vol. 183, No. 2, pp. 185–95, DOI: 10.1006/jsvi.1995.0248.

Guler, K., and Celep, Z.. (1995b). Static and dynamic responses of a circular plate on a tensionless elastic foundation: *J Sound Vibrat*, Vol. 183, No. 2, pp. 185–95, DOI: 10.1006/jsvi.1995.0248.

Güler, K., and Guler, K.. (2004). Circular Elastic Plate Resting on Tensionless Pasternak Foundation: *Journal of Engineering Mechanics*, Vol. 130, No. 10, pp. 1251–1254, DOI: 10.1061/(asce)0733-9399(2004)130:10(1251).

Gunerathne, S., Seo, H., Lawson, W.D., and Jayawickrama, P.W. (2018). Analysis of edge-to-center settlement ratio for circular storage tank foundation on elastic soil: *Computers and Geotechnics*, Vol. 102, No. April, pp. 136–147, DOI: 10.1016/j.compgeo.2018.05.008.

Gunerathne, S., Seo, H., Lawson, W.D., and Jayawickrama, P.W. (2019). Variational approach for settlement analysis of circular plate on multilayered soil: *Applied Mathematical Modelling*, Vol. 70, pp. 152–170, DOI: 10.1016/j.apm.2019.01.009.

Gupta, A.P., and Bhardwaj, N.. (2004). Vibration of rectangular orthotropic elliptic plates of quadratically varying thickness resting on elastic foundation: *Journal of Vibration and Acoustics, Transactions of the ASME*, Vol. 126, No. 1, pp. 132–40, DOI: 10.1115/1.1640654.

Gupta, U.S., Lal, R., and Jain, S.K. (1990). Effect of elastic foundation on axisymmetric vibrations of polar orthotropic plates of variable thickness: *Journal of Sound and Vibration*, Vol. 139, No. 3, pp. 503–513.

Hamarat, M.A., Çalık Karaköse, Ü.H., and Orakdöğen, E. (2012). Seismic Analysis of Structures Resting on Two Parameter Elastic Foundation: *15th World Conference on Earthquake Engineering (15WCEE)*, No. 1940.

Hassan, A.H.A., and Kurgan, N. (2020). Bending Analysis of Thin FGM Skew Plate Resting on Winkler Elastic Foundation Using Multi-Term Extended Kantorovich Method: *Engineering Science and Technology, an International Journal*, Vol. 23, No. 4, pp. 1–13, DOI: 10.1016/j.jestch.2020.03.009.

Hemsley, J.A. (1987). “Influence of wall superstructure on the foundation interaction analysis of a circular raft.” *Proceeding of Institute of Civil Engineers*,, p. 115–142.

Hetenyi, M. (1950). A general solution for the bending on an elastic foundation of arbitrary continuity: *Journal of Applied Physics*, Vol. 21, No. 1, pp. 55–58.

Hetenyi, M. (1946). *Beams on Elastic Foundation: Theory with Applications in the Fields of Civil and Mechanical Engineering*, Univ. of Michigan Press, Ann Arbor, Michigan.

Hinton, E. (1988). *Numerical methods and software for dynamic analysis of plates and shells*, Pineridge Press, Swansea.

Hooper, J.A. (1974). Analysis of a circular raft in adhesive contact with a thick elastic layer: *Geotechnique*, Vol. 24, No. 4, pp. 561–580.

Hooper, J.A. (1975). Elastic settlement of a circular raft in adhesive contact with a transversely isotropic medium: *Geotechnique*, Vol. 25, No. 4, pp. 691–711.

Hooper, J.A., and West, D.J. (1983). "Structural analysis of a circular raft on yielding soil." *Proceeding Institute of Engineers,*, p. 205–222.

Hughes, T.J.R. (1987). *The Finite Element Method. Linear Static and Dynamic Finite Element Analysis*, Prentice-Hall: Englewood Cliffs, NJ.

Hughes, T.J.R., and Cohen, M. (1978). The "Heterosis" Finite Element for Plate Bending: *Compurers & Structures*, Vol. 9, pp. 445–450.

Iguchi, M., and Luco, J.E. (1981). Dynamic response of flexible rectangular foundation on an elastic half space: *Earthquake Engineering and Structural Dynamics*, Vol. 9, pp. 239–249.

Ishkova, A.G. (1947). Exact solution of the problem of a circular plate in bending on an elastic half-space under the action of a uniformly distributed axisymmetrical load: *Dokl. Akad. Nauk. S.S.S.R.*, Vol. 4, pp. 129–132.

Janes, R.L. (1962). Digital computer solution for pavement deflections",: *Journal of Portland Cement Association*, Vol. 4, No. 3, pp. 30–36.

Jianguo, W., Xruxr, W., and Maoruang, H. (1992). Fundamental Solutions and Boundary Integral Equations for Reissner's Plates on Two Parameter Foundations: *International Journal of Solids and Structures*, Vol. 29, No. 10, pp. 1233–1239.

Jones, R., and Mazumdar, J.A. (1980). A note on the behavior of plates on an elastic foundation: *Journal of Applied Mechanics*, Vol. 47, pp. 191–192, DOI: 10.1115/1.3153602.

Jones, R., and Xenophontos, J. (1977). The Vlasov Foundation Model: *Int. J. mech. SCi.*, Vol. 19, pp. 317–323.

Joodaky, A., and Joodaky, I. (2015). A Semi-Analytical Study on Static Behavior of Thin Skew Plates on Winkler And Pasternak Foundation: *International Journal of Mechanical Sciences*, Vol. 100, pp. 322–327, DOI: 10.1016/j.ijmecsci.2015.06.025.

Kant, T. (1982). Numerical Analysis of Thick Plates: *Computer Methods in Applied Mechanics and Engineering*, Vol. 31, pp. 1–18.

Kant, T., Owen, D, R, J., and Zienkiewicz, O.C. (1982). A Refined Higher-Order C^o Plate Bending Element: *Compurers & Structures*, Vol. 15, No. 2, pp. 177–183.

Karaşin, H., Gülkan, P., and Aktas, G. (2015). A finite grid solution for circular plates on elastic foundations: *KSCE Journal of Civil Engineering*, Vol. 19, No. 4, pp. 1157–1163, DOI: 10.1007/s12205-014-0713-x.

Katsikadelis, J.T., and Kallivokas, L.F. (1986). Clamped Plates on Pasternak-Type Elastic Foundation by the Boundary Element Method: *Journal of Applied Mechanics*, Vol. 53, No. December, pp. 909–17.

Katsikadelis, J.T., and Kallivokas, L.F. (1988). Plates on bi-parametric elastic foundation by BDIE method: *Journal of Engineering mechanics division, ASCE*, Vol. 114, pp. 847–875.

Ketabdari, M.J., Allahverdi, A., Boreyri, S., and Ardestani, M.F. (2016). Free vibration analysis of homogeneous and FGM skew plates resting on variable Winkler-Pasternak elastic foundation: *Mechanics and Industry*, Vol. 17, No. 1, DOI: 10.1051/meca/2015051.

Kim, C.S., and Dickinson, S.M. (1989). On the free, transverse vibration of annular and circular, thin, sectorial plates subject to certain complicating effects: *Journal of Sound and Vibration*, Vol. 134, No. 3, pp. 407–421, DOI: 10.1016/0022-460X(89)90566-X.

Kobayashi, H., and Sonoda, K. (1989). Rectangular mindlin plates on elastic foundations: *International Journal of Mechanical Science*, Vol. 31, No. 9, pp. 679–91.

Koning, H. (1997). "Stress distribution in a homogeneous anisotropic, elastic, semi-infinite solid." *Proceeding of 4Th International Conference on Soil Mechanics and Found Engineering, London*,, p. 335–338.

Krenk, S., and Schimdt, H. (1981). Vibration of elastic circular plate on an elastic half-space-a direct approach: *Journal of Applied Mechanics*, Vol. 81, pp. 161–168.

Krishnamoorthy, C.S. (1987). *Finite Element Analysis-Theory and Programming*, Tata McGraw Hill Publishing Company Ltd., New Delhi.

Lam, K.Y., Wang, C.M., and He, X.Q. (2000). Canonical exact solutions for Levy-plates on two-parameter foundation using Green's functions: *Engineering Structures*, Vol. 22, No. 4, pp. 364–378, DOI: 10.1016/S0141-0296(98)00116-3.

Laura, P.A.A., Gutierrez, R.H., Sanzi, H.C., and Elvira, G. (1995). The lowest axisymmetrical frequency of vibration of a circular plate partiallyembedded in a Winkler foundation: *Journal of Sound and Vibration*, Vol. 185, pp. 915–19.

Leissa, A.W. (1993). *Vibration of plates*, Acoustical Society of America, Sewickley, PA.

Lenczner, D. (1962). Bending moments and pressures on model footings: *I. Concr. Constr. Eng.*, Vol. 57, pp. 181–187.

Liew, B.K.M., and Han, J.-B. (1997). Bending Analysis of Simply Supported Shear Deformable Skew Plates: No. March, pp. 214–221.

Liu, H., Liu, F., Bai, H., and Yang, R. (2016). Free vibration of thick annular sector plate on Pasternak foundation with general boundary conditions: *Journal of Vibroengineering*, Vol. 18, No. 3, pp. 1692–1706, DOI: 10.21595/jve.2016.16717.

Mandal, J.J., and Ghosh, D.. . . (1999). Prediction of elastic settlement of rectangular raft foundation- a coupled FE - BE approach: *International Journal for Numerical and Analytical Methods in Geomechanics*, Vol. 23, No. March 1998, pp. 263–273.

Mandal, J.J., and Roy, T. (2015). Prediction of elastic settlement of rectangular piled raft foundation: *Japanese Geotechnical Society Special Publication*, Vol. 2, No. 34, pp. 1228–1232, DOI: https://doi.org/10.3208/jgssp.IND-31.

Mar, M., Alvapplllai, A., Faruque, M.O., and Zaman, M. (1991). "Dynamic Response of Foundations on Two- Parameter Media." *Second International Conference on Recent Advances in Geotechnical Earthquake Engineering & Soil Dynamics*,, p. 679–684.

Meghre, A.S., and Kadam, K.N. (2014). *Finite Element Method in Structural Analysis*, First Edit Ed., Khanna Publishers, New Delhi.

Meghre, A.S., and Kadam, K.N. (2010). Higher order thick circular plates subjected to distributed loads: *Journal of Institution of Engineers (India), Civil Engineering Division*, Vol. 90, pp. 43–47.

Melerski, E.S. (1989). Circular plate analysis by finite differences: energy approach: *Journal of Engineering Mechanics, ASCE*, Vol. 115, pp. 1205–24.

Melerski, E.S. (1997). Numerical modelling of elastic interaction between circular rafts and cross-anisotropic media: *Computers and Structures*, Vol. 64, No. 1–4, pp. 567–578, DOI: 10.1016/S0045-7949(96)00132-0.

Mishra, R.C., and Chakrabarti, S.K. (1997). Shear and attachment effects on the behaviour of rectangular plates resting on tensionless elastic foundation: *Engineering Structures*, Vol.

19, No. 7, pp. 551–567, DOI: 10.1016/S0141-0296(97)00122-3.

Molla, M.K.A., and Ray, D.P. (1994). Analysis of flexible rectangular raft foundation under dynamic loading: *Compurers & Structures*, Vol. 52, No. 5, pp. 1079–1091.

Morley, L.S.D. (1963). *Skew Plates and Strucrures*, Pergamon Press, Oxford.

Mostafa Shaaban, A., and Rashed, Y.F. (2013). A coupled BEM-stiffness matrix approach for analysis of shear deformable plates on elastic half space: *Engineering Analysis with Boundary Elements*, Vol. 37, No. 4, pp. 699–707, DOI: 10.1016/j.enganabound.2012.12.005.

Narita, Y. (1985). Natural frequencies of free, orthotropic elliptical plates: *Journal of Sound and Vibration*, Vol. 100, pp. 83–89.

Oin, O.H. (1995). Hybrid - Trefftz finite element method for Reissner plates on an elastic foundation: *Computer Methods In Applied Mechanics and Engineering*, Vol. 122, pp. 379–92.

Olson, M.D., and Lindberg, G.M. (1970). Annular and circular sector finite elements for plate bending: *International Journal of Mechanical Sciences*, Vol. 12, No. 1, pp. 17–33, DOI: 10.1016/0020-7403(70)90003-2.

Omurtag, M.H., Özütok, A., Aköz, A.Y., and Özcelikörs, Y. (1997). Free vibration analysis of Kirchoff plates on an elastic foundation by mixed finite element formulation based on Gâteaux differential: *International Journal for Numerical Methods in Engineering*, Vol. 40, pp. 297–317.

Özdemir, Y.I. (2018). Eigenvector and eigenvalue analysis of thick plates resting on elastic foundation with first order finite element: *Challenge Journal of Structural Mechanics*, Vol. 4, No. 2, pp. 61–76.

Ozgan, K., and Daloglu, A.T. (2007). Alternative plate finite elements for the analysis of thick plates on elastic foundations: *Structural Engineering and Mechanics*, Vol. 26, No. 1, pp. 69–86.

Ozgan, K., and Daloglu, A.T. (2009). Application of the modified Vlasov model to the free vibration analysis of thick plates resting on elastic foundations: *Shock and Vibration*, Vol. 16, No. 5, pp. 439–454, DOI: 10.3233/SAV-2009-0479.

Özgan, K., and Daloğlu, A.T. (2008). Effect of transverse shear strains on plates resting on elastic foundation using modified Vlasov model: *Thin-Walled Structures*, Vol. 46, No.

11, pp. 1236–1250, DOI: 10.1016/j.tws.2008.02.006.

Özgan, K., and Daloğlu, A.T. (2012). Free vibration analysis of thick plates on elastic foundations using modified Vlasov model with higher order finite elements: *Indian Journal of Engineering and Materials Sciences*, Vol. 19, No. 4, pp. 279–291.

Özgan, K., and Daloğlu, A.T. (2015). Free vibration analysis of thick plates resting on Winkler elastic foundation: *Challenge Journal of Structural Mechanics*, Vol. 1, No. 2, pp. 78–83.

Paiva de, J.B., and Butterfield, R. (1997). Boundary Element Analysis of plate-soil interaction: *Compurers & Structures*, Vol. 64, No. 1–4, pp. 319–328.

Pasternak, P.L. (1954). On a New Method of Analysis of an Elastic Foundation by Means of Two Foundation Constants: *Gosudarstvennoe Izdatelstvo Literaturi po Stroitelstuvei Arkhitekture, Moscow* .,.

Petyt, M. (1990). *Introduction to finite element vibration analysis*, Cambridge University Press, Cambridge.

Pickett, G., and McCormick, F.J. (1951). “Circular and rectangular plates under lateral loads and supported by an elastic solid medium.” *Proc. 1st U. S. Nat. Congr. Appl. Mech.*,, p. 331–338.

Pickett, G., Raville, M.E., Janes, W.C., and McCormick, F.J. (1951). Deflections, moments and reactive pressures for concrete pavements: *Kanas State College Bulletin No. 65.*,.

Providakis, C.P. (1997). Transient boundary element analysis of elasto-plastic plates on elastic foundation: *Soil dynamics & Earthquake Engineering*, Vol. 16, pp. 21–27.

Qin, Q.H. (1994). Hybrid Trefftz finite-element approach for plate bending on an elastic foundation: *Applied Mathematical Modelling*, Vol. 18, No. 6, pp. 334–339, DOI: 10.1016/0307-904X(94)90357-3.

Rajapakse, R.K.N.D., and Selvadurai, A.P.S. (1986). On the performance of Mindlin plate elements in modelling Plate-elastic medium interaction: a comparative study: *International Journal for Numerical Methods in Engineering*, Vol. 23, pp. 1229–1244.

Rajesh, K., and Saheb, K.M. (2018). Free vibration analysis of Mindlin plates resting on pasternak foundation using coupled displacement method: *Archive of Mechanical Engineering*, Vol. 65, No. 1, pp. 107–128, DOI: 10.24425/119412.

Rao, N.S.V.K. (1998). *Vibration Analysis and Foundation Dynamics*, Wheeler Publishing, New Delhi.

Rao, B.L., and Rao, K.C. (2013). Vibrations of Elastically Restrained Circular Plates Resting on Winkler Foundation: *Arabian Journal for Science and Engineering*, Vol. 38, No. 11, pp. 3171–3180, DOI: 10.1007/s13369-012-0457-1.

Rashed, Y.F., Aliabadi, M.H., and Brebia, C.A. (1998). The boundary element method for thick plates on a Winkler foundation: *International Journal for Numerical Methods in Engineering*, Vol. 41, pp. 1435–1462.

Reissner, E. (1947). On Bending of Elastic Plate: *Quarterly of Applied Mathematics*, Vol. 5, No. 1, pp. 55–68.

Rouzegar, J., and Sharifpoor, R.A. (2015). Flexure of thick plates resting on elastic foundation using two-variable refined plate theory: *Archive of Mechanical Engineering*, Vol. 62, No. 2, pp. 181–203, DOI: 10.1515/meceng-2015-0011.

Salari, M., Bert, C.M., and Striz, A.G. (1987). Free vibration of a solid circular plate free at its edge and attached to a Winkler foundation: *Journal of Sound and Vibration*, Vol. 118, pp. 188–91.

Sapountazakis, E.J., and Katsikadelis, J.T. (1992). Unilaterally supported plates on elastic foundations by the boundary element method: *Journal of Applied Mechanics*, Vol. 58, pp. 580–586.

Savidis, S.A., and Richter, T. (1979). Dynamic response of elastic plates on the surface of the half-space: *International Journal for Numerical and Analytical methods in Geomechanics*, Vol. 3, pp. 245–254.

Selvaduari, A. (1979). *Elastic analysis of soil-foundation interaction*, Amsterdam: Elsevier.

Sengupta, D. (1993). Direct computation of moment, shear and reaction in flat plates using a triangular element free from locking: *Compurers & Structures*, Vol. 48, pp. 843–50.

Sengupta, D. (1995). Performance Study of A Simple Finite Element In The Analysis of Skew Rhombic Plates: *Computers & Structures*, Vol. 54, No. 6, pp. 1173–82.

Sengupta, D. (1991). Stress Analysis of Flat Plates With Shear Using Explicit Stiffness Matrix: *International Journal for Numerical Methods in Engineering*, Vol. 32, No. October, pp. 1389–1409.

Sharma, S., and Shivani, S. (2011). Free Vibration Analysis of Circular Plate of Variable Thickness Resting on Pasternak Foundation: *Journal of InternationalAcademy of*

Physical Sciences, Vol. 15, No. January 2011, pp. 1–13.

Shi, D.Y., Shi, X.J., and Li, W.L. (2014). In-plane vibration analysis of annular sector plates with arbitrary boundary supports: *Zhendong Gongcheng Xuebao/Journal of Vibration Engineering*, Vol. 27, No. 1, pp. 1–8.

Shukla, S.K., Gupta, A., and Sivakugan, N. (2011). Analysis of Circular Elastic Plate Resting on Pasternak Foundation by Strain Energy Approach: *Geotechnical and Geological Engineering*, Vol. 29, No. 4, pp. 613–618, DOI: 10.1007/s10706-011-9392-2.

Smaill, J.S. (1990). Dynamic response of circular plates on elastic foundation: linear and non-linear deflection: *Journal of Sound and Vibration*, Vol. 139, No. 3, pp. 487–502.

Srinivasa, C. V, Suresh, Y.J., Kumar, W.P.P., and Banagar, A.R. (2018). Bending behavior of simply supported skew plates: *International Journal of Scientific & Engineering Research*, Vol. 9, No. 5, pp. 21–26.

Straughan, W. (1990). Analysis of plates on elastic foundation.: *A dissertation in Civil Engineering, Graduate School of Texas Tech. University,in Partial Fulfillment of the Requirements for the Degree of Doctor of Philosophy.*,.

Syngellakis, S., and Bai, C. (1993). On the application of the boundary element method to plate-half-space interaction: *Engineering Analysis with Boundary Elements*, Vol. 12, pp. 119–25.

Tameroglu, S.S. (1996). Vibration of clamped rectangular plate on elastic foundations subjected to uniform compressive forces: *Journal of Engineering mechanics division, ASCE*, Vol. 122, No. 8, pp. 714–718.

Terzaghi, K. (1955). Evaluation of Coefficients of Subgrade Reaction: *Geotechnique*, Vol. 5, No. 4, pp. 297–326.

Timoshenko, S.P., and Woinowsky-Krieger, W. (1970). *Theory of Plates and Shells*, McGraw-Hill: New York.

Turhan, A. (1992). A Consistent Vlasov Model for Analysis of Plates on Elastic Foundations Using the Finite Element Method: *A dissertation in Civil Engineering, Graduate School of Texas Tech. University,in Partial Fulfillment of the Requirements for the Degree of Doctor of Philosophy.*,.

Utku, M., Ergin, C., and Inceleme, I. (2000). Circular plates on elastic foundations modelled with annular plates: *Computers & Structures*, Vol. 78, pp. 365–374.

Vallabhan, C.V.G.V.G., and Das, Y.C. (1991a). A refined model for beams on elastic foundations: *International Journal of Solids and Structures*, Vol. 27, No. 5, pp. 629–637, DOI: 10.1016/0020-7683(91)90217-4.

Vallabhan, C.V.G., and Das, Y.C. (1991b). Analysis of Circular Tank Foundations: *J. Engng. Mech., ASCE.*, Vol. 117, No. 4, pp. 789–797.

Vallabhan, C.V.G.G., and Das, Y.C. (1991c). Modified Vlasov Model for Beams on Elastic Foundations: *J. Geotech. Engrg.*, Vol. 117, No. 6, pp. 956–966.

Vallabhan, C.V.G., and Das, Y.C. (1988). Parametric Study of Beams on Elastic Foundations: *Journal of Engineering mechanics division, ASCE*, Vol. 114, No. 12, pp. 2072–82.

Vallabhan, C.V.G., Straughan, W.T., and Das, Y.C. (1991). Refined model for analysis of plates on elastic foundations: *Journal of Engineering Mechanics*, Vol. 117, pp. 2830–43.

Vesić, A.S. (1961). Bending of Beams Resting on Isotropic Elastic solid: *Journal of Engineering mechanics division, ASCE*, Vol. 87, No. EM2, pp. 35–53.

Vlasov, V.Z., and Leont'ev, U.N. (1966). Beams, plates and shells on elastic foundations: *Israel Program for Scientific Translations*, p. 357.

Wang, C.Y. (2005). Fundamental frequency of a circular plate supported by a partial elastic foundation: *Journal of Sound and Vibration*, Vol. 285, pp. 1203–1209.

Wang, X., and Yuan, Z. (2018). Buckling analysis of isotropic skew plates under general in-plane loads by the modified differential quadrature method: *Applied Mathematical Modelling*, Vol. 56, pp. 83–95, DOI: 10.1016/j.apm.2017.11.031.

Weeën, F. V. (1982). Application of the boundary integral equation method to Reissner's plate model: *International Journal for Numerical Methods in Engineering*, Vol. 18, pp. 1–10.

Whittaker, W.L., and Christiano, P. (1982). Dynamic response of plate on elastic half-space: *Journal of Engineering Mechanics Division, ASCE*, Vol. 108, pp. 133–154.

Winkler, E. (1867). *Die Lehre von der Elastizitat und Festigkeit*, Dominicus, Prague.

Wu, L., and Lee, W. (2003). Dynamic Analysis of Circular Plate On Elastic Foundation by EFHT Method: *The Chinese Journal of Mechanics-Series A*, Vol. 19, No. 3, pp. 337–347.

Xenalevina Sidara, S.C., and Maknun, I.J. (2020). Convergence behavior of DKMQ element in functionally graded material (FGM) skew plate: *AIP Conference Proceedings*, Vol. 2296, No. November, DOI: 10.1063/5.0030634.

Xiao, J.R. (2001). Boundary element analysis of unilateral supported Reissner plates on elastic foundations: *Computational Mechanics*, Vol. 27, No. 1, pp. 1–10.

Yue, F., Wang, F., Jia, S., Wu, Z., and Wang, Z. (2020). Bending Analysis of Circular Thin Plates Resting on Elastic Foundations Using Two Modified Vlasov Models: *Mathematical Problems in Engineering*, Vol. 2020, pp. 1–12, DOI: 10.1155/2020/2345347.

Yue, F., Wu, Z., Yang, H., and Li, M. (2019). Iterative technique for circular thin plates on Gibson elastic foundation using modified Vlasov model: *Theoretical and Applied Mechanics Letters*, Vol. 9, No. 5, pp. 312–319, DOI: 10.1016/j.taml.2019.04.007.

Zheng, X.J., and Zhou, Y.H. (1988). Exact solution of nonlinear circular plate on elastic-foundation: *Journal of Engineering Mechanics-ASCE*, Vol. 114, pp. 1303–16.

Zienkiewicz, O.C., and Taylor, R.L. (1991). *The Finite Element Method. Solid and Fluid Mechanics and Non-inerarity*, (4th edn.) Ed., McGraw-Hill: London.

25.06.2024

25/06/2024

Dr. Jagat Jyoti Mandal
Ex-Professor, NIT Durgapur & NITTTR, Kolkata
Chartered Engineer & Geotechnical Consultant

25/06/24

Dr. Debasish Bandyopadhyay
Professor
Dept. of Construction Engineering
Jadavpur University, Salt Lake
Kolkata - 700 106